

D ynam ics of glassy system s

L eticia F . C ugliandolo

Laboratoire de P hysique T heorique, E cole N orm ale Superieure,
24 rue Lhom ond 75231 P aris C edex 05 France and

Laboratoire de P hysique T heorique et H autes E nergies, Jussieu,
1er etage, T our 16, 4 P lace Jussieu, 75252 P aris C edex 05, France

O ctober 12, 2002

A bstract

T hese lecture notes can be read in two ways. T he first two Sections contain a review of the phenom enology of several physical system s with slow nonequilibrium dynam ics. In the Conclusions we sum m arize the scenario for this temporal evolution derived from the solution to som e solvable m odels (p spin and the like) that are intim ately connected to the m ode coupling approach (and sim ilar ones) to super-cooled liquids. At the end we list a number of open problem s of great relevance in this context. T hese Sections can be read independently of the body of the paper where we present som e of the basic analytic techniques used to study the out of equilibrium dynam ics of classical and quantum m odels with and without disorder. W e start the technical part by brie y discussing the role played by the environm ent and by introducing and com paring its representation in the equilibrium and dynam ic treatm ent of classical and quantum system s. W e next explain the role played by explicit quenched disorder in both approaches. Later on we focus on analytical techniques; we expand on the dynam ic functional m ethods, and the diagram m atic expansions and resum m ations used to derive m acroscopic equations from the m icroscopic dynam ics. W e show why the m acroscopic dynam ic equations for disordered m odels and those resulting from self-consistent approxim ations to non-disordered ones coincide. W e review som e generic properties of dynam ic system s evolving out of equilibrium like the m odi cations of the fluctuation-dissipation theorem , generic scaling form s of the correlation functions, etc. F inally we solve a fam ily of m ean- eld m odels. T he connection between the dynam ic treatm ent and the analysis of the free-energy landscape of these m odels is also presented. W e use pedagogical exam ples all along these lectures to illustrate the properties and results.

Contents

1	Introduction	6
2	Some physical systems out of equilibrium	8
2.1	Domain growth	8
2.2	Glasses	10
2.3	Spin-glasses	13
2.4	Quantum fluctuations	14
2.5	Rheology and granular matter	15
2.6	Elastic manifolds in random potentials	16
2.7	Aging	17
2.8	Summary	19
3	Theoretical approach	20
4	Systems in contact with environments	22
4.1	Modeling the coupled system	22
4.1.1	Statics	23
4.1.2	Dynamics	24
5	Observables and averages	25
5.1	Classical systems	26
5.2	Quantum problems	28
5.3	Average over disorder	29
6	Time dependent probability distributions	29
6.1	The Fokker { Planck and Kramers equations	29
6.2	Approach to equilibrium	30
6.3	Equilibrium dynamics	31
7	The fluctuation { dissipation theorem (fdt)	33
7.1	Static fdt	33
7.2	Dynamic fdt	33
7.3	Quantum fdt	34
7.4	Examples	34
7.4.1	Harmonic oscillator and diffusion	34
7.4.2	A driven system	35
7.4.3	No Einstein relation	35
7.4.4	A complex bath	35
8	Dynamic generating functionals	36
8.1	Classical models	36
8.2	Supersymmetry (susy)	38
8.3	Connection with the replica formalism	39
8.4	Quantum models	39

8.5	Average over disorder	42
9	Dynam ic equations	43
9.1	A useful derivation for fully-connected m odels	43
9.1.1	C lassical system s	43
9.1.2	Q uantum m odels	47
9.2	Beyond fully-connected m odels	50
9.2.1	C lassical m odels	50
9.2.2	Q uantum m odels	53
9.3	F ield equations	54
9.4	The therm odynam ic lim it and tim e-scales	54
9.5	Single spin equation	55
10	D iagram m atic techniques	56
10.1	Perturbative solution	56
10.2	The m ode coupling approxim ation (m ca)	57
10.3	m ca and disordered m odels	58
10.4	m ca for super-cooled liquids and glasses	60
11	G lassy dynam ics: G eneric results	61
11.1	The weak-ergodicity breaking scenario	61
11.2	The weak long-term m emory scenario	63
11.3	Slow tim e-reparam etrization invariant dynam ics	64
11.4	C orrelation scales	65
11.4.1	P roperties	66
11.4.2	D e nition of a characteristic tim e	70
11.5	M odi cations of fdt	71
11.5.1	T im e dom ain	71
11.5.2	F requency dom ain	72
11.5.3	T im e-reparam etrization invariant form ulation	72
11.5.4	fdt part	74
11.5.5	D i usion	75
12	Solution to m ean- eld m odels	75
12.1	N um erical solution	75
12.2	Solution at high tem peratures	76
12.3	Solution at low -T	78
12.3.1	The Lagrange m ultiplier	78
12.3.2	The stationary regim e	79
12.3.3	The aging regim e	80
12.3.4	The Edwards-Anderson param eter	81
12.3.5	F luctuation -dissipation relation	82
12.3.6	D iscontinuous classical transition	83
12.3.7	The classical threshold level	83
12.3.8	Two p m odels	84
12.3.9	sk m odel and sim ilar	85

12.3.10	Mode dependence	85
12.3.11	Quantum fluctuations	85
12.3.12	Driven dynamics	86
13	Modifications of fdt in physical systems	87
13.1	Domain growth	87
13.2	Structural glasses	89
13.3	Spin-glasses	89
13.4	Rheology	90
13.5	Vibrated models and granular matter	91
13.6	Driven vortex systems	91
13.7	Quantum fluctuations	91
13.8	Systems of finite size: preasymptotic behavior	91
13.9	Critical dynamics	92
13.10	Connection with equilibrium	93
14	Effective temperatures	94
14.1	Thermodynamical tests	95
14.1.1	How to measure a temperature	95
14.1.2	Zeroth law	98
14.1.3	Auxiliary thermal baths	100
14.2	Temperature fixing by susy breaking	101
14.3	Fictive temperatures	101
14.4	Nonequilibrium thermodynamics	101
14.5	Statistical mechanics	101
15	Metastable states	102
15.1	Equilibrium	103
15.2	Static tap approach	105
15.3	The tap equations	107
15.4	Stability of, and barriers between, the tap solutions	108
15.5	Index dependent complexity	109
15.6	Weighted sums over tap solutions	109
15.7	Accessing metastable states with replicas	110
15.8	Dynamics and quantum systems	112
16	Conclusions	112
17	Perspectives	117
A	Generalized Langevin equations	119
B	The Kubo formula	121
C	The response in a Langevin process	121
D	Grassmann variables and supersymmetry	122

1 Introduction

Graduate and undergraduate courses on statistical mechanics and thermodynamics are usually devoted to the theory of macroscopic systems in thermal equilibrium. In many experimental realizations, actually some of the more interesting ones at present, the situation is, however, very different. The systems are in contact with equilibrated environments but, for one reason or another, they do not manage to equilibrate with them. The systems evolve in time in an out of equilibrium manner.

The list of systems evolving out of equilibrium is very long. The reasons for not reaching equilibrium with the environment are also varied. The most common cases are those in which the time needed to equilibrate the sample falls beyond the experimental time-window. We discuss them in the context of domain growth, phase separation and classical and quantum glassy systems. Another important cause for lack of equilibration is the action of external forces that drive the samples out of equilibrium. In this context we discuss the rheological properties of glass forming liquids and glassy materials, that are closely related to the relaxation of the same systems. The driven dynamics of granular matter is another example of this kind. Finally, we briefly touch another type of problem that has received much attention in recent years: the relaxation and weakly driven dynamics of elastic manifolds in random potentials that model magnetic domain walls in disordered materials, superconductors, Wigner crystals, etc.

A common feature among the relaxing and weakly driven examples cited above is that they evolve very slowly. Thus, they belong to a particular class of the full set of non-equilibrium systems. Exploiting the fact that their dynamics is slow, and other more subtle properties that we shall discuss along these notes, we can hope to develop a common theoretical description for all of them.

In these lectures we focus on the study of a family of simple models that can be adapted to mimic the above mentioned physical systems. Typically, these models are fully connected interacting spin systems or models of interacting particles in finite dimensions. They can be seen as the equivalent of the fully connected Ising model for ferromagnetism that correctly predicts the existence of a thermodynamic transition and the nature of the two phases but fails to describe the dependence on dimensionality or the precise critical behavior. Similarly, the schematic models do not include a notion of distance inside the system. This crude approximation allows one to solve the dynamics explicitly, paying the price of losing information about the behavior in real space. Models of finite manifolds embedded in finite dimensional spaces and under the effect of random potentials are generalizations of the schematic models that capture partial spatial information. They are also solvable analytically. Interestingly enough, one finds that these models realize several phenomenological approaches to glassy physics that have been known for long. Moreover, their dynamic macroscopic equations coincide with those arising from the self-consistent approximations used to analyze more realistic models as, for instance, the mode-coupling approach to super-cooled liquids. Having an exact solution is very important in many respects. Firstly, it establishes the phenomenological approaches on firmer bases. Secondly, it allows one to set clear limits of validity of

the self-consistent approximations to realistic models. Thirdly, being defined by interacting potentials their free-energy density is accessible to analytical studies, from which one obtains the organization of metastable states and relates it to the dynamic properties. Fourthly, many important and common features of systems evolving slowly out of equilibrium have been discovered in the analytic solution to these models. Fifthly, one is able to identify some of the missing ingredients needed for a more accurate description of real systems. Even if their treatment has been too tough to implement correctly yet, it is important to know in which direction one could try in improving the analytical study. In short, they constitute a very useful "laboratory" where one identifies general trends that can be later tested numerically and experimentally in more realistic models and real materials.

Although the models on which we concentrate are simple in the sense discussed above one needs to master many analytical methods to extract all the richness of their behavior. These methods are not completely standard and are not comprehensively described in textbooks or lecture notes. For this reason, we try to present a rather complete and detailed introduction to them. We also discuss the scenario for glassy dynamics that stems out of this analysis. Finally, we mention several lines for future work that are currently being explored by several groups trying to go beyond the fully-connected and infinite dimensional models.

The lecture notes are organized as follows. In the next Section we introduce the phenomenology of the physical systems we are interested in paying special attention to the dynamic properties that we later describe analytically. The rest of the lecture notes are more technical. We start by reviewing very briefly several theoretical approaches to the glassy problem in Section 3. This summary is certainly not exhaustive but it may serve as a source of references. Since in the rest of the notes we shall develop classical and quantum systems in parallel we devote Section 4 to discuss how should one model the coupling between a system and its environment in both cases. In Section 5 we set the notation and we define several useful observables for spin and particle systems. The subject of Section 6 is a brief discussion of Fokker-Planck and Kramers processes and how they describe the approach to equilibrium. In the following Section we introduce the fluctuation-dissipation theorem, valid for systems evolving in equilibrium. Once these generic properties are established it will become simpler to discuss how they are modified in a system that evolves far from equilibrium. In Section 8 we explain the functional formalism that allows one to derive a generic dynamic effective action and the dynamic equations that we present in Section 9. We also introduce the very useful super-symmetric formulation of classical stochastic processes. In Section 10 we discuss an alternative method to obtain approximate dynamic equations. We focus on the mode-coupling (mc) approximation to show how averaging over disorder in some random models eliminates the same family of diagrams that the mc procedure neglects for non-disordered ones. The rest of the lectures are dedicated to the solution to the dynamic equations of the schematic models. We present it in as much generality as possible in Section 11. We discuss three generic results that were obtained when solving these equations without assuming equilibrium: the definition of correlation scales (Section 11.4), the modifications of the fluctuation-dissipation

theorem (Section 13) and the definition of effective temperatures (Section 14). We also discuss how these properties appear in variations of the models that mimic the physical systems introduced in Section 2 and in finite toy models, simulations and experiments. Finally, in Section 15 we relate the dynamic results to the organization of metastable states via the static and dynamic approach of Thouless, Anderson and Palmer (tap). We briefly discuss the connection between it and the studies of the potential energy landscape (Edwards measure and inherent structure approach). Finally, in Section 16 we summarize the scenario for the glass transition and glassy dynamics derived from solvable mean-field models and present some of the lines for future research in this area.

2 Some physical systems out of equilibrium

In this Section we summarize the phenomenology of a number of systems with slow dynamics. We especially signal the features that we expect to capture with an analytical approach.

2.1 Domain growth

Out of equilibrium relaxational dynamics occurs, for instance, when one suddenly quenches a system with ferromagnetic interactions from its high temperature phase into its low temperature phase. When the system is in contact with a thermal bath at temperature $T > T_c$ (T_c is the Curie critical temperature) the system is disordered and the instantaneous averaged magnetization vanishes at all times. (The average refers here to a coarse graining over a region of linear size, ℓ , with $\ell \gg \xi$ and ξ the correlation length.) All the one-time properties, such as the instantaneous averaged magnetization or the static magnetic susceptibility, can be computed using the Gibbs-Boltzmann distribution, P_{gb} . The system evolves in time but in a very simple manner controlled by P_{gb} . All properties of the equilibrium dynamics hold and any two-time correlation function is invariant under translations of time. Instead, if one externally and suddenly changes T to set it below the Curie temperature, $T < T_c$, the system evolves from the very disordered initial condition via the growth of domains of up and down magnetic order. With simple arguments one shows that the typical linear size of the domains grows as a power of the time spent in the low temperature phase, $R(t_w) = \xi(T) t_w^{1/z}$ [1]. We call waiting-time, t_w , the time spent since the entrance in the low- T phase. The dynamic exponent z depends on the kind of microscopic dynamics considered, e.g. for non-conserved order parameter $z = 2$ while for conserved order parameter $z = 3$. All T -dependence is concentrated in the prefactor $\xi(T)$. After the initial quench the system is a superposition of up and down domains and the magnetization averaged over the full system ($\ell = L$) vanishes. During coarsening domains grow. This is a scaling regime in which the system is statistically invariant under rescaling by the typical length $R(t)$. Typically, at a time $t_{req} \propto L^z$ the system orders and the averaged magnetization, m , equals the magnetization of the conquering domain, say $m > 0$. Restricted

ergodicity or equilibrium within one ergodic component holds in the sense that time and ensemble averages can be exchanged if and only if the time average is taken over a time window $t_{\text{req}} < t < t_{\text{erg}}$ and the ensemble average is restricted to the configurations with positive magnetization. Since a rare fluctuation might lead the system to reverse from $m > 0$ to $m < 0$ another, still longer, characteristic time, t_{erg} , appears. This time is also a function of the size of the system L and it is such that for times that are much longer than it complete ergodicity is restored. One can estimate it to be of Arrhenius type $t_{\text{erg}} \sim \exp[cL^{d-1}/(k_B T)]$, with c a constant, d the dimension of space and cL^{d-1} the free-energy barrier to be surmounted to go from one ergodic component to the other.

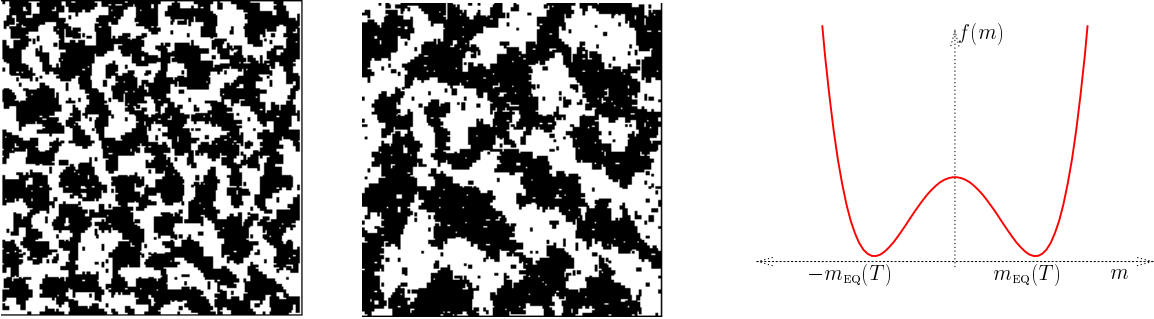


Figure 1: Two snapshots of a 2d cut of a 3d lattice undergoing ferromagnetic domain growth with non-conserved order parameter after a quench from $T > T_c$ to $T < T_c$ at time $t = 0$. On the left, $t_w = 10^3$ Monte Carlo steps (MCS). On the right, $t_w = 10^5$ MCS. Sketch of the Landau free-energy density $f(m)$ in the low- T phase. The evolution of the system is partially described by the evolution of a point in this free-energy landscape. Just after the quench $m = 0$ and coarsening is visualized in this plot as a static point on top of the barrier. After t_{req} the point falls into the well around the magnetization of the conquering domain. After t_{erg} ergodicity is restored and the point jumps the barrier via thermal activation [2].

The low temperature phase can also be reached with an annealing, e.g. by modifying the external temperature in steps of length ΔT and magnitude $\Delta T < 0$ until reaching the working temperature T . Since the entrance in the low- T phase the system coarsens. If the prefactor $\tau(T)$ increases with T , after a time t_w since crossing T_c a system prepared with a slow cooling rate will have much larger structures than one of the same age that has been quenched into the ordered phase. The dynamics in isothermal conditions is basically identical in both cases but the starting configuration at the initial temperature T is however very different, the annealed system looking older than the quenched one. The presence or absence of cooling rate dependences as well as the effect of temperature on the low- T dynamics allow one to distinguish among different glassy systems. We shall come back to this issue when discussing structural and spin glasses.

On the right panel of Fig. 1 we plot the two-welled Landau free-energy density

$f(m)$ against m . Transverse to the m direction there are $2^{L^d} - 1$ other directions that complete the phase space of the spin model. Note that when $L \rightarrow 1$ phase space is infinite dimensional even if real space is finite dimensional, $d < 1$. If one wishes to view the dynamics as the wandering of a point, that represents the instantaneous configuration of the system, in the free-energy landscape, the one-dimensional plot in Fig. 1 might be useful only if used carefully. The initial configuration after a quench corresponds to the top of the barrier ($m = 0$). This unstable point hides the $2^{L^d} - 1$ states, for $L \rightarrow a$, transverse directions (a is the lattice spacing). The domain growth process takes place while the representative point sits on the top of the barrier. Falling into one well corresponds to the growth of the conquering domain. Finally, jumping over the barrier is the activated process of reversing the full system. As long as $t < t_{\text{req}}$ the dynamics is highly non-trivial while viewed on this plot it looks trivial, with the representative point simply sitting on the border between the two basins of attraction of the equilibrium states $m = \pm m_{\text{eq}}$ [3].

Importantly enough, both t_{req} and t_{erg} grow with L and, if the thermodynamic limit $L \rightarrow 1$ is taken at the outset, diverging times with L cannot be reached and physical times are always smaller than t_{req} . The system cannot equilibrate with its environment and the non-equilibrium domain growth process goes on for ever.

2.2 Glasses

The domain growth example is very useful to visualize a non-equilibrium evolution. The mechanism behind the dynamics is clear and the growth of order can be easily identified. In other systems that undergo a non-equilibrium evolution whether there is a growing order controlling the evolution is still an open question. Glassy systems are one such example.

Understanding the glass transition and glassy dynamics is one of the greatest challenges in theoretical physics. The glassy problem can be summarized as follows [4]. Take a liquid at high temperature T_i and quench it at a constant rate, $r = -dT/dt$. On each temperature step, the viscosity relaxes rather quickly and with a simple analysis one estimates its asymptotic value to trace a curve $\eta(T)$ that is sketched in the left panel of Fig. 2 (red curve). This curve has several remarkable features. At very high temperature $\eta(T)$ very slowly grows with decreasing T . Decreasing the external temperature still the system approaches the crystallization (or melting) transition T_m . If the cooling rate r is sufficiently fast, this transition is avoided and the system enters a metastable super-cooled liquid phase where the viscosity grows very quickly with decreasing T . Indeed, one typically observes that when T changes by, say, 100°C , the viscosity jumps by approximately 10 orders of magnitude. In consequence, the dynamics of the liquid slows down enormously. For several liquids the form of the $\eta(T)$ curve can be described with a Vogel-Fulcher law,

$$\eta(T) = \eta_0 \exp \frac{A}{T - T_0} ; \quad (2.1)$$

that predicts a divergence of $\eta(T)$ when $T \rightarrow T_0$. These liquids are conventionally called fragile. Within the experimental precision T_0 coincides with the Kauzmann

temperature T_K where the extrapolation of the difference between the entropy of the liquid and the crystal vanish.) However, this fitting procedure can be criticized for several reasons. In many cases the form of the fitting function strongly depends on the temperature window chosen for the fit. Even more important is the fact that the dynamics becomes so slow when T decreases that the time needed to equilibrate the sample goes beyond the minimal cooling rate, or the maximum time reachable in the experience. Below a temperature T_g ($> T_0$) one can no longer equilibrate the sample. One of the most clear signatures of the absence of equilibrium below T_g is the fact that the measurement of, e.g., the volume as a function of temperature, depends on the cooling rate, r , used to reach T . Moreover, T_g decreases with decreasing cooling rate. Hence, the so-called "glass transition" is not a true thermodynamic transition but a dynamic crossover from the super-cooled liquid phase, where the dynamics is slow but occurs as in equilibrium [5], to the glass phase where the system does not manage to equilibrate with its environment. These features are schematically shown in the right panel of Fig. 2. Going back to the interpretation of Eq. (2.1), some authors extrapolate it below T_g , where viscosity measurements are not possible, and interpret the divergence at T_0 as the signature of a true thermodynamic transition. This means that even in the limit of vanishing cooling rate one would observe a transition from the super-cooled liquid to an ideal glass phase (still metastable with respect to the crystal) at T_0 . Others prefer a scenario in which Eq. (2.1) has no meaning below T_g .

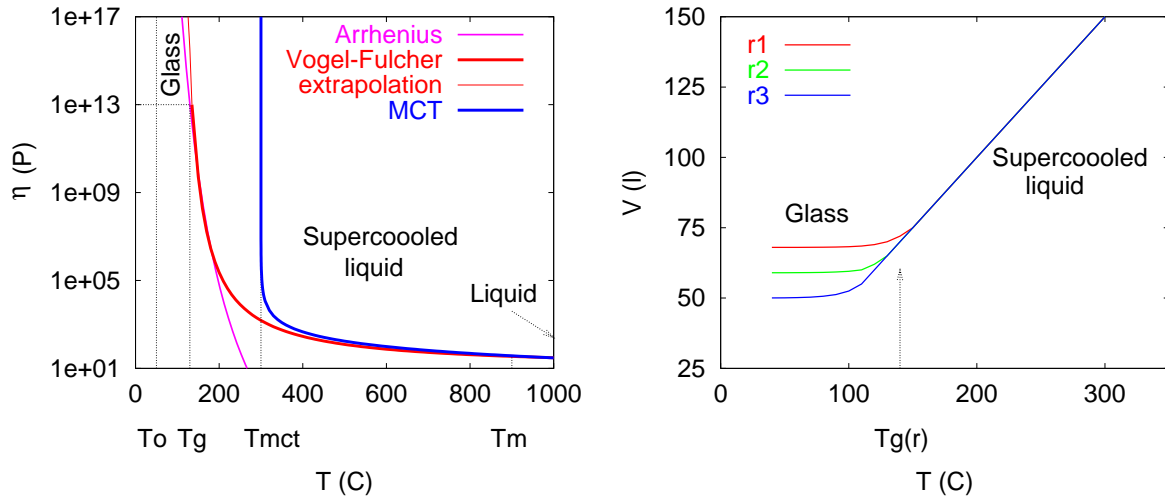


Figure 2: Left: sketch of the viscosity against temperature approaching T_g . Rough comparison between different scaling forms. (Arrhenius: $A = 3900\text{C}$, $\eta_0 = 10^6\text{P}$. Vogel-Fulcher: $A = 500\text{C}$, $T_0 = 100\text{C}$, $\eta_0 = 10\text{P}$. mct: $\eta_0 = (T - T_d)^{-\alpha}$ with $T_d = 300\text{C}$, $\alpha = 0.7$, $\eta_0 = 1700\text{P}$.) Right: cooling rate dependence of the volume, $r_1 > r_2 > r_3$.

In this sense, it is important to stress that the viscosity of many glass forming liquids, as the silica materials that give rise to window glass, is well fitted by an

An Arrhenius law

$$\tau(T) = \tau_0 \exp \frac{A}{T} \quad (2.2)$$

that diverges at $T \rightarrow 0$. These are the so-called strong glasses. It has been suggested that actually all glasses are strong since one can always fit $\tau(T)$ with an Arrhenius law if the temperature window used for the fit is close enough to T_g (as suggested in Fig. 2). This is the reason why some authors prefer a scenario in which the super-cooled liquid phase extends all the way up to $T = 0$ when an infinitely slow cooling rate is used. The curve labeled mct in the same figure shows the prediction of the models we shall discuss in these notes (spin models and mode-coupling theory). In short, this approach predicts a dynamic transition at T_d that is typically higher than T_g , with a power law divergence of τ . Albeit this and other defects, this approach is successful in many respects since it yields a satisfactory qualitative description of the phenomenology of super-cooled liquids and glasses.

For the purpose of our discussion the important point to stress is the fact that the liquid falls out of equilibrium at the (cooling rate dependent) temperature T_g . Indeed, even the "state" reached by the system below T_g depends on the cooling rate as seen, for instance, in measurements of volume, entropy, etc. as functions of T , see the right panel in Fig. 2. The slower the cooling rate, the deeper one penetrates below the threshold level corresponding to $\tau \rightarrow 1$. The dynamics below T_g occurs out of equilibrium since $t_{eq} > t_{exp}$, see the sketch in Fig. 3. The properties of the system cannot be described with the use of P_{gb} and a more sophisticated analysis has to be developed.

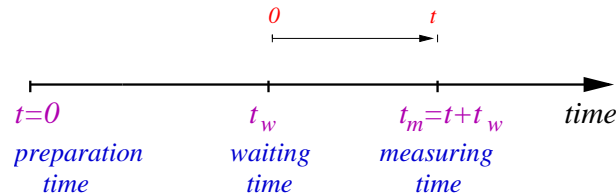


Figure 3: Characteristic times. The waiting and measuring times are experimental times t_{exp} . The equilibration time t_{eq} can be shorter or longer than them leading to equilibrium or non-equilibrium dynamics, respectively.

The above paragraphs were devoted to the discussion of the liquid to glass transition and it is implicitly assumed that the system was made of molecules in interaction. In the case of simple liquids, in which the constituents have no structure, one can describe the relevant interactions with a two body potential

$$E = \sum_{i < j} V(\mathbf{r}_i - \mathbf{r}_j) : \quad (2.3)$$

Hard spheres are the simplest example of this kind where the only interaction are hard core ones that forbid the penetration of one particle by another. Adding polymers in the solution that hosts the spheres one can tune a repulsive interaction between the particles. (See Fig. 4-left below for a snapshot of one such experimental

system [6].) Favorite potentials used in numerical simulations are the Lennard-Jones and soft-sphere ones

$$V(\mathbf{r}_i - \mathbf{r}_j) = 4 \epsilon_{ij} \left[\left(\frac{\sigma_{ij}}{r_{ij}} \right)^{12} - \left(\frac{\sigma_{ij}}{r_{ij}} \right)^6 \right] \quad (2.4)$$

To avoid crystallization one usually uses a binary system with N_A particles with mass m_A and N_B particles with mass m_B . The parameter σ_{AA} fixes the length scale, ϵ_{AA} the energy scale and m_A the mass scale. The time scale is then given by $t_0 = m_A \sigma_{AA}^2 / \epsilon_{AA}$. For a given density, e.g. $\rho = 1.2$, an adequate choice of the remaining parameters yields the expected properties of a liquid or a glass with a numerical transition at a temperature T_g where the relaxation time goes beyond the time accessible with the simulation. In the soft-sphere model one only keeps the repulsive term in the potential. Many other types of glasses are known in Nature. For instance, plastics as PVC whose mesoscopic constituents are polymers also undergo a glass transition very similar to the one described previously. Several types of interactions between the monomers that form the macromolecules are also of two-body type and they are repertoriated in the literature. The dynamics of particle systems is given by Newton's equations.

2.3 Spin-glasses

More exotic types of glasses have been studied for long. Spin-glasses have attracted the attention of experimentalists and theoreticians as a prototypical system with quenched disorder [7, 8, 9, 10]. These systems are magnetic alloys in which magnetic impurities are replaced in a magnetically inert host. The impurities occupy random positions and are not displaced within the sample in experimental times. The interactions between the impurities depend on the distance between them. Since the latter are random, the interactions themselves take random values that change in sign very quickly. A number of experimental realizations exist. As in other glassy systems, spin-glasses fall out of equilibrium at a transition temperature T_g when usual cooling rate procedures are used. From experimental and numerical results near T_g complemented with standard critical analysis, it is rather generally believed that the transition between the paramagnetic and the spin-glass phase is, in this case, a true thermodynamic transition. This is at variance with what occurs in structural and polymeric glasses. Another important difference with structural glasses and systems undergoing simple coarsening as ferromagnets is that the magnitude of cooling rate dependences is quite negligible suggesting that for spin-glasses the preferred configurations at one temperature are totally different from the ones at any other temperature. Still, slightly farther away from the transition one can no longer equilibrate the spin-glasses and observes typical non-equilibrium effects.

Edwards and Anderson proposed a simplified model for spin-glasses in which one represents the magnetic impurities with Ising spins placed on the vertices of a three dimensional cubic lattice. The random nature of the interactions are mimicked with first neighbors random interactions between the spins taken from a Gaussian

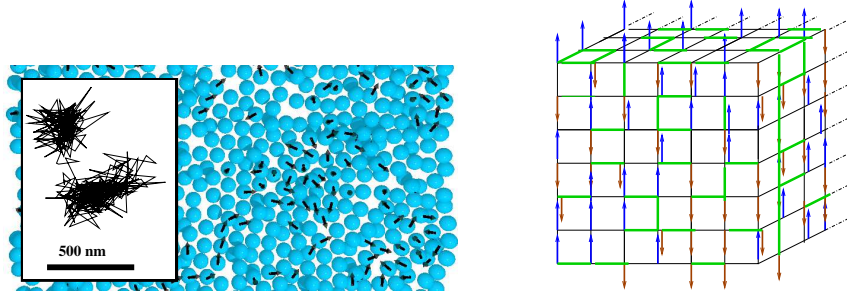


Figure 4: Different types of glasses: on the left, a colloidal system (image taken from [6]); on the right a representation of the 3d Edwards spin-glass model.

(or bimodal) probability distribution with zero mean and variance $[J_{ij}^2] = J^2 = (2z)$ where z is the connectivity of the lattice. (Hereafter we denote with square brackets the average over disorder.) The Hamiltonian is

$$H_J[S] = \sum_{\langle ij \rangle} J_{ij} s_i s_j : \quad (2.5)$$

where the vector S encodes the full set of spins in the sample $S = (s_1; s_2; \dots; s_N)$ and $\langle ij \rangle$ represents nearest neighbors on the lattice. In the fully connected limit in which each spin interacts with all others the sum runs over all pair of spins and the unusual normalization of the J_{ij} s, $[J_{ij}^2] = J^2 = (2N)$, ensures a correct thermodynamic limit. This is the Sherrington-Kirkpatrick (sk) model.

For many years it was common lore that the presence of explicit quenched disorder made spin-glasses intrinsically different from glasses where no quenched random forces have been identified. This belief was in part motivated by the analytical treatment used to study the equilibrium properties of the spin-glass phase in sk, namely, the replica trick. More recently, after a series of seminal papers by Kirkpatrick, Thirumalai and Wolynes [11], and the later solution to the non equilibrium dynamics of several glassy models [12, 13], it has been realized that the presence of quenched disorder is not that relevant. All glasses can be analyzed on the same footing. The schematic mean-field model for glasses, the p spin model, has quenched Gaussian interactions and its Hamiltonian is

$$H_J[S] = \sum_{i_1 i_2 \dots i_p} J_{i_1 i_2 \dots i_p} s_{i_1} s_{i_2} \dots s_{i_p} : \quad (2.6)$$

($[J_{i_1 \dots i_p}] = 0$ and $[J_{i_1 \dots i_p}^2] = J^2 p! = (2N^{p-1})$, we henceforth set $J = 1$.) Glauber's rule for Ising spins or Langevin equations for soft spins define the microscopic evolution.

2.4 Quantum fluctuations

Different driving dynamics slightly modify the picture just presented. Quantum glassy phases, where quantum fluctuations are at least as important as thermal activation, have been identified in a number of materials. Two such examples are

the spin glass compound and the amorphous insulator studied in [14] and [15], respectively. Another interesting realization is the so-called Coulomb glass in which localized electrons interact via Coulomb two-body potentials and hop between localization centers [16]. In all these systems the dynamics is extremely slow and strong history dependence as well as other glassy features have been observed.

Models for magnetic compounds are constructed with $SU(2)$ spins while models for particle systems are quantized with the usual commutation relations between coordinate and momenta. In both cases the dynamics is fixed by Heisenberg equations.

2.5 Rheology and granular matter

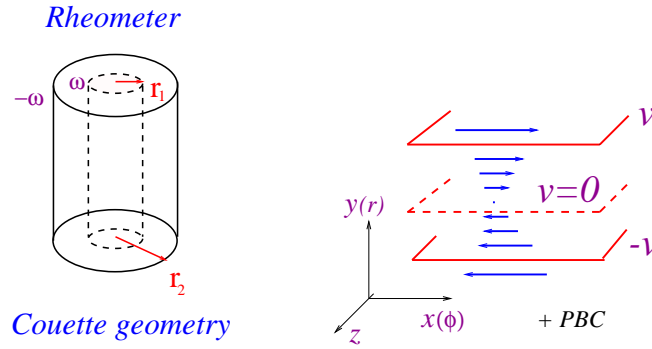


Figure 5: Left: A Couette cell used to shear a liquid. The internal and external walls turn with opposite angular velocities and the fluid is included in between them. Right: a cut of the Couette cell. (pbc: periodic boundary conditions.)

The above examples concern systems that are not able to reach equilibrium with their environments in a reasonable time but that, let evolve on astronomical time-scales, will eventually equilibrate. Other ways of establishing non-equilibrium states with slow dynamics are possible if one externally drives the samples [17].

A dense liquid can be driven to a slow out of equilibrium stationary regime by a weak shear. A shear is an example of a force that does not derive from a potential, i.e. it cannot be written as $\vec{f} = -\nabla V = \nabla \varphi$. The simplest way to apply a shear on a liquid is by means of a rheometer. In Fig. 5 we show one with a Couette geometry. The shear modifies the dynamic equations for the fluid by adding an advection $\vec{v} \cdot \nabla (\varphi; t)$. In the planar limit $\vec{v} = \gamma \hat{y}$ where \vec{v} is the velocity of the fluid, γ its density and γ the shearing rate. One mimics such a force in a spin system with a non-symmetric force, i.e. the force exerted by the spin i on the spin j is not equal to the force exerted by the spin j on the spin i [18, 19], e.g.

$$\vec{f}_i = \sum_{j \neq i}^X J_{ij} \vec{s}_j \quad \text{with } J_{ij} \neq J_{ji} : \quad (2.7)$$

(The motivation to define such a force comes from neural nets where the synapses have a direction.) It is clear that this force cannot be written as the variation of

a potential energy with respect to s_i , it violates detail balance, and an equilibrium measure cannot describe its effects [20].

A weak shear has a spectacular effect on the relaxation of liquids [21]. Usually, the viscosity as a function of the shear rate, $\dot{\gamma}$, has a Newtonian plateau at small $\dot{\gamma}$ that crosses over to a decreasing function that is approximately given by $\dot{\gamma}^{-2=3}$. Hence, by shearing the liquid one facilitates its flow and the relaxation time decreases with increasing $\dot{\gamma}$. Moreover, one introduces a shear-dependent time scale τ_{sh} that plays an important role in aging experiments as discussed in Section 2.7.

Another family of materials that have captured the attention of experimentalists and theoreticians in recent years is granular matter [22]. Since the potential energy needed to displace a macroscopic grain by a distance equal to its diameter, mgd , is much larger than the characteristic thermal energy, $k_B T$, thermal activation is totally irrelevant for systems made of macroscopic grains. Therefore, in the absence of external driving granular matter is blocked in metastable states and there exists no statistical mechanics approach capable of describing its static behavior. Instead, when energy is pumped in in the form of shearing, vibration or tapping, transitions between the otherwise metastable states occur and granular matter slowly relaxes towards configurations with higher densities. When trying to model these systems it is also important to keep in mind that dissipation is not given by the usual Ohmic form proportional to the velocity of the grains, $\dot{\mathbf{x}}$, but it is much more cumbersome. Glassy features such as hysteresis as a function of the amount of energy injected, slow dynamics [22], and non stationary correlations [23, 24, 25] have been exhibited.

The effect of the external drive can be described by applying time-dependent oscillatory forces, e.g. $f_i(\mathbf{r}; t) = A \sin(\mathbf{r} \cdot \mathbf{t})$, to each spin variable in model (2.6) [26]. One could also include complicated sources of dissipation by modifying the noise kernels obtained in Section 4 for a usual equilibrated bath.

2.6 Elastic manifolds in random potentials

The motion of a d dimensional directed elastic manifold embedded in an N dimensional space in the presence of quenched random disorder has a bearing in several areas of physics [27, 28]. (The total dimension of space is $d + N$.) The case $d = 0$ represents a particle in a random potential. With $d = 1, N = 2$ and an attractive punctual disorder one models, for instance, a single vortex in a dirty superconductor. When $d = 2$ and $N = 1$ one describes the dynamics of a directed interface in three dimensions. The standard model is

$$H = \int d^d \mathbf{x} \left(\frac{1}{2} \dot{\tilde{\mathbf{r}}}(\mathbf{x})^2 + V(\tilde{\mathbf{r}}; \mathbf{x}) \right) \quad (2.8)$$

where $\tilde{\mathbf{r}}(\mathbf{x}) = (\tilde{r}_1; \dots; \tilde{r}_N)(\mathbf{x})$ and $\mathbf{x} = (x_1; \dots; x_d)$ represents the transverse position of the point \mathbf{x} on the manifold and $V(\tilde{\mathbf{r}}; \mathbf{x})$ is a Gaussian random potential, with zero mean and correlations $[V(\tilde{\mathbf{r}}; \mathbf{x})V(\tilde{\mathbf{r}}^0; \mathbf{x}^0)] = N V(\tilde{\mathbf{r}} - \tilde{\mathbf{r}}^0)^2 = N \delta^d(\mathbf{x} - \mathbf{x}^0)$.

The study of these problems has been boosted by the advent of high- T_c superconductivity. Other physical systems that are modeled with similar Hamiltonians

are Wigner crystals, vortex lattices, charge density waves, etc. in the presence of disorder. All these problems have an underlying periodic structure that is modified by elastic distortions, topological defects and external quenched disorder. They can be set into motion with an external force and the velocity-force characteristics has several interesting features that have been much studied. One observes a depinning transition at $T = 0$, creep dynamics when the applied force is weak and $T > 0$, hysteresis, etc. (The driven motion is achieved, for instance, by applying an external current in the case of the vortex systems and the current-voltage characteristics is monitored.) The relaxational and driven dynamics of these systems show similarities but also marked differences with that of glasses and spin-glasses that are possibly due to the existence of an ordered underlying structure.

2.7 Aging

Aging means that older systems relax in a slower manner than younger ones [29]. One defines the age of a system as the time spent in the phase under study. For instance, the age of a system that is suddenly quenched from high- T to low- T is simply t_w . The aging properties are studied by monitoring the time evolution of correlation and response functions. In the former experiments one lets the system evolve and compares its configuration at the waiting-time t_w with the one reached at the subsequent time $t_w + t_w$. In the latter one perturbs the system at t_w with, e.g. a dc or an ac field, and follows the evolution of the linear response to the perturbation. In the glassy phase both correlations and responses depend on t_w in an aging manner and, within the experimentally accessible time-window, this trend does not show any tendency to stop. At temperatures that are close but above T_g one observes "interrupted aging", that is, a dependence on the age of the system until it reaches the equilibration time ($t_w > t_{eq}$) where the dynamics crosses over to an equilibrium one. In equilibrium correlation and response measurements are related in a system independent manner by the fluctuation-dissipation theorem (see Section 7). Out of equilibrium this general relation does not hold and, as we shall explain in Sections 13 and 14, important information can be extracted from its modifications.

Aging has an easy interpretation within coarsening systems. While the averaged domain size $R(t_w)$ grows with t_w , its rate of increase $d_{t_w} R(t_w)$ decreases, e.g. $d_{t_w} R(t_w) \propto t_w^{z-1}$ in the example explained in Section 2.1. The motion of interfaces slows down as time elapses. Comparing the configuration at t_w and at a later time $t_w + t_w$, one finds a clear separation of time-scales depending on the relative value of t_w with respect to t_w . If $\chi_0(t_w) = 1 - d_{t_w} \ln R(t_w)$, one has $R(t_w + t_w) = R(t_w) + d_{t_w} R(t_w) \approx R(t_w)$, and the domain walls do not move. The overlap between the configurations at t_w and $t_w + t_w$ is a sum of overlaps between domains of one and another type. (This holds when the ratio between the number of spin in the surface of the domains and in the bulk vanishes in the thermodynamic limit. Some non-standard systems have fractal scaling of the interfaces and the volume of the domains might also have a fractal dimensionality [30].) Due to thermal fluctuations within the domains, the correlation decays as in equilibrium

from 1 at equal times to $m_{eq}^2(T)$ when τ increases while still satisfying the constraint $\tau_0(t_w)$. For τ 's beyond this limit, the correlations decay below $m_{eq}^2(T)$ since the interfaces move and one compares configurations with very different domain structures as shown, for instance, in the two snapshots in Fig. 1.

In structural glasses, a pictorial explanation of aging is also possible in aging that each particle sees a cage made of its neighbors. When τ is short compared to a characteristic time $\tau_0(t_w)$ each particle rapidly rattles within its cage and the decorrelation is only characterized by thermal fluctuations. The correlations decay in a stationary manner from its value at equal times to a value called q_{ea} that will be defined precisely in Section 12 [in the domain growth example $q_{ea} = m_{eq}^2(T)$]. When τ increases, the motion of the particles destroys the original cages and one sees the structural relaxation. The waiting-time dependence implies that the cages are still when time evolves. The motion of a tagged particle is depicted in the left panel of Fig. 4 [6]. One sees how it first rattles within a cage to later make a long displacement and start rattling within another cage.

In spin-glasses no consensus as to which is the origin of aging has been reached. Still, the qualitative behavior of correlations and responses is rather close to the one in domain growth and structural glasses. In Fig. 6 we show the decay of the thermomagnetic magnetization (an integrated linear response) and the correlations between the fluctuations of the magnetization in a spin-glass [31, 32].

Shearing may have a very strong effect on an aging system. In some cases it introduces a characteristic time t_{sh} that yields the longest relaxation time. Thus, aging is interrupted for waiting-times that are longer than t_{sh} (see Fig. 7). This effect has been known for long experimentally [21] and it has been found and explored recently within the theoretical framework that we review [33, 34]. Experiments in other soft glassy materials with aging and aging interrupted by shear can be found in [35]. Some examples where the effect of shearing is not as spectacular are also known. For instance, in a phase separating mixture sheared in one direction the domains stop growing in the transverse direction while they continue to grow longitudinally (see [19] and references therein). This is a subject of intensive research.

Granular matter is usually driven with periodic forces or tapping. These perturbations pump energy into the system that is evacuated via friction and introduce a time-scale t_{osc} that is simply the period of the oscillation. How these forces influence the aging properties is much less known and it is the subject of current investigations. For the moment, most of the work in this direction has been numerical [24, 25] and also analytical within the kind of models we shall solve [26] (see [23] for some experimental studies).

The aging properties of relaxing manifolds in random potentials have been found analytically [36] and numerically [37]. The experiment of Portier et al [38] shows aging features in a high- T_c superconductor [39] that are also observed numerically [40, 41]. However, other experimental studies using different protocols have not exhibited these properties [42]. More experiments are needed to get a better understanding of the non-equilibrium relaxation of these systems. An external electric current drives a vortex system in its transverse direction due to Lorentz forces. How the longitudinal and transverse aging properties of the system are modified in the

moving phases is another problem that deserves further study [43]. The comparison between the dynamics of the moving vortex lattice, the tapped dynamics of granular matter and the sheared dynamics of dense liquids is also interesting and begins to be done.

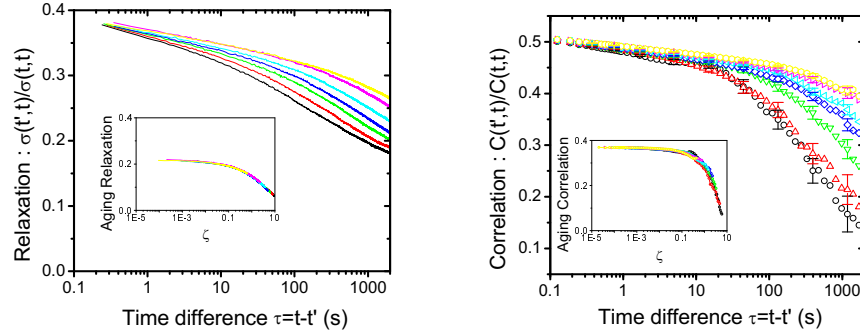


Figure 6: Aging in the thio spinel insulator spin-glass. Decay of the thermoremanent magnetization (left) and correlations between magnetic fluctuations (right). From left to right curves for increasing waiting-times. Inset: scaling. (Curves taken from [32], see [31] and [32] for details.)

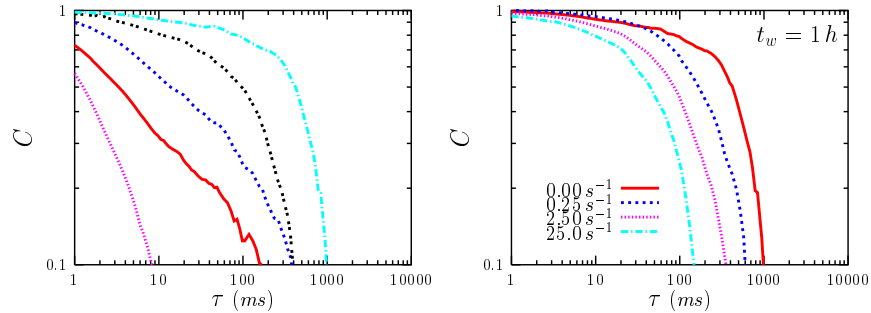


Figure 7: Aging and interrupted aging in laponite. Decay of the correlation function in a relaxing (left) and a sheared (right) sample. In the aging case different curves correspond to increasing waiting-times from left to right, $t_w = 10; 20; 30; 40; 50$ min. (note that the decay occurs for t_w since the waiting-times are rather short and the sample is still very far from equilibrium; cfr. with the results in A. Knaebel et al in [35]). In the sheared case, the sample has been let wait for $t_w = 1$ h, four shear rates, $\dot{\gamma}$, with values indicated in the key were applied at this instant and the decay of the stationary correlation was recorded [44].

2.8 Summary

In this Section we introduced several examples of macroscopic systems that evolve with a slow non-equilibrium macroscopic dynamics. The microscopic dynamics governing the evolution of the constituents of each system is very different. For systems undergoing domain growth and classical glasses, T is the external control parameter that generates fluctuations. For glasses at very low T thermal fluctuations are almost completely irrelevant while quantum fluctuations become important and drive

the dynamics. For granular matter T is again irrelevant and the system's relaxation is due to the external drive. In the elastic systems an underlying ordered structure is visible and may cause important differences in the macroscopic dynamics with respect to other glassy systems where no quasi-order has been identified. A ubiquitous phenomenon in these slowly evolving systems out of equilibrium is (sometimes interrupted) aging or the breakdown of stationarity. Even if all these systems seem to be totally different, a common formalism to study their macroscopic dynamics is now being used and a common picture starts to develop.

In the rest of these lectures we shall explain the main technical tools needed to study simplified models for these real systems. We shall describe the main features of the outcoming scenario making contact with the phenomenology introduced in this Section.

3 Theoretical approach

Besides many phenomenological descriptions of the glass transition and glassy dynamics proposed long ago, recently, several theoretical approaches have been developed. In the following we briefly describe some of the main ones.

Dynamics in the phase space.

The instantaneous configuration of the full system is a point in phase space that moves as time goes on (see the right panel in Fig. 1). In a whole family of models one assumes a free-energy landscape on phase space with wells and barriers and proposes that the point evolution is given by some dynamic prescription on this space. Choosing a convenient distribution and organization of wells and barriers, aging effects are captured by such models. (An average over different systems or over different parts of the same system is implicitly assumed in order to obtain smooth results for the observables.) In "trap models", for instance, each well has an associated trapping-time such that once the system falls in the trap it has to wait this trapping-time to escape from it. A useful choice is a Levy distribution of trapping-times that is not bounded (this is related to assuming that the depth of wells is not bounded from below). The dynamics is such that whenever the point leaves a trap a complete "renewal" takes place in the sense that in the next time step it chooses any trap from the ensemble with equal probability. For simple probability reasons one can prove that at a time t_w after the starting time the system will be trapped in a well with life-time t_w . This model is due to J-P Bouchaud and it leads to aging [45, 46, 47, 48] (for other trap models in the glassy context see [49]).

Domain growth.

A different approach most commonly used to describe the dynamics of spin-glasses assumes that the evolution is driven by the growth of domains of two (or a few) competing phases. The non-equilibrium dynamics is then very similar to ferromagnetic coarsening slowed down by the existence of disorder and/or competing interactions. To obtain concrete predictions one either uses scaling arguments that

lead to the "droplet model" for spin-glasses [50] and its extension to other glassy systems or one solves exactly simple models in low dimensions, typically $d = 1$ [51, 52]. A drawback of this approach is that it has been hard to identify the growing structures in glassy systems.

Kinetic models.

A third approach used to model the dynamics of glasses consists in proposing purely kinetic models with no underlying energy function. The dynamic rules are chosen so as to slow down the dynamics and lead to a dynamic arrest at some critical temperature or density. Interestingly enough some tuning the nature of the constraints these models may behave as strong, fragile or may even show a fragile-to-strong crossover and they can have non-trivial long-lasting nonequilibrium dynamics without having an underlying static transition. Several such models exist, see [51] for a collection of articles on this subject and [53].

Mean-field models.

Many of the recent developments in the understanding of the similarities in the behavior of a priori so different systems as the ones described in Section 2 are based on the analysis of mean-field models. These models are defined by Hamiltonians with long range interactions [e.g. sum over all pairs of spins in Eq. (2.5)] or in infinite dimensions [e.g. take $N \rightarrow \infty$ in Eq. (2.8)]. Sometimes it is convenient to include quenched disordered interactions though this is not necessary.

The static properties of these models are accessible by the usual statistical mechanics analysis complemented by the less standard replica trick when disorder exists [9]. The organization of metastable states or, in other words, the full structure of the relevant Landau-type free-energy landscape, is also accessible with time-independent calculations called trap approach in the context of spin-glass theory [56].

As for dynamics we first have to define how the microscopic variables evolve in time. In classical particle systems Newton equations determine their evolution. In quantum systems Heisenberg equations do the same. Since in realistic situations the systems of interest are in contact with their environments we present the modelization of the coupled systems in Section 4. We show how the effect of the environment translates into noise in both cases. For classical models the elimination of the bath variables leads to Langevin equations. Non-potential forces and vibrations in classical systems are easily included by adding terms to the Langevin equations. Once the microscopic dynamics is given the techniques described in the rest of the notes allow us to solve these schematic models.

These models capture many properties of real systems. Nevertheless, their mean-field character implies many drawbacks. For example, one finds that they have sharp dynamic (with no thermodynamic anomaly) and static transitions at temperatures T_d and T_s , ($T_d > T_s$). The relationship between the dynamic solution and the organization of metastable states in the relevant free-energy landscape can be made precise and it allows us to understand the existence of these two separate transitions. In real systems, however, there is no sharp dynamic transition since T_g is actually a crossover, while T_s might not exist (recall the discussion on T_0 in Section 2.2).

In spite of this and other defects, one of the interests in these models and their solutions is that they have a great power of prediction of so far unknown effects and that they act as a source of inspiration for searching new features in the numerical and experimental study of more realistic models and systems. The rather accurate comparison to numerical simulations [57, 58, 59], and, to the extent of their availability, experiments [31, 60, 61, 62, 32], supports the proposal that the mechanism in these models is similar to the one responsible for the glass transition, and the glassy dynamics, in real materials. Indeed, there is growing consensus in that they provide an exaggerated realization of the actual glassy phenomenon. It is worth mentioning too that some of the features found in the mean-field models that we shall explain below have also been analysed within the other approaches mentioned above.

In the following we present the asymptotic analytic solution to this family of models. Some of the ingredients missing in their full analytic solution, that would render their description of real materials more accurate, have been identified (analysis of the dynamics in time-scales that diverge with N , description of dynamic heterogeneities, etc.). For the moment, their complete analytical treatment has proven too difficult but some recent articles report partial success and suggest interesting ways to follow up. We shall come back to these issues in the Conclusions and Perspectives.

4 Systems in contact with environments

In the typical experimental protocols discussed in Section 1 one quenches the sample and subsequently follows its evolution in time. Once arrived at the final point in parameter space, if no external forces are applied, the system relaxes and its energy density decreases towards an asymptotic value. Hence, the system is not isolated, but in contact with an environment that acts as a source of dissipation. The system plus environment is "closed" while the system alone is "open". The first question to answer is how to model the coupled classical and quantum system.

4.1 Modeling the coupled system

The nature of the environment, e.g. whether it can be modeled by a classical or a quantum ensemble, depends on the problem under study. The choice of the coupling between system and environment is determined by the symmetry properties of the system and by physical intuition. Weiss' textbook [63] has a very complete description of this problem. We here explain the main ingredients of the modelization. The generic problem we want to study is

$$H_{\text{tot}} = H_{\text{syst}} + H_{\text{env}} + H_{\text{int}} + H_{\text{counter}} : \quad (4.1)$$

Until otherwise stated, we focus on a single particle coupled to an environment. H_{syst} is the Hamiltonian of the isolated particle, $H_{\text{syst}} = \frac{p^2}{2M} + V(q)$, with p and q its momentum and position. H_{env} is the Hamiltonian of a thermal bath

that, again for simplicity, we take to be an ensemble of N independent harmonic oscillators

$$H_{\text{env}} = \sum_{a=1}^{N_b} \frac{1}{2m_a} \dot{x}_a^2 + \frac{m_a \omega_a^2}{2} x_a^2 : \quad (4.2)$$

This is indeed a very usual choice since, for example, it may represent phonons. H_{int} is the coupling between system and environment. We restrict the following discussion to an interaction that is linear in the oscillator and particle coordinates, $H_{\text{int}} = q \sum_{a=1}^{N_b} c_a x_a$, with c_a the coupling constants. The calculations can be easily generalized to an interaction with a more complicated dependence on the system's coordinate, $F(q)$, that may be dictated by the symmetries of the system. We discuss the last term, H_{counter} , below.

4.1.1 Statics

Classical problems

Let us first show how the static properties of a classical system are modified by its interaction with a classical thermal bath. If the coupled system is in equilibrium, it is described by a partition function given by a sum over the combined phase space of the system and environment. Having chosen a bath of harmonic oscillators, the integration over the bath variables can be readily performed; this calculation yields the reduced partition function that is written as an integration over the phase space of the system only. One can easily prove that the mass of the system gets (negatively) renormalized due to the coupling to the environment [64]. Therefore one introduces the counter-term

$$H_{\text{counter}} = \frac{1}{2} \sum_{a=1}^{N_b} \frac{c_a^2}{m_a \omega_a^2} q^2 \quad (4.3)$$

in such a way to eliminate the mass renormalization and to recover the partition function of the isolated system.

Quantum problems

If one includes quantum fluctuations to describe the system and environment, the situation is slightly more complex. The relevant quantity to study is the density matrix of the full system that, for instance, can be represented as a path integral on imaginary time [65]. The contribution of the environment to the effective action is quadratic and its variables can be integrated away to yield a reduced density matrix. As opposed to the classical case, the interaction with the reservoir not only induces a (negative) mass renormalization but it also generates a retarded quadratic interaction

$$Z_h = \int_0^Z d^0 x(\tau) K(\tau, 0) x(0) \quad (4.4)$$

controlled by the kernel

$$K(\tau) = \frac{2}{\hbar} \sum_{n=1}^{\infty} \frac{\omega_n^2}{\omega_n^2 + \tau^2} \exp(i\omega_n \tau); \quad (4.5)$$

with ω_n the Matsubara frequencies, $\omega_n = 2\pi n/\hbar$, n an integer in $(-1; 1)$ and $I(\omega)$ the spectral density of the bath,

$$I(\omega) = \frac{1}{2} \sum_{a=1}^N \frac{c_a^2}{m_a \omega_a} \delta(\omega - \omega_a); \quad (4.6)$$

that is a smooth function of ω usually taken to be $I(\omega) = \gamma \omega^s \exp(-\omega/\omega_s)$; with the "friction coefficient", γ a constant, ω_s a high frequency cut-off and s a parameter that characterizes different baths: $s = 1$ is Ohmic (and leads to the usual white noise when $\omega_s \rightarrow \infty$), $s > 1$ is super-Ohmic and $s < 1$ is sub-Ohmic. As in the classical case, one includes a counter-term to cancel the mass renormalization but the retarded interaction (4.4) cannot be eliminated.

4.1.2 Dynamics

The distinction between the effect of a reservoir on the statistic properties of a classical and a quantum system is absent from a full dynamic treatment where the coupling to the environment always leads to a retarded interaction. In classical problems one generally argues that the retarded interaction can be simply replaced by a local one, i.e. one uses white noises, if long enough time-scales are explored. In quantum problems the same simplification is not justified in general.

Classical problems

The dissipative dynamics of a classical system in contact with an environment is usually described by a phenomenological Langevin equation. If the system is simply given by a particle of mass M , whose position is denoted by q , this equation reads

$$M \ddot{q}(t) + \int_0^t \gamma(t-\tau) \dot{q}(\tau) d\tau = -V'(q(t)) + \xi(t) \quad (4.7)$$

$$\langle \xi(t) \xi(\tau) \rangle = k_B T \gamma(t-\tau) \quad (4.8)$$

where $\gamma(t-\tau)$ is a retarded friction and $\xi(t)$ is a time-dependent Gaussian random force with zero mean and correlation given by Eq. (4.8). We adopt angular brackets to denote averages over the noise.

The Langevin equation was first introduced in the context of Brownian motion and later used in a variety of problems with dissipation. It can be derived from the coupled system defined in Eq. (4.1) [66, 63] (see Appendix A). Indeed, if one assumes that the initial coordinates and momenta of the oscillators have a canonical distribution at an inverse temperature β [shifted by the coupling to the particle $x_a(0) \rightarrow x_a(0) - q = (m_a \omega_a^2)^{-1} q(0)$], Newton's equation for the evolution of the particle becomes Eq. (4.7). The random nature of the force is due to the randomness in the initial values of the position and momenta of the oscillators. The use of an equilibrium measure for the distribution of the oscillators implies the invariance under time translations of the friction kernel, $\gamma(t-\tau)$, and its relation to the noise-noise correlation in Eq. (4.8). The latter is a fluctuation-dissipation theorem that holds for the bath variables (see Appendix A and Section 7). Different forms of

$\langle \epsilon(t, t_0) \rangle$ can be generated by different choices of the ensemble of oscillators. Typically, the decay of $\langle \epsilon(t, t_0) \rangle$ occurs in a finite relaxation time, τ . When the minimum observation time is of the order of or shorter than τ one has a "colored noise". Instead, when it is much longer than τ , any time difference satisfies $t - t_0 \gg \tau$ and the kernel can be approximated with a delta function $\langle \epsilon(t, t_0) \rangle \approx 2\tau \delta(t - t_0)$, which corresponds to a white noise. For the classical problems we shall deal with the white-noise approximation is adequate.

Once the Langevin equation has been established on a firmer ground, it can be used as a starting point to study the dynamics of more complicated classical systems in contact with classical environments. The description of the dynamics of a macroscopic system with dissipation is then given by N coupled Langevin equations with N the number of dynamic degrees of freedom. (In this case one usually couples an independent set of oscillators to each microscopic variable of the system, other choices lead to more complicated equations.) Time-dependent, $f_i(t)$, and constant non-potential forces, f_i^{np} , as the ones applied to granular matter and in rheological measurements are simply included as part of the deterministic force. In the white noise limit

$$M \ddot{q}_i(t) + \gamma \dot{q}_i(t) = -\frac{\partial V(q)}{\partial q_i(t)} + f_i(t) + f_i^{np} + \xi_i(t); \quad (4.9)$$

$$\langle \xi_i(t) \xi_j(t_0) \rangle = 2\gamma k_B T \delta_{ij} \delta(t - t_0); \quad (4.10)$$

A continuous Langevin equation for classical spins is usually written replacing the hard Ising constraint $s_i = \pm 1$ by a soft one implemented with a potential term of the form $V(s_i) = u(s_i^2 - 1)^2$ with u a coupling strength that one eventually takes to infinity. The soft spins are continuous unbounded variables $s_i \in (-\infty, \infty)$ but the potential energy favors the configurations with s_i close to ± 1 . Even simpler models are constructed with spherical spins, that are also continuous variables globally constrained to satisfy $\sum_{i=1}^N s_i^2 = N$.

Quantum problems

Even if several attempts to write down quantum versions of the Langevin equation appeared in the literature, these methods remain very much model dependent and difficult to generalize [63]. A more convenient way to analyze the dynamics of a coupled system and environment with quantum fluctuations is the functional Schwinger-Keldysh formalism. We postpone the discussion of the effect of the quantum reservoir on the quantum system to Section 8 where we introduce this formalism. In short, the effect of the environment is to introduce retarded terms in the dynamic action that are similar to the ones in Eq. (4.4) but in real time. The white approximation is not acceptable and one is forced to keep the non-local in time kernels.

5 Observables and averages

As usual in statistical and quantum mechanics meaningful quantities are averaged observables. For an equilibrated system, due to ergodicity, one can either take

an ensemble average or an average over a sufficiently long time-window. Out of equilibrium these do not coincide in general. In this Section we define averaging procedures for classical and quantum problems out of equilibrium and we set the notation used in the rest of the notes.

5.1 Classical systems

The interaction with the environment induces fluctuations and the Langevin equation is solved in a probabilistic sense,

$$q_k^{\text{sol}}(t) = F[(\zeta_k); q_0; t] : \quad (5.1)$$

The index k labels different realizations of the thermal history, i.e. different realizations of the noise at each instant. q_0 is the initial condition $q_0 = q(0)$ and (ζ_k) encodes all noise values in the interval $[0; t]$. We discretize time, $t_a = a$ with the time spacing and $a = 0; 1; \dots$. The total time is $t = T$. We shall be interested in the limit $T \rightarrow \infty$ and $\Delta t \rightarrow 0$ with t fixed. Equation (5.1) means that there is a different solution for each noise history.

Any one-time functional of q , $A[q](t)$, must be averaged over all histories of the thermal noise to obtain a deterministic result

$$\langle A[q](t) \rangle = \lim_{N \rightarrow \infty} \frac{1}{N} \sum_{k=1}^N A[q_k^{\text{sol}}](t) P(\zeta_k) = \int D\zeta P(\zeta) A[q^{\text{sol}}](t) : \quad (5.2)$$

N is the number of noise realizations. $P(\zeta_k)$ is the probability distribution of the k -th thermal history. For a Gaussian noise

$$P(\zeta_k) \propto \exp \left[-\frac{1}{2k_B T} \sum_{a,b} \zeta_k(t_a) \zeta_k(t_b) \right] : \quad (5.3)$$

The measure of the functional integral is just $D\zeta = \prod_a d\zeta(t_a)$.

Two-time functions characterize the out of equilibrium dynamics in a more detailed way and they are defined as

$$C_{AB}(t; t^0) = \langle A[q](t) B[q](t^0) \rangle = \int D\zeta P(\zeta) A[q^{\text{sol}}](t) B[q^{\text{sol}}](t^0) : \quad (5.4)$$

The observable $B[q]$ is measured at time t^0 , the observable $A[q]$ is measured at time t for each noise realization and the average is taken afterwards.

The instantaneous linear response is also a two-time function. Imagine that q represents the position of a Brownian particle that one kicks with a weak perturbing force at time $t^0 = t_a$ (see Fig. 8). The subsequent position of the particle is modified by the perturbation. The linear response is given by the comparison of the perturbed dynamics with the unperturbed one, in which no force has been applied, up to linear order in the perturbation:

$$R_{AB}(t; t^0) = \frac{\langle A[q](t) \rangle - \langle A[q](t) \rangle_{h_B=0}}{h_B(t^0)} : \quad (5.5)$$



Figure 8: Left: an instantaneous perturbation applied at t_a . Right: a step perturbation applied at t_a and held constant for all subsequent times.

The subindex B indicates that the perturbation applied at t^0 is conjugated to the observable $B[q]$ when the Hamiltonian is modified as $H \rightarrow H + h_B B[q]$. The subindex A indicates that we examine how the observable $A[q]$ at time t reacts to the perturbation. At the end of the calculation we set $h_B = 0$ to extract the linear response. Keeping $h_B \neq 0$ yields information about the nonlinear terms in the response function. For causal systems the response function vanishes if $t^0 > t$.

In future Sections we shall be interested in the integrated linear response rather than the instantaneous one. This quantity represents the linear response of the system to a step-like perturbation of duration $t - t^0$ that starts at t^0 , as represented on the right panel of Fig. 8:

$$R_{AB}(t; t^0) = \int_{t^0}^t dt^0 R_{AB}(t; t^0) : \quad (5.6)$$

Rather often results are presented in the frequency domain. One defines the Fourier transform and its inverse

$$\tilde{A}(\omega) = \int_{-\infty}^{\infty} dt \exp(-i\omega t) A(t); \quad A(t) = \int_{-\infty}^{\infty} \frac{d\omega}{2\pi} \exp(i\omega t) \tilde{A}(\omega) : \quad (5.7)$$

For a stationary process, the linear susceptibility, $\tilde{\chi}_{AB}(\omega)$, is simply given by the Fourier transform of the linear response (5.5). However $R_{AB}(t; t^0)$ is not necessarily stationary out of equilibrium. Hence, we define two generalized linear susceptibilities,

$$\tilde{\chi}_{AB}^{(1)}(\omega; t^0) = \int_{t^0}^{\infty} dt \exp(-i\omega t) R_{AB}(t^0 + t; t^0); \quad (5.8)$$

$$\tilde{\chi}_{AB}^{(2)}(\omega; t) = \int_{-\infty}^{\infty} dt^0 \exp(-i\omega t^0) R_{AB}(t; t^0); \quad (5.9)$$

that reduce to the well-known expression for $\tilde{\chi}_{AB}(\omega)$ in a stationary system. Note that in the first line we kept the shorter time t^0 fixed while in the second line we kept the longer time t fixed. These expressions have a real and an imaginary part that yield the in-phase ($\tilde{\chi}^{(0)}$) and the out-of-phase ($\tilde{\chi}^{(1)}$) susceptibilities, respectively. The integrations run over positive values of t only due to causality.

Up to this point we have discussed the simple case in which observables only depend on time. More generally, one is interested in extending the above definitions to field theories. In the context of liquids, glasses, etc. the generic observables A

and B depend on the positions and momenta of the particles. A key quantity is the density $\rho(\mathbf{r};t) = \frac{1}{N} \sum_{i=1}^N \delta(\mathbf{r} - \mathbf{r}_i(t))$, where \mathbf{r} is a d -dimensional vector in real space and \mathbf{r}_i are the positions of the N particles in the system. From the density-density correlator $N^{-1} G(\mathbf{r};t; \mathbf{r}^0; t^0) = \frac{1}{N} \langle \rho(\mathbf{r} + \mathbf{r}^0; t) \rho(\mathbf{r}^0; t^0) \rangle$ one defines the more useful van Hove correlator $G_{vh}(\mathbf{r};t; \mathbf{r}^0; t^0) = \frac{1}{N} \int d^d r^0 G(\mathbf{r};t; \mathbf{r}^0; t^0)$, that measures the probability of finding a particle i within a volume $d^d r$ around the point \mathbf{r} at time t given that there was a particle j at the origin at time t^0 . The normalization factor fixes the number of particles, $\int d^d r G_{vh}(\mathbf{r};t) = N$. The density-density and van Hove correlators can be naturally separated in two contributions, a self and a distinct part. In the former, one adds over equal particles only while in the latter one adds over distinct particles. The two-time intermediate scattering function is constructed with the components of the real-space Fourier transform of the density at different times: $N^{-1} F(\mathbf{k};t; t^0) = \langle \rho(\mathbf{k};t) \rho(\mathbf{k};t^0) \rangle = \langle \rho(\mathbf{k};t) \rho(-\mathbf{k};t^0) \rangle$. When times are equal one recovers the structure factor, $S(\mathbf{k};t) = F(\mathbf{k};t;t)$ that at long times approaches a limit $S(\mathbf{k};t) \rightarrow S(\mathbf{k})$ even for glassy systems.

The two-time intermediate scattering function is measurable via neutron scattering. Indeed, one can easily extend the proof described e.g. in [67] to the non-equilibrium case, to show that the cross-section per nucleus is related to the intermediate scattering function. This relation suggests to call the self and distinct correlators, incoherent and coherent ones, respectively. Many times, one defines the correlators of the local density fluctuations, $\rho(\mathbf{r};t) - \bar{\rho}(t) = \rho(\mathbf{r};t) - \frac{1}{V} \int d^d r' \rho(\mathbf{r}';t)$. The modification of the correlations defined above follow straightforwardly. A detailed description of the properties of these correlations in an equilibrated liquid can be found in [67].

Up to now we have only discussed one-point and two-point functions. In general problems, higher order functions are not trivially related to the previous ones and bear richer information. These are four-point functions, $\langle A(t) B(t^0) C(t^0) D(t^0) \rangle$, or any other form of a more general type. In most of the solvable models we shall discuss below, and in most of the approximations used to analyze realistic models, higher-order functions do not appear. The reasons for their disappearance are manifold. In simplified models one can simply prove that higher order functions are exactly given in terms of one and two-point functions. In more realistic cases, higher order functions are approximated with expressions that depend on one and two-point functions only. This is done, for instance, in Gaussian approximations and mode-coupling theory. However, a complete solution to a finite dimensional model should be able to predict the behavior of such higher order correlations.

5.2 Quantum problems

A quantum mechanical operator, \hat{A} , in the Heisenberg representation evolves according to

$$\hat{A}(t) = \exp \left(\frac{iHt}{\hbar} \right) \hat{A}(0) \exp \left(-\frac{iHt}{\hbar} \right) \quad (5.10)$$

Ensemble averages are defined as $\langle \hat{A}(t) \rangle = \text{Tr} \hat{A}(t) \hat{\rho}(0) = \text{Tr} \hat{A}(0) \hat{\rho}(t)$, where $\hat{\rho}(0)$ is the initial density operator and the trace is defined in the usual way, $\text{Tr}[\hat{A}] = \text{Tr}[\hat{A} \hat{1}]$.

$P_{ij} = \langle j | i \rangle$, with f, g an orthonormal basis in Fock space. The normalization factor is the partition function $Z = \text{Tr} \hat{\rho}(0)$. Two-time dependent correlation functions are introduced as $\langle \hat{A}(t) \hat{B}(t^0) \rangle = Z^{-1} \text{Tr} \hat{A}(t) \hat{B}(t^0) \hat{\rho}(0)$. Clearly $\langle \hat{A}(t) \hat{B}(t^0) \rangle \neq \langle \hat{B}(t^0) \hat{A}(t) \rangle$ and one can define symmetrized and anti-symmetrized correlations:

$$C_{fA, gB}(t; t^0) = \frac{1}{2} \langle \hat{A}(t) \hat{B}(t^0) + \hat{B}(t^0) \hat{A}(t) \rangle; \quad (5.11)$$

$$C_{[A, B]}(t; t^0) = \frac{1}{2} \langle \hat{A}(t) \hat{B}(t^0) - \hat{B}(t^0) \hat{A}(t) \rangle; \quad (5.12)$$

respectively. The linear response and the integrated linear response are defined just as in the classical case, see Eqs. (5.5) and (5.6). In linear response theory, in and out of equilibrium, $R_{AB}(t; t^0)$ and the anti-symmetrized correlation $C_{[A, B]}(t; t^0)$ are related by the Kubo formula [68] (see Appendix B)

$$R_{AB}(t; t^0) = \frac{i}{\hbar} \langle [\hat{A}(t); \hat{B}(t^0)] \rangle = \frac{2i}{\hbar} \langle C_{[A, B]}(t; t^0) \rangle; \quad (5.13)$$

5.3 Average over disorder

Time independent quenched random forces and interactions exist in some of the models and systems that we study. We shall be mostly interested in quantities averaged over the distribution of disorder that we denote with square brackets $\langle \dots \rangle$.

Averaging over disorder is a delicate matter when one wishes to compute static properties. For instance, one has to resort to the sometimes contested replica trick [69]. We shall see in Section 8 that in a full dynamic treatment with no special initial conditions there is no need to introduce replicas and the formalism is totally free from ambiguities.

6 Time dependent probability distributions

In Section 4 we derived a Langevin equation with white noise as the microscopic dynamic equation controlling the evolution of the classical problems we shall study. In this Section we prove some properties of the equilibrium dynamics of classical models with dynamics given by these equations. One can simply modify this proof for a generic Markov process, a classical problem with colored noise and a quantum model.

6.1 The Fokker-Planck and Kramers equations

The Fokker-Planck and Kramers equations are particular master equations that hold exactly for a Langevin process with white noise. The probability distribution of the thermal noise, $P(\dots)$, induces a time-dependent probability distribution of the dynamic variables q and v (or $p = v/M$):

$$P(q; v; t) = \int \mathcal{D} P(\dots) q \dot{q}^{\text{sol}}(t) v \dot{v}^{\text{sol}}(t); \quad (6.1)$$

that satisfies the Kramers equation

$$\frac{\partial P(q;v;t)}{\partial t} = \frac{\partial}{\partial q} (vP(q;v;t)) + \frac{\partial}{\partial v} \left[v + \frac{V^0(q)}{M} + \frac{k_B T}{M} \frac{\partial}{\partial v} \right] P(q;v;t) : \quad (6.2)$$

For colored noises one cannot derive a simple differential equation for $P(q;v;t)$; indeed, it is clear that in these cases the stochastic process is not Markovian. The averages over them all histories can be expressed in terms of $P(q;v;t)$, $\langle A[q;v] \rangle(t) = \int_{-\infty}^{\infty} \int_{-\infty}^{\infty} A[q;v] P(q;v;t) dq dv$.

When the inertial term in the Langevin equation can be dropped, $P(q;v;t)$ is replaced by an exclusive function of q , $P(q;t)$, defined as

$$P(q;t) = \int_{-\infty}^{\infty} dv P(q;v;t) \quad (6.3)$$

and determined by the Fokker-Planck equation,

$$\frac{\partial P(q;t)}{\partial t} = \frac{\partial}{\partial q} [P(q;t) V^0(q)] + k_B T \frac{\partial^2}{\partial q^2} P(q;t) : \quad (6.4)$$

It is very important to note that the balancing of factors on the right-hand-side (rhs) of the Fokker-Planck and the Kramers equations is a direct consequence of the equilibration of the noise (see Appendix A). This relation is known under the name of Einstein relation or fluctuation-dissipation theorem of the second kind (according to Kubo). We shall see its implications below.

6.2 Approach to equilibrium

In this Section we focus, for simplicity, on the Fokker-Planck equation (6.4). In order to ensure the equilibration of the system at long times P_{gb} must be a stationary solution of the Fokker-Planck equation. Introducing $P / \exp(-V)$ in Eq. (6.4) one realizes that any other ratio between the factors in front of the first and second term on the rhs of the Fokker-Planck equation would not allow for this asymptotic solution.

We still have to show that P_{gb} is the actual asymptotic solution reached by the dynamic process, $\lim_{t \rightarrow \infty} P(q;t) = P_{gb}$. An easy and elegant proof relies on a mapping between the Fokker-Planck and the Schrodinger equations [68]. Introducing

$$P(q;t) = \psi_0(q) p(q;t) = c e^{-\beta V(q)} p(q;t) \quad (6.5)$$

with c a positive constant, one has

$$\frac{\partial p(q;t)}{\partial t} = -k_B T \frac{\partial^2}{\partial q^2} p(q;t) - \frac{1}{2} V''(q) p(q;t) + \frac{1}{4} (V'(q))^2 p(q;t) = H_{fp} p(q;t) : \quad (6.6)$$

This is a Schrodinger equation in imaginary time. Note however that $p(q;t)$ here is a probability density and plays the role of a wave function while in true quantum mechanics it is the modulus squared of the wave function which has a probability

interpretation. If the term between square brackets grows to infinity sufficiently fast when $q \rightarrow \pm 1$ the spectrum of the Fokker-Planck Hamiltonian H_{fp} is discrete. It is now easy to check that $\phi_0(q)$ is the ground state of H_{fp} , i.e. a positive definite eigenvector with eigenvalue $E_0 = 0$. We write $p(q;t) = \sum_n c_n \phi_n(q) \exp(-E_n t)$ with $\phi_n(q)$ the eigenvector associated to the eigenvalue E_n , $E_n > 0$ when $n > 0$. When $t \rightarrow \infty$ all terms vanish apart from the one with $n = 0$, $\lim_{t \rightarrow \infty} p(q;t) = c_0 \phi_0(q) = \phi_0(q)$, where we used $c_0 = \int_{\mathbb{R}} dq \phi_0(q) p(q;0) = \int_{\mathbb{R}} dq p(q;0) = 1$. This expression implies $\lim_{t \rightarrow \infty} P(q;t) = \phi_0^2(q) = c^2 \exp(-2V(q))$ and the conservation of probability allows one to compute the normalization constant, $c^{-2} = \int_{\mathbb{R}} dq \exp(-2V(q))$. Thus P_{gb} is indeed the asymptotic solution to the Fokker-Planck equation [68].

Note that this argument assumes that a sufficiently long t ($t > t_{eq}$) is reached such that only the $n = 0$ term survives in the sum. This hypothesis does not hold in the asymptotic analysis for the relaxing models we analyze in the next Sections. In the low- T phase the equilibration time grows with the size of the system, $t_{eq}(N) \rightarrow \infty$, while in the analysis we only consider times that are finite with respect to N . Moreover, when non-potential or time-dependent forces are exerted on the system, see Eq. (4.9), the transformation (6.5) is not sufficient to deal with their effect and equilibrium cannot be established.

Just as in usual quantum mechanics one can use an operator notation to represent the Fokker-Planck equation. Indeed, identifying $\partial/\partial q$ with the operator \hat{p} the usual commutation relations between momentum and coordinate are recovered. The probability distribution $P(q;t)$ is then identified with a quantum time-dependent "state" $|\mathcal{P}(t)\rangle$. With these new names, the Fokker-Planck equation reads

$$\frac{\partial |\mathcal{P}(t)\rangle}{\partial t} = \hat{H}_{fp} |\mathcal{P}(t)\rangle \quad \text{with} \quad \hat{H}_{fp} = \hat{p} \hat{V}^0(q) - k_B T \hat{p}^2 \quad (6.7)$$

$|\mathcal{P}(t)\rangle$ is obtained from the evolution of an initial state $|\mathcal{P}(0)\rangle$ with the operator $\exp(-\hat{H}_{fp} t)$.

6.3 Equilibrium dynamics

All average values (5.2) can be computed using $P(q;t)$ as $\langle A[q](t) \rangle = \int_{\mathbb{R}} dq A[q] P(q;t)$. If we pursue the identification with the quantum mechanics formulation and we associate the bra $\langle j|$ to the "wave function" identical to 1 we write the average as $\langle A[q](t) \rangle = \langle \hat{A}[q] |\mathcal{P}(t)\rangle$. The normalization of the probability distribution reads $\langle \hat{1} |\mathcal{P}(t)\rangle = 1$. Clearly, if the system reached equilibrium at a time t_0 , all averages of one-time quantities are time-independent henceforth.

Any correlation $C_{AB}(t; t^0)$ for two "local" functions of the variable q can be expressed as

$$\begin{aligned} C_{AB}(t; t^0) &= \int_{\mathbb{R}} dq \int_{\mathbb{R}} dq^0 \int_{\mathbb{R}} dq^0 A[q] T(q^0; t^0 | q; t) B[q^0] T(q^0; 0 | q^0; t^0) P(q^0; 0) \\ &= \langle \hat{A}[q] \exp(-\hat{H}_{fp}(t - t^0)) \hat{B}[q] \exp(-\hat{H}_{fp} t^0) |\mathcal{P}(0)\rangle \quad (6.8) \end{aligned}$$

In the transition probabilities, T , we included the time-dependence to clarify their meaning. In the second line we used the quantum mechanical notation. If the time

t^0 is longer than the equilibration time, the probability density at t^0 reached the equilibrium one, $\text{Tr} \rho(t^0) = \text{Tr} \rho(0) = P_{\text{gb}}(\mathbf{q}^0)$. Equivalently, $\langle \mathcal{B}(t^0) \rangle = \langle \mathcal{B} \rangle$. Two properties follow immediately:

Stationarity: Since the transition probability is a function of the time-difference only, $T(\mathbf{q}; t; \mathbf{q}^0; t^0) = T(\mathbf{q}; \mathbf{q}^0; t - t^0) = \langle \mathcal{A} \rangle \exp(-\hat{H}_{\text{fp}}(t - t^0))$ the correlation is invariant under translations of time for $t^0 > t_{\text{eq}}$.

Onsager relations: $\langle \mathcal{A}[\mathbf{q}](t) \mathcal{B}[\mathbf{q}](t^0) \rangle = \langle \mathcal{A}[\mathbf{q}](t^0) \mathcal{B}[\mathbf{q}](t) \rangle$ for any two observables \mathcal{A} and \mathcal{B} that depend only on the coordinates. Indeed,

$$\begin{aligned} \langle \mathcal{A}(t^0) \mathcal{B}(t) \rangle &= \langle \mathcal{A} e^{\hat{H}_{\text{fp}}(t - t^0)} \mathcal{B} \rangle_{\text{gb}} = \langle \mathcal{A} e^{\hat{H}_{\text{fp}}(t - t^0)} \mathcal{B} \rangle_{\text{gb}} \\ &= \langle \mathcal{A} e^{\hat{H}_{\text{fp}}(t - t^0)} \mathcal{B} \rangle_{\text{gb}} = \langle \mathcal{A} e^{\hat{H}_{\text{fp}}(t - t^0)} \mathcal{B} \rangle_{\text{gb}} \\ &= \langle \mathcal{A} e^{\hat{H}_{\text{fp}}(t - t^0)} \mathcal{B} \rangle_{\text{gb}} : \end{aligned} \quad (6.9)$$

The proof is completed by showing that $e^{\hat{H}_{\text{fp}}(t - t^0)} e^{\hat{V}} = e^{\hat{H}_{\text{fp}}(t - t^0)}$ for all $t - t^0$ which is equivalent to $\hat{H}_{\text{fp}} = e^{\hat{V}} \hat{H}_{\text{fp}} e^{-\hat{V}}$. The latter can be checked directly using the Fokker-Planck Hamiltonian. The matrix elements $\langle \mathbf{q}; t | \hat{H}_{\text{fp}} | \mathbf{q}^0; t^0 \rangle = T(\mathbf{q}; t | \mathbf{q}^0; t^0)$ and $\langle \mathbf{q}; t | \hat{H}_{\text{fp}} | \mathbf{q}^0; t^0 \rangle = T(\mathbf{q}; t | \mathbf{q}^0; t^0)$ yield the transition probabilities and the first equation in this paragraph can be recast as $T(\mathbf{q}; t | \mathbf{q}^0; t^0) e^{-\hat{V}(\mathbf{q})} = T(\mathbf{q}; t | \mathbf{q}^0; t^0) e^{-\hat{V}(\mathbf{q})}$ which is detailed balance.

Similarly, one proves that the linear response $R_{\text{AB}}(t; t^0)$ is also stationary when $P(\mathbf{q}^0; t^0) = P_{\text{gb}}(\mathbf{q}^0)$. We represent the instantaneous infinitesimal perturbation $h(t^0)$ as the kick between $t_a = -2$ and $t_b = 2$ in Fig. 8-left. The Fokker-Planck Hamiltonian in the presence of the field is $\hat{H}_{\text{fp}}^h = \hat{H}_{\text{fp}} + h \hat{B}[\mathbf{q}] + k_B T \hat{H}_{\text{fp}}$ while \hat{H}_{fp} is the Fokker-Planck operator in no field. The average in a field reads

$$\langle \mathcal{A}[\mathbf{q}](t) \rangle_h = \langle \mathcal{A}[\mathbf{q}] e^{\hat{H}_{\text{fp}}(t - t^0)} e^{\hat{H}_{\text{fp}}^h(t^0 - t^0)} e^{\hat{H}_{\text{fp}}(t^0 - t^0)} \rangle_{\text{gb}} : \quad (6.10)$$

and the variation with respect to h yields

$$\frac{\langle \mathcal{A}[\mathbf{q}](t) \rangle_h}{\langle \mathcal{A}[\mathbf{q}](t) \rangle} = \langle \mathcal{A}[\mathbf{q}] e^{\hat{H}_{\text{fp}}(t - t^0)} \frac{\hat{H}_{\text{fp}}^h - \hat{H}_{\text{fp}}}{h} e^{\hat{H}_{\text{fp}}(t^0 - t^0)} \rangle_{\text{gb}} : \quad (6.11)$$

with $h = h$. The factor between parenthesis equals $(\hat{H}_{\text{fp}}^h - \hat{H}_{\text{fp}}) e^{\hat{H}_{\text{fp}}(t^0 - t^0)} = \hat{H}_{\text{fp}}^h e^{\hat{H}_{\text{fp}}(t^0 - t^0)}$. Taking the limit $h \rightarrow 0$ and evaluating at $h = 0$ one has

$$R_{\text{AB}}(t; t^0) = \langle \mathcal{A}[\mathbf{q}] e^{\hat{H}_{\text{fp}}(t - t^0)} (\hat{B}[\mathbf{q}] - \langle \hat{B}[\mathbf{q}] \rangle) e^{\hat{H}_{\text{fp}}(t^0 - t^0)} \rangle_{\text{gb}} : \quad (6.12)$$

From this expression one recovers several properties of the response:

Causality: The same derivation for $t^0 > t$ yields

$$R_{\text{AB}}(t; t^0) = \langle \mathcal{B}[\mathbf{q}] e^{\hat{H}_{\text{fp}}(t - t^0)} (\hat{A}[\mathbf{q}] - \langle \hat{A}[\mathbf{q}] \rangle) e^{\hat{H}_{\text{fp}}(t^0 - t^0)} \rangle_{\text{gb}} : \quad (6.13)$$

Since $\langle \mathcal{B} \rangle = 0$, $R(t; t^0) = 0$ for all $t < t^0$.

Stationarity: When $\langle \mathcal{A} \rangle = \langle \mathcal{B} \rangle = 0$ one has

$$R_{\text{AB}}(t; t^0) = \langle \mathcal{A}[\mathbf{q}] e^{\hat{H}_{\text{fp}}(t - t^0)} (\hat{B}[\mathbf{q}] - \langle \hat{B}[\mathbf{q}] \rangle) \rangle_{\text{gb}} = R_{\text{AB}}^{\text{st}}(t - t^0) : \quad (6.14)$$

Response at equal times: $\lim_{t \rightarrow t^0} R_{AB}(t; t^0) = \hbar^{-1} \langle \hat{A}^0[q] \hat{B}^0[q] \exp(-\hat{H}_{fp} t^0) \rangle$.
 If $\hat{A}[q] = \hat{B}[q] = \hat{q}$ then $\hat{A}^0[q] = \hat{B}^0[q] = 1$ and $\lim_{t \rightarrow t^0} R_{AB}(t; t^0) = \hbar^{-1} \langle \hat{q}^2 \rangle = 1$ from conservation of probability.

Fluctuation-dissipation theorem: We postpone its discussion to Section 7.2.

Onsager relations: Using the relation between correlation and responses dictated by the fdt one finds that the Onsager relations must also hold between responses.

7 The fluctuation-dissipation theorem (fdt)

The fluctuation-dissipation theorem (fdt) relates the correlations of spontaneous fluctuations to the induced fluctuations in equilibrium. It is a model independent relation between the linear response and its associated correlation function that takes different forms for classical and quantum system. The latter reduces to the former when quantum fluctuations become irrelevant. In this Section we present several proofs of the fdt. When the equilibration hypothesis is not justified, this relation does not necessarily hold.

7.1 Static fdt

Many relations between correlations of fluctuations and susceptibilities are known in statistical mechanics. All these are different statements of the static fdt.

Take for instance a perfect gas. The fluctuations in the density $\rho = n/V$ where n is the number of particles within a sub volume V of a system with N particles and volume V , are defined as: $\delta \rho = (\rho - \langle \rho \rangle)$. In the thermodynamic limit $N \rightarrow \infty$; $V \rightarrow \infty$ with $N/V = \rho$ fixed, these are related to the isothermal compressibility $\chi_T = -1/V \partial V / \partial P$ via $\langle \delta \rho^2 \rangle = (k_B T)^{-1} \chi_T / V$. This relation is a form of fdt.

For a system in equilibrium with a thermal reservoir at temperature T one has

$$\frac{\hbar \langle \delta A^2 \rangle}{\hbar} = \hbar \langle (\delta A - \delta A_i)^2 \rangle \quad (7.1)$$

for any observable A . The average $\langle \delta A^2 \rangle$ is calculated with the partition function of the system in the presence of a small field coupled to A in such a way that the Hamiltonian reads $H = H_0 - \hbar A$. For a magnetic system this equation relates the magnetic susceptibility to the magnetization fluctuations.

7.2 Dynamic fdt

There are several proofs of this theorem. Here we focus on a Fokker-Planck process. In Section 6.3 we computed R_{AB} and C_{AB} in equilibrium. Taking the derivative of Eq. (6.8) with respect to t^0 one finds

$$\begin{aligned} \frac{\partial C_{AB}(t-t^0)}{\partial t^0} &= \hbar \langle \hat{A}[q] \exp(-\hat{H}_{fp}(t-t^0)) (-i k_B T \hat{B}^0[q]) \rangle_{gb} \\ &= k_B T R_{AB}(t-t^0) \end{aligned} \quad (7.2)$$

for $t - t_0 > 0$. Note that since in equilibrium the averages of one-time quantities are constant one can replace $C_{AB}(t - t_0)$ by the connected correlation $C_{AB}^c(t - t_0)$. $C_{AB}(t - t_0) = \langle A(t)B(t_0) \rangle$ in the left-hand-side (lhs) and the fdt also reads $C_{AB}^c(t - t_0) = k_B T R_{AB}(t - t_0)$. In integrated form

$$k_B T R_{AB}(t - t_0) = C_{AB}(t - t_0) - C_{AB}(t - t_0) = C_{AB}^c(t - t_0) - C_{AB}(t - t_0) : (7.3)$$

7.3 Quantum fdt

Proofs and descriptions of the quantum fdt can be found in several textbooks [70, 68]. Here, we express it in the time-domain and in a mixed time-Fourier notation that gives us insight as to how to extend it to the case of glassy non-equilibrium dynamics.

If at time t_0 a quantum system has reached equilibrium the density operator $\hat{\rho}(t_0)$ is just the Boltzmann factor $\exp(-\hat{H})/Z$. As in Section 6.3 it is then immediate to show that time-translation invariance (tti) holds $C_{AB}(t; t_0) = C_{AB}(t - t_0)$. In addition, from the definition of $C_{AB}(t; t_0)$ in Eq. (5.11) one proves the kms properties $C_{AB}(t; t_0) = C_{BA}(t_0; t + i\hbar) = C_{BA}(t - i\hbar; t_0)$. Assuming, for definiteness, that $t > 0$ it is easy to verify the following equation

$$C_{fA, Bg}(\omega) + \frac{i\hbar}{2} R_{AB}(\omega) = C_{fA, Bg}(\omega) - \frac{i\hbar}{2} R_{AB}(\omega); \quad (7.4)$$

where $\omega = t + i\hbar/2$. This is a way to express fdt through an analytic continuation to complex times. In terms of the Fourier transformed $\tilde{C}_{AB}(\omega)$ defined in Eq. (5.7) the kms properties read $\tilde{C}_{AB}(\omega) = \exp(-\hbar\omega) \tilde{C}_{BA}(-\omega)$ and lead to the following relation between Fourier transforms of symmetrized and anti-symmetrized correlations: $\tilde{C}_{[A, B]}(\omega) = \tanh \frac{\hbar\omega}{2} \tilde{C}_{fA, Bg}(\omega)$. Using now the Kubo relation (5.13) one obtains the quantum fdt

$$R_{AB}(t - t_0) = \frac{i}{\hbar} \int_{t_0}^t dt \exp(-i\omega(t - t_0)) \tanh \frac{\hbar\omega}{2} \tilde{C}_{fA, Bg}(\omega); \quad (7.5)$$

with the representation $\int_0^{\infty} dt \exp(i\omega t) = \lim_{\epsilon \rightarrow 0^+} \int_0^{\infty} dt \exp(i\omega t - \epsilon t) = \frac{1}{i\omega + \epsilon} = \frac{1}{i\omega} + i\pi\delta(\omega)$,

$$\tilde{R}_{AB}(\omega) = \frac{1}{\hbar} \lim_{\epsilon \rightarrow 0^+} \int_{-1}^1 d\omega' \frac{1}{\omega' + i\epsilon} \tanh \frac{\hbar\omega'}{2} \tilde{C}_{fA, Bg}(\omega') \quad (7.6)$$

from which we obtain the real and imaginary relations between $\text{Im} \tilde{R}_{AB}(\omega)$, $\text{Re} \tilde{R}_{AB}(\omega)$ and $\tilde{C}_{fA, Bg}(\omega)$. If $\hbar\omega = 2\pi$, $\tanh(\hbar\omega/2) = 1$ and Eq. (7.5) becomes the classical fdt, Eq. (7.2).

7.4 Examples

7.4.1 Harmonic oscillator and diffusion

The simplest example in which one sees the modifications of the fdt at work is a one-dimensional harmonic oscillator with no inertia coupled to a white bath. One

nds

$$k_B T \frac{R(t; t^0)}{\partial_{t^0} C(t; t^0)} = \begin{cases} 1 & \text{if } k > 0 \\ 1 + \exp\left(\frac{2kt^0}{k_B T}\right) & \text{if } k = 0 \\ 0 & \text{if } k < 0 \end{cases} \quad (7.7)$$

for times $t \rightarrow t^0$ and $t^0 \rightarrow \infty$ with k the harmonic constant of the oscillator. Thus, when there is a confining potential and P_{gb} can be defined the fdt holds. Instead, when the potential is flat ($k = 0$) or unbounded from below ($k < 0$) no normalizable P_{gb} can be defined and the fdt is modified.

If one keeps inertia, the calculations are slightly more involved but one can carry them through to show that momenta and coordinates behave very differently [71]. Since the probability distribution of the momenta very rapidly reaches a Maxwellian for all values of k these variables equilibrate and fdt holds for them. This is the reason why the kinetic energy of a particle system serves to calibrate the external temperature. The coordinates, instead, behave as in (7.7) depending on the value of k .

7.4.2 A driven system

Take now a symmetric two-dimensional harmonic oscillator $V(x; y) = \frac{k}{2}(x^2 + y^2)$ and apply the non-potential force $f(x; y) = (y; -x)$ on it. This force makes a particle turn within the potential well and one can check, by direct calculation, that the fdt does not hold.

7.4.3 No Einstein relation

If the bath is such that the Einstein relation between friction and noise correlation does not hold, the fdt for the system variables does not hold either. Again, this can be easily checked using a harmonic oscillator.

7.4.4 A complex bath

Let us couple a harmonic oscillator to a complex bath made of two parts: a white bath ($\gamma_1 \neq 0$) with friction coefficient γ_1 at temperature T_1 and a coloured bath with friction kernel $\gamma(t) = \gamma_2 \exp[-\gamma_2 t]$ kept at temperature T_2 [72]. The complex bath induces two time-scales (see Section 11.4 for its precise definition) in the dynamics of the oscillator: the correlation is stationary but it decays in two steps, from q_1 at equal times to an "Edwards-Anderson parameter" q_{ea} for time differences $t \rightarrow \infty$, that are shorter than a characteristic time τ_0 and from q_{ea} to zero for longer t 's. The parameters q_1 , q_{ea} and τ_0 are functions of k , the friction coefficients γ_1 and γ_2 and the two temperatures T_1 and T_2 . In Fig. 9 we display the correlation decay and the parametric plot of the integrated linear response, χ , against the correlation, C , constructed using $t \rightarrow \infty$ as a parameter that runs from $t \rightarrow 0$ ($C = q_1$; $\chi = 0$) to $t \rightarrow \tau_0$ ($C = q_{ea}$; $\chi = 1$). (See Section 11.5.3.) The fdt predicts a linear relation between χ and C with a slope $1/(k_B T)$ for systems equilibrated with a reservoir at temperature T . In this problem though "there is no T " since the system

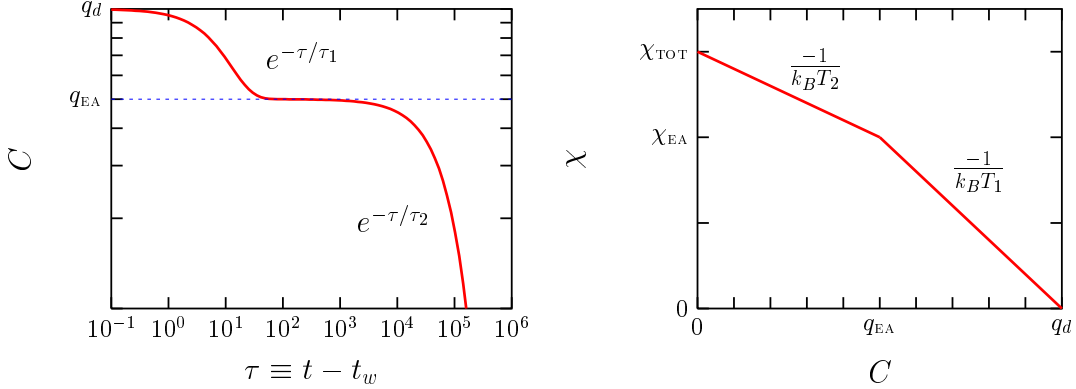


Figure 9: Left: Decay of the correlation for a harmonic oscillator coupled to a mixed bath. Right: parametric plot of the integrated linear response against the correlation.

is coupled to a bath with two temperatures and two time-scales. Surprisingly, one finds that the rapid decay is controlled by the temperature of the fast bath, T_1 , while the subsequent, slower, decay is controlled by the temperature of the slow bath, T_2 .

A similar phenomenon, now self-induced, appears in glassy models. These interacting systems are coupled to an external white bath at temperature T_1 . Their dynamics is such that several time-scales, each with its own "temperature" is generated. We shall show how this arises in solvable models in Section 12 and we shall prove that the fd relation can indeed be used to define an "effective temperature" in Section 14.

8 Dynamic generating functionals

In this Section we present the functional methods used to analyze the dynamics of classical [73] and quantum [74] models coupled to environments. We discuss the relation between the two approaches. The generating functionals, with their effective actions, are the adequate starting point to apply perturbation theory (when it is accepted), self-consistent approximations such as the mode-coupling approach, or even more sophisticated techniques as the functional renormalization group.

8.1 Classical models

For a classical system coupled to a classical environment, we use as a starting point a stochastic equation with an additive noise $\dot{q}(t) = E q(q)$. For instance, if we deal with a massive particle governed by the Langevin equation, Eq. (4.7) $E q(q) = M \dot{q} + \int_0^t dt' \dot{q}(t') q(t') + V'(q)$.

Any averaged observable, e.g. $\langle h A[q] \rangle(t)$ in Eq. (5.2), can be computed from the variation of a dynamic generating functional Z with respect to a time-dependent

source :

$$\langle hA[q]i(t) \rangle = \frac{Z[\lambda]}{Z[\lambda=0]} = \frac{Z}{Z[\lambda=0]} \int D P[\lambda] e^{\int_{t^0}^t dt^0 \lambda^{(0)} A[q^{sol}](t^0)} : \quad (8.1)$$

Since the probability distribution $P[\lambda]$ is normalized to one, $Z[\lambda=0] = 1$, and the average is automatically normalized. The idea is to derive a useful expression for the generating functional Z by introducing the functional identity

$$1 = \int D q (q - q^{sol}) = \int D q \left(\int E q[q](t) \det \frac{E q[q](t)}{q(t^0)} \right) : \quad (8.2)$$

In the first integral an integration and delta function is applied on each time slice and the compact notation actually represents $\int_a [dq(a) \delta(q(a) - q^{sol}(a))]$. The second identity follows from a change of variables in the functional integral. If the stochastic equation has only one solution, one can eliminate the absolute value in the determinant, and

$$Z[\lambda] = \int D \lambda D q P[\lambda] \left(\int E q[q](t) \det \frac{E q[q](t)}{q(t^0)} \right) \exp \int_{t^0}^t dt^0 \lambda^{(0)} A[q](t^0) : \quad (8.3)$$

This expression can be recast in a more convenient form by using the exponential representation of the delta function

$$\left(\int E q[q](t) \right) / \int D i\dot{q} \exp \int_0^{Z_t} dt^0 i\dot{q}(t^0) \left((t^0) \int E q[q](t^0) \right) \quad (8.4)$$

(the constant of proportionality is numeric, a power of 2, and irrelevant for the calculation of averages, thus we omit it), and the determinant through the introduction of a pair of fermionic variables [65]

$$\det \frac{E q[q](t)}{q(t^0)} = \int D \bar{D} \exp \int_0^{Z_t} dt^0 \int_0^{Z_t} dt^0 \bar{D}(t^0) \frac{E q[q](t^0)}{q(t^0)} D(t^0) : \quad (8.5)$$

Having used these identities, the generating functional becomes a functional integral over $q, i\dot{q}, \bar{D}$ and D . Since λ appears in quadratic terms of the effective action only, the functional integral over λ can be simply calculated. We obtain

$$\begin{aligned} Z[\lambda; \hat{\lambda}] &= \int D q D i\dot{q} D \bar{D} \exp(S_{eff}) \\ S_{eff} &= \int_0^{Z_t} dt^0 \int_0^{Z_t} dt^0 i\dot{q}(t^0) k_B T (t^0 - t^0) (t^0 - t^0) i\dot{q}(t^0) + \int_0^{Z_t} dt^0 \bar{D}(t^0) \frac{E q[q](t^0)}{q(t^0)} D(t^0) \\ &\quad + \int_0^{Z_t} dt^0 (i\dot{q}(t^0) E q[q](t^0) - \bar{D}(t^0) q(t^0) - \hat{\lambda}(t^0) i\dot{q}(t^0)) \end{aligned} \quad (8.6)$$

where we have introduced a new source $\hat{\lambda}(t)$ coupled to the auxiliary variable $i\dot{q}(t)$.

In Appendix C we prove the following very useful relations

$$R(t; t^0) = hq(t) i\dot{q}(t^0) i \quad (8.7)$$

$$\frac{1}{2} k_B T \int_0^{Z_t} dt^0 ((t^0; t^0) + (t^0; t^0)) R(t; t^0) = hq(t) (t^0) i : \quad (8.8)$$

Usually, the kernel $(t^0; t^0)$ is symmetric $(t^0; t^0) = (t^0; t^0)$ and the latter relation simplifies. For a white noise $(t^0; t^0) = 2 \delta(t - t^0)$ and $2 k_B T R(t; t^0) = hq(t) (t^0) i$.

8.2 Supersymmetry (susy)

In the white noise limit Z in Eq. (8.6) can be written in a much more compact form if one introduces the superfield formulation of stochastic processes explained in [65, 76, 77], see Appendix D. One first enlarges (space)-time to include two Grassmann coordinates \bar{t} and $\bar{\theta}$, i.e. $t \rightarrow a = (t; \bar{\theta})$. The dynamic variable $q(t)$ and the auxiliary variable $i\dot{q}(t)$ together with the fermionic ones $\psi(t)$ and $\bar{\psi}(t)$ are encoded in a superfield,

$$(a) = q(t) + \bar{\psi}(t) + \bar{\theta}(t) + i\dot{q}(t)\bar{\theta} : \quad (8.9)$$

With these definitions,

$$Z[a] = \int d^2a \exp \left[-\frac{1}{2} \int da (a) (D_a^{(2)}) (a) \right] \int da V[a(a)] + \int da (a) (a) \quad (8.10)$$

with $a = (t; \bar{\theta})$, $da = dt d\bar{\theta}$, and the dynamic operator $D_a^{(2)}$ defined as

$$D_a^{(2)} = 2k_B T \frac{\partial^2}{\partial \bar{\theta} \partial \theta} + 2 \frac{\partial^2}{\partial \bar{\theta} \partial t} - \frac{\partial}{\partial t} M \frac{\partial^3}{\partial \bar{\theta} \partial \theta^2} : \quad (8.11)$$

If the model is spherically constrained, $D_a^{(2)} \rightarrow D_a^{(2)} - \delta(a) \lambda$ with $\lambda(a)$ a super Lagrange multiplier introduced to enforce the constraint. The delta function $\delta(a-b)$ is defined in Appendix D and it satisfies $\int db \delta(a-b) f(b) = f(a)$. The supersymmetric notation allows one to encode in the single super correlator $Q(a;b)$ all correlators and responses. The generalization to a system with N degrees of freedom is immediate.

Symmetries

The properties of the equilibrium dynamics, i.e. the invariance under time-translations, the fluctuation-dissipation theorem, etc., are consequences of the symmetries of the supersymmetric action. The non-equilibrium dynamic solution spontaneously breaks these symmetries.

For a stochastic process with a white noise the susy group is generated by three operators [76, 65, 77]:

$$D^0 = k_B T \frac{\partial}{\partial \bar{\theta}} + \frac{\partial}{\partial t} \quad D^0 = \frac{\partial}{\partial \bar{\theta}} \quad D^0 D^0 + D^0 D = \frac{\partial}{\partial t} \quad (8.12)$$

with $D^0 = D^0 = 0$. We can construct an extension of this group that acts on two-point (in general n -point) functions, as

$$\begin{aligned} D^0(a;b) &= D^0(a) + D^0(b) \\ D^0(a;b); D^0(a;b) &= \frac{\partial}{\partial t} + \frac{\partial}{\partial \bar{\theta}} : \end{aligned} \quad (8.13)$$

The meaning of the three generators can be understood when they are made to act on $Q(a;b)$. Firstly, causality plus probability conservation imply (irrespective of equilibration): $D^0(a;b)Q(a;b) = 0$, This equation serves to select the non-vanishing

terms in the super correlator. It imposes $\langle \hat{q}(t) \hat{q}(t^0) \rangle = 0$ and the fact that all components involving only one \hat{q} and $\bar{\hat{q}}$ vanish. Then

$$Q(a; b) = C(t; t^0) \langle \bar{\hat{q}}(t) \hat{q}(t^0) \rangle = R(t; t^0) \quad (8.14)$$

(the bifermionic correlator $\langle \bar{\hat{q}}(t) \hat{q}(t^0) \rangle$ equals the response $R(t; t^0)$). The susy action [the exponent in Eq. (8.10)] vanishes if evaluated on such correlators (when $\hat{q} = \bar{\hat{q}} = 0$). The other two generators imply

$$(\partial_t + \partial_{t^0}) Q(a; b) = 0 \quad \forall t, t^0; \quad D^0(a; b) Q(a; b) = 0 \quad \forall t, t^0 : \quad (8.15)$$

When is a system unable to reach equilibrium? In terms of symmetries this question can be addressed as follows. In driven system the dynamical actions break susy explicitly. They are externally kept far from equilibrium by the forcing. If susy is not explicitly broken two possibilities arise. Either the system evolves from its initial condition during an out of equilibrium transient in which neither stationarity nor fdt hold until the equilibration time t_{eq} is reached and equilibrium establishes. In this language, susy is unbroken by the boundary conditions. On the contrary, if the system never achieves equilibrium the equilibration time diverges and cannot be reached in the calculation. The effect of the initial conditions is then to break susy [77, 78] and consequently violate the equilibrium properties even for long times. susy is then spontaneously broken. The initial conditions play for susy the same role played in ordinary symmetry-breaking by space boundary conditions: if the symmetry is spontaneously broken their effect extends away from them, in this case for all times.

8.3 Connection with the replica formalism

The effective action in Eq. (8.10) is a kinetic minus a potential term $V[\hat{q}]$. When applying the replica trick to compute the free-energy a replicated effective potential $V[\hat{q}^a]$ appears. A connection between the two formalisms, that is based on the similarity between the zero-dimensional replica space and the susy one, has been exploited. Roughly speaking, many properties of the replica overlap $Q^{ab} = \frac{1}{N} \sum_{i=1}^N \hat{q}_i^a \hat{q}_i^b$ finds a counterpart in the dynamic susy correlator $Q(a; b)$. For instance, a summation over a replica index, $\sum_{a=1}^n$ when $n \rightarrow 0$, translates into an integration over the supercoordinate $d\hat{q}_a$. For the moment, though, the connection is empirical and a formalization of the relation between the two approaches would be welcome.

8.4 Quantum models

The Schwinger-Keldysh formalism [74] allows one to analyze the real-time dynamics of a quantum system. The starting point is the time dependent density operator

$$\hat{\rho}_{tot}(t) = e^{-\frac{i}{\hbar} \hat{H}_{tot} t} \hat{\rho}_{tot}(0) e^{\frac{i}{\hbar} \hat{H}_{tot} t} : \quad (8.16)$$

Introducing identities, an element of the time-dependent density matrix reads

$$\begin{aligned} \langle q_a^0; x_a^0; q_a^0; x_a^0; t \rangle &= \int_1^Z dQ dQ^0 dX_a dX_a^0 \langle q_a^0; x_a^0 \rangle e^{-\frac{i}{\hbar} \hat{H}_{tot} t} \mathcal{D}[X_a] \\ &\quad \langle q_a^0; x_a^0 \rangle \hat{\rho}_{tot}(0) \mathcal{D}[X_a] \langle q_a^0; x_a^0 \rangle e^{\frac{i}{\hbar} \hat{H}_{tot} t} \langle q_a^0; x_a^0 \rangle ; \end{aligned} \quad (8.17)$$

where q is the coordinate of the particle and x_a are the coordinates of the oscillators. The first factor is the coordinate representation of the evolution operator and it can be represented as a functional integral. The third factor can also be represented in functional form. They read

$$\langle q^0; x_a^0 | e^{\frac{i}{\hbar} \hat{H}_{\text{tot}} t} | q^+; x_a^+ \rangle = \int_{q^+(0)=Q}^{q^+(t)=q^0} \int_{x_a^+(0)=X_a}^{x_a^+(t)=x_a^0} Dq^+ Dq^+ Dq^+ Dq^+ e^{\frac{i}{\hbar} S_{\text{tot}}} \quad (8.18)$$

$$\langle q^0; x_a^0 | e^{\frac{i}{\hbar} \hat{H}_{\text{tot}} t} | q^0; x_a^0 \rangle = \int_{q(0)=Q^0}^{q(t)=q^0} \int_{x_a(0)=X_a^0}^{x_a(t)=x_a^0} Dq Dq Dq Dq e^{\frac{i}{\hbar} S_{\text{tot}}} \quad (8.19)$$

Interestingly enough, the evolution operator in Eq. (8.19) gives rise to a path integral going backwards in time, from $q(t) = q^0; x_a(t) = x_a^0$ to $q(0) = Q^0; x_a(0) = X_a^0$. The full time-integration can then be interpreted as being closed, going forwards from $t_0 = 0$ to t and then backwards from t to $t_0 = 0$. This motivates the name "closed time path formalism". A doubling of degrees of freedom ($q^+; q$) appeared and it is intimately linked to the introduction of Lagrange multipliers in the functional representation of the stochastic dynamics in the classical limit.

The action S_{tot} has the usual four contributions, from the system, the reservoir, the interaction and the counter-term. The action of the system reads

$$S_{\text{sys}}^+ [q^+(t); q^+(t)] = \int_0^t dt \left[\frac{M}{2} \dot{q}^+(t)^2 - V(q^+(t)) + q^+(t) \dot{q}^+(t) \right] \quad (8.20)$$

where we have introduced a time-dependent source $q^+(t)$. Similarly, we introduce a source $q(t)$ in the path integral going backwards in time.

Since we are interested in the dynamics of the system under the effect of the reservoir we compute the reduced density matrix

$$\rho_{\text{red}}(q^0; q^0; t) = \int_1^{Z_1} dx_a \langle q^0; x_a | \hat{j}_{\text{tot}}^0(t) | q^0; x_a \rangle \quad (8.21)$$

The initial density operator $\hat{j}_{\text{tot}}^0(0)$ has the information about the initial state of the whole system. If one assumes that the system and the bath are set in contact at $t = 0$, $\hat{j}_{\text{tot}}^0(0)$ factorizes $\hat{j}_{\text{tot}}^0(0) = \hat{j}_{\text{sys}}^0(0) \hat{j}_{\text{env}}^0(0)$. (Other initial preparations, where the factorization does not hold, can also be considered and may be more realistic in certain cases.) If the environment is initially in equilibrium at an inverse temperature β , $\hat{j}_{\text{env}}^0(0) = Z_{\text{env}}^{-1} \exp(-\beta \hat{H}_{\text{env}})$. For a bath made of harmonic oscillators the dependence on the bath variables is quadratic and they can be traced away to yield:

$$\rho_{\text{red}}(q^0; q^0; t) = \int_1^{Z_1} dQ \int_1^{Z_1} dQ^0 \int_{q^+(0)=Q}^{q^+(t)=q^0} Dq^+ \int_{q(0)=Q^0}^{q(t)=q^0} Dq e^{\frac{i}{\hbar} S_{\text{eff}}} \langle q^0; x_a | \hat{j}_{\text{sys}}^0(0) | q^0; x_a \rangle$$

with $S_{\text{eff}} = S_{\text{sys}}^+ + S_{\text{sys}} + S_{\text{th}}$. The last term has been generated by the interaction with the environment and it reads

$$S_{\text{th}} = \int_0^t dt \int_0^t dt' \left[q^+(t) q(t') - q(t) q^+(t') \right] + i \int_0^t dt \int_0^t dt' \left[q^+(t) q(t') - q(t) q^+(t') \right] \quad (8.22)$$

The noise and dissipative kernels and are given by

$$\gamma(t) = \int_0^{Z-1} d! I(!) \coth \frac{1}{2} \hbar! \cos(! (t)) ; \quad (8.23)$$

$$\eta(t) = \frac{d}{dt} \langle \hat{Q}(t) \rangle = \int_0^{Z-1} d! I(!) \sin(! (t)) : \quad (8.24)$$

In these equations, $I(!)$ is the spectral density of the bath, already defined in Eq. (4.6). is defined in the first identity and as we shall see below it plays the same role as the friction kernel in classical problems with colored noise.

Next, we have to choose an initial density matrix for the system. One natural choice, having in mind the quenching experiments usually performed in classical systems, is the diagonal matrix $\rho_{\text{red}}^{\text{red}}(0) = \rho_{\text{red}}^{\text{red}}(0)$ that corresponds to a random "high-temperature" situation and that allows one to simplify considerably

$$\rho_{\text{red}}^{\text{red}}(q^0; q^0; t) = \int_0^{Z-1} dQ \int_{q^+(0)=Q}^{q^+(t)=q^0} Dq^+(t) \int_{q^-(0)=Q}^{q^-(t)=q^0} Dq^-(t) e^{\frac{i}{\hbar} S_{\text{eff}}} : \quad (8.25)$$

Another representation of $\rho_{\text{red}}^{\text{red}}$ is obtained by renaming the variables

$$q = \frac{1}{2}(q^+ + q^-) \quad i\hat{q} = \frac{1}{\hbar}(q^+ - q^-) : \quad (8.26)$$

and rewriting the effective action as a function of q and $i\hat{q}$. The new form is useful to establish contact with the generating functional for classical systems. The thermal parts simply become

$$S_{\text{th}} = \int_0^Z dt^0 \int_0^Z dt^0 \hbar i \hat{q}(t^0) (t^0 - t^0) 2q(t^0) + i \int_0^Z dt^0 \int_0^Z dt^0 \hbar i \hat{q}(t^0) (t^0 - t^0) \hbar i \hat{q}(t^0)$$

as for a Langevin process in a colored noise. When $\hbar \rightarrow 0$, the full effective action approaches the classical one as can be verified by expanding in powers of \hbar , and keeping only the leading terms. If, moreover, the limit $\beta \rightarrow 1$ is taken, the kernels and become proportional to functions and one recovers a white noise. Keeping $\hbar > 0$ the rotated version allows one to treat classical and quantum problems in parallel.

If one generalizes the above system to be one described by a field $\hat{\phi}_i$ with $i = 1; N$ components, the symmetrized correlation function $C_{ij}(t; t^0) = \frac{1}{2} \langle \hat{\phi}_i(t) \hat{\phi}_j(t^0) + \hat{\phi}_j(t^0) \hat{\phi}_i(t) \rangle$ (where the hats represent operators) is given by

$$C_{ij}(t; t^0) = \frac{\hbar^2}{2} \left[\frac{1}{\gamma_{ij}(t) \gamma_{ji}(t^0)} + \frac{1}{\gamma_{ji}(t^0) \gamma_{ij}(t)} \right] \rho_{\text{red}}^{\text{red}} = 0 \quad (8.27)$$

$[C_{ij}(t; t^0) = C_{ji}(t^0; t)]$. Using the Kubo formula (5.13) the linear response function can be expressed in terms of the averaged commutator, $R_{ij}(t; t^0) = i\hbar \langle [\hat{\phi}_i(t); \hat{\phi}_j(t^0)] \rangle$ and

$$R_{ij}(t; t^0) = \frac{\hbar}{i} \left[\frac{1}{\gamma_{ij}(t) \gamma_{ji}(t^0)} - \frac{1}{\gamma_{ji}(t^0) \gamma_{ij}(t)} \right] \rho_{\text{red}}^{\text{red}} = 0 : \quad (8.28)$$

(The hats represent operators.) It is also useful to write the correlation and response in terms of the fields $\hat{\phi}_i^+$, $\hat{\phi}_i$ and their rotated counterparts

$$2C_{ij}(t; t^0) = \langle \hat{\phi}_i^+(t) \hat{\phi}_j(t^0) + \hat{\phi}_j^+(t^0) \hat{\phi}_i(t) \rangle = \langle \hat{\phi}_i(t) \hat{\phi}_j(t^0) + \hat{\phi}_j(t^0) \hat{\phi}_i(t) \rangle; \quad (8.29)$$

$$R_{ij}(t; t^0) = \frac{i}{h} \langle \hat{\phi}_i^+(t) \hat{\phi}_j^+(t^0) - \hat{\phi}_j(t^0) \hat{\phi}_i(t) \rangle = \langle \hat{\phi}_i(t) \hat{\phi}_j^+(t^0) - \hat{\phi}_j(t^0) \hat{\phi}_i(t) \rangle; \quad (8.30)$$

8.5 Average over disorder

In general one is interested in the evolution of a model in which the configuration of disorder is typical. One could either attempt to solve the dynamics for one such disorder realization or one can assume that the behavior of a typical system is described by the averaged behavior over all systems, each weighted with its probability. Since the former procedure is more difficult than the latter one usually studies the dynamics averaged over disorder and computes:

$$\langle \hat{A}(t) \rangle = \frac{\int \mathcal{D}J \mathcal{D}D \int \mathcal{D}\hat{\phi} \hat{A}[\hat{\phi}; \hat{\phi}^+] e^{-S_{\text{eff}}[\hat{\phi}, \hat{\phi}^+]}}{\int \mathcal{D}J \mathcal{D}D \int \mathcal{D}\hat{\phi} e^{-S_{\text{eff}}[\hat{\phi}, \hat{\phi}^+]}}; \quad (8.31)$$

J represents here the random exchanges in Eq. (2.5). Similarly, one can perform an average over a random potential in a problem as the one defined in Eq. (2.8).

One of the advantages of using a dynamic formalism is that when the initial conditions are uncorrelated with disorder there is no need to use the replica trick to average over disorder [75]. Indeed, the classical generating functional is constructed from a path integral that is identical to 1 (and hence independent of disorder) in the absence of sources. The same holds for the quantum Schwinger-Keldysh generating functional, $\text{Tr} \hat{\rho}_{\text{red}}(0) = 1$, since we have chosen a diagonal density matrix as the initial condition for the system. Thus,

$$\langle \hat{A}(t) \rangle = \int \mathcal{D}J \mathcal{D}D \int \mathcal{D}\hat{\phi} \hat{A}[\hat{\phi}; \hat{\phi}^+] e^{-S_{\text{eff}}[\hat{\phi}, \hat{\phi}^+]}, \quad (8.32)$$

and these averages can be simply computed from $\langle Z_J \rangle$ [79].

If the initial condition is correlated with the random exchanges or the random potential, the situation is different. One such example is the study of the equilibrium dynamics of a disordered model, i.e. the study of the evolution of initial conditions taken from P_{gb} . In this case, the use of replicas to average $\ln Z$ is unavoidable and one is forced to treat replicated dynamic correlators. For classical models this has been discussed in [80]. For quantum problems the difficulty of the calculation increases since one needs to work in a mixed real and imaginary time formalism [81]. The initial density operator is a Boltzmann factor that is represented with the Matsubara formalism while the real-time dynamics is written with the Schwinger-Keldysh approach. Mixed correlators and responses intervene in the dynamic equations.

9 Dynamic equations

In this Section we present three derivations of the dynamic equations for the macroscopic order parameters that use the classical or quantum dynamic generating functionals as starting points. Each method is better adapted for different kinds of models.

9.1 A useful derivation for fully-connected models

9.1.1 Classical systems

Even if the use of the susy notation is not necessary to derive the dynamic equations [82], it is very useful in several aspects. Firstly, it allows to establish contact with the replicated version of the static partition function and the further study of this quantity; secondly, it is very useful as a bookkeeping tool; thirdly, it allows us to develop more sophisticated techniques and enable to derive the dynamic equations of models without fully connected interactions. For all these reasons, we preferred to introduce the susy formalism in Section 8.2 and use it here.

Since for classical models the use of white noises is rather generally justified we shall stick to this case. Moreover, we shall drop the inertial contribution to further simplify the presentation. We analyze here models with N variables $\tilde{\mathbf{x}} = (\tilde{x}_1; \dots; \tilde{x}_N)$ of the kind discussed in Section 2. In susy notation the dynamical generating functional after setting the sources to zero reads

$$Z = \int \mathcal{D} \tilde{\mathbf{x}} \exp \left[- \frac{1}{2} \sum_i \tilde{x}_i(a) \left(D_a^{(2)} \right)_{ij} \tilde{x}_j(a) + V[\tilde{\mathbf{x}}] \right] \quad (9.1)$$

with $\tilde{\mathbf{x}}$ and $\tilde{\mathbf{x}}_a$ two superfields, the latter imposing the spherical constraint $(\tilde{x}_s(a) = \tilde{x}(t) + \text{fermionic} + \tilde{\lambda}(t))$, $\tilde{\lambda}(t)$ is a Lagrange multiplier that fixes the measure of integration and $\tilde{\lambda}(t)$ enters the Langevin equation). Soft spins with their corresponding potential energy can be studied in a similar way though their treatment is slightly more complicated. The potential energy of a rather generic fully connected disordered model can be expressed as a series expansion of the form

$$V[\tilde{\mathbf{x}}] = g \sum_{r=0}^{\infty} F_r \sum_{i_1 < \dots < i_{r+1}} J_{i_1 \dots i_{r+1}} \tilde{x}_{i_1} \dots \tilde{x}_{i_{r+1}}; \quad (9.2)$$

For each r the sum is taken over all possible groups of $r+1$ spins. The fully-connected character of the model implies that there is no notion of distance or geometry. $J_{i_1 \dots i_{r+1}}$ are random interactions taken from a Gaussian distribution with zero mean and variance $[J_{i_1 \dots i_{r+1}}^2] = (r+1)!(2N)^r$, just as in the model in Eq. (2.6). Thus (9.2) is a Gaussian random potential with

$$[V(\tilde{\mathbf{x}}(a))V(\tilde{\mathbf{x}}(b))] = N g^2 \sum_{r=0}^{\infty} F_r^2 \frac{\tilde{\mathbf{x}}(a) \tilde{\mathbf{x}}(b)}{N} = N V \frac{\tilde{\mathbf{x}}(a) \tilde{\mathbf{x}}(b)}{N} : \quad (9.3)$$

The scalar product in the second member is defined as $\tilde{a} \cdot \tilde{b} = \sum_{i=1}^P \tilde{a}_i \tilde{b}_i$. The bullet means that the powers are taken locally in the super-coordinates a and b and they do not involve an operational product, see Appendix D. The term $r = 0$ corresponds to a random field linearly coupled to the spin, the term $r = 1$ is quadratic in the fields while for $r \geq 2$ we obtain higher order interactions. If $F_r = F_p \delta_{r,p}$ for $p \geq 2$ and all other $F_r = 0$ one recovers a spherical p spin model. If two parameters are non-zero one obtains a model with two p spin terms. The model of a particle in an infinite dimensional spherical random environment correlated as in (2.8) also falls in this category if one can expand the correlator in a power series.

The disordered averaged generating functional reads

$$Z[D] = \int \mathcal{D}a \mathcal{D}b e^{-\sum_{i=1}^R \int da \frac{1}{2} \sum_{i=1}^P \tilde{a}_i \tilde{a}_i (a) + \sum_{i=1}^R \int da \sum_{i=1}^P \tilde{a}_i \tilde{a}_i (a) + \frac{N}{2} \int da \sum_{i=1}^P \tilde{a}_i \tilde{a}_i (a) + \sum_{i=1}^R \int da \sum_{i=1}^P \tilde{a}_i \tilde{a}_i (a) + \frac{N}{2} \int da \sum_{i=1}^P \tilde{a}_i \tilde{a}_i (a)} : \quad (9.4)$$

Introducing the order parameter $Q(a;b) = N^{-1} \sum_{i=1}^P \tilde{a}_i \tilde{a}_i (a) \tilde{a}_i \tilde{a}_i (b)$ through

$$1 / \int \mathcal{D}Q \mathcal{D}iQ e^{-\frac{1}{2} \int da \sum_{i=1}^P \tilde{a}_i \tilde{a}_i (a) + \sum_{i=1}^R \int da \sum_{i=1}^P \tilde{a}_i \tilde{a}_i (a) + \frac{N}{2} \int da \sum_{i=1}^P \tilde{a}_i \tilde{a}_i (a) + \sum_{i=1}^R \int da \sum_{i=1}^P \tilde{a}_i \tilde{a}_i (a) + \frac{N}{2} \int da \sum_{i=1}^P \tilde{a}_i \tilde{a}_i (a)} \quad (9.5)$$

yields

$$Z[D] = \int \mathcal{D}Q \mathcal{D}iQ \exp \left[-\frac{1}{2} \int da \sum_{i=1}^P \tilde{a}_i \tilde{a}_i (a) + \sum_{i=1}^R \int da \sum_{i=1}^P \tilde{a}_i \tilde{a}_i (a) + \frac{N}{2} \int da \sum_{i=1}^P \tilde{a}_i \tilde{a}_i (a) + \sum_{i=1}^R \int da \sum_{i=1}^P \tilde{a}_i \tilde{a}_i (a) + \frac{N}{2} \int da \sum_{i=1}^P \tilde{a}_i \tilde{a}_i (a) \right] : \quad (9.6)$$

(Again we omit irrelevant normalization constants.) Note that all terms in the exponent are order N if the integrals yield finite contributions. We call the models for which this is true "mean-field" since the saddle-point evaluation of the integral when $N \rightarrow \infty$ is exact without including fluctuations. There is however a caveat in this reasoning that we discuss in Section 9.4.

The saddle-point values for the Landau fields Q are simply related to correlations of the original spins. Indeed, evaluating the generating function in Eq. (9.6) with a saddle-point approximation

$$0 = \frac{S}{Q(a;b)} \left(\sum_{i=1}^N h_i \tilde{a}_i (a) \tilde{a}_i (b) \right) i_{Z[Q]} ; \quad (9.7)$$

where the average on the rhs is taken with the generating functional

$$Z[Q] = \int \mathcal{D}Q \mathcal{D}iQ e^{-\frac{1}{2} \int da \sum_{i=1}^P \tilde{a}_i \tilde{a}_i (a) + \sum_{i=1}^R \int da \sum_{i=1}^P \tilde{a}_i \tilde{a}_i (a) + \frac{N}{2} \int da \sum_{i=1}^P \tilde{a}_i \tilde{a}_i (a) + \sum_{i=1}^R \int da \sum_{i=1}^P \tilde{a}_i \tilde{a}_i (a) + \frac{N}{2} \int da \sum_{i=1}^P \tilde{a}_i \tilde{a}_i (a)} : \quad (9.8)$$

Opening up the susy notation Eq. (9.7) implies, as expected,

$$\begin{aligned} N C_{sp}(t_1; t_2) &= \sum_{i=1}^N h_i \tilde{a}_i(t_1) \tilde{a}_i(t_2) i_{Z[Q]} ; & N \hat{Q}_{sp}(t_1; t_2) &= \sum_{i=1}^N h_i \tilde{a}_i(t_1) \tilde{a}_i(t_2) i_{Z[Q]} ; \\ N R_{sp}(t_1; t_2) &= \sum_{i=1}^N h_i \tilde{a}_i(t_1) \tilde{a}_i(t_2) i_{Z[Q]} ; & N R_{sp}^y(t_1; t_2) &= \sum_{i=1}^N h_i \tilde{a}_i(t_1) \tilde{a}_i(t_2) i_{Z[Q]} : \end{aligned}$$

Going back to Eq. (9.6) we can now shift $i\bar{Q}, \bar{Q} \rightarrow (D_a^{(2)}(t)) (a-b) \bar{Q}(a;b)$, and integrate over i

$$[\mathbb{Z}] = \int \mathcal{D}Q \mathcal{D}\bar{Q} e^{-\frac{N}{2} \int da db \left[D_a^{(2)}(a;b) \bar{Q}(a;b) + (D_a^{(2)}(t)) (a-b) Q(a;b) - V(Q(a;b)) \right]} e^{\frac{i}{2} \text{Tr} \text{Ln} \bar{Q}} ;$$

Using a saddle-point evaluation, we eliminate \bar{Q} , $[\mathbb{Z}] = \int \mathcal{D}Q \exp[-N S_{\text{eff}}(Q)]$,

$$2S_{\text{eff}}(Q) = \int da db \left[D_a^{(2)}(a;b) Q(a;b) - V(Q(a;b)) \right] - \text{Tr} \text{Ln} Q ; \quad (9.9)$$

The saddle-point equation over Q , $S_{\text{eff}} = Q = 0$, yields the dynamic equation

$$(D_a^{(2)} + (t)) (a-b) + Q^{-1}(a;b) + V'(Q(a;b)) = 0 ; \quad (9.10)$$

that takes a more convenient form after multiplying operationally by Q :

$$(D_a^{(2)} + (t))Q(a;b) + (a-b) + da^0 (a;a^0)Q(a^0;b) = 0 ; \quad (9.11)$$

with the self-energy defined as

$$(a;b) - V'(Q(a;b)) = g^2 \sum_{r=0}^X F_r^2 (r+1) Q(a;b)^{-r} ; \quad (9.12)$$

We have recasted the saddle-point dynamic equation in the form of a Schwinger-Dyson equation. The dynamic field is here a susy correlator that encodes the usual correlation function, the advance and retarded linear responses and the fourth correlator (that vanishes for causal problems):

$$\begin{aligned} \bar{G}_o^{-1}(t)R(t;t^0) &= (t-t^0) + 2 \hat{Q}(t;t^0) + \int dt^0 [(t;t^0)R(t^0;t^0) + D(t;t^0)\hat{Q}(t^0;t^0)] ; \\ \bar{G}_o^{-1}(t)C(t;t^0) &= 2 k_B T R(t^0;t) + \int dt^0 (t;t^0)C(t^0;t^0) + \int dt^0 D(t;t^0)R(t^0;t^0) ; \\ \bar{G}_o^{-1Y}(t)R^Y(t;t^0) &= (t-t^0) + \int_0^{Z-1} dt^0 {}^Y(t^0;t)R(t^0;t^0) + \int dt^0 \hat{^Y}(t;t^0)C(t^0;t^0) \\ &\quad + 2 \hat{^Y}(t)C(t;t^0) ; \\ \bar{G}_o^{-1Y}(t)\hat{Q}(t;t^0) &= \int dt^0 {}^Y(t;t^0)\hat{Q}(t^0;t^0) + \int dt^0 \hat{^Y}(t;t^0)R(t^0;t^0) + 2 \hat{^Y}(t)R(t;t^0) ; \end{aligned}$$

with $\bar{G}_o^{-1}(t) = M \hat{Q} + Q_t + (t)$, $\bar{G}_o^{-1Y}(t) = M \hat{Q}^Y + Q_t^Y + (t)$, ${}^Y(t;t^0) = (t^0;t)$ and

$$(t;t^0) = g^2 \sum_{r=0}^X F_r^2 (r+1) r C^{r-1}(t;t^0) R(t;t^0) \quad (9.13)$$

$$D(t;t^0) = g^2 \sum_{r=0}^X F_r^2 (r+1) C^r(t;t^0) \quad (9.14)$$

$$\hat{^Y}(t;t^0) = g^2 \sum_{r=0}^X F_r^2 (r+1) r C^{r-1}(t;t^0) \hat{Q}(t;t^0) : \quad (9.15)$$

We set to zero all fermionic correlators. We call the above integro-differential equations the Schwinger-Dyson equations for R , C , R^Y and \hat{Q} , respectively.

Causality can be used to simplify the four Schwinger-Dyson equations considerably. For $t^0 > t$ one has $R(t; t^0) = 0$ while for $t > t^0$ one has $R(t^0; t) = 0$. Rewriting the equations for R and R^y with these two choices of times one easily sees that $\hat{Q}(t; t^0) = 0$ for all t and t^0 (note that \hat{Q} is symmetric in t and t^0) and $\phi_0(t) = 0$ for all t . Thus, the equation for \hat{Q} vanishes identically when causality holds. In the following we search for causal solutions and we work with their simplified version. We loose in this way the possibility of finding solutions that break causality which are related to instantons [65]. We shall come back to this point later. If we focus on the case $t > t^0$ the dynamic equations simplify to

$$\overline{G}_0^{-1}(t)R(t; t^0) = \int_{t^0}^t dt^m (t; t^m)R(t^m; t^0); \quad (9.16)$$

$$\overline{G}_0^{-1}(t)C(t; t^0) = \int_0^{t^0} dt^m D(t; t^m)R(t^0; t^m) + \int_0^t dt^m (t; t^m)C(t^0; t^m); \quad (9.17)$$

In their integrated form they read

$$R(t; t^0) = G_0(t; t^0) + \int_{t^0}^t dt^m \int_{t^0}^{t^m} dt^m G_0(t; t^m) (t^m; t^m)R(t^m; t^0); \quad (9.18)$$

$$C(t; t^0) = \int_0^{t^0} dt^m \int_0^{t^0} dt^m R(t; t^m) D(t^m; t^m) R(t^0; t^m); \quad (9.19)$$

with the propagator given by $G_0^{-1}(t; t^0) = (t^0 | \overline{G}_0^{-1}(t) | t)$.

The equation for $\phi(t)$ can be derived from the Schwinger-Dyson equation by imposing the spherical constraint through the evaluation at $t = t^0$. Multiplying operationally by G_0^{-1} one obtains

$$\begin{aligned} \phi(t) = & \int_0^t dt^m [(t; t^m)C(t; t^m) + D(t; t^m)R(t; t^m)] \\ & + M \int_0^t dt^m \int_0^{t^m} dt^m (\partial_t R(t; t^m)) D(t^m; t^m) (\partial_t R(t; t^m)) \\ & + M^2 \int_0^t \partial_t R(t; s) \partial_{st}^2 C(s; t) \int_{s!}^t \partial_{st}^2 R(t; s) \partial_{t^0} C(s; t^0) ds : \end{aligned} \quad (9.20)$$

The last two terms are a consequence of having a kinetic term with second derivatives. It can be easily identified with minus the second-derivative of the correlation at equal times by taking the limit $t^0 \rightarrow t$ in Eq. (9.17). Thus

$$\phi(t) = \int_0^t dt^m [(t; t^m)C(t; t^m) + D(t; t^m)R(t; t^m)] - M \frac{\partial^2}{\partial t^2} C(t; t^0) : \quad (9.21)$$

One way of deriving the equation for $\phi(t)$ for a Langevin process with white noise and no inertia goes as follows. Considering $t > t^0$ in the complete Schwinger-Dyson equation for C and taking $t^0 \rightarrow t$, and considering $t < t^0$ in the same equation and taking $t^0 \rightarrow t^+$, one finds

$$\lim_{t^0 \rightarrow t} \partial_t C(t; t^0) = \lim_{t^0 \rightarrow t^+} \partial_t C(t; t^0) = 2k_B T \quad (9.22)$$

where we used $R(t; t^0) = 1$. The derivative of C has a cusp at $t = t^0$. The symmetry of the correlation function about $t = t^0$ implies $C(t^0 + \epsilon; t^0) = C(t^0 - \epsilon; t^0)$ and an expansion up to first order in ϵ implies $\lim_{t \rightarrow t^0} \partial_t C(t; t^0) = \lim_{t \rightarrow t^0} \partial_t C(t^0; t)$. From Eq. (9.22) one has $\lim_{t \rightarrow t^0} \partial_t C(t; t^0) = -k_B T$. Now, one rewrites the complete equation for C exchanging t and t^0 and adds this equation to the same equation in the limit $t \rightarrow t^0$: $\lim_{t \rightarrow t^0} (\partial_t C(t; t^0) + \partial_{t^0} C(t; t^0)) = -2\langle \epsilon(t) \rangle + \lim_{t \rightarrow t^0} [\text{rhs eq. for } C + \text{rhs eq. for } C(t^0; t)]$. From the discussion above the lhs vanishes and the rhs implies

$$\langle \epsilon(t) \rangle = k_B T + \int_0^Z dt^0 [\langle \epsilon(t; t^0) C(t; t^0) + D(t; t^0) R(t; t^0) \rangle] : \quad (9.23)$$

For the spherical p spin model $\langle \epsilon(t) \rangle$ is simply related to the energy density $E(t)$. Indeed, take the Langevin equation evaluated at time t , multiply it by $s_i(t^0)$, sum over all sites, average over the noise and take the limit $t \rightarrow t^0$. Repeat this procedure with the Langevin equation evaluated at t^0 and multiplying by $s_i(t)$. Adding the resulting equations and using $\sum_{i=1}^N s_i(t) s_i(t^0) = 2 \langle E(t) \rangle$ (see Appendix C) we have $\langle \epsilon(t) \rangle = \lim_{t \rightarrow t^0} \sum_i \frac{H_J(s(t))}{s_i(t)} s_i(t^0) + k_B T$ that for the spherical p spin model becomes

$$\langle \epsilon(t) \rangle = pE(t) + k_B T : \quad (9.24)$$

Thanks to the mean-field character of the model the action is proportional to N and the saddle-point evaluation is exact when $N \rightarrow \infty$. For the fully connected models considered in this Section the self-energy is given by a rather simple function of the interactions. In Section 9.2 we present a more powerful method that allows us to derive a similar equation for dilute (as opposed to fully connected) disordered models. For finite dimensional problems none of these procedures are exact. An effective action in terms of local order parameters $Q_i(a; b)$ can be written but the evaluation of the generating functional by saddle-point has to include fluctuations [83, 84].

9.1.2 Quantum models

The similarity between the effective action for classical and quantum models can be exploited to derive the dynamic equations of a quantum system in a very similar manner to what we have just done for classical models [85]. Even if the susy notation is not useful for quantum problems we can still use a compact notation. We first encode the variables $q; i\bar{q}$ in a vector. The quadratic terms in the action can be condensed into one term by introducing the operator

$$\begin{aligned} \mathcal{O}_p(t; t^0) &= \begin{pmatrix} \mathcal{O}_p^{++}(t; t^0) & \mathcal{O}_p^+(t; t^0) \\ \mathcal{O}_p^{+-}(t; t^0) & \mathcal{O}_p(t; t^0) \end{pmatrix} = f \mathcal{O}_p(t; t^0) g; \\ \mathcal{O}_p^{++}(t; t^0) &= (M \partial_t^2 + \epsilon^+(t)) \langle t | \bar{\psi} | t^0 \rangle - 2i \langle t | \bar{\psi} | t^0 \rangle \\ \mathcal{O}_p^+(t; t^0) &= 2 \langle t | \bar{\psi} | t^0 \rangle + 2i \langle t | \bar{\psi} | t^0 \rangle \\ \mathcal{O}_p^{+-}(t; t^0) &= 2 \langle t | \bar{\psi} | t^0 \rangle + 2i \langle t | \bar{\psi} | t^0 \rangle \\ \mathcal{O}_p(t; t^0) &= (M \partial_t^2 + \epsilon(t)) \langle t | \bar{\psi} | t^0 \rangle - 2i \langle t | \bar{\psi} | t^0 \rangle \end{aligned} \quad (9.25)$$

in such a way that

$$S_{\text{eff}}[\tilde{\gamma}^+; \tilde{\gamma}] = \frac{1}{2} \int dt \int dt^0 \tilde{\gamma}^+(t) \text{Op}(\tilde{\gamma}; t^0) \tilde{\gamma}(t^0) + \int dt V[\tilde{\gamma}^+] + \int dt V[\tilde{\gamma}] \quad (9.26)$$

where Greek indices label γ and the sum convention is assumed.

Introducing the order parameter $Q(\tilde{\gamma}; t^0) = N^{-1} \sum_i \gamma_i(t) \gamma_i(t^0)$ via the identity

$$1 / \int dQ \exp \left(\int dt \int dt^0 \hat{Q}(\tilde{\gamma}; t^0) \gamma(\tilde{\gamma}; t^0) \right) = \int d\hat{Q} \exp \left(\int dt \int dt^0 \hat{Q}(\tilde{\gamma}; t^0) \gamma(\tilde{\gamma}; t^0) - N \int dt^0 Q(\tilde{\gamma}; t^0) \right); \quad (9.27)$$

the full action can be rewritten as

$$S_{\text{eff}}[\tilde{\gamma}^+; \tilde{\gamma}] = \frac{1}{2} \int dt \int dt^0 \tilde{\gamma}^+(t) \text{Op}(\tilde{\gamma}; t^0) \tilde{\gamma}(t^0) + \int dt \int dt^0 \hat{Q}(\tilde{\gamma}; t^0) \gamma(\tilde{\gamma}; t^0) \\ + \frac{N}{2} \int dt \int dt^0 \hat{Q}(\tilde{\gamma}; t^0) Q(\tilde{\gamma}; t^0) + \frac{N}{2} \int dt \gamma^+(t) \gamma(t) + \int dt V[\tilde{\gamma}^+] + \int dt V[\tilde{\gamma}]; \quad (9.28)$$

The stationary-point values of $Q(\tilde{\gamma}; t^0)$ are related to the "physical" correlations and responses defined in Eqs. (8.29) and (8.30) as follows

$$N Q^{++}(\tilde{\gamma}; t^0) = \overline{\gamma^+(t) \gamma^+(t^0)} = N C(\tilde{\gamma}; t^0) + \frac{i\hbar}{2} (R(\tilde{\gamma}; t^0) + R(t^0; \tilde{\gamma})); \quad (9.29)$$

$$N Q^+(\tilde{\gamma}; t^0) = \overline{\gamma^+(t) \gamma(t^0)} = N C(\tilde{\gamma}; t^0) + \frac{i\hbar}{2} (R(\tilde{\gamma}; t^0) - R(t^0; \tilde{\gamma})); \quad (9.30)$$

$$N Q^{-}(\tilde{\gamma}; t^0) = \overline{\gamma^-(t) \gamma^-(t^0)} = N C(\tilde{\gamma}; t^0) - \frac{i\hbar}{2} (R(\tilde{\gamma}; t^0) - R(t^0; \tilde{\gamma})); \quad (9.31)$$

$$N Q(\tilde{\gamma}; t^0) = \overline{\gamma(t) \gamma(t^0)} = N C(\tilde{\gamma}; t^0) + \frac{i\hbar}{2} (R(\tilde{\gamma}; t^0) + R(t^0; \tilde{\gamma})); \quad (9.32)$$

with $N C(\tilde{\gamma}; t^0) = \sum_i C_{ii}(\tilde{\gamma}; t^0)$ and $N R(\tilde{\gamma}; t^0) = \sum_i R_{ii}(\tilde{\gamma}; t^0)$. It is easy to check that these functions satisfy the identity $Q^{++}(\tilde{\gamma}; t^0) + Q^-(\tilde{\gamma}; t^0) - Q^+(\tilde{\gamma}; t^0) - Q(\tilde{\gamma}; t^0) = 0$. At the classical level this identity reduces to the condition $\hat{\gamma}(t) \hat{\gamma}(t^0) = 0$ for all pairs of times t, t^0 . In what follows we do not break this identity and hence do not allow for solutions that break causality.

The functional integration over $\gamma_i(t)$ and $\gamma_i(t^0)$ is now quadratic and can be performed. Symmetrizing the operator Op with respect to the Greek indices and times the integral over the fields γ amounts to replacing the quadratic term in $i\hbar S_{\text{eff}}$ by

$$\frac{N}{2} \int dt \int dt^0 \text{Tr} \log \left(\frac{1}{\hbar} \text{Op}_{\text{symm}}(\tilde{\gamma}; t^0) + \frac{1}{\hbar} \hat{Q}(\tilde{\gamma}; t^0) \right); \quad (9.33)$$

At this stage, all terms in the action depend upon the "macroscopic" quantities \hat{Q} ; Q and γ and are proportional to N . Since it is easier to write the equations in matrix notation, we encode \hat{Q} and Q in two matrices

$$\hat{Q} = \begin{pmatrix} \hat{Q}^{++} & \hat{Q}^{+} \\ \hat{Q}^{-} & \hat{Q} \end{pmatrix} \quad Q = \begin{pmatrix} Q^{++} & Q^{+} \\ Q^{-} & Q \end{pmatrix}$$

and we define

$$F[Q](t; t^0) = \frac{g^2}{2h} \int_{t^0}^t F_r^2(r+1) \frac{(Q^{++}(t; t^0))^r}{(Q^+(t; t^0))^r} \frac{(Q^+(t; t^0))^r}{(Q^-(t; t^0))^r} dt; \quad (9.34)$$

the saddle-point with respect to $i\hat{Q}^-(t; t^0)$ yields $i\hat{Q}^-(t; t^0) = \frac{h}{i} Q^{-1}(t; t^0) \circ p(t; t^0)$. The matrix and time-operator inverse of Q is denoted Q^{-1} . The saddle-point equation with respect to $Q^-(t; t^0)$ yields $i\hat{Q}^-(t; t^0) = \frac{i}{2h} F[Q](t; t^0)$. These saddle-point equations imply, in a compact matrix and time-operator notation,

$$\frac{i}{h} \circ p_{\text{symm}} Q = I - \frac{1}{2h^2} F[Q] Q; \quad (9.35)$$

where I is the identity: $I(t; t^0) = \delta(t - t^0)$ and we denote with a cross the standard operational product in matrix and time (see Appendix D). The saddle-point with respect to $i\hat{Q}^+$ yields

$$i\hbar = (\circ p + i\hat{Q}^+)^{-1}(t; t) = i\hbar Q^{++}(t; t); \quad (9.36)$$

and similarly for Q^- . These equations lead to the spherical constraint.

The dynamic equations for the auto-correlation and response follow from the set of equations (9.34)–(9.35) and the definitions of the dynamic order parameters given in Eqs. (9.29)–(9.32). More precisely, the equation of motion for the response function follows from the subtraction of the $++$ and $+-$ components of Eq. (9.35):

$$M \partial_t^2 + \frac{1}{2} \dot{C}(t) + \frac{1}{2} \int_{t^0}^t dt^0 \dot{C}(t^0) R(t^0; t^0) = \frac{1}{2} \dot{C}(t) \\ \frac{g^2}{2h} \int_{t^0}^t F_r^2(r+1) \int_{t^0}^t dt^0 \frac{h}{2} (Q^{++}(t; t^0))^r (Q^+(t; t^0))^r R(t^0; t^0); \quad (9.37)$$

and the equation of motion for the correlation follows from the addition of the $++$ and $+-$ components of Eq. (9.35):

$$M \partial_t^2 + \frac{1}{2} \dot{C}(t) + \frac{1}{2} \int_{t^0}^t dt^0 \dot{C}(t^0) R(t^0; t^0) + \frac{1}{2} \int_{t^0}^t dt^0 \dot{C}(t^0) C(t^0; t^0) \\ = \frac{g^2}{2h} \int_{t^0}^t F_r^2(r+1) \int_{t^0}^t dt^0 \frac{h}{2} (Q^{++}(t; t^0))^r Q^+(t^0; t^0) \\ (Q^+(t; t^0))^r Q^-(t^0; t^0); \quad (9.38)$$

Written in this way, Eq. (9.38) is complex. Its imaginary part yields $\dot{C}(t) + \frac{1}{2} \int_{t^0}^t dt^0 \dot{C}(t^0) R(t^0; t^0) = 0$. Moreover, since the response is causal, products of advanced $R(t; t^0)$ and retarded $R(t^0; t)$ responses vanish identically for all $t; t^0$: $R(t; t^0)R(t^0; t) = 0$, $\forall t; t^0$ and one can show that for any integer $k > 0$ and any constants c_1, c_2 , $[C(t; t^0) + c_1 R(t; t^0) + c_2 R(t^0; t)]^k = [C(t; t^0) + c_1 R(t; t^0)]^k + [C(t; t^0) + c_2 R(t^0; t)]^k$. Using this property one has $(Q^{++}(t; t^0))^r (Q^+(t; t^0))^r = 2i \text{Im} [C(t; t^0)]^k$.

$\frac{i\hbar}{2}R(t;t^0)]$ and $\text{Im}[(Q^{++}(t;t^0))^*Q^{+}(t^0;t^0) - (Q^{+}(t;t^0))^*Q^{-}(t^0;t^0)] = 2C(t^0;t^0)$
 $\text{Im}[C(t;t^0) - \frac{i\hbar}{2}R(t;t^0)] = \hbar R(t;t^0)\text{Re}[C(t;t^0) - \frac{i\hbar}{2}(R(t;t^0) + R(t^0;t))]^*$. We can identify the self-energy $\tilde{\Sigma}$ and the vertex \tilde{D} as

$$\tilde{\Sigma}(t;t^0) = 4(t-t^0)\tilde{\Sigma}(t;t^0) - D(t;t^0) - 2\hbar(t-t^0)\tilde{D}(t;t^0)$$

$$\tilde{\Sigma}(t;t^0) = \frac{g^2}{\hbar} \int_0^x F_r^2(x+1) \text{Im}[C(t;t^0) - (i\hbar)R(t;t^0)]^* ; \quad (9.39)$$

$$\tilde{D}(t;t^0) = \frac{g^2}{2} \int_0^x F_r^2(x+1) \text{Re}[C(t;t^0) - (i\hbar)(R(t;t^0) + R(t^0;t))]^* : \quad (9.40)$$

Note that the total self-energy $\tilde{\Sigma}$ and vertex \tilde{D} are real and have two contributions of different origin: one arises from the interaction of the system and the bath ($\tilde{\Sigma}$ and \tilde{D}) and one is caused by the non-linearities stemming from the average over disorder ($\tilde{\Sigma}$ and \tilde{D}).

The dynamic equations can then be written in the compact form (9.13) – (9.13). It is important to realize that the self-energy $\tilde{\Sigma}(t;t^0)$ is proportional to the response function $R(t;t^0)$, which in turns implies $\tilde{\Sigma}(t;t^0) = \tilde{\Sigma}(t;t^0) = 0$ for $t < t^0$. This means that the upper limit of integration in Eqs. (9.13) and (9.13) is t , which renders the equations explicitly causal. There are no more independent equations for R and C . The other two equations that can be obtained from Eq. (9.35) are the equation for $R(t^0;t)$, that is equivalent to Eq. (9.13), and one equation that identically cancels by virtue of the identity between two-point correlators.

Real and imaginary parts of Eqs. (9.36) and the one for Q combined with the saddle-point equation for $\tilde{\Sigma}$ imply the equal times conditions $C(t;t) = 1$; $R(t;t) = 0$. In addition, from Eq. (9.37) one obtains that the first derivative of the response function is discontinuous at equal times:

$$\lim_{t^0 \rightarrow t^-} \partial_t R(t;t^0) = \frac{1}{M} ; \quad \lim_{t^0 \rightarrow t^+} \partial_t R(t;t^0) = 0 ; \quad (9.41)$$

while from Eq. (9.38) one obtains that the first derivative of the correlation is continuous:

$$\lim_{t^0 \rightarrow t^-} \partial_t C(t;t^0) = \lim_{t^0 \rightarrow t^+} \partial_t C(t;t^0) = 0 : \quad (9.42)$$

In conclusion, Eqs. (9.13), (9.13) and (9.21) are the complete set of equations that determines the dynamics of the system.

9.2 Beyond fully-connected models

9.2.1 Classical models

A very useful formalism to study the statics of classical dilute disordered models with the replica trick has been introduced by Monasson [86] generalising the previous work of Motzishaw and de Dominicis [87]. The parallel between the static calculation using replicas and the dynamic formalism, once expressed in terms of superfields, exists also at the level of this approach. The presentation in this Section follows very

closely the one in [88] where the dynamic formalism apt to analyze dilute disordered models was introduced.

The dilute spin-glass, or Viana-Bray model in its Ising version, is a spin model defined on a random graph with average connectivity c and pair random exchanges taken from the probability distribution $P(J_{ij}) = (1 - c/N) \delta(J_{ij}) + c/N [\frac{1}{2} \delta(J_{ij} - J) + \frac{1}{2} \delta(J_{ij} + J)]$. For the sake of simplicity we consider the spherical version of this model. Let us define $c(\cdot)$ as the fraction of sites with super-field ϕ_i identical to a chosen value

$$c(\cdot) = \frac{1}{N} \sum_{i=1}^N \delta(\phi_i - \cdot); \quad (9.43)$$

for all values of the super-coordinate a . Note that $\int da c(a) = 1$. Similarly to what we have done when introducing $Q(a;b)$ in Eq. (9.5) we enforce the definition of $c(\cdot)$ in the generating functional by introducing an identity in its path integral representation: $1 = \int da \delta(c(\cdot) - \frac{1}{N} \sum_{i=1}^N \delta(\phi_i - a)) = \int da \delta(c(\cdot) - \frac{1}{N} \sum_{i=1}^N \delta(\phi_i - a)) \exp[\int da \delta(c(\cdot) - \frac{1}{N} \sum_{i=1}^N \delta(\phi_i - a))]$. We obtain

$$Z = \int da \delta(c(\cdot) - \frac{1}{N} \sum_{i=1}^N \delta(\phi_i - a)) \exp[\int da \delta(c(\cdot) - \frac{1}{N} \sum_{i=1}^N \delta(\phi_i - a)) \sum_{i=1}^N \delta(\phi_i - a)] + \frac{N}{2} \int da c(a) (D_a^{(2)} + S(a)) (a) da V[a];$$

$V[a] = \sum_{ij} J_{ij} \phi_i(a) \phi_j(a)$. Once written in this form, the average over disorder can be simply performed and the disordered averaged generating functional becomes $[Z] = \int da \delta(c(\cdot) - \frac{1}{N} \sum_{i=1}^N \delta(\phi_i - a)) \exp(-N G)$ with

$$G = \int da \delta(c(\cdot) - \frac{1}{N} \sum_{i=1}^N \delta(\phi_i - a)) \left[\frac{1}{N} \sum_{i=1}^N \delta(\phi_i - a) + \frac{1}{2} \int da c(a) (D_a^{(2)} + S(a)) (a) + H_{eff} \right]$$

and $\exp(-N H_{eff}) = \int da V[a]$. With the notation $N H_{eff}$ we suggest that H_{eff} is of order one. We shall discuss this very important issue below.

The second term in G is now the only term where the ϕ_i 's appear and all of them contribute in exactly the same form. One can then replace the sum over i by a factor N times $\delta(\phi_i - a)$ and exponentiate the functional integral over the representative super-field ϕ_i , $\int d\phi_i \exp(\phi_i \delta(\phi_i - a)) = \exp(N \ln \int d\phi \exp(\phi \delta(\phi - a)))$. The saddle-point equation on $\delta(\phi)$ reads $\delta(\phi) = \frac{\ln c(\cdot)}{N} \ln \int d\phi \exp(\phi \delta(\phi - a))$. Replacing this expression for $\delta(\phi)$ and using the fact that $\int da c(a) = 1$, the generating functional averaged over disorder becomes $[Z] = \int da \delta(c(\cdot) - \frac{1}{N} \sum_{i=1}^N \delta(\phi_i - a)) \exp[-N S_{eff}(c)]$ with

$$S_{eff}(c) = \int da c(a) \ln c(a) + \frac{1}{2} \int da c(a) (D_a^{(2)} + S(a)) (a) + H_{eff};$$

The first term is an entropic contribution, the second term is a kinetic energy and the third one is the potential energy.

The difficulty now arises as to how to compute the effective Hamiltonian H_{eff} . For fully connected models as the ones discussed in the previous Section H_{eff} can

be calculated exactly and one recovers the dynamic equations that were already known (see below). For dilute disordered models, or models defined on a random graph, H_{eff} is still a quantity of order one. In this sense we still call them mean-field models. This property allows us to pursue the calculation with a saddle-point approximation. H_{eff} is determined by a set of iterative approximations. For finite dimensional models the situation worsens still since a saddle-point approximation cannot be used without taking into account the fluctuations around it.

Gaussian approximation

In this Section we assume that we deal with any model such that the effective action S_{eff} is indeed of order N . In a first step we resort to a Gaussian approximation, in which one proposes:

$$c(\cdot) = (\det Q)^{-1/2} e^{\frac{1}{2} \sum_{i,j}^R \text{dadb}_{ij}(\mathbf{a}) Q^{-1}_{ij}(\mathbf{a};\mathbf{b}) \cdot \mathbf{b}} : \quad (9.44)$$

The denominator ensures the normalization of $c(\cdot)$ and $Q(\mathbf{a};\mathbf{b})$ is correctly given by the averaged correlator: $Q(\mathbf{a};\mathbf{b}) = N^{-1} \sum_{i,j}^R \frac{1}{N} \langle \mathbf{a}_i \mathbf{a}_j \rangle \langle \mathbf{b}_i \mathbf{b}_j \rangle e^{\frac{1}{2} \sum_{i,j}^R \text{dadb}_{ij}(\mathbf{a}) Q^{-1}_{ij}(\mathbf{a};\mathbf{b}) \cdot \mathbf{b}}$ with $N = (\det Q)^{-1/2}$. After rather simple manipulations the c -dependent effective action can be expressed in terms of $Q(\mathbf{a};\mathbf{b})$, $2S_{\text{eff}}(Q) = \text{Tr} \ln Q + \sum_{i,j}^R \text{dadb}_{ij}(\mathbf{a}) \langle \mathbf{b}_i \mathbf{b}_j \rangle + \sum_{i,j}^R \text{dadb}_{ij}(\mathbf{a}) Q(\mathbf{a};\mathbf{b}) - 2H_{\text{eff}}(Q)$. Its variation with respect to Q yields:

$$\frac{\delta S_{\text{eff}}(Q)}{\delta Q} = 0 = \frac{1}{2} Q^{-1}(\mathbf{a};\mathbf{b}) + \frac{1}{2} \langle \mathbf{b}_a \mathbf{b}_a \rangle + \sum_{i,j}^R \text{dadb}_{ij}(\mathbf{a}) Q(\mathbf{a};\mathbf{b}) - \frac{H_{\text{eff}}(Q)}{Q(\mathbf{a};\mathbf{b})} : \quad (9.45)$$

Multiplying this equation operationally by $Q(\mathbf{b};\mathbf{a}^0)$ (see Appendix D) the dynamic equation takes the more familiar form (9.11) with $\langle \mathbf{a};\mathbf{a}^0 \rangle = \frac{1}{2} H_{\text{eff}}(Q) = Q(\mathbf{a};\mathbf{a}^0)$.

One example: the infinite range p spin model

The p spin spherical model is a particular case of the model in (9.2) with

$$\begin{aligned} 4H_{\text{eff}} &= \frac{1}{N} \sum_{i_1, \dots, i_p}^X \frac{1}{N^{p-1}} \sum_{j_1, \dots, j_p}^Z \text{dadb}_{i_1 j_1}(\mathbf{a}) \dots \text{dadb}_{i_p j_p}(\mathbf{a}) = \sum_{i_1, \dots, i_p}^Z \text{dadb}_{i_1 j_1}(\mathbf{a}) \dots \text{dadb}_{i_p j_p}(\mathbf{a}) \frac{1}{N} \sum_{i=1}^N \mathbf{a}_i \mathbf{a}_i \\ &= \sum_{i_1, \dots, i_p}^Z \langle \mathbf{a}_{i_1} \mathbf{a}_{i_1} \rangle \dots \langle \mathbf{a}_{i_p} \mathbf{a}_{i_p} \rangle c(\mathbf{a}_{i_1}) \dots c(\mathbf{a}_{i_p}) \sum_{j_1, \dots, j_p}^Z \text{dadb}_{j_1 i_1}(\mathbf{a}) \dots \text{dadb}_{j_p i_p}(\mathbf{a}) \\ &= \sum_{j_1, \dots, j_p}^Z \text{dadb}_{j_1 i_1}(\mathbf{a}) \dots \text{dadb}_{j_p i_p}(\mathbf{a}) \langle \mathbf{a}_{i_1} \mathbf{a}_{i_1} \rangle \dots \langle \mathbf{a}_{i_p} \mathbf{a}_{i_p} \rangle c(\mathbf{a}_{i_1}) \dots c(\mathbf{a}_{i_p}) \end{aligned} \quad (9.46)$$

Replacing the Gaussian Ansatz (9.44), H_{eff} becomes a simple function of $Q(\mathbf{a};\mathbf{b})$:

$$H_{\text{eff}}(Q) = \frac{1}{4} \sum_{i,j}^Z \text{dadb}_{ij} Q^{-1}(\mathbf{a};\mathbf{b}) : \quad (9.47)$$

The full expression for the effective action $S_{\text{eff}}(Q)$ is identical to Eq. (9.9). A way to prove that the Gaussian Ansatz (9.44) is exact for this model is to check that the exact equation for $c(\cdot)$ coincides with the one obtained from the Gaussian Ansatz and the saddle-point evaluation.

A second example: the dilute spherical spin-glass

In this case the effective Hamiltonian $H_{\text{eff}}(c)$ reads

$$2H_{\text{eff}}(c) = \int \int d\mathbf{a} d\mathbf{a}' c(\mathbf{a}) c(\mathbf{a}') \cosh J \mathbf{a} \cdot \mathbf{a}' : \quad (9.48)$$

With the Gaussian Ansatz, this expression becomes

$$2H_{\text{eff}}(Q) = \int \frac{d\mathbf{Q}}{\det(1 - J^2 Q^2)} : \quad (9.49)$$

The self-energy can only be expressed as a series expansion or a functional:

$$(a;b) = \int d\mathbf{Q} (1 - J^2 Q^2)^{-1} (a;b) = \int d\mathbf{Q} \sum_{k=0}^{\infty} J^{2k} Q^{(2k+1)} (a;b) : \quad (9.50)$$

Using the first expression for one derives the dynamic equation

$$(c-1)J^2 Q^2 (a;b) + (a-b) = D_a^{(2)} \int d\mathbf{Q} (J^2 Q^3) (a;b) : \quad (9.51)$$

Otherwise, if we use the second expression we obtain a dynamic equation involving a series. Note that this equation is much more complicated than the one for the fully connected p spin spherical model. The derivatives act on functionals of the correlator Q in this case. Moreover, the Gaussian approximation is not exact for dilute models. An iterative method can be implemented to go beyond this approximation. It was introduced in [88] but we shall not describe it here.

9.2.2 Quantum models

Once we have presented the method for the classical dynamics, its extension to a quantum system is simple. The important point to remark about the previous derivation is that the susy notation has been used, mostly, as a bookkeeping device. In the quantum case a susy formalism is not useful. Instead, it is convenient to use the formalism apt to take the classical limit, encoding the variables $(q; \dot{q})$ in a two-component (column) vector \tilde{v} , and defining a (line) vector \mathbf{v} :

$$\tilde{v}_i = \begin{pmatrix} q_i \\ \dot{q}_i \end{pmatrix}, \quad \mathbf{v} = \begin{pmatrix} 1 \\ \frac{i\hbar}{2} \end{pmatrix};$$

the effective action reads

$$S_{\text{eff}} = S_{\text{kin}}(\mathbf{v}, \tilde{v}_i) = S_{\text{kin}}(\mathbf{v}, \tilde{v}_i) + S_{\text{pot}}(\mathbf{v}, \tilde{v}_i) = S_{\text{pot}}(\mathbf{v}, \tilde{v}_i) + S_{\text{th}}(\tilde{v}_i) \quad (9.52)$$

with the thermal part of the action written as

$$S_{\text{th}}(\tilde{v}) = \int dt \int dt^0 \tilde{v}_i^t(t) A(t-t^0) \tilde{v}_i(t^0) : \quad (9.53)$$

Calling $a = 1;2$ the vector indices, the notation becomes identical to the susy one, with a here playing the rôle of the coordinate in super-space $a = (t; \bar{t})$ in the classical problem. Just as in the previous Section, one introduces the identity (9.43), where a is now interpreted as a vector index, to rewrite the generating functional. The analysis of the kinetic and thermal part of the effective action follows the same lines as the one presented for the classical problem.

9.3 Field equations

Once we have written the dynamic action in terms of ϕ_i and $\hat{\phi}_i$ the "field equations" follow from exact properties of the functional integration [65]. Indeed,

$$\begin{aligned} 0 &= \int \mathcal{D}\phi \mathcal{D}\hat{\phi} \frac{1}{\hat{\phi}_i(t)} e^{-S_{\text{eff}}[\phi; \hat{\phi}] + \int_C dt^0 (\phi_i(t^0) \hat{\phi}_i(t^0) + \hat{\phi}_i(t^0) \hat{\phi}_i(t^0))} \\ &= \int \mathcal{D}\phi \mathcal{D}\hat{\phi} \frac{S_{\text{eff}}(\phi; \hat{\phi}_i)}{\hat{\phi}_i(t)} + \hat{\phi}_i(t) e^{-S_{\text{eff}}(\phi; \hat{\phi}_i) + \int_C dt^0 (\phi_i(t^0) \hat{\phi}_i(t^0) + \hat{\phi}_i(t^0) \hat{\phi}_i(t^0))} : \end{aligned}$$

The subindex C in the integrals stands for "time contour" and it can describe the usual integration from the initial time to infinity for classical models or the closed time path for quantum ones. Taking now the variation with respect to the source $\hat{\phi}_j(t^0)$ and evaluating at $\phi = \hat{\phi} = 0$ for all times and components we find

$$0 = \langle \phi_{ij}(t^0) \hat{\phi}_j(t^0) \frac{S_{\text{eff}}(\phi; \hat{\phi}_i)}{\hat{\phi}_i(t)} \rangle^* \quad (9.54)$$

where the brackets denote an average with the measure weighted by the dynamic action S_{eff} . If, instead one takes the variation with respect to $\phi_j(t^0)$ and later evaluates at $\phi = \hat{\phi} = 0$ one obtains:

$$\langle \hat{\phi}_i(t) \frac{S}{\phi_j(t^0)} \rangle^* = 0 : \quad (9.55)$$

A way to derive dynamic equations for the two-point correlators amounts to use Wick's theorem and rewrite these averages as a sum over all possible factorizations in products of two point-functions. This is of course exact if the action is quadratic but it is only a Gaussian approximation for more general models. This kind of derivation has been mainly used in the study of the dynamics of manifolds in random potentials [89].

9.4 The thermodynamic limit and time-scales

It is very important to stress that the dynamic equations derived with the saddle-point approximation hold only when $N \rightarrow \infty$ before any long-time limit is taken. They describe the dynamics in finite time-scales with respect to N and they cannot capture the crossover from the non-equilibrium relaxation to the equilibrium dynamics reached in time scales that diverge with N [remember that $t_{\text{eq}}(N)$].

Previous attempts to study the dynamics of disordered glassy systems assumed that these same equations hold for the equilibrium dynamics when N is finite and time-scales diverge with N [90]. This assumption is wrong as shown by several inconsistencies found in the solution at low temperatures: (i) the asymptotic values of one time-quantities do not necessarily coincide with the values calculated with the equilibrium distribution. (ii) the solution exhibited violates the fluctuation-dissipation theorem. These two results are not compatible with equilibrium.

In order to study the equilibrium dynamics of these models one should (i) start from random initial conditions but reach times that grow with N or (ii) impose equilibrium initial conditions. The second route has been implemented (though without solving the full dynamic problem) by Houghton, Jain and Young [80]. They showed that in this case one is forced to introduce the replica trick to average over disorder.

The dynamic equations here derived are correct when $N \rightarrow 1$ at the outset. Since times are always finite with respect to N , when $t_{eq}(N)$ diverges with N the dynamics is not forced to reach equilibrium and there is no contradiction if the solution violates the equilibrium theorems.

9.5 Single spin equation

In the limit $N \rightarrow 1$ one can also write the full action S_{eff} in terms of a single variable. This is at the expense of modifying the thermal kernel and the interaction term in a self-consistent way, through the introduction of terms arising from the non-linear interactions (the vertex and self-energy, respectively). For a classical model with white external noise the single variable equation reads

$$M_i(t) + \gamma_i(t) + \int_0^t dt' \gamma_i(t, t') \dot{x}_i(t') = \dot{x}_i(t) + \gamma_i(t) : \quad (9.56)$$

Its generalisation is straightforward. There are two noise sources in this equation: $\gamma_i(t)$ is the original white noise while $\gamma_i(t)$ is an effective (Gaussian) noise with zero mean and correlations self-consistently given by $\langle \gamma_i(t) \gamma_j(t') \rangle = \delta_{ij} D(t, t')$. The vertex $D(t, t')$ plays the rôle of the colored noise correlation in a usual Langevin equation. The self-energy $\gamma_i(t, t')$ appears here in the place of an 'integrated friction'. A solution of the problem can be attempted numerically using this equation and the self-consistent definitions of γ and D .

This procedure is not particularly useful for the analysis of 'polynomial' models since the transformation into a Q -dependent effective action can be done exactly. It does however become useful for dealing with models whose single-spin effective action has higher order interaction terms. An example is the quantum spin model. This procedure is similar to the one used in dynamic mean-field theory [91].

Interestingly enough, as shown in Section 7.4, a rather damped harmonic oscillator coupled to a bath made of a white and a coloured part at different temperatures acquires two time-scales controlled by the two temperatures involved. We see that a similar structure might appear for the glassy system if the self-energy and vertex self-consistently arrange to act on each degree of freedom as the friction and noise-noise correlator of a complex bath. We shall see that this is indeed what happens to mean-field models. We believe that a similar mechanism arises in finite dimensional glassy models as well [72].

10 Diagrammatic techniques

In this Section we first describe the perturbative solution to the Langevin process and how it is used to construct series expansions for the correlations and responses. Self-consistent approximations, such as the mode coupling or the self-consistent screening, correspond to a selection of a subset of diagrams from the full series. The connection with disordered models is demonstrated. The presentation is very close to the one in [92]. An extension to quantum problems is possible using the generating functional formalism.

10.1 Perturbative solution

Let us focus on a single scalar degree of freedom, q , with potential energy

$$V(q) = \frac{\gamma(t)}{2} q^2 + \frac{g}{3!} q^3; \quad (10.1)$$

and dynamics given by the Langevin Eqs. (4.7) and (4.8) in the white noise limit. We take the initial condition $q(t=0) = 0$. $\gamma(t)$ is a time-dependent function that we fix at the end of the derivation by requiring $C(t;t) = 1$. In vector models it is the Lagrange multiplier that self-consistently imposes a spherical constraint. Note that this potential is not bounded from below. Setting $G_0(t;t^0) = [\gamma(t) + \gamma(t^0) + M\gamma(t^0)]^{-1}$, a perturbative expansion for $q(t)$ in powers of the noise is easily written as

$$q(t) = (G_0 \circ \gamma)(t) + \frac{g}{2} (G_0 \circ [G_0 \circ G_0 \circ \gamma])(t) + \dots \quad (10.2)$$

where \circ means a time convolution, $(G_0 \circ f)(t) = \int_0^t dt^0 G_0(t;t^0) f(t^0)$, and \circ is a simple product at equal times. This notation is equivalent to the one used in the susy formalism, see Appendix D. Causality implies $G_0(t;t^0) = 0$ for $t < t^0$. If inertia can be neglected $G_0(t;t^0) = \exp\left(-\int_{t^0}^t \gamma(t') dt'\right)$. If one keeps the second-time derivative $G_0(t;t^0)$ takes a more complicated form. Equation (10.2) can be graphically represented as in Fig. 10. Crosses indicate noise and oriented lines indicate the bare propagator G_0 . Each vertex carries a factor $g=2$. Note that the unknown q is evaluated at time t while the noises are evaluated at all previous times.

Figure 10: Terms $O(g^0)$, $O(g^1)$ and $O(g^2)$ in the perturbative solution to the Langevin equation.

The expansion for q leads to two expansions for the correlation and response. In simple words, the former corresponds to sandwiching, i.e. averaging over the noise, the usual product of two series as the one in Fig. 10 evaluated at different times t and t^0 . Due to the average over the Gaussian noise noise factors have to be taken by pairs. Let us illustrate this with a few examples.

The first term in the expansion is the result of averaging two $O(g^0)$ terms (first term in Fig. 10):

$$C_0(t; t^0) = h(G_0(t)) (G_0(t)) = 2 k_B T \int_0^{t^0} dt G_0(t; t^0) G_0(t^0; t^0); \quad (10.3)$$

Fig. 11. We depict this term and its contributions to more complicated diagrams with a single crossed line, see the first graph in Fig. 11. The term $O(g)$, as well as all terms which are odd powers of g , vanishes. There are two contributions to the term $O(g^2)$. One is the result of multiplying a term $O(g^2)$ with a term $O(g^0)$ and it is a tadpole, see the second graph in Fig. 11; we assume this term and all its corrections are included in the contributions from the time-dependent mass and we henceforth ignore them. The other comes from multiplying two $O(g)$ terms, see the third graph in Fig. 11.

Higher order terms are of two types: they either dress the propagators or they dress the vertices, see the last two diagrams in Fig. 11. These two terms are order $O(g^4)$. The first one follows from averaging two $O(g^2)$ contributions while the second one is the result of averaging an $O(g^3)$ and an $O(g)$ term. The full series yields the exact perturbative expansion for C .

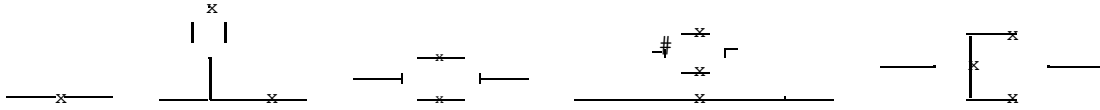


Figure 11: From left to right: $O(g^0)$, two $O(g^2)$ and two $O(g^4)$ terms in the series for C . The next to last diagram dresses the propagator and the last term dresses the vertex. The former is kept in the mca while the latter is neglected.

The series expansion for the response follows from the relation (8.8) in the white noise limit. In graphical terms we obtain it by multiplying the series in Eq (10.2) and Fig. 10 evaluated at time t by a noise evaluated at time t^0 and taking the average.

10.2 The mode coupling approximation (mca)

The diagrammatic expansions for C and R can be represented analytically by introducing the kernels $\Gamma(t; t^0)$ and $D(t; t^0)$ through the Schwinger-Dyson equations (9.18) and (9.19) in their integral form. Each of them is a compact notation for a series of diagrams. These equations are exact perturbatively. However, for a generic model one cannot compute the kernels Γ and D exactly.

The mode coupling approach amounts to approximating the kernels $\Gamma(t; t^0)$ and $D(t; t^0)$ in the following way. One takes their values at $O(g^2)$ and substitutes in them the bare propagator G_0 and the bare correlation C_0 by their dressed values, i.e. by R and C themselves. For the model defined in Eq. (10.1) this yields

$$\Gamma(t; t^0) = g^2 C(t; t^0) R(t; t^0); \quad (10.4)$$

$$D(t; t^0) = 2 k_B T \left(\Gamma(t; t^0) + \frac{g^2}{2} C^2(t; t^0) \right); \quad (10.5)$$

This approximation neglects "vertex renormalization" in the sense that all diagrams correcting the values of the lines are taken into account while all diagrams correcting the vertices are neglected. For instance, one keeps the fourth diagram in Fig. 11 that represents a line correction, while leaving aside the fifth diagram drawn in the same figure that represents a vertex correction.

The same procedure can be implemented using the susy representation of the dynamics. Each line represents the super field and the super-correlator follows from the sandwich of two series for the super-field evaluated at different super-coordinates a and b .

The Schwinger-Dyson equations can be recast, after multiplying by G_0^{-1} , into the form (9.16) and (9.17) for a random potential (9.2) with only one term $r = p = 3$. Applying the mca to the trivial (and ill-defined) model (10.1) we derived the dynamic equations for the $p = 3$ spin spherical model! On the one hand, this result is worrying since it shows that the mca can be rather uncontrolled and it can generate glassy behavior by itself. On the other hand, since the same equations hold in the mca of a model of interacting particles with realistic interactions, this calculation allows one to understand why the dynamic equations of the mct for super-cooled liquids coincide with the ones of disordered spin models above T_d . In the next Subsection we show how the diagrams neglected in the mca vanish in a disordered model with a large number of components. (See also [93] for other recent discussions of the meaning and range of validity of the mca and mct.)

10.3 mca and disordered models

The first to notice that the mca for a "quadratic" dynamic equation corresponds to the exact dynamic equation of a disordered problem with a large number of components was Kraichnan [94] in the context of the Navier-Stokes equation. More recently, Franz and Hertz showed that the "schematic mct equations of the F_p group" for super-cooled liquids are identical to those arising from a spin model with pseudo-random interactions between groups of three spins [95]. (The schematic mct focus on a chosen wavevector.)

Indeed, for the example chosen in this Section, one easily demonstrates that the diagrams retained by the mca are precisely those which survive if one modifies the initial model (10.1) and considers instead the following disordered problem [92]. First, let us upgrade q to a vector with N components or "colors" i , where $i = 1; 2; \dots; N$. Second, let us modify the potential energy (10.1) into

$$V(\tilde{\mathbf{r}}) = g \sum_{i < j < k}^X J_{ijk} \tilde{r}_i \tilde{r}_j \tilde{r}_k \quad (10.6)$$

with couplings J_{ijk} that are independent quenched Gaussian random variables of zero mean and variance $[J_{ijk}^2]_J = 1/N^{p-1} = 1/N^2$. (p is the number of spins in each term in V .) In the large N limit, the noise and disorder averaged correlation and response of this modified model obey Eqs. (9.16) and (9.17) with $\tilde{\mathbf{r}}$ and D given by Eqs. (10.4) and (10.5), respectively. The fact that these equations are recovered can be seen either directly on the perturbation theory, or using the functional methods

given in Section 8. Since we want to stress that the diagrams neglected in the mca vanish exactly for this model we use here the first approach.

The bare propagator is diagonal in the color indices, $G_{oij} = G_o \delta_{ij}$. The vertex is now proportional to the random exchanges J_{ijk} . The perturbative solution to the Langevin equation reads

$$\dot{\phi}_i(t) = (G_o \ddot{\phi}_i(t) - \sum_{j,k} J_{ijk} G_o (\dot{\phi}_j - \dot{\phi}_k)(t) + \dots) \quad (10.7)$$

One is interested in computing the self-correlation averaged over the noise and disorder, $N^{-1} \sum_{i=1}^N [\phi_i(t) \phi_i(t^0)]$. The latter average eliminates all terms with an odd number of couplings. Similarly, since $J_{ijk} \neq 0$ only if all indices i, j, k are different, tadpole contributions as the one in the second graph in Fig. 11 vanish (the noise-noise correlation enforces that two indices in the random exchange must coincide). Finally, one can check that due to the scaling with N of the variance of the disordered interactions, vertex corrections as the one in the last graph in Fig. 11 are sub-leading and vanish when $N \rightarrow \infty$. Instead, all line corrections remain finite in the thermodynamic limit. We can check this statement in the two examples shown in Fig. 11 extended to include color indices. The vertex correction has four random exchanges that due to the averaging over the noise are forced to match as, e.g. $J_{ijk} J_{jlm} J_{mni} J_{kln}$ leaving 6 free-indices. Averaging over disorder one identifies the indices of two pairs of J 's, e.g. $i = l$ and $k = m$, this yields a factor $(1/N^2)^2$ and, at most, it leaves 4 color indices over which we have to sum from 1 to N (i, j, k, n). We have then an overall factor $1/N^4 \cdot N^4 = 1$ and this term vanishes when one normalises the correlation by N . Instead, in the line correction, after averaging over the noise, we are left with 6 free indices, e.g. $J_{ikj} J_{kln} J_{lmn} J_{inj}$, the average over the noise only imposes $k = n$ in its most convenient contribution, and the overall factor is $1/N^4 \cdot N^5 = N$. This term contributes to the normalised global correlation.

Interestingly enough, the equivalence between the mca and a disordered system extends to an arbitrary non-linear coupling $F(q)$. Expanding F in a power series $F(q) = \sum_{r=2}^{\infty} \frac{F_r}{r!} q^r$ the mca leads to

$$(\ddot{\phi}; \dot{\phi}^0) = g^2 \sum_{r=2}^{\infty} \frac{F_r^2}{(r-1)!} C^{r-1}(\ddot{\phi}; \dot{\phi}^0) R(\dot{\phi}; \dot{\phi}^0); \quad (10.8)$$

$$D(\ddot{\phi}; \dot{\phi}^0) = 2 k_B T (\ddot{\phi} - \dot{\phi}^0) + g^2 \sum_{r=2}^{\infty} \frac{F_r^2}{r!} C^r(\ddot{\phi}; \dot{\phi}^0); \quad (10.9)$$

Note that for r odd, there appears an additional "tadpole" contribution in Eq. (10.8), which we have assumed again that it has been re-absorbed into the mass term $\ddot{\phi}(t)$. The dynamic equations can also be obtained as the exact solution of the Langevin dynamics of N continuous spins ϕ_i interacting through the potential

$$V_J[\tilde{\phi}] = g \sum_{r=2}^{\infty} \frac{F_r}{r!} \sum_{i_1 < \dots < i_{r+1}} J_{i_1 \dots i_{r+1}} \tilde{\phi}_{i_1} \dots \tilde{\phi}_{i_{r+1}} \quad (10.10)$$

where $J_{i_1 \dots i_{r+1}}$ are quenched independent Gaussian variables with zero mean and $[(J_{i_1 \dots i_{r+1}})^2] / N^r$. Therefore the mc equations for a single dynamic variable

in contact with a heat reservoir and under an arbitrary nonlinear potential $F(\mathbf{q})$ describe exactly a fully-connected spin-glass problem with arbitrary multi-spin interactions or a particle evolving in an N dimensional space in a quenched random potential $V[\mathbf{r}]$ with a Gaussian distribution with zero mean and variance (9.3) [96, 89]. Let us note that in order to be well defined, the model given by V must be supplemented by a constraint preventing the field ϕ from exploding in an unstable direction set by the coupling tensor $J_{i_1 \dots i_{r+1}}$. This problem is cured by imposing the spherical constraint $\sum_{i=1}^N \phi_i^2(t) = N C(t; t) = N$.

The extension of the mapping to a space dependent $\phi(\mathbf{x}; t)$ (or to a multicomponent field) is straightforward. Several interesting physical examples involve an equation of the type:

$$\frac{\partial \hat{\phi}(\mathbf{k}; t)}{\partial t} = -(\mathbf{k}^2 + \gamma) \hat{\phi}(\mathbf{k}; t) + \sum_{r=2}^{\infty} \frac{F_r}{r!} L_r(\mathbf{k}; \mathbf{k}_1; \dots; \mathbf{k}_r) \hat{\phi}(\mathbf{k}_1; t) \dots \hat{\phi}(\mathbf{k}_r; t) + \xi(\mathbf{k}; t)$$

where $\hat{\phi}(\mathbf{k}; t)$ is the Fourier transform of $\phi(\mathbf{x}; t)$, and $\xi(\mathbf{k}; t)$ a Gaussian noise such that $\langle \xi(\mathbf{k}; t) \xi^*(\mathbf{k}'; t') \rangle = 2 k_B T (\mathbf{k} + \mathbf{k}') \delta(t - t')$. The Kardar-Parisi-Zhang (kpz) equation [97] corresponds to $r = 2$, $L_2(\mathbf{k}; \mathbf{k}_1; \mathbf{k}_2) = [\mathbf{k}_1 \cdot \mathbf{k}_2] \mathbf{k}_1 + \mathbf{k}_2 + \mathbf{k}$, while domain coarsening in the ϕ^4 theory corresponds to $r = 3$, $L_3(\mathbf{k}; \mathbf{k}_1; \mathbf{k}_2; \mathbf{k}_3) = \mathbf{k}_1 + \mathbf{k}_2 + \mathbf{k}_3 + \mathbf{k}$, with a negative γ [1]. The Navier-Stokes equation is similar to the kpz case with, however, an extra tensorial structure due to the vector character of the velocity field. The correlation and response functions now become \mathbf{k} dependent, $\langle \phi(\mathbf{k} + \mathbf{k}'; t) \phi^*(\mathbf{k}; t') \rangle = \langle \phi(\mathbf{k}; t) \phi^*(\mathbf{k}'; t') \rangle$ and $\langle \phi(\mathbf{k} + \mathbf{k}'; t) R(\mathbf{k}; t; t') \rangle = \langle \phi(\mathbf{k}; t) R(\mathbf{k}'; t; t') \rangle$. The generalized mc equations then read (assuming that the structure factors are invariant under the permutation of $\mathbf{k}_1; \dots; \mathbf{k}_r$):

$$\begin{aligned} \langle \phi(\mathbf{k}; t; t^0) \rangle &= g^2 \sum_{r=2}^{\infty} \frac{F_r^2}{(r-1)!} \sum_{\mathbf{k}_1; \dots; \mathbf{k}_r} L_r(\mathbf{k}; \mathbf{k}_1; \dots; \mathbf{k}_r) L_r(\mathbf{k}_r; \mathbf{k}_1; \dots; \mathbf{k}_r) \\ &\quad C(\mathbf{k}_1; t; t^0) \dots C(\mathbf{k}_r; t; t^0) R(\mathbf{k}_r; t; t^0) \end{aligned} \quad (10.11)$$

$$\begin{aligned} D(\mathbf{k}; t; t^0) &= 2 k_B T \delta(t - t^0) + g^2 \sum_{r=2}^{\infty} \frac{F_r^2}{r!} \sum_{\mathbf{k}_1; \dots; \mathbf{k}_r} L_r(\mathbf{k}; \mathbf{k}_1; \dots; \mathbf{k}_r)^2 \\ &\quad C(\mathbf{k}_1; t; t^0) \dots C(\mathbf{k}_r; t; t^0) \end{aligned} \quad (10.12)$$

where $\langle \phi(\mathbf{k}; t; t^0) \rangle$ and $D(\mathbf{k}; t; t^0)$ are defined in analogy with Eqs. (10.8) and (10.9).

10.4 mca for super-cooled liquids and glasses

In the last 20 years the mca has been much used in the study of super-cooled liquids. Starting from the realistic interactions between the constituents of a liquid, Gotze et al [98] used the mca together with an assumption of equilibrium to derive a dynamic equation for the density-density correlator. This analysis led to the schematic mode coupling theory (mct) [99] of super-cooled liquids and generalisations [100] (with no reference to wave-vector dependence) and to more sophisticated versions that include

a dependence on space [98]. The difference between these models lies on the form of the kernels and D. Kirkpatrick, Thirumalai and Wolynes [11] realized in the late 80s that the schematic mode coupling equation [99] is identical to the dynamic equation for the spin-spin correlator in the disordered Potts or p spin model, building a bridge between the study of structural and spin glasses. Why these models and not sk? This will become clear when we present their dynamic and static behavior.

In this Section we explained why the dynamic equation of a disordered model and the one stemming from a m.c.a. of a model with more realistic interactions coincide: the terms neglected in the latter vanish exactly in the former. The example studied here serves also to signal the danger in using a m.c.a. One could conclude that a trivial model has a highly non-trivial dynamics, this being generated by the approximation itself.

In the derivation of the dynamic equations presented in this Section no assumption of equilibrium was used. Therefore, these equations hold also in the low temperature phase where equilibrium is lost. It is then natural to propose that the dynamics of the p spin spherical model below T_d schematically describes the dynamics of glasses just as its dynamics above T_d yields the schematic m.c.t. of super-cooled liquids [13]. To go beyond the schematic theory while still keeping a single mode description (as in [100]) one simply has to consider $p_1 + p_2$ spherical disordered models. Moreover, the dynamics of a manifold in a random potential is described by dynamic equations with a K dependence that goes beyond the single mode m.c.t.

Recently, Latz showed how the generic dynamic equations derived in this Section can also be obtained starting from the microscopic fluid system and using the m.c. approximation though with no equilibration assumption [102]. Alternative derivations of mode-coupling equations are discussed in [93]

Kawasaki and Kim [103] derived the same schematic m.c. equation using a non-disordered quadratic Hamiltonian for densities and velocities complemented with random non-linear dynamic equations. Interestingly enough, in this case the m.c.t. arises from a model with trivial statics and complex dynamics. Tuning the ratio between the number of density variables and velocity variables they even managed to include the so-called "hopping term" that softens the dynamic transition [98, 101]. Is worth noting that in Kawasaki and Kim's model this term is not due to thermally activated processes but to the effect of the velocity-like variables through the complex dynamics.

11 Glassy dynamics: Generic results

Before presenting the explicit solution to the mean-field models we state some generic features of the low- T dynamics that we believe hold in general.

11.1 The weak-ergodicity breaking scenario

Figure 12-right shows a sketch of the decay of the correlation as obtained from the numerical solution to the dynamic equations for the mean-field models (see

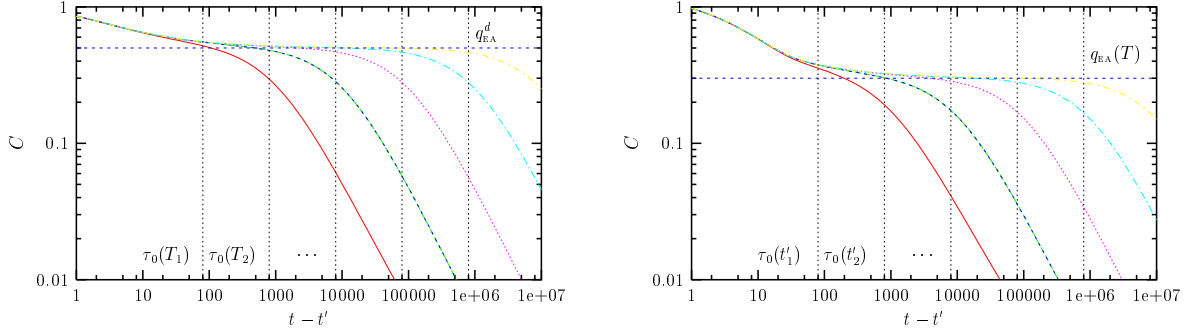


Figure 12: Left: Sketch of the decay of the stationary correlations in the high T phase close to T_d , $T_1 > T_2 > \dots$. Right: Sketch of the decay of the aging correlations in the low T phase, at fixed $T < T_d$, $t_1^0 < t_2^0 < \dots$

Section 12.1). It develops a separation of time scales in the long t^0 limit. It first approaches a plateau at q_{ea} in a stationary manner and it then decays below this value with an explicit waiting-time dependent form. For each waiting-time there is a sufficiently long t such that the correlation decays to zero. These properties are included in the weak-ergodicity breaking (web) scenario that states that, for $t \rightarrow \infty$, C decays in such a way that

$$\lim_{t^0 \rightarrow \infty} C(t; t^0) = q_{ea} + C_{st}(t - t^0) \quad (11.1)$$

$$\lim_{t \rightarrow \infty} C_{st}(t - t^0) = 0 \quad \Rightarrow \quad \lim_{t \rightarrow \infty} \lim_{t^0 \rightarrow \infty} C(t; t^0) = q_{ea} \quad (11.2)$$

$$\lim_{t \rightarrow \infty} C(t; t^0) = 0 \quad \text{at fixed } t^0: \quad (11.3)$$

Equation (11.2) defines the Edwards-Anderson order parameter, q_{ea} . For finite t^0 there is a crossover between two time-scales controlled by a waiting-time dependent characteristic time $\tau_0(t^0)$ that is a growing function of t^0 whose precise form depends on the model. For large $t - t^0$ such that $t - t^0$ is small with respect to $\tau_0(t^0)$, the correlation function first decays from 1 to q_{ea} in a stationary manner. At long $t - t^0$ it goes further below q_{ea} to eventually reach 0 in a manner that depends both upon t and t^0 (the aging effect). This behavior suggests the presence of at least two time-sectors in which the dynamics is stationary and non-stationary, respectively. We shall see that the number of time-scales, or more precisely correlation scales, depends on the model.

We write C as the sum of a stationary and an aging contribution:

$$C(t; t^0) = C_{st}(t - t^0) + C_{ag}(t; t^0): \quad (11.4)$$

The matching conditions at equal times between C_{st} and C_{ag} are $C(t; t) = 1$ implying $C_{st}(0) + C_{ag}(t; t) = 1$ with $C_{st}(0) = 1 - q_{ea}$ and $C_{ag}(t; t) = q_{ea}$. Together with Eq. (11.2) they ensure that in the two-time sector in which C_{st} decays from 1 to 0, C_{ag} is just a constant q_{ea} . Instead, in the two-time sector in which C_{ag} decays from q_{ea} to 0, C_{st} vanishes identically.

The new web [45, 12] reflects the fact that for short time-differences the system behaves as if it were trapped in some region of phase space of size q_{ea} suggesting ergodicity breaking. However, it is always able to escape this region in a time-scale $\tau_0(t^0)$ that depends upon its age t^0 . Hence, trapping is gradual and ergodicity breaking is weak. q_{ea} depends on temperature when $T < T_d$.

We have already described, phenomenologically, such a separation of time-scales in the decay of correlation functions when we discussed the domain growth problem and glassy dynamics in Section 2. The first term describes in this case the fast fluctuations within domains while the second term characterises the domain growth itself. A second example where such a separation of time-scales occurs are the trap models in phase space. The first term corresponds to the dynamics within the traps while the second describes the wandering of the system from trap to trap. In glasses, the first term corresponds to the rapid rattling of each particle within its cage while the second one describes the destruction of the cages and hence the structural relaxation.

In driven models rendered stationary by a weak perturbation we also find a separation of time-scales with τ_0 increasing with weaker strengths of the perturbation. We can also propose that C and R separate in two terms, both being stationary but evolving in different time-scales.

In classical purely relaxational models governed by a Langevin equation with no inertia the correlation functions are monotonic with respect to both times t and t^0 , as it is easily checked numerically. Inertia introduces oscillations and the decay can be non-monotonic. The magnitude of the oscillations depends upon the relative value of the mass M with respect to the other parameters in the problem. However, for a wide choice of parameters the oscillations appear only in the stationary regime, the aging dynamics having a monotonic decay towards zero. This is relevant since it allows one to use the general properties of monotonic correlation functions proven in [104] and discussed in Section 11.4 to find the two-time scaling of $C_{\text{ag}}(t; t^0)$.

11.2 The weak long-term memory scenario

Regarding the response function, we propose a similar separation in two terms:

$$R(t; t^0) = R_{\text{st}}(t - t^0) + R_{\text{ag}}(t; t^0) \quad (11.5)$$

with $R_{\text{st}}(t - t^0) = \lim_{t^0 \rightarrow 1} R(t; t^0)$. The matching conditions close to equal times are different for a model with or without inertia. In the former case, $R(t; t) = 0$, $R(t; t^-) = 1/M$ while in the latter, using the Ito convention, $R(t; t) = 0$; $R(t; t^-) = 1/M$. In both cases the equal times condition implies $R_{\text{st}}(0) = 0$, $R_{\text{ag}}(t; t) = 0$ while the next-to-main diagonal values yield $R_{\text{st}}(\infty) = 1/M$; $R_{\text{ag}}(t; t^-) = 0$ and $R_{\text{st}}(\infty) = 1/M$; $R_{\text{ag}}(t; t^-) = 0$, respectively.

The response tends to zero when times get far apart, and its integral over a finite time-interval as well:

$$\lim_{t \rightarrow 1} R(t; t^0) = 0; \quad \lim_{t \rightarrow 1} \int_0^{t^0} dt R(t; t^0) = 0 \quad \text{fixed } t^0: \quad (11.6)$$

These properties imply

$$\lim_{t \rightarrow \ell+1} \lim_{t^0 \rightarrow 1} R(t; t^0) = 0 \quad \lim_{t \rightarrow \ell+1} R_{st}(t - t^0) = 0; \quad \lim_{t \rightarrow \ell+1} R_{ag}(t; t^0) = 0 : (11.7)$$

However, the contribution of the response to the dynamic equations and to other measurable quantities is not trivial. Examining the integral of the response function over a growing time interval one finds that even if the response vanishes, it yields a contribution to the integration. Figure 15-left shows the integrated linear response (5.6). Using (11.5)

$$(t; t^0) = \int_{t^0}^t dt^0 [R_{st}(t - t^0) + R_{ag}(t; t^0)] = R_{st}(t - t^0) + R_{ag}(t; t^0) : (11.8)$$

If, for long enough t^0 , the contribution of the second term in (11.8) were negligible, $(t; t^0)$ should be a stationary quantity. Instead, for all t^0 's studied and for t long enough one clearly sees a waiting-time dependence that can only come from the integration of the second term. This is a weak long-term memory (wltm), the system has an "averaged" memory of its past.

When a system is in equilibrium, the response is simply related to the correlation via fdt. We then assume (and test on the dynamic equations) that the dynamics in the stationary regime satisfies fdt:

$$R_{st}(\omega) = \frac{1}{k_B T} \frac{dC_{st}(\omega)}{d\omega} = 0; \\ R_{st}(\omega) = \frac{2}{h} \lim_{\omega \rightarrow 0} \frac{d|\omega|}{2} \frac{1}{|\omega| + i} \tanh \frac{h|\omega|}{2} C_{st}(|\omega|) \quad (11.9)$$

in a classical and quantum problem, respectively. One can formally prove that fdt has to hold for any generic relaxing model for short time-differences [105], see Section 11.5.4. For longer time-differences, when C_{ag} and R_{ag} vary in time while C_{st} and R_{st} have decayed to zero, one cannot assume the validity of fdt and, as we shall see, the equations have a solution that explicitly modifies fdt.

11.3 Slow time-reparametrization invariant dynamics

We have already mentioned that the correlations decay monotonically (only below q_{pa} if $M \neq 0$). The main insight coming from the numerical solution to the full equations is that the dynamics becomes slower and slower for fixed waiting-time and as $t - t^0$ increases. In the stationary regime $\partial_{t^0} [C(t; t^0); R(t; t^0)]$ and $\partial_{t^0} [C(t; t^0); R(t; t^0)]$ are not negligible with respect to the terms in the rhs of Eqs. (9.16) and (9.17). On the contrary, in the second decay below q_{pa} , C and R decay in a much slower manner such that, $\partial_t C(t; t^0) \approx (t)C(t; t^0)$ and $\partial_{t^0} C(t; t^0) \approx (t)C(t; t^0)$ (similarly for R), and the time-derivatives can be neglected.

We choose the following strategy to solve the equations in the long t^0 limit where a sharp separation of time-scales can be safely assumed. First, we take advantage of the fact that one-time quantities approach a limit, as one can verify numerically, and write the asymptotic form of Eq. (9.23) for $\omega \rightarrow 0$. The integrals on the rhs are

approximated using the separation of C and R in two terms that vary in different time-scales that we assume are well-separated. We detail this calculation below. As regards to the equations for C and R , we proceed in two steps. On the one hand, we choose $t \ll t^0$ short in such a way that $C > q_{ea}$ and we write the dynamic equations for C_{st} and R_{st} . On the other hand, we take t and t^0 widely separated so as $C < q_{ea}$ and we write the dynamic equations for C_{ag} and R_{ag} . In this way we double the number of unknown functions and equations but we simplify the problem enough as to make it solvable.

Once the time-derivatives are neglected and the integrals are approximated as we explain in Section 12.3.3 the aging equations become invariant under reparametrizations of time $t \rightarrow h(t)$ that transform the two-point functions as

$$C_{ag}(t; t^0) \rightarrow C_{ag}(h(t); h(t^0)); \quad R_{ag}(t; t^0) \rightarrow [dh(t^0)] R_{ag}(h(t); h(t^0)) : \quad (11.10)$$

This is not an exact invariance of the dynamic equations. It is only generated when dropping the time-derivatives. This invariance was first noticed by Sompolinsky [90] in his study of the equilibrium dynamics (see also [8] and it later appeared in the nonequilibrium dynamics [12, 104, 96, 72, 106]. We shall see that this approximation forbids us to solve completely the dynamic equations, in particular, to fix the time scaling (select $h(t)$).

11.4 Correlation scales

Take three ordered times $t_3 \geq t_2 \geq t_1$. The correlations are $C(t_i; t_j) = \frac{1}{N} \sum_k h s_k(t_i) s_k(t_j) i_{cos_{ji}}$. The monotonicity of the decay of the correlations with respect to the longer time (keeping the shorter time fixed) and the shorter time (keeping the longer time fixed) allows us to derive general properties that strongly constrain the possible scaling forms. Indeed, one can relate any three correlation functions via triangle relations [104] constructed as follows. Using the fact that the decay is monotonic, one can invert the relation between correlation and times to write, for example, $t_2 = g(C(t_2; t_1); t_1)$ with $g : [0; 1] \times [0; 1] \rightarrow [0; 1]$. This allows us to rewrite $C(t_3; t_1)$ as

$$C(t_3; t_1) = C(g(C(t_3; t_2); t_2); t_1) = C(g(C(t_3; t_2); g(C(t_2; t_1); t_1)); t_1) : \quad (11.11)$$

We now define a real function $f(x; y)$, $f : [0; 1] \times [0; 1] \rightarrow [0; 1]$, by taking the limit $t_1 \rightarrow 1$ while keeping the intermediate correlations fixed

$$\lim_{t_1 \rightarrow 1} C(t_3; t_1) = f(C(t_3; t_2); C(t_2; t_1)) : \\ C(t_2; t_1) \text{ and } C(t_3; t_2) \text{ fixed}$$

The fact that the limit exists is a reasonable working assumption. This function completely characterizes the correlations and their scales in the asymptotic limit. (Note that we defined f using the correlation between the longest time and the intermediate as the first argument.)

11.4.1 Properties

The definition of the function f , as well as the properties shown in this Subsection, are model independent. The form taken by f for each model is determined by the dynamic equations.

Time reparametrization invariance The function f is invariant under reparametrizations of time that satisfy (11.10).

Associativity Take now four times $t_4 \leq t_3 \leq t_2 \leq t_1$. The correlation between t_4 and t_1 can be written in two ways

$$\begin{aligned} C(t_4; t_1) &= f(C(t_4; t_2); C(t_2; t_1)) = f(f(C(t_4; t_3); C(t_3; t_2)); C(t_2; t_1)) ; \\ C(t_4; t_1) &= f(C(t_4; t_3); C(t_3; t_1)) = f(C(t_4; t_3); f(C(t_3; t_2); C(t_2; t_1))) : \end{aligned}$$

Thus f satisfies $f(f(x; y); z) = f(x; f(y; z))$, i.e. it is an associative function.

Identity. If one takes $t_1 = t_2$

$$C(t_3; t_1) = f(C(t_3; t_2); C(t_2; t_1)) = f(C(t_3; t_1); C(t_1; t_1)) = f(C(t_3; t_1); 1) ; \quad (11.12)$$

for all $C(t_3; t_1) \in [0; 1]$. Equivalently, if one takes $t_2 = t_3$

$$C(t_3; t_1) = f(C(t_3; t_2); C(t_2; t_1)) = f(C(t_3; t_3); C(t_3; t_1)) = f(1; C(t_3; t_1)) ; \quad (11.13)$$

for all $C(t_3; t_1) \in [0; 1]$. The correlation at equal times acts as the identity since $x = f(x; 1)$ and $y = f(1; y)$ for all $x, y \in [0; 1]$.

Zero. Taking t_3 and t_2 much larger than t_1 in such a way that $C(t_2; t_1) \rightarrow 0$ and $C(t_3; t_1) \rightarrow 0$ while $C(t_3; t_2) > 0$,

$$0 = C(t_3; t_1) = f(C(t_3; t_2); C(t_2; t_1)) \rightarrow f(C(t_3; t_2); 0) : \quad (11.14)$$

Equivalently, taking $t_3 \rightarrow t_2$ and t_1 , then $C(t_3; t_2) \rightarrow 0$ and $C(t_3; t_1) \rightarrow 0$ while $C(t_2; t_1) > 0$ and one has

$$0 = C(t_3; t_1) = f(C(t_3; t_2); C(t_2; t_1)) \rightarrow f(0; C(t_2; t_1)) : \quad (11.15)$$

The minimum correlation acts as a zero of $f(x; y)$ since $0 = f(x; 0)$ and $0 = f(0; y)$ for all $x, y \in [0; 1]$. (This property can be easily generalised if the correlation approaches a non-zero limit.)

Bound. Given that we assume that the system drifts away in phase space, $C(t_2; t_1)$ decays as a function of t_2 for t_1 fixed, and $C(t_2; t_1)$ increases as a function of t_1 for t_2 fixed. This property implies

$$y = f(1; y) \leq f(x; y) \leq y; \quad x < 1; \quad x = f(x; 1) \leq f(x; y) \leq x; \quad y < 1 : \quad (11.16)$$

Therefore $f(x; y) \leq \min(x; y)$.

Forms for f In [104] we proved that

$$f(x;y) = |^{-1}(|(x)|(y)) \quad \text{Isomorphic to the product} \quad (11.17)$$

$$f(x;y) = \min(x;y) \quad \text{Ultrametricity} \quad (11.18)$$

are the only possible forms that satisfy the properties of f shown above. Note that for $|$ equal to the identity the first type of function becomes simply $f(x;y) = xy$, hence the name. It is also possible to prove that the first kind of function (11.17) is only compatible with the time scaling [107, 104]

$$C(t_2;t_1) = |^{-1} \frac{h(t_2)}{h(t_1)} \quad (11.19)$$

with $h(t)$ a monotonically growing function. The actual correlation can have a piecewise form. Here, instead of reproducing the proofs given in [104] we explain these statements reviewing the scaling forms found for some physical systems and in the analytic solution to mean-field models.

Examples: domain growth

The correlation decays in two steps, see the right panel in Fig. 12 and for $C > q_{ea} = m_{eq}^2$ the decay is stationary:

$$C_{21} \quad C(t_2;t_1) = q_{ea} + C_{st}(t_2 - t_1); \quad (11.20)$$

and it can be put in the form (11.19) using $h(t) = \exp(\ln t)$ and $|^{-1}(x) = q_{ea} + C_{st}(x)$. Any three correlation satisfying (11.20) also verify $t_3 - t_1 = C_{st}^{-1}(C_{31} - q_{ea}) = t_3 - t_2 + t_2 - t_1 = C_{st}^{-1}(C_{32} - q_{ea}) + C_{st}^{-1}(C_{21} - q_{ea})$ that implies

$$C_{31} = C_{st}[C_{st}^{-1}(C_{32} - q_{ea}) + C_{st}^{-1}(C_{21} - q_{ea})] + q_{ea} : \quad (11.21)$$

This equation is equivalent to (11.17). This means that any three correlations above q_{ea} can be related with an f that is isomorphic to the product, see (11.17), with $|_{st}^{-1}(x) = C_{st}(\ln x) + q_{ea}$ and $|_{st}(x) = \exp(C_{st}^{-1}(x - q_{ea}))$.

When the times are such that the domain walls move, the self-correlation decays below q_{ea} in an aging manner, with

$$C_{21} \quad C(t_2;t_1) = C_{ag}(t_2;t_1) = |_{ag}^{-1} \frac{R(t_2)}{R(t_1)} ; \quad (11.22)$$

$|_{ag}^{-1}(1) = q_{ea}$ and $|_{ag}^{-1}(0) = 0$. It is obvious that any three correlations below q_{ea} also satisfy (11.17)

Take now $t_3 = t_2 + t_{32}$ with $t_{32} < t_0(t_2)$ and $C_{32} > q_{ea}$, and t_3 and t_2 sufficiently larger than t_1 ($t_3 = t_1 + t_{31}$ with $t_{31} > t_0(t_1)$ and $t_2 = t_1 + t_{21}$ with $t_{21} > t_0(t_1)$) such that $C_{31} < q_{ea}$ and $C_{32} < q_{ea}$. One has

$$\begin{aligned} C_{31} &= |_{ag}^{-1} \frac{R(t_3)}{R(t_1)} = |_{ag}^{-1} \frac{R(t_3)}{R(t_2)} (|_{ag}^{-1} |_{ag}^{-1}) \frac{R(t_2)}{R(t_1)} \\ &= |_{ag}^{-1} \frac{R(t_3)}{R(t_2)} |_{ag}(C_{21}) = C_{21} : \end{aligned}$$

The last identity is a consequence of $R(t_3) = R(t_2) = 1$ since for a sufficiently small ϵ , $R^0(t_2) = R(t_2) = 1$.

Thus, when the times are such that two correlations, say with values a and b , are both greater than q_{ea} one explores the dynamics in the stationary regime and $f(a; b)$ is isomorphic to the product. When they are both smaller than q_{ea} one explores the dynamics in the aging coarsening regime and again $f(a; b)$ is isomorphic to the product though with a different function f . Finally, if $a > q_{ea}$ and $b < q_{ea}$, $f(a; b) = \min(a; b)$ and one finds dynamic ultrametricity.

The structure discussed in the context of the domain growth problem is indeed generic. Some special values of the correlation act as "fixed points" of $f(a; a)$, $f(a; a) = a$. A "correlation scale" spans the values of correlations comprised between two subsequent fixed points. Within a correlation scale f is isomorphic to the product. Any two correlations falling into different correlation scales are related by an ultrametric f . In the domain growth example 1, q_{ea} and 0 are fixed points that are simple to visualize physically. In more abstract models as the spin-glass the form of f is more involved, with a stationary scale between 1 and q_{ea} and a dense set of fixed points, hence correlation scales, that fill the interval $[0; q_{ea}]$.

Scaling functions

Most solvable models, numerical data and experimental results can be described with only two correlation scales, a stationary and a slow one. Several scaling functions $h(t)$ for the slow decay have been proposed in the literature. In the following we summarize and discuss the main ones. In Fig. 13 we compare the decay of the correlation from q_{ea} for three of the four laws discussed below.

Power law: $h(t) = at^{-\alpha}$. This is the simplest scaling also called simple aging. Ferromagnetic domain growth realizes this form with $\alpha = 1/2$ for non conserved dynamics and $\alpha = 1/3$ for conserved dynamics [1]. Several solvable models have simple aging, an example being the classical spherical $p = 2$ model [108, 109]. In [12] it was conjectured that a power law also characterized the aging dynamics of the fully connected p spin-model with $p \geq 3$. This was later confirmed with the algorithm of Kim and Latz [110] that allows one to reach much longer times. Aging below T_c in the simplest trap model also scales with this law [45]. The molecular dynamic simulations of Lennard-Jones mixtures show this type of scaling too. Note that for all α , C scales as a function of $t_2 = t_1$.

Enhanced power law: $h(t) = \exp(-\ln(t-t_0))$ This law yields the most accurate description of spin-glass experimental data. The exponent typically takes a possibly T -dependent value about 2 [31].

Stretched exponential: $h(t) = \exp(-(t-t_0)^\beta)$ This law has been proposed to describe the slowing down of the full correlation above the critical temperature. As far as we know, no aging model that satisfies a scaling (11.19) with a stretched exponential has been found yet.

Logarithm: $h(t) = \ln(t-t_0)$ In the Fisher and Huse droplet model for spin-glasses, activated dynamics is assumed and the domains are found to grow as $R(t) \sim \ln(t-t_0)$.

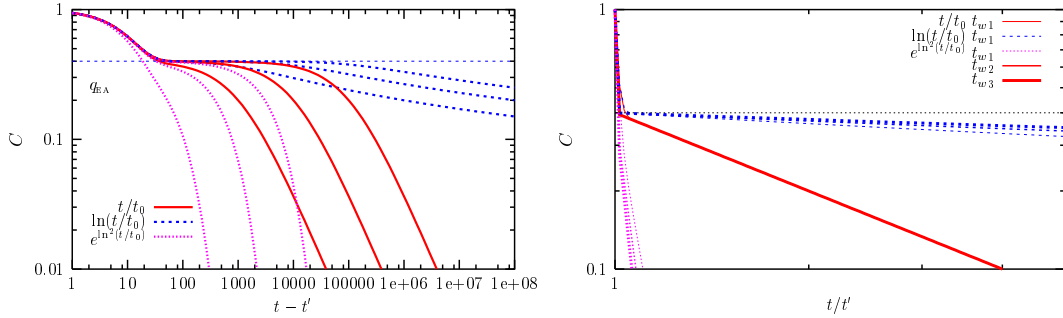


Figure 13: Comparison between three $h(t)$ s, power law, enhanced power law and logarithm. Plot of $C(t; t') = (1 - q_{ea}) \exp(-(t - t')/t_0) + q_{ea} h(t) = h(t')$ against the time-difference $t - t'$ (on the left) and against the ratio of times t/t' (on the right) for three waiting times. Note the drift of the curves in the right panel. For the logarithmic law (sub-aging) the curves drift towards the left for increasing waiting-time. Instead, for the enhanced power law (super-aging) the curves drift to the right for increasing waiting-time. For the power law (simple aging) the scaling is perfect. In real systems the decay of the stationary part towards q_{ea} is much slower than exponential (typically power law with a small exponent) and the separation of time-scales is not so neat.

This leads to $C(t_2; t_1) = g(\ln(t_2/t_0) - \ln(t_1/t_0))$. However, this law does not fit the aging experimental data [31].

Dynamic ultrametricity: Even though it seems mysterious at first sight there is a simple graphical construction that allows one to test it. Take two times $t_3 > t_1$ such that $C(t_3; t_1)$ equals some prescribed value, say $C(t_3; t_1) = 0.3 = C_{31}$. Plot now $C(t_3; t_2)$ against $C(t_2; t_1)$ using $t_2, t_1 \in [t_3, \infty)$ as a parameter. Depending on the value of C_{31} with respect to q_{ea} we find two possible plots. If $C(t_3; t_1) > q_{ea}$, for long enough t_1 , the function f becomes isomorphic to the product. Plotting then $C(t_3; t_2)$ for longer and longer t_1 , the construction approaches a limit in which $C(t_3; t_2) = C_{31} C(t_2; t_1)$. If, instead, $C_{31} < q_{ea}$, in the long t_1 limit the construction approaches a different curve. We sketch in Fig. 14 two possible outcomes of this construction. On the right, we represent a model with two correlation scales, ultrametricity holds between them and within each of them f is isomorphic to the product. On the left instead we represent a model such that dynamic ultrametricity holds for all correlations below q_{ea} . The construction approaches, in the long t_1 limit, the broken curve depicted in the sketch.

The spin-glass [104] and the dynamics of manifolds in an infinite dimensional embedding space in the presence of a random potential with long-range correlations [96, 36] have ultrametric decays everywhere within the aging regime. This scaling is also found in the trap model at the critical temperature [46]. Dynamic ultrametricity in infinite dimensional systems has been searched numerically. There is some evidence for it in the 4dEA model. In 3d instead the numerical data does not

support this scaling [59, 111]. Whether this is due to the short times involved or if the scaling asymptotic is different in 3d is still an open question.

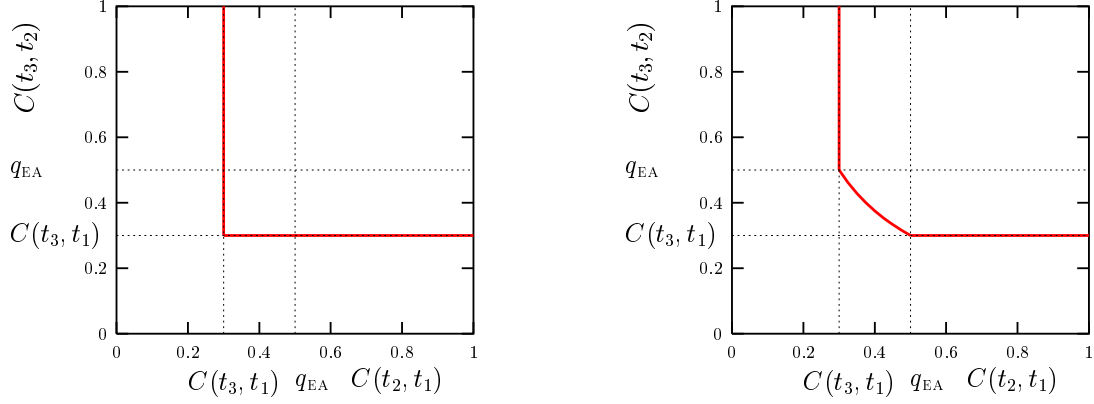


Figure 14: Sketch of a check of ultrametricity using the parametric plot $C(t_3; t_2)$ against $C(t_3; t_1)$ for $C(t_3; t_1) = 0.3 < q_{EA}$ fixed. On the left an ultrametric model, on the right a model with two correlation scales.

11.4.2 Definition of a characteristic time

Expanding the argument in (11.19) for $t_2 = t_1 + \delta t$ with δt one nds, to leading order,

$$\frac{h(t_1)}{h(t_2)} = 1 - \frac{t_c(t_1)}{t_1} \frac{h^0(t_1)}{h(t_1)} + \dots; \quad (11.23)$$

with $O(\delta t^2)$ $h^0(t_1) = h^2(t_1) + h^0(t_1) = h(t_1)$ corrections. The characteristic time $t_c(t_1)$ is given by

$$t_c(t_1) = \begin{cases} t_1 & \text{Power law} \\ t_1 [\ln^{-1}(t_1/t_0)] & \text{Enhanced power law} \\ t_1 (t_0/t_1) & \text{Stretched exponential} \\ t_1 \ln(t_1/t_0) & \text{Logarithm} \end{cases}$$

Note that $t_c(t_1)$ is defined close to the limit of equal times and (11.23) does not make sense for large δt . Rather often in the literature, the scaling variable $x = \delta t/t_1$ has been used even for large values of δt . This scaling is incompatible with the general properties of the triangular relations recalled in Section 11.4.1 if the exponent a is larger than 1 [116]. See the right panel in Fig. 13 to see the different trends of these scalings when plotted as functions of t/t_1 .

For the power law $t_c(t_1)$ scales just as t_1 . In the cases of the stretched exponential and the enhanced power law, $t_c(t_1)$ has a slower growth than the linear dependence if $\alpha > 0$ in the first case and $\alpha > 1$ in the second. This behavior has been called sub-aging. For the logarithm $t_c(t_2)$ grows faster than linearly. This function belongs to a different class that we called super aging [31].

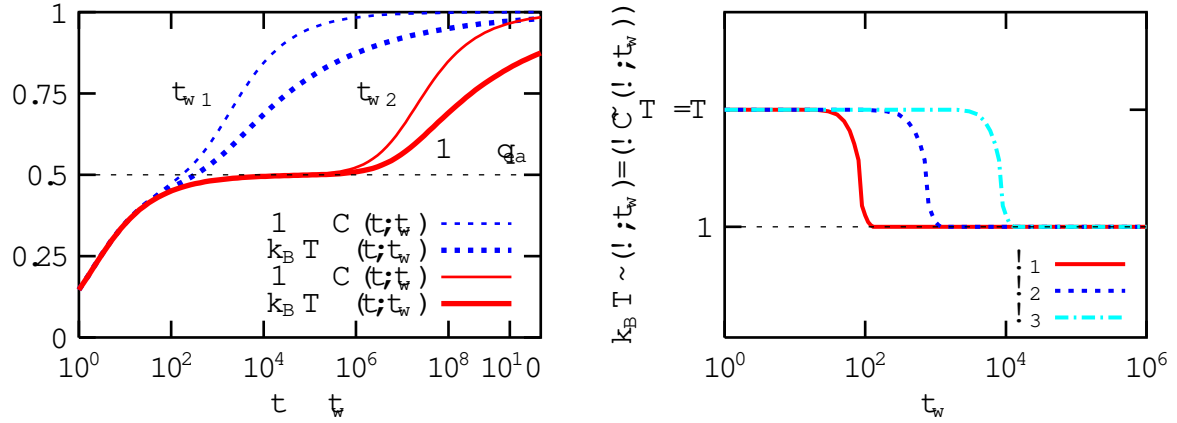


Figure 15: Left: sketch of the modification of fdt in the time-domain. Right: sketch of the modification of fdt in the frequency domain for a glassy system, $T_1 > T_2 > T_3$.

11.5 Modifications of fdt

One of the most important outcomes of the analytic solution to the mean-field glassy models [12, 104] is the need to modify the fluctuation-dissipation relations between linear responses, $R(t; t_w)$, and their partner correlations between spontaneous fluctuations, $C(t; t_w)$, when $T < T_d$. In this Subsection we discuss different ways of presenting the modification of fdt expected in rather generic systems with slow dynamics.

11.5.1 Time domain

The fdt is a linear relation between $R(t; t_w)$ and $C(t; t_w)$ for any pair of times $(t; t_w)$, see Eq. (7.3). In early simulations of the 3d Ising model [57] as well as in the analytic solution to fully-connected disordered models a modification of this relation below T_d appeared [12]. Plotting $k_B T(t; t_w)$ and $1/C(t; t_w)$ for t_w fixed as a function of $\ln(t/t_w)$ one typically obtains the pair of curves schematically shown on the left panel of Fig. 15. The two functions go together until t/t_w reaches a characteristic time $t_0(t_w)$ and they then depart demonstrating that fdt does not hold beyond this time-scale. The characteristic time $t_0(t_w)$ is of the order of the time needed to reach the plateau in the correlation function (this holds for mean-field models but it is not certain in finite dimensional systems). Summarizing

$$t/t_w < t_0(t_w) \quad \text{fdt holds in the fast scale;} \quad (11.24)$$

$$t/t_w > t_0(t_w) \quad \text{fdt is modified in the slow scale;} \quad (11.25)$$

with $t_0(t_w)$ an increasing function of t_w that depends on the system considered (see Fig. 12).

11.5.2 Frequency domain

As explained in Section 5.1 taking a Fourier transform with respect to the time difference while keeping t_w fixed allows one to work in a mixed frequency-time domain. Since many experimental set-ups are prepared to apply ac-fields it is particularly important to predict the aspect fdt modification have when using these parameters. The condition $t \ll t_w < \tau_0(t_w)$ to explore the fast relaxation roughly translates into $\omega \gg \tau_0(t_w)$, i.e. for a fixed waiting-time high frequencies are required. The longer the waiting time the lower the frequency one has to use to see this scale since $\tau_0(t_w)$ increases with t_w . Instead, when $t \ll t_w > \tau_0(t_w)$ one has $\omega \ll \tau_0(t_w)$, and very low frequencies are needed to explore the slow scale. These conditions imply

$$\begin{aligned} \omega \gg \tau_0(t_w) &> 1 && \text{fdt holds in the fast scale;} \\ \omega \ll \tau_0(t_w) &< 1 && \text{fdt does not hold in the slow scale:} \end{aligned} \quad (11.26)$$

Reversing the argument above, if one weakly perturbs the sample with an ac-field of a fixed frequency ω_1 at a chosen time t_w , one can follow the deviation from fdt using t_w as the control parameter. This procedure yields the solid line on the right panel of Fig. 15. Choosing now a lower frequency $\omega_2 (< \omega_1)$ the crossover from the slow to the fast regime occurs at a larger value of t_w . One obtains then the dotted curve on the right panel of Fig. 15. So on and so forth, the smaller the frequency of the applied ac-field the longer the slow regime lasts and the longer one sees deviations from fdt. (Note that the probe does not modify the dynamics.) In the Figure we chose to sketch the behavior of a system with only two-time scales, in which the fdt ratio takes two constant values separated at single breaking point in which the correlation reaches the plateau value q_{ea} . This procedure is commonly employed experimentally, see Section 13.2 where we discuss the measurements of Grigera and Israeloff for glycerol [60].

11.5.3 Time-reparameterization invariant formulation

A more interesting way of displaying the modification of the fdt has been suggested by the analytic solution to the mean-field models discussed in Section 12.3. One of its advantages is that it allows one to classify the systems into sort of "universality classes" according to the form the fdt modification takes.

The analytic solution is such that, in the asymptotic limit in which the waiting-time t_w diverges after $N \rightarrow 1$, the integrated linear response approaches the limit

$$\begin{aligned} \lim_{t_w \rightarrow 1} C(t; t_w) &= C \quad (C) \\ C(t; t_w) &= C \end{aligned} \quad (11.27)$$

when t_w and t diverge while keeping the correlation between them fixed to C [104]. Deriving this relation with respect to the waiting time t_w , one finds that the opposite of the inverse of the slope of the curve $C(C)$ is a parameter that replaces temperature

in the differential form of the fdt. Thus, using Eq. (11.27) one defines

$$k_B T_{\text{eff}}(C) = \left(\frac{d\bar{\chi}}{dC} \right)^{-1}; \quad (11.28)$$

that can be a function of the correlation. Under certain circumstances one can show that this quantity has the properties of a temperature [112] in the sense to be described in Section 14.

One of the advantages of this formulation is that, just as in the construction of triangle relations, times have been "divided away" and the relation (11.27) is invariant under the reparametrizations of time defined in Eq. (11.10).

Equation (11.27) is easy to understand graphically. Let us take a waiting time t_w , say equal to 10 time units after the preparation of the system (by this we mean that the temperature of the environment has been set to T at the initial time) and trace $\bar{\chi}(t; t_w)$ against $C(t; t_w)$ using t as a parameter (t varies between t_w and infinity). If we choose to work with a correlation that is normalized to one at equal times, the parametric curve starts at the point $(C(t_w; t_w) = 1; (\bar{\chi}(t_w; t_w) = 0))$ and it arrives at the point $(C(t \rightarrow \infty; t_w) = \bar{C}; (\bar{\chi}(t \rightarrow \infty; t_w) = \bar{\chi}))$. Without loss of generality we can assume that the correlation decays to zero, $\bar{C} = 0$. This first curve is traced in red in Figs. 16. Now, let us choose a longer waiting time, say $t_w = 100$ time units, and reproduce this construction. One finds the green curves in Figs. 16. Equation (11.27) states that if one repeats this construction for a sufficiently long waiting time, the parametric curve approaches a limit $\bar{\chi}(C)$, represented by the blue curves.

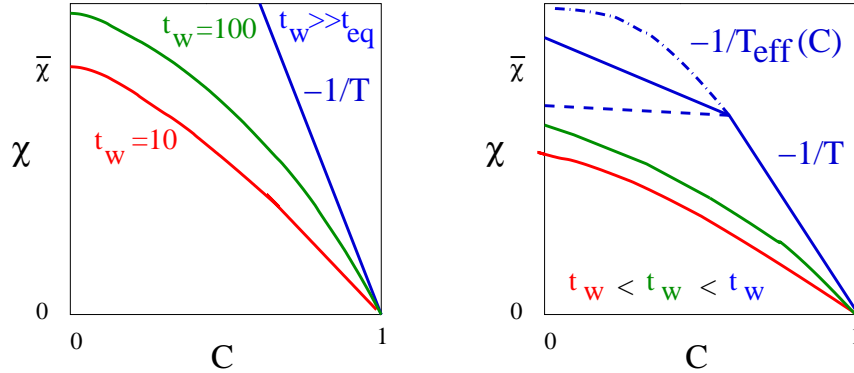


Figure 16: The asymptotic behavior of the integrated linear response against the correlation in a parametric plot, for fixed waiting time and using t as a parameter. Left: behavior in equilibrium. Right: behavior in a slowly relaxing system out of equilibrium. See text for an explanation.

When the system equilibrates with its environment, the construction approaches a straight line with slope $-1/(k_B T)$ as predicted by the fdt. This is the result shown in the left panel of Fig. 16. Instead, for non-equilibrium systems evolving slowly the asymptotic limit is different, it is given by a curve $\bar{\chi}(C)$. For solvable fully-connected models one distinguishes three families, as drawn in the right panel of Fig. 16. They correspond to some systems undergoing domain growth [109] (e.g. the $O(N)$ model

in $d = 3$ when $N \rightarrow 1$), systems behaving like structural glasses [12, 89, 36] (e.g. the p -spin model) and spin-glasses [104, 96, 89, 36] (e.g. the SK model). Several numerical studies in more realistic models of the three cases tend to confirm this classification [58]. However, two provisos are in order. First, one has to be very cautious about the numerical results given the very short time scales and rather small system sizes accessible in simulations [113]. Second, as shown in Section 13.1, at least one system that undergoes domain growth, the ferromagnetic chain, has a non-trivial $\phi(C)$ like the one found for the SK model.

We have already found these asymptotic $\phi(C)$ curves when we discussed the dynamics of a (at) harmonic oscillator in contact with a complex bath made of subsystems with different characteristic times and temperatures (Section 7.4.4). Here we claim that the same structure arises in a glassy model coupled to a white-bath. Different values of the effective temperature are self-generated in the system.

This plot is invariant under reparametrisations of time $t \rightarrow \tilde{t}(t)$ acting on the two-point functions as in Eqs.(11.10). A different choice of the functions h only changes the speed with which the $\phi(C)$ curve is traced but not its form.

11.5.4 fdt part

The formalism used in Section 7 to derive the fdt can be used to obtain a bound on fdt violations [105]. Indeed, one bounds the difference between response and variation of the correlation with the Cauchy-Schwartz inequality leading to

$$k_B T R(t_w + t_w; t_w) - Q_C(t_w + t_w; s) \Big|_{s=t_w} \leq \frac{c}{c} \frac{d_{t_w} H(t_w)}{d_{t_w} H(t_w)} \quad (11.29)$$

where c is a constant and $H(t_w) = \int_0^R dq P(q; t_w) (E(q) - k_B T \ln P(q; t_w))$ is a positive definite function that monotonically decreases towards the free-energy when the system eventually equilibrates [70]. One finds a similar bound for Kramers processes and a generalization that includes the power input when time-dependent or non-potential forces are applied. For systems such that $d_{t_w} H(t_w) \neq 0$ sufficiently fast when $t_w \rightarrow 1$ the bound implies that the lhs vanishes in this limit. This can be achieved in two ways: either each term is finite and the difference between them vanishes or each term tends to zero independently. The former possibility is what happens in the fast regime where fdt holds. The latter holds in the slow regime where both the response and the variation of the correlation are very small but the relation between them does not follow fdt. One derives a more useful bound by integrating (11.29) over time:

$$k_B T (t_w + t_w; t_w) - C(t_w + t_w; t_w) + C(t_w; t_w) \leq \frac{c}{c} \int_{t_w}^{t_w + t_w} dt \frac{d_{t_w} H(t_w)}{d_{t_w} H(t_w)} : \quad (11.30)$$

The terms in the lhs are now always finite while the value of the rhs depends on the relation between the time-difference and the waiting-time t_w . For sufficiently short t_w such that the rhs vanishes fdt has to be satisfied in its integrated form. This result explains the existence of a common straight-line with slope $-1/(k_B T)$ in the nonequilibrium curves in Fig. 16. For sufficiently long t_w such that the rhs

takes a finite value $\beta \hbar$ can be violated. In this second scale a departure from the straight line of slope $\beta \hbar = (k_B T)^{-1}$ can occur and it is indeed what happens in systems with slow non-equilibrium dynamics, see the right panel in Fig. 16. One sees how a separation of time-scales in the dynamics induces the $\beta \hbar$ violations.

In driven systems the bound depends on the power input and only vanishes in the limit of vanishing applied forces. The $\beta \hbar$ is not even enforced in the fast scale and deviations start as soon as C decays from 1. However, as we shall see below, the modification of $\beta \hbar$ follows a very similar pattern to the one shown in Fig. 16 with the strength of the applied force playing a similar role to the one of the waiting-time here.

11.5.5 Diffusion

In these Lectures we focus on models with a bounded self-correlation for an observable with zero average that is normalised at equal times. If the averaged observable does not vanish but the equal-time correlation reaches a time-independent limit one can still use the simple self-correlation in the generalisations of $\beta \hbar$. However, in more general diffusive model with an unbounded time-dependent equal-time correlator it is more natural to compare the behaviour of the "displacement" $C(t; t^0) = \langle \phi(t) \phi(t^0) \rangle$ (that vanishes by definition at equal times) to the linear response. In normal diffusion these are linked by $R(t; t^0) = \beta \hbar^{-1} C(t; t^0)$. In glassy models like the massless manifold in a random potential and others this relation is modified [36, 37, 71, 164].

12 Solution to mean-field models

In this Section we turn our attention to the solution to the Schwinger-Dyson equations derived in previous Sections. We start by describing the simplest numerical algorithm that solves these equations and we next briefly discuss the asymptotic analytic solution at high temperatures. Next we describe in quite detail the solution at low T .

12.1 Numerical solution

One can attempt a numerical solution to the set of causal integro-differential equations (9.16), (9.17) together with the equation for the Lagrange multiplier $\lambda(t)$. One of the questions we would like to explore is whether they encode a non-equilibrium evolution as the one described in the Introduction and Section 2.

The correlation $C(t; t^0)$ and response $R(t; t^0)$ are two-time quantities, that is, they depend on t (which physically corresponds to the time of observation) and t^0 (which corresponds to the age of the system). In the simplest algorithm one discretises the two-times plane with a uniform grid, $t^0 = j \hbar$ and $t = i \hbar$. The correlation and response on the diagonal and the next-to-main diagonal of the two-times plane $(i; j)$ are known, see Eqs. (9.41) and (9.42), for all times.

The time-derivatives $\partial_t^2 C(t; t^0)$ and $\partial_t^2 R(t; t^0)$ in their discretized form are used to update the two-point functions. Due to causality, to advance one time step, the integrals only need values of C and R that are already known. This algorithm is simple and efficient but it is severely limited by the computer storage capacity. Since one has to store C and R for all previous time steps, the memory used grows as i^2 and this number becomes rather quickly prohibitive. In standard pcs one can use $i_{\max} = 10^4$, get an acceptable precision for $\epsilon = 0.1$ and reach total times of the order of 10^3 .

In the quantum case the presence of non local kernels χ and ϕ , that appear convoluted with C and R , renders the numerical solution harder. The larger the cut-off, the smaller the iteration step we need to compute these integrals with a good precision. The maximum total time is of the order of 10^2 in this case.

A different starting point for a numerical solution is the single variable equation (9.56). This route was followed by Eissfeller and Oppenheimer for spin-glasses [114] and it is usually used in the so-called dynamic mean-field theory [91]. Again, this method is limited by the storage capacity.

The knowledge of the qualitative features of the solution helps one devising a more performant algorithm with a variable two-time grid. As we shall see from the analytic solution, C and R vary rapidly when times are near the diagonal $j = i$ and decay very slowly far from it. Kim and Latz have exploited this property and wrote such an algorithm for the spherical p spin model reaching total times of the order of 10^8 [110].

Finally, one can think of an iterative search where one starts from a trial form of C and R and uses the dynamic equations to extract the new form. One can expect to obtain the solution by repeating this procedure until the iteration converges to a fixed point. This method would allow one to look for solutions of the full set of Schwinger-Dyson equations that break causality.

The numerical solution for the causal problem, found with the simple uniform grid, has been of great help in deriving the asymptotic analytic solution. In the following we describe how this solution builds up.

12.2 Solution at high temperatures

At high temperature the system equilibrates with its environment since

$$t_{eq}(N \rightarrow \infty; T) = \infty : \quad (12.1)$$

The mere existence of an asymptotic limit implies that one-time quantities as, e.g., the energy density, $E(t)$, or the Lagrange multiplier, $\lambda(t)$, have to approach an asymptotic limit, $\lim_{t \rightarrow \infty} E(t) = E_1$ and $\lim_{t \rightarrow \infty} \lambda(t) = \lambda_1$. In equilibrium $E_1 = E_{eq}$ and similarly for all one-time quantities. Two time-quantities, as C and R , depend on times but only through time differences as explained in Section 6.

To solve the high T dynamics one first assumes that after a transient equilibrium is reached and a solution of the form $\lambda(t) \rightarrow \lambda_1$,

$$C(t; t^0) \rightarrow C_{st}(t - t^0); \quad R(t; t^0) \rightarrow R_{st}(t - t^0) \quad (12.2)$$

with R_{st} and C_{jbst} related by $f dt$, for long waiting-times t^0 and all time-differences $t - t^0$, exists. These properties also apply to D and C that behave as a correlation and a response, respectively. This Ansatz should solve Eqs. (9.16) and (9.17) when $T > T_d$, with T_d the dynamic critical temperature. In order to prove it we take t^0 long and we assume that we can separate the integrals in Eqs. (9.17) and (9.16) in a preasymptotic and an asymptotic contribution,

$$\int_0^{t^0-1} dt^0 + \int_0^{t_{eq}} dt^0 + \int_{t_{eq}}^{t^0-1} dt^0 : \quad (12.3)$$

Next, we assume that the two-point functions decay as fast as to ensure that all preasymptotic contributions vanish, e.g. $\int_0^{t_{eq}} dt^0 A(t; t^0) B(t^0; t^0) = 0$ when t and $t - t^0$ are in the asymptotic regime. Using the Ansatz (12.2) and this assumption the integrals in the rhs of Eq. (9.17), for a classical problem, read

$$\begin{aligned} & \int_{t_{eq}}^{t^0} dt^0 D_{st}(t - t^0) \frac{1}{k_B T} \frac{\partial C_{st}(t^0 - t^0)}{\partial t^0} + \int_{t_{eq}}^t dt^0 \frac{1}{k_B T} \frac{\partial D_{st}(t - t^0)}{\partial t^0} C_{st}(t^0 - t^0) \\ &= \frac{1}{k_B T} \int_{t_{eq}}^{t^0} dt^0 \frac{\partial}{\partial t^0} [D_{st}(t - t^0) C_{st}(t^0 - t^0)] + \frac{1}{k_B T} \int_{t^0}^t dt^0 \frac{\partial D_{st}(t - t^0)}{\partial t^0} C_{st}(t^0 - t^0) \end{aligned}$$

The first integral in the rhs is a total derivative and it can be readily evaluated, it yields $D_{st}(t - t^0) C_{st}(0) - D_{st}(t - t_{eq}) C_{st}(t^0 - t_{eq}) = D_{st}(t)$ where we assumed that t and t^0 are well in the asymptotic regime in such a way that $C_{st}(t^0 - t_{eq}) = 0$, and we defined $t^0 = t$. Integrating by parts the last integral in the rhs one finally obtains the high T equation for the correlation

$$G_o^{-1}(\omega) C_{st}(\omega) = \frac{1}{k_B T} D_{st}(0) C_{st}(\omega) - \frac{1}{k_B T} \int_0^\omega d\omega' D_{st}(\omega - \omega') d_o C_{st}(\omega') \quad (12.4)$$

with $G_o^{-1}(\omega) = M d_2 + d + \omega_1$. One can check that Eq. (9.16) coincides with Eq. (12.4) under the same assumptions. To prove this statement one has to integrate Eq. (9.16) with respect to t^0 from t_{eq} to t^0 taking care of the fact that t^0 appears in the lower limit of the integral.

Equation (12.4) for the spherical spin model coincides with the schematic mc equation [98, 115]. This equation has a decaying solution above a sharp critical temperature that we call $T_{mct} = T_d$ where the assumptions of $f(t)$ and $f dt$ are justified. After a short transient (eliminated by the limit $t^0 \rightarrow t_{eq}$) the system equilibrates with its environment even if the thermodynamic limit has already been taken. At very high T the decay to zero is very fast and typical of, say, a high- T liquid. Closer to T_d , however, a very interesting structure appears. The solution takes the form sketched in the left panel in Fig. 12. In a logarithmic scale one sees a two step relaxation develop with a first relatively quick decay towards a plateau at a value that we call q_{ea}^d and next a slower relaxation towards zero. The length of the plateau increases when temperature approaches T_d from above and it diverges at T_d . At T_d the height of the plateau, q_{ea}^d , follows from the asymptotic analysis of Eq. (12.4). If one loosely considers q_{ea}^d to be an order parameter, the high temperature analysis yields $q_{ea}^d > 0$ [see Eq. (12.30)] and the transition is

discontinuous. It is important to stress that, as we shall see below, this does not mean that the model has a first order thermodynamic transition. All susceptibilities are continuous when going across T_d even though $q_{ea}^d > 0$. In the mode-coupling literature these transitions are called type B.

The details of the asymptotic analysis of the schematic mc equation and its relation with the behavior of real systems has been discussed at length in the literature (see, e.g. [115]). We shall not develop it here. With the purpose of future comparison with the low- T solution we just recall that the approach and departure from the plateau (beta relaxation) occurs with two power laws:

$$C_{st}(\omega) \sim \frac{q_a^d}{\omega^a} + c_a \omega^{-a} + \dots \quad C_{st}(\omega) \sim \frac{q_a^d}{\omega^b} + c_b \omega^{-b} + \dots \quad (12.5)$$

given by

$$\frac{1}{k_B T_d} \frac{\omega^2 (1+b)}{(1+2b)} = \frac{1}{k_B T_d} \frac{\omega^2 (1-a)}{(1-2a)} = \frac{1}{2} \frac{V^{\infty}(q_{ea}^d)}{(V^{\infty}(q_{ea}^d))^{3/2}} : \quad (12.6)$$

A similar analysis can be done for a quantum model.

12.3 Solution at low $-T$

Three families of mean-field models have been found so far. In this Section we present the solution to the spherical mean-field descriptions of ferromagnetic domain growth and structural glasses in some detail. We use a generic notation that allows us to treat the classical and quantum problem simultaneously. The presentation follows [85]. By the end of this Subsection we discuss the generalisation of these results to models of "spin-glass" type, models with spatial dependence and the effect of different microscopic dynamics.

The numerical solution to the dynamic equations at low T shows no evidence for an arrest in the waiting-time dependence of the decay of C and R . In this regime of temperatures,

$$t_{eq}(N; T < T_d) \rightarrow 1 \quad (12.7)$$

and the equations do not admit the choice of a $t^0 > t_{eq}$. In order to consider the crossover towards the equilibration regime one should revisit the derivation of the dynamic equations allowing for $N \rightarrow \infty$. This program has not been pursued in the literature and it remains one of the most interesting open problems in the field.

12.3.1 The Lagrange multiplier

We approximate the integral in Eq. (9.21) by separating its support in three intervals

$$t^0 : 0 \rightarrow 0; \quad t^0 : 0 \rightarrow t; \quad t^0 : t \rightarrow t : \quad (12.8)$$

The first time-interval contains only finite times t^0 . Hence, all correlations and responses of the form $C(t; t^0)$ and $R(t; t^0)$ vanish due to Eqs. (11.3) and (11.7). In the last time-interval t^0 is close to t in the sense that correlations of the kind $C(t; t^0)$ are of the form $C_{st}(t - t^0) + q_{ea}$ and similarly for the responses. Finally, in the intermediate time-interval the C and R vary in the aging regime. Of course, we

are sloppy in that we do not precise what are the values of t_0 and t_1 . The definitions of correlation scales given in Section 11.4 correct this in precision exchanging the time limits by limits in the correlation. Within these assumptions the asymptotic value of $\langle \chi(t) \rangle$ is given by

$$\begin{aligned} \chi_1 = & A_1 + q_{\text{ea}} \int_0^{Z_1} dt^0 \langle \chi_{\text{st}}(t^0) \rangle + \tilde{D}_{q_{\text{ea}}} \int_0^{Z_1} dt^0 \langle R_{\text{st}}(t^0) \rangle \\ & + \int_0^{Z_1} dt^0 [\langle \chi_{\text{st}}(t^0) \rangle C_{\text{st}}(t^0) + D_{\text{st}}(t^0) \langle R_{\text{st}}(t^0) \rangle] + \text{Last} \end{aligned} \quad (12.9)$$

(see Appendix E). χ_1 and D are made of two terms, one contribution from the bath and one contribution from the interactions (see Eqs. (9.39) and (9.40)). We called Last a term that equals $M \langle \chi_{\text{st}}^2(t^0) \rangle_{t=0}$ in a model with inertia (classical or quantum) and simply $k_B T$ in classical models without inertia. A_1 is the aging contribution:

$$A_1 = \lim_{t \rightarrow \infty} \int_0^{Z_t} dt^0 [\langle \chi_{\text{ag}}(t; t^0) \rangle C_{\text{ag}}(t; t^0) + D_{\text{ag}}(t; t^0) \langle R_{\text{ag}}(t; t^0) \rangle] : \quad (12.10)$$

The bath does not contribute to the integrals in A_1 when the kernels χ and χ_{ag} decay sufficiently fast to zero as to yield vanishing integrals. This is trivially true for a white noise. It can be a working assumption for colored noises based on a weak limit of the strength of the coupling to the noise (see, however, [118]). More precisely, we are neglecting terms of the form $\lim_{t \rightarrow \infty} \int_0^{Z_t} dt^0 A(t - t^0) B(t; t^0)$ where A is either χ or χ_{ag} and B is either C_{ag} or R_{ag} . In this case

$$A_1 = \lim_{t \rightarrow \infty} \int_0^{Z_t} dt^0 \chi_{\text{ag}}(t; t^0) C_{\text{ag}}(t; t^0) + \tilde{D}_{\text{ag}} \int_0^{Z_t} dt^0 \chi_{\text{ag}}(t; t^0) R_{\text{ag}}(t; t^0) : \quad (12.11)$$

The second and third terms in Eq. (12.9) come from the constant (non-zero) limit of the first decay of the correlation $q_{\text{ea}} = \lim_{t \rightarrow \infty} \lim_{t^0 \rightarrow 1} C(t; t^0)$ and the vertex $\tilde{D}_{q_{\text{ea}}} = \lim_{t \rightarrow \infty} \lim_{t^0 \rightarrow 1} \tilde{D}(t; t^0)$. For the classical spherical p spin model $\tilde{D}_{q_{\text{ea}}} = \frac{p}{2} q_{\text{ea}}^{p-1}$ and this equation also holds for its quantum extension if we use $\lim_{t \rightarrow \infty} \langle R_{\text{st}}(t) \rangle = q_a$, a property of the wltm scenario. The integral over the stationary parts can be simply performed using fdt for classical problems but they cannot in quantum problems.

12.3.2 The stationary regime

If $(t; t^0)$ are such that $C(t; t^0) > q_{\text{ea}}$, $C(t; t^0) = q_{\text{ea}} + C_{\text{st}}(t - t^0)$ and $R(t - t^0) = R_{\text{st}}(t - t^0)$. The Schwinger-Dyson equation for R in this time sector reads

$$M \langle \chi^2 \rangle + \chi_1 \langle R_{\text{st}} \rangle = \langle \chi \rangle + \int_0^Z dt^0 \langle \chi_{\text{st}}(t - t^0) \rangle R_{\text{st}}(t^0) \quad (12.12)$$

and it keeps the same form as in the high-temperature phase, apart from the fact that the constant χ_1 has contributions from the aging regime. The Schwinger-Dyson equation for C reads

$$\begin{aligned} M \langle \chi^2 \rangle + \chi_1 (q_{\text{ea}} + C_{\text{st}}) = & A_1 + q_{\text{ea}} \int_0^{Z_1} dt^0 \langle \chi_{\text{st}}(t^0) \rangle + \tilde{D}_{q_{\text{ea}}} \int_0^{Z_1} dt^0 \langle R_{\text{st}}(t^0) \rangle \\ & + \int_1^{Z_1} dt^0 [\langle \chi_{\text{st}}(t + t^0) \rangle C_{\text{st}}(t^0) + D_{\text{st}}(t + t^0) \langle R_{\text{st}}(t^0) \rangle] : \end{aligned} \quad (12.13)$$

One can now Fourier-transform both equations

$$R_{st}(\omega) = \frac{1}{M\omega^2 + \gamma_{st}(\omega)} ;$$

$$M\omega^2 + \gamma_{st}(\omega) C_{st}(\omega) + \gamma_{ea}(\omega) = A_1 + \gamma_{ea}(\omega) + \tilde{D}_{ea} R_{st}(\omega) + \gamma_{st}(\omega) C_{st}(\omega) + D_{st}(\omega) R_{st}(\omega) :$$

The formal solution to the equation for C_{st} is

$$C_{st}(\omega) = \gamma_{ea} + A_1 + \gamma_{ea}(\omega) + \tilde{D}_{ea} R_{st}(\omega) + \gamma_{st}(\omega) R_{st}(\omega) + D_{st}(\omega) R_{st}(\omega) :$$

The first term on the rhs has an imaginary and a real part. The imaginary part vanishes identically since, due to fdt, both $\text{Im } R_{st}(\omega)$ and $\text{Im } \gamma_{st}(\omega)$ are proportional to $\tanh(\hbar\omega/2)$ which is zero at $\omega = 0$ for classical and quantum problems. Concerning the real part of this first term, as we have assumed that $C_{st}(\omega)$ goes to zero for $\omega \rightarrow 1$, we need to impose the self-consistent condition

$$\gamma_{ea} + A_1 + \gamma_{ea}(\omega = 0) + \tilde{D}_{ea} R_{st}(\omega = 0) = 0 : \quad (12.14)$$

This is the condition that fixes γ_{ea} . We shall find it again in the next section as the matching condition between the stationary and aging regimes. The final equation for $C_{st}(\omega)$ is

$$C_{st}(\omega) = D_{st}(\omega) R_{st}(\omega) : \quad (12.15)$$

One can check that these calculations are consistent with the results from §11. Actually, the integrals in equation for $\gamma(t)$ involving the stationary parts can be evaluated with the help of the equations for R_{st} and C_{st} , Eqs. (12.14) and (12.15), and yield once again Eq. (12.14).

Similarly to the high-temperature case one can now show that fdt for $\tilde{\gamma}_{st}$ and \tilde{D}_{st} implies fdt for R_{st} and C_{st} . The remainder of the proof, i.e. to show that fdt between R_{st} and C_{st} implies fdt between $\tilde{\gamma}_{st}$ and \tilde{D}_{st} depends only upon the form of $\tilde{\gamma}_{st}$ and \tilde{D}_{st} as functions of R_{st} and C_{st} and is not modified from the one discussed in Section 12.2.

12.3.3 The aging regime

If we now choose the time $t; t^0$ to be well-separated so as to have $C(t; t^0) = C_{ag}(t; t^0)$, γ_{ea} and $R(t; t^0) = R_{ag}(t; t^0)$, the weak and weak limit hypotheses allow us to throw the second time derivatives on the lhs. We assume that their contribution is much weaker than the one of each of the integral terms on the rhs. This is an assumption that we have to verify at the end of the calculation, once the solution for C_{ag} and R_{ag} is known. It corresponds to the over-damped limit.

Using the approximation described in Appendix E, the equation for R in the aging regime becomes

$$\gamma_{ag}(t; t^0) = \tilde{\gamma}_{ag}(t; t^0) \int_0^{\omega_1} d\omega R_{st}(\omega) + R_{ag}(t; t^0) \int_0^{\omega_1} d\omega \gamma_{st}(\omega) + \int_{t^0}^t dt^0 \tilde{\gamma}_{ag}(t; t^0) R_{ag}(t^0; t^0) \quad (12.16)$$

and we call it the R_{ag} -eq. Similarly, the equation for C becomes

$$\begin{aligned} {}_1 C_{ag}(t; t^0) = & C_{ag}(t; t^0) \int_0^{Z_1} d^0 R_{st}(\cdot^0) + \tilde{D}_{ag}(t; t^0) \int_0^{Z_1} d^0 R_{st}(\cdot^0) \\ & + \int_0^{Z_t} dt^0 \tilde{\sim}_{ag}(t; t^0) C_{ag}(t^0; t^0) + \int_0^{Z_{t^0}} dt^0 \tilde{D}_{ag}(t; t^0) R_{ag}(t^0; t^0) \end{aligned} \quad (12.17)$$

and we call it the C_{ag} -eq. In all integrals over the slow regime we neglected the contributions of the noise kernels $\tilde{\sim}$ and \tilde{D} and we approximated $\tilde{\sim}_{ag}(t; t^0) \sim \tilde{\sim}_{ag}(t; t^0)$ and $\tilde{D}_{ag}(t; t^0) \sim \tilde{D}_{ag}(t; t^0)$ (again, see [118] for a discussion on the effect of a strong bath).

12.3.4 The Edwards-Anderson parameter

The Edwards-Anderson parameter, q_{ea} , is determined self-consistently from the matching of $\lim_{t \rightarrow 1} {}_1 C_{ag}(t; t) = \lim_{t \rightarrow 1} {}_1 C(t; t^0) = q_{ea}$. Taking the limit $t^0 \rightarrow t$ in the R_{ag} -eq and C_{ag} -eq one obtains

$${}_1 R_{ag}(t; t) = \tilde{\sim}_{ag}(t; t) \int_0^{Z_1} d^0 R_{st}(\cdot^0) + R_{ag}(t; t) \int_0^{Z_1} d^0 R_{st}(\cdot^0); \quad (12.18)$$

$${}_1 q_{ea} = A_1 + q_{ea} \int_0^{Z_1} d^0 R_{st}(\cdot^0) + \tilde{D}_{ag}(t; t) \int_0^{Z_1} d^0 R_{st}(\cdot^0); \quad (12.19)$$

The first equation admits the solution $R_{ag}(t; t) = 0$ since $\tilde{\sim}_{ag}(t; t)$ is proportional to $R_{ag}(t; t)$ { see Eq. (9.39). This corresponds to the high-temperature solution where there is no aging regime. Here we concentrate on the other possibility. The response becomes smaller and smaller as time passes { though its integral over an infinite interval gives a finite contribution. If we neglect all terms that are proportional to $R_{ag}(t; t)$ with respect to terms that are proportional to q_{ea} , only the first term in the power expansions of $\tilde{\sim}$ and \tilde{D} survive and

$$\tilde{\sim}_{R_{q_{ea}}} = \lim_{t \rightarrow 1} \frac{\tilde{\sim}_{ag}(t; t)}{{}_1 R_{ag}(t; t)} \quad \tilde{D}_{q_{ea}} = \lim_{t \rightarrow 1} \tilde{D}_{ag}(t; t) \quad (12.20)$$

that for the p spin model become

$$\tilde{\sim}_{R_{q_{ea}}} = \frac{p(p-1)}{2} q_{ea}^{p-2} \quad \tilde{D}_{q_{ea}} = \frac{p}{2} q_{ea}^{p-1}; \quad (12.21)$$

in accord with the large limit of the stationary values (see Section 12.3.2). Equations (12.18) and (12.19) become

$${}_1 = \tilde{\sim}_{R_{q_{ea}}} \int_0^{Z_1} d^0 R_{st}(\cdot^0) + \int_0^{Z_1} d^0 R_{st}(\cdot^0); \quad (12.22)$$

$${}_1 q_{ea} = A_1 + q_{ea} \int_0^{Z_1} d^0 R_{st}(\cdot^0) + \tilde{D}_{q_{ea}} \int_0^{Z_1} d^0 R_{st}(\cdot^0); \quad (12.23)$$

The second equation is the same as the one arising from the end of the stationary regime, Eq. (12.14).

From Eqs. (12.14) and (12.15) one derives

$$\lim_{\omega \rightarrow 0} \omega R_{st}(\omega) = R_{st}(\omega = 0) = \frac{1}{\lim_{\omega \rightarrow 0} \omega R_{st}(\omega)}; \quad (12.24)$$

and

$$\lim_{\omega \rightarrow 0} \omega R_{st}(\omega) = R_{st}^2(\omega = 0); \quad (12.25)$$

We remind that the factor $R_{st}^2(\omega = 0)$ can be written in terms of the stationary correlation function using (12.25); therefore this is a closed equation for the correlation that determines q_{ea} . In the case of the p-spin model it reads

$$1 = \frac{p(p-1)}{2} q_{ea}^{p-2} \frac{1}{h} \lim_{\omega \rightarrow 0} \omega \frac{d}{d\omega} \tanh \frac{h \omega}{2} C_{st}(\omega) : \quad (12.26)$$

In the classical case, the integral can be readily computed and the final equation for q_{ea} is

$$\frac{p(p-1)}{2} q_{ea}^{p-2} (1 - q_{ea})^2 = (k_B T)^2; \quad (12.27)$$

that coincides with the result for the purely relaxational dynamics [12]. For $p \geq 3$ fixed, q_{ea} is a function of temperature. Equation (12.27) can be solved graphically. The lhs has a bell shape. It vanishes at $q_{ea} = 0; 1$ and it reaches a maximum at $q_{ea}^{max} = (p-2)/p$. The equation has two solutions for all temperatures $(k_B T)^2 < (k_B T^{max})^2 = p(p-1)/2 [(p-2)/p]^2 (2-p)^2$, these merge at T^{max} and disappear for higher T 's. The physical solution corresponds to the branch on the right of the maximum, the one that continues the solution $q_{ea} = 1$ at $T = 0$. The minimum value of q_{ea} is reached at the dynamic critical temperature $T_d (< T^{max})$, where $q_{ea}^d = q_{ea}(T_d) > q_{ea}^{max}$.

12.3.5 Fluctuation - dissipation relation

In order to advance further we have to relate the response to the correlation. If we assume that

$$R_{ag}(t; t^0) = \frac{1}{k_B T} \frac{\partial C_{ag}(t; t^0)}{\partial t^0}; \quad (12.28)$$

with T the value of an effective temperature (see Section 14) that is determined by Eqs. (12.23) and (12.24) $0 = A_1 - \frac{q_{ea}}{R_{st}(\omega = 0)} + \lim_{\omega \rightarrow 0} \omega R_{st}(\omega)$. Using Eq. (12.28) and the equivalent relation between $\tilde{\chi}_{ag}$ and $\tilde{\chi}'_{ag}$, we obtain $A_1 = (k_B T)^{-1} \lim_{t \rightarrow 1} \tilde{\chi}'_{ag}(t; t) C_{ag}(t; t) = (k_B T)^{-1} q_{ea} \tilde{\chi}'_{ag}$ and

$$\frac{1}{k_B T} = \frac{p(p-2)}{q_{ea}} R_{st}(\omega = 0) = \lim_{\omega \rightarrow 0} \omega \frac{d}{d\omega} \frac{2(p-2)^2}{p(p-1)} q_{ea}^{p-2}; \quad (12.29)$$

In the classical limit $T = T_c = (p-2)/(1 - q_{ea}^c) = q_{ea}^c$ and the result in [12] is recovered. Note that both in the classical and quantum case, $T \rightarrow 1$ if $p = 2$. Since the

case $p = 2$ is formally connected to ferromagnetic domain growth in $d = 3$ (in the mean-field approximation) there is no memory neither in the classical nor in the quantum domain growth.

The Ansatz in Eq. (12.28) solves classical and quantum aging equations. The modification of the fdt in this regime became thus classical even when quantum fluctuations exist. This is an interesting sort of decoherent effect that will become clearer when we shall discuss the interpretation of this results in terms of effective temperatures.

Using Eq. (12.28) for all values of C below q_{ea} we assumed that there is only one aging correlation scale in the problem. Interestingly enough, one does a more general analysis using the formalism described in Section 11.4 and find that the dynamic equations force the solution to have only one aging correlation scale [78].

12.3.6 Discontinuous classical transition

The classical dynamic critical point ($T_d; h = 0$) can arise either when $q_{ea} \neq 0$ or when $T \neq T_c$. For the p spin model, using Eqs. (12.27) and (12.29) the latter holds and [12]

$$(k_B T_d)^2 = \frac{p(p-2)}{2(p-1)^2} \quad q_{ea}^d = \frac{p-2}{p-1} : \quad (12.30)$$

The transition is discontinuous since the order parameter q_{ea} jumps at T_d . However, it is still of second order thermodynamically since there are no thermodynamic discontinuities, all susceptibilities being continuous across T_d . For instance,

$$\lim_{t \rightarrow t_w} \chi(t; t_w) = \frac{1}{k_B T} (1 - q_a) + \frac{1}{k_B T} q_{ea} \neq \frac{1}{k_B T} \quad \text{when } T \neq T_d \text{ at } T_d : \quad (12.31)$$

The dynamic transition occurs at a value T_d that is higher than the static transition temperature T_s . The latter is fixed as the temperature where replica symmetry breaking occurs (using the standard prescription to fix the parameters in the Parisi Ansatz to compute the free-energy density) [167]. This feature is an explicit realisation of the discussion on T_g and T_0 in Section 2. They are sharp in this model.

12.3.7 The classical threshold level

The asymptotic energy density reads $E_1 = \frac{1}{p} \int_0^1 dt^0 [\chi(t; t^0) C(t; t^0) + D(t; t^0) R(t; t^0)]$ where we used Eq. (9.24). Replacing the solution found above we obtain

$$E_1 = \frac{1}{2} \frac{1}{k_B T} (1 - q_a^p) + \frac{1}{k_B T} q_{ea}^p \quad E_{th} : \quad (12.32)$$

If one compares this expression with the equilibrium energy density, found studying the partition function [167], one discovers that [12]

$$E_1 = E_{th} > E_{eq} : \quad (12.33)$$

Thus, the non-equilibrium dynamics does not approach the equilibrium level asymptotically but it reaches a threshold level that is extensively higher than equilibrium

(note that the inequality (12.33) holds for the energy density). The name threshold is motivated by a similarity with percolation (in phase space) that we shall discuss in Section 15 [12].

12.3.8 Two p models

In Section 12.3.4 we took the limit $t^0 \rightarrow t$, or equivalently, $C_{ag} \rightarrow q_{ea}$ in the equations for the slow part of the response and the correlation and this lead us to Eqs. (12.25) and (12.29) for q_{ea} and T . Let us now take subsequent variations of this equation with respect to the correlation and evaluate them in the same limit. It is easy to see that if we neglect the contributions from the integral between t^0 and t , assuming that the integrands are analytic in this limit, we get new equations linking T and q_{ea} that, for generic models, are not compatible. Indeed, as we shall see below, the pure spherical spin model is the only one for which the solution is given by an analytic function $\chi^2(x)$ when $x \rightarrow 1$.

The way out of this contradiction is to propose that the correlation approaches the plateau at q_{ea} with a power law decay and that it departs from it with another non-trivial power law [89, 36]:

$$C_{st}(t, t^0) = (1 - q_{ea}) + c_a^{(1)}(t - t^0)^{-a} + c_a^{(2)}(t - t^0)^{-2a} + \dots \quad (12.34)$$

$$C_{ag}(t; t^0) = q_{ea} - c_b^{(1)} \frac{h(t^0)^{1-b}}{h(t)} - c_b^{(2)} \frac{h(t^0)^{1-2b}}{h(t)} + \dots \quad (12.35)$$

with $c_a^{(i)}$ and $c_b^{(i)}$ constants. If the exponent b is smaller than one, the integrals generated by taking derivatives with respect to C_{ag} do not vanish when $t^0 \rightarrow t$. The expansion of the stationary and aging equations around q_{ea} in the exponents a and b . One finds [89]

$$\frac{1}{k_B T} \frac{((1+b))^2}{(1+2b)} = \frac{1}{k_B T} \frac{((1-a))^2}{(1-2a)} = \frac{1}{2} \frac{V'''(q_{ea})}{(V''(q_{ea}))^{3/2}} \quad (12.36)$$

that are to be confronted to Eqs. (12.5) and (12.6) for the high T behavior. We recall that $V(C)$ is the correlation of the random potential. Importantly enough, the exponents a and b are now T -dependent and they are related via an equation in which T enters.

Classical spherical spin model

Since $V(C) = C^2$ using Eqs. (12.25) and (12.29) to $x = T$ and q_{ea} one finds $((1+b))^2 = (1+2b) = 1+2$ and $b = 1$ for all $T < T_d$. The exponent a interpolates between $a = 1+2$ at $T \rightarrow 0$ and $a = 1$ at $T \rightarrow T_d$ since $((1-a))^2 = (1-2a) = T/(2T)$.

Classical mixed $p_1 + p_2$ spherical spin model

For adequate choices of the coefficients in $V(C) = a_1 C^{p_1} + a_2 C^{p_2}$ (see below) one finds T -dependent exponents $a(T)$ and $b(T)$.

Ultrametric limit

It is interesting to notice that $(1+b)^2 = 1+2b$ is bounded by one. Thus, Eq. (12.36) constrains the random potentials for which a solution with only two correlation scales exists. For a particle in a power-law correlated random potential one sees the transition towards an ultrametric-like solution arrives when the potential goes from short-range to long-range correlated [89]. To our knowledge this has not been found in a static calculation. An interpretation of the exponents a and b , and this consequence, in terms of the properties of the trap free-energy landscape is not known either.

12.3.9 sk model and similar

A different family of models, to which the sk model belongs, are solved by an ultrametric Ansatz, $C_{31} = f(C_{32}; C_{21})$, for all correlations below q_{ea} . The $\langle C \rangle$ plot yields a non-trivial curve (instead of a straight line) for $C \in [0; q_{\text{ea}}]$. The transition is continuous $q_{\text{ea}}^d = 0$. These models are called type A in the mct literature.

Indeed, for a generic disordered model with random potential correlated as in Eq. (9.3), one finds that the solution is ultrametric if and only if [89]

$$\frac{V^{\text{m}}(C)}{V^{\text{m}}(q_{\text{ea}})} \frac{V^{\text{m}}(q_{\text{ea}})^{1/3=2}}{V^{\text{m}}(C)} < 1 : \quad (12.37)$$

This bound constrains, for instance, the values of the coefficients in a polynomial random potential for which the dynamic solution is ultrametric. The fdt is modified with a C dependent factor given by $T = T_{\text{eff}}(C) = q_{\text{ea}} V^{\text{m}}(C) / V^{\text{m}}(q_{\text{ea}}) = (4(V^{\text{m}}(C))^{3=2})$.

12.3.10 Mode dependence

The models we solved so far have no spatial dependence. The manifold problem (2.8) has an internal structure that leads to a mode-dependence. This model has been solved for generic potential correlations [36]. We summarize the outcome without presenting its detailed derivation. All modes are slaved to one in the sense that one has to solve for the dynamics of one of them and the mode-dependence follows from an algebraic equation. The value of the effective temperature does not depend on the mode. The mathematical reason for this is the slaved structure of the equations. The physical reason is that all interacting observables evolving in the same time-scale have to partially equilibrate and acquire the same effective temperature (see Section 14). The height of the plateau, q_{ea} , is a k dependent quantity. The approach to it and departure from it also depends on k but only via the prefactors; the exponents a and b , see Eqs. (12.34) and (12.35), are the same for all modes.

Mode-coupling equations including a wave-vector dependence have been derived by Latz using the Mori-Zwanzig formalism; the structure of the solution to these equations shares the properties just described [102].

12.3.11 Quantum fluctuations

The simplest effect of quantum fluctuations is to introduce oscillations in the first step of relaxation. These disappear at long enough time-differences and they are

totally suppressed from the second decay, that superficially looks classical [85, 106].

The Edwards-Anderson parameter q_{EA} depends upon T and h . As expected, quantum fluctuations introduce further fluctuations in the stationary regime and they decrease the value of q_{EA} , $q_{\text{EA}}(T; h \neq 0) < q_{\text{EA}}(T; h = 0)$.

The modification of $f(t)$ in the quantum model is of a rather simple kind: R_{ag} and C_{ag} are related as in the classical limit. For the quantum extension of the spin model there are two correlation scales, one with the temperature of the environment, T , the other with another value of the effective temperature, T^* , that depends on T , h and the characteristics of the environment. This is a kind of decoherent effect.

As regards to the transition from the glassy to the liquid or paramagnetic phase, an interesting effect appears. Keeping all other parameters fixed, the plane $(T; h^2 = (JM))$ is separated in these two phases by a line that joins the classical dynamic critical point $(T_d; h = 0)$ and the quantum dynamic critical point $(T = 0; h_d)$. Close to the classical dynamic critical point the transition is discontinuous but of second order thermodynamically until it reaches a tricritical point where it changes character to being of first order. This behavior is reminiscent of what has been reported for the quantum spin-glass studied in [14].

A still more dramatic effect of quantum mechanics is related to the very strong role played by the quantum environment on the dynamics of a quantum system. Indeed, the location of the transition line depends very strongly on the type of quantum bath considered and on the strength of the coupling between system and environment [118].

12.3.12 Driven dynamics

The effect of non potential forces can be mimicked with a force as the one in (2.7) [18, 19] where the strength of the force, σ , is analogous to the shear stress σ . For strengths that are not too strong, the dynamics presents a separation of time scales with a fast approach to the plateau and a slow escape from it that is now, however, also stationary. Indeed, after a characteristic time t_{sh} the full dynamics becomes stationary though the system is still far from equilibrium. One defines a structural relaxation time, τ_R , as the time needed to reach, say, a correlation equal to a half. One relates the structural relaxation to the viscosity via $\eta = \int_0^\infty dt C(t)$. The scaling of τ_R with the shear rate $\dot{\gamma} = \sigma/\eta$ has been successfully confronted to the behavior in rheological experiments in super-cooled liquids and glasses [19]. In terms of the general scalings discussed in Section 11.4, the correlations are characterised by two different functions $\phi(t)$, one for the fast decay towards the plateau and another for the slow decay from the plateau, while the functions $h(t)$ are simple exponentials.

Interestingly enough, from the study of $f(t)$ violations above (though close to) and below T_d , when the forcing is weak, one extracts a still well-defined slope of the $\log(C)$ plot when C evolves in the slow scale [18, 121, 19]. This means that an effective temperature can also be identified for these systems kept explicitly out of equilibrium (see also [172]).

Oscillatory forces, as the ones used to perturb granular matter, have a different effect. Aging is not stopped in a finite region of the phase diagram (T -strength of the

force-frequency of the force) [26]. An effective temperature can still be defined as the slope of the $\langle C \rangle$ plot drawn using stroboscopic time, with a point per oscillatory cycle.

13 Modifications of fdt in physical systems

In this Section we discuss the realizations of the modifications of fdt in each of the physical systems presented in Section 2.

The asymptotic curves in Fig. 16 have a rather peculiar form. They are linear with slope $-1/(k_B T)$ when the correlation decreases from 1 to the plateau value q_{ea} . After this breaking point, when the correlation decays towards zero, the curve is non-trivial, taking the three forms described in Section 11.5.3 for ferromagnetic domain-growth (in $d > d_c$), structural glasses and spin-glasses. The separation between these two parts is sharp when the dynamics has a sharp separation of time-scales. In Section 11.5.4 we gave a formal explanation for the existence of the first scale where fdt holds for any relaxing system. Here and in the two next Subsections we give more intuitive arguments for the validity of fdt in the fast regime in the context of the physical systems discussed in the Introduction.

For the sake of comparison we show in Fig. 18 the form of the $\langle C \rangle$ plot for a p spin model adapted to mimic a structural glass (the original model), a sheared liquid or glass, vibrated granular matter and a quantum glass.

13.1 Domain growth

The separation of time-scales is easy to visualize in the case of a system undergoing domain growth. If the two times t and t_w are not very different, the domain walls do not move between t and t_w and the dynamics consists of spins flips within the domains due to thermal fluctuations. This dynamics is identical to the equilibrium dynamics since the system can be thought of as being a patchwork of independent equilibrated finite systems of linear size $R(t_w)$. It is then natural that the fdt holds in this time scale. On the contrary, if t grows in such a way that t_w becomes of the order of $R(t_w)$, the domains grow and the non-equilibrium dynamics takes place. The motion of the domain walls in the presence of an external perturbing random field introduced to measure the staggered response is due to two competing factors: on the one hand, the system tends to diminish the curvature of the interfaces due to surface tension, on the other hand the random field tends to pin the domain walls in convenient places. The full response of the walls is approximately [119]

$$\chi_1(t + t_w; t_w) = \rho(t_w) \chi_s(t + t_w; t_w) R^{-1}(t_w) \chi_s(t + t_w; t_w) \quad (13.1)$$

where $\rho(t_w)$ is the density of interfaces and $\chi_s(t + t_w; t_w)$ is the integrated response of a single wall. The contribution of a single interface depends on dimensionality and, for a ferromagnetic Ising model with first neighbor interactions and non-conserved

order parameter it has been estimated to be

$$s(t_w; t_w) = t \quad \text{with} \quad \begin{cases} (3-d)=4 & d < 3 \\ 0 & d > 3 \end{cases}$$

and $0.33 + 0.066 \ln$ in $d = 3$ [119]. Thus, below the critical dimension $d_c = 3$ the response of a single interface grows indefinitely with the time-difference. The same trend though with a different value of d_c and with slightly different exponents has been obtained for a continuous spin model. Still, for all $d > 1$, s decays sufficiently fast as to compensate the growth of s , s vanishes and the integrated linear response function gets stuck at the value reached at the end of the stationary time scale, $s_{eq} = (k_B T)^{-1} (1 - m_{eq}^2)$. In the slow regime the parametric plot is then given by a flat straight line with vanishing slope, see the dashed line in the right panel of Fig. 16. Instead, the case $d = 1$ behaves in a totally different way: $(t + t_w)$ still decays as $(t + t_w)^{-1/2}$ while s grows as $t^{1/2}$, thus, in the regime of times such that $t = t_w$ is finite the interfaces do contribute to the integrated response and the (C) curve is non-trivial. As explained in [119] these results can be easily interpreted as follows. When $d > d_c$ the curvature driven mechanism dominates and the interface response decreases with t . When $d < d_c$ instead this mechanism is weakened while the field driven motion, and consequently the single interface response, becomes more important. In the limit $d = 1$ the curvature driven mechanism disappears, s compensates exactly the decay in s and s is non-trivial [119].

Besides the qualitative arguments just presented, the ferromagnetic Ising chain is completely solvable and very instructive [170, 120, 48]. The transition occurs at $K = J = (k_B T)^{-1}$ and this limit can be reached either by letting $T \rightarrow 0$ or $J \rightarrow 1$. The latter is better adapted to compute the integrated linear response and one finds

$$(C) = \frac{P}{2} \arctan \frac{P}{2 \cot \frac{P}{2} C} : \quad (13.2)$$

The fast regime is eliminated for this choice of parameters and the full (C) curve is given by this equation. This model is a concrete example of a system undergoing domain growth that has a non-trivial (C) . For finite J (or finite T) the equilibration time is finite and, for $t_w \rightarrow t_{eq}$ the trivial $(C) = 1 = (k_B T)$ must be reached. However, for fixed $t_w \rightarrow t_{eq}$ one still finds a very rich structure: the master curve (C) corresponding to $J \rightarrow 1$ is followed from $C(t_w; t_w) = 1$ down to $C_{eq} = C(t_{eq}; t_w)$. For longer time-differences, $t + t_w > t_{eq}$ the system equilibrates and (C) departs from the master curve and approaches the point $(0; 1 = (k_B T))$. The point of departure C_{eq} depends on J and t_w . For fixed t_w , C_{eq} increases with increasing J ; for fixed J , C_{eq} increases with increasing t_w . Corberi et al also argued that even if the form of C and R depend on the microscopic dynamics, the (C) curve should be universal.

Note an unexpected feature of this result: when $J \rightarrow 1$, even if the correlation and response vary in a single time-scale with a simple aging scaling, the (C) relation is a continuous function. This property poses some problems for the interpretation of the slope of the (C) plot as an effective temperature (see Section 14) as well as the relation between statics and dynamics discussed in Section 13.10. It would be interesting to identify the generic origin of these "contradictions".

For some time it has been argued that systems undergoing domain growth cannot have a non-trivial $\chi(C)$. This example, even though in $d = 1$, demonstrates that this is not true. It would be extremely interesting to construct a coarsening model in higher dimensions with a non-trivial contribution to the integrated response coming from the interfaces in such a way that $\chi(C)$ be non-trivial.

13.2 Structural glasses

For glassy systems, where no such growth of order has been identified yet, the form of the fdt modification is different from the one found for domain growth. These systems still show a separation of time-scales in the sense that the correlation decays in two sharply separated steps as suggested by numerical studies. The asymptotic parametric curve has the form of the solid line in Fig. 16. One can argue in terms of caging motion to get an intuitive interpretation of why fdt holds in the fast correlation scale. Indeed, in this correlation-scale the time-different t_w is so short that each particle moves within a rather "solid" cage formed by its neighbors. Loosely speaking, the cages act as a confining potential on each particle. The rapid motion is again due to thermal fluctuations and the dynamics is like the one expected in equilibrium: it is then no surprise that fdt holds. For the moment there is no easy interpretation for the form of the second part of the parametric curve. Why does it have a non-zero constant slope or, equivalently, a single finite value of the effective temperature? This result was obtained using fully-connected models and it was later checked numerically in a number of more realistic glassy models [58].

Two sets of experiments using laponite [61] and glycerol [60] have investigated the modifications of fdt in glasses. The former is explained in [61]. In the latter Grigera and Israeloff [60] monitored the time-evolution of the fd ratio for glycerol at $T = 179.8\text{K}$, the glass transition being at $T_g = 196\text{K}$. The measurements were done at fixed frequency $\omega = 7.7\text{Hz}$ and the results presented in the manner described in Section 11.5.2. For a perfect time-scale separation the curve should have a step-like form as sketched in the right panel of Fig. 15 and also included with line-points in Fig. 13.2. The experience shows that the fd ratio evolves very slowly from T to T_g with a very long transient between one and the other. Measurements at lower frequencies should yield a more sharp separation between the two steps.

13.3 Spin-glasses

The parametric curve for the fully-connected sk model for spin-glasses is given by the curve with a varying slope in the right panel of Fig. 16. This result corresponds to having a succession of temporal scales each one with an effective temperature, $T_{\text{eff}}(C)$. The question as to whether this behavior also applies to the finite dimensional case remains open. The only results available for the moment and, most probably, for a long while are numerical and experimental. For the time-scales explored, the parametric curves obtained have a very mild curvature. In order to decide beyond doubt if the asymptotic plot is curved it is necessary to perform a very careful analysis of the times and sizes explored (see [113]).

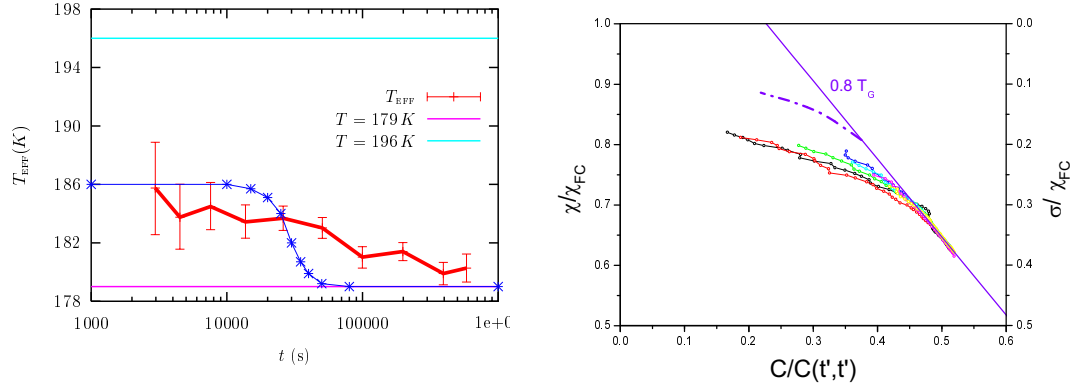


Figure 17: Left: the waiting-time evolution of the effective temperature of glycerol [60]. Right: the parametric (C) plot for thiopinel, an insulator spin-glass [32].

Very recently Herisson and Ocio studied the evolution of the correlations in the magnetization fluctuations (noise) and the thermomagnetic magnetization (integrated response) of thiopinel, an insulator spin-glass [32]. Their aim was to obtain the parametric curve (C) . In the right panel of Fig. 13.2 we show their results. It is important to note that even the experimental data is very far away from the expected nonequilibrium asymptote that is estimated to be given by the dotted-dashed curve in the figure. (for more details on this experiment see [32].)

13.4 Rheology

In Section 2 we have already explained that a non potential external force might stop aging. When the strength of this force is small, the separation of time-scales is still present but the dynamics becomes stationary. This fact makes the dynamics much simpler when observed in the time domain but it still captures some of the interesting features of non-equilibrium. For instance, the correlation function of a super-cooled liquid under homogeneous shear approaches a non-equilibrium stationary state and the parametric construction of Fig. 16 yields the same results where the waiting-time dependence is replaced by a shearing rate dependence. Thus, the red curve corresponds to a rather strong shearing rate, the green curve to a shearing rate of intermediate magnitude and the blue curves to the limit of vanishing shearing rate depending on the underlying system studied. These results were first obtained by solving the dynamics of a fully-connected model with non-symmetric interactions as the one introduced in Eqs. (2.7) and (4.9) [18, 34]. The numerical study of Lennard-Jones mixtures under uniform shear performed by Berthier and J-L Barrat completed the study of this framework [121] (see also [172] and [19]).

In Section 14 we present the interpretation of the modification of $\chi(t)$ in terms of self-generated effective temperatures. Let us use this language here to explain these results and motivate further studies in other systems with different microscopic dynamics. Within the effective temperature interpretation, we see that $T_{\text{eff}}(C) > T$ control the slow relation. In slightly more technical terms, the correlation scales

in which the time derivatives of the correlation are negligible with respect to the correlation itself evolve according to a temperature that is given by the modification of the fdt relation. This fact suggests that the effective temperatures should appear in systems in which the microscopic dynamics is not necessarily thermal but in which a separation of time-scales rapid-slow is self-generated as time passes.

13.5 Vibrated models and granular matter

In fact, a similar modification to fdt has also been observed for glassy models driven by a time-dependent oscillatory force that mimics the perturbations used to move granular matter [26]. In this case, since the perturbation introduces its own characteristic time $t_c / \omega = 1$ it is more convenient to present the data using stroboscopic time, i.e. using a single point for each cycle. Modifications of fdt in models for granular matter were studied in [122, 123, 25].

13.6 Driven vortex systems

The effective temperature has also been observed in the transverse motion of a driven vortex system [43]. Very interestingly, T_{eff} shares many quantitative properties with the "shaking temperature" of Koshelev and Vinokur [173].

13.7 Quantum fluctuations

Even more spectacular are the results for glassy models in which quantum fluctuations are important and keep a separation of fast-slow time-scales [85, 106]. The fast scale is fully controlled by the quantum dynamics and the fdt takes the complicated quantum form described in Section 7. In the slow scale though the quantum fdt is no longer valid and it is replaced by a modified classical form in which the deviations from the classical fdt depend on the strength of quantum fluctuations. The dynamics in the slow scale supercially looks classical. This result was found in the solution to mean-field models (quantum extensions of the p spin and sk, fully connected $SU(N)$). It is important to notice that Monte Carlo simulations of quantum problems in real-time are not possible.

13.8 Systems of finite size: preasymptotic behavior

The previous discussion shows that the correlation scales (time-scales) play a very important role in the global behavior of the systems. For relaxational systems we argued that the asymptotic parametric curve appears in the limit $\lim_{t_w \rightarrow 1} \lim_{N \rightarrow 1}$. The thermodynamic limit that is taken first ensures that the equilibration time, t_{eq} , diverges and cannot be reached by the waiting-time. For a system of finite size, $N < +1$, the equilibration time is a function of N . In consequence, the limit curve (C) has a lifetime that is bounded by t_{eq} . When the waiting-time becomes of the same order of magnitude as t_{eq} , the curve (C) starts changing to approach the equilibrium asymptote, the straight line of slope $-1/(k_B T)$. The way in which the

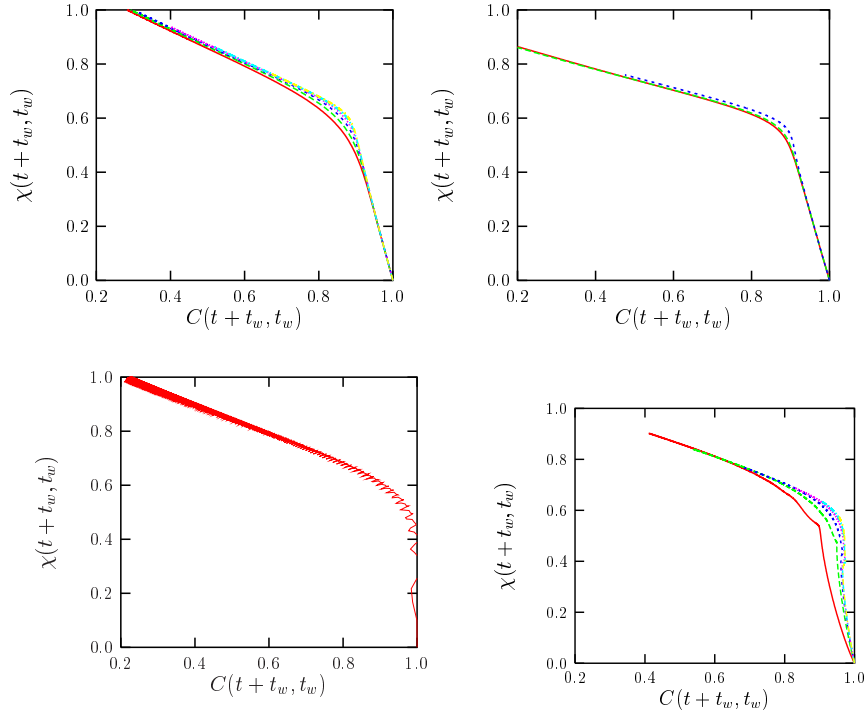


Figure 18: The parametric (C) plot for the p -spin model: relaxational dynamics (upper left panel) [12], with asymmetric interactions (upper right panel) [18], under the effect of an oscillatory field (lower left panel) [26] and with quantum fluctuations (lower right panel) [85]. The different curves on each panel correspond to different waiting-times.

approach to equilibrium is achieved is not known in general. It is a very difficult problem even for fully-connected models and there is little hope to solve a problem in sufficient detail as to be able to determine all the crossovers. This might be possible for the $O(N)$ model of ferromagnetic growth or for the spherical spin disordered model. Crisanti and Ritort [160] analysed the crossover to equilibrium in the p -spin model with numerical simulations.

13.9 Critical dynamics

Godreche and Luck studied the coarsening dynamics of ferromagnetic models quenched to the critical point T_c . Spatial correlations develop in the system but only up to a length scale that grows as $(t + t_w)^{1/z_c}$ with z_c the dynamic critical exponent. The equilibrium magnetization, m_{eq} , and, hence, q_{ea} , vanish. Still, the dynamics is highly non-trivial. For finite though long t_w a stationary regime for $t < t_w$ and an interrupted aging regime for $t_0 < t_w < t_0 + t_w$ can be identified even if they are not clearly separated by a plateau in the correlation at a finite q_{ea} . In the former

regime, the correlation and response are stationary and satisfy fdt. In the latter

$$C(t; t_w) \sim t_w^{-2} = {}^2F_C \frac{t}{t_w} ; \quad (t; t_w) \sim t_w^{-2} = {}^2F \frac{t}{t_w} ; \quad (13.3)$$

with and the usual static critical exponents and F_C and F two scaling functions. As t_w increases the stationary regime arrives up to lower values of C and when t_w grows to infinity the full decay is stationary as in equilibrium. Since the interrupted aging part of C and R decay only algebraically with t_w the (C) plot for finite though long t_w is very rich with a non-trivial functional form. Similar results were obtained for the critical dynamics of the XY model [124].

13.10 Connection with equilibrium

The relation

$$T \frac{d^2 (C)}{dC^2} \bigg|_{C=q} = \lim_{h \rightarrow 0} P_h(q) ; \quad (13.4)$$

between the static and non-equilibrium dynamic properties of slowly decaying systems, where (C) is the non-equilibrium relation between integrated response and correlation function as defined in Eq. (11.27) and $P_h(q)$ is the probability distribution of overlaps¹ in the perturbed Gibbs state, became apparent from the analytic solution to some mean-field models.

This relation holds in the exact solution to the SK model [104] and the problem of a finite dimensional manifold embedded in an infinite dimensional space in the presence of a random potential with long-range correlations [96, 36]. It is not verified in the exact solution to the p spin model and the manifold in a random potential with short range correlations. The reason for this discrepancy is that for the latter models the dynamics in the $t_w \rightarrow 1/N \rightarrow 1$ limit approaches the threshold and not equilibrium. More precisely, all generalized susceptibilities, and in particular the energy density, approach a limit $\lim_{t_w \rightarrow 1/N \rightarrow 1} \chi^{gen}(t_w) = \chi_{th}^{gen} \neq \chi_{eq}^{gen}$. In all cases the dynamics occurs in a region of phase space that is different from the one sampled in equilibrium and, for p spin models and the like it has different statistical properties. For the former models, even if still the region of phase space explored by the dynamics is different from the one corresponding to the equilibrium states, its statistical properties can be thought to be somehow equivalent, since $\lim_{t_w \rightarrow 1/N \rightarrow 1} \chi^{gen}(t_w) = \chi_{th}^{gen} = \chi_{eq}^{gen}$, and the relation (13.4) holds.

More recently, Franz, Mezard, Parisi and Pelti proposed that the connection (13.4) goes beyond mean-field and applies to finite d systems in which all dynamic susceptibilities converge to their equilibrium values, linking in this way the (easy to measure) non-equilibrium dynamic properties of realistic models to the (hard to measure) equilibrium properties of the same models. Since a threshold level as the one found for the p spin model cannot subsist for ever in finite d, they argued that the validity of Eq. (13.4) should be rather generic.

¹The overlaps are given by the correlation between two equilibrated configurations.

Several comments are in order. Corberi et al showed that there is a non-trivial nonequilibrium dynamic $\chi(C)$ that does not satisfy Eq. (13.4) in one dimensional coarsening systems where the interface response does not vanish asymptotically (see Section 13.1). Even if the hypothesis of convergence of the generalized susceptibilities is not verified in this model, it provides a very simple example where the relation (13.4) does not hold. It might be possible to extend this result to domain growth in $d > 1$ with an interface geometry such that the domain wall response does not vanish asymptotically. This problem deserves further study.

Based on numerical simulations, Marinari et al claimed [125] that the relation (13.4) is verified in the 3d eam. As pointed out by Berthier, Holdsworth and Sellitto in the context of the xy model [124] and by A. Barrat and Berthier [113] in the context of the 2d and 3d eam models, one has to be extremely careful when extrapolating the numerical results obtained for finite waiting-time out of equilibrium and finite size in equilibrium. Indeed, these authors showed that one can tune the finite waiting-time and the finite size to have a relation like (13.4) well before the asymptotic limits are reached and even in the trivial phase of the xy and 2d eam models.

Finally, it is worth stressing that a non-trivial $\chi(C)$ has been found in explicitly out of equilibrium situations for which equilibrium is trivial as, for instance, in rheological measurements of super-cooled liquids or in the long-time dynamics of super-cooled liquids before equilibration is reached. Indeed, non-trivial $\chi(C)$ curves have been found in glassy model above the putative T_g in Lennard-Jones systems and at finite T in models for which $T_g = 0$ like the kinetically constrained lattice models [53, 54].

In conclusion, a better determination of which are the conditions under which (13.4) holds is necessary.

14 Effective temperatures

Temperature has remained an ill-defined concept until the development of thermodynamics and statistical mechanics. Evidently, the fact that a quantity, called temperature, must characterize the sensation of coldness or warmth has been known since the old times. However, temperature was usually confused with heat.

The thermodynamics is an empirical theory based on four postulates that has been developed to determine some properties of the macroscopic objects without knowing the details of their constituents and interactions. After t_{eq} , an isolated and finite system reaches an equilibrium macroscopic state that can be characterized by a small number of parameters, the state variables. Temperature is one of these parameters. The first law states that energy is conserved in an isolated system after having established the equivalence between heat and work. The zeroth law states that if two systems are in thermal equilibrium with a third, then they are also in equilibrium between them. The temperature is determined by an auxiliary measurement. One sets a thermometer in contact with the system, waits until thermal equilibrium is established and then determines the temperature by calibrating the reading of the thermometer. If one repeats this procedure with a second system,

equilibrated with the first one, the first law ensures that the thermometer will itself be in equilibrium with the second system and, consequently, its reading will yield the same temperature. Hence, all systems in thermal equilibrium among them are at the same temperature.

The statistical mechanics establishes a bridge between the mechanical description of the microscopic constituents of the system and its macroscopic behavior. It yields a precise sense to the concept of temperature. To illustrate this statement, let us take an isolated system in the microcanonical ensemble with volume V and internal energy U . The entropy of the system is defined as $S(U) = k_B \ln \Omega(U)$ with $\Omega(E)dE$ the number of accessible states with mean energy between E and $E + dE$. The microcanonical definition of temperature is given by $1/(k_B T) = \partial S(E)/\partial E$, evaluated at $E = U$. The development of statistical mechanics allows one to show that this definition is equivalent to the thermodynamic one. One can equally find it with the canonical and grandcanonical formalisms.

The previous paragraphs describe the behavior of systems in thermal equilibrium. What can one say about the systems that evolve out of equilibrium? Can one define a temperature for them? Or is it at least possible for a subclass of nonequilibrium systems? If this holds true, can one use this definition as a first step towards the development of a thermodynamics and a statistical mechanics for systems far from equilibrium?

Hohenberg and Shraiman discussed the possibility of defining a temperature for certain systems out of equilibrium [126] using the modification of fdr . In Ref. [112] we critically studied the definition of such an effective temperature, T_{eff} , we insisted on the need to reach a regime with slow dynamics (related to small entropy production) to be able to define such a "state variable" and we demonstrated the importance of analyzing it in separated time-scales. In this Section we show in which sense the expected properties of a temperature are satisfied by T_{eff} and we display some numerical tests.

14.1 Thermodynamical tests

14.1.1 How to measure a temperature

In normal conditions, the temperature of an object is measured by coupling it to a thermometer during a sufficiently long time interval such that all heat exchanges between thermometer and system take place and the whole system equilibrates. Let us call $t = 0$ the instant when thermometer and system are set in contact. For simplicity, we choose to describe the thermometer with a single variable x . In order to have a statistical measure of the object's temperature [127, 72] we couple the thermometer to M independent copies of the system. Each system is characterized by a variable $\tilde{\omega}$, $\tilde{\omega} = 1; \dots; M$. The energy of the total system is

$$E_{tot} = m \frac{x^2}{2} + V(x) + \sum_{\tilde{\omega}=1}^M E(\tilde{\omega}) - \frac{k}{M} x \sum_{\tilde{\omega}=1}^M A[\tilde{\omega}];$$

with $V(x)$ the potential energy of the isolated thermometer and $E(\tilde{\omega})$ the one

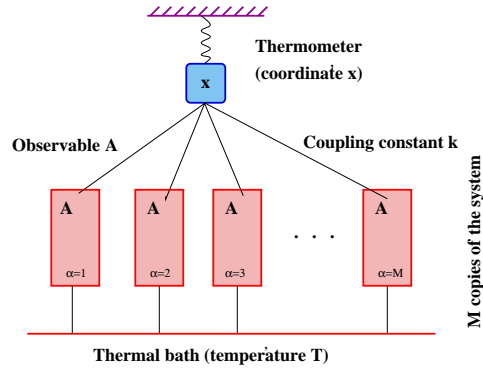


Figure 19: Coupling between a thermometer and the observable A of the system.

of the i th isolated system. Note the similarity between this coupled model and the treatment of system + environment done in Section 4 and the discussion on the harmonic oscillator coupled to a complex bath in Section 7.4.4. For a given value of M , the last term acts as an infinitesimal field $kx = \frac{k}{M}$ that is coupled to the observable A of each copy. The equation of motion of the thermometer reads

$$m \ddot{x}(t) = -\frac{\partial V(x)}{\partial x(t)} - \frac{k}{M} \sum_{i=1}^M A_i(t) \quad (14.1)$$

Again for simplicity we choose an observable A with vanishing mean $\langle A_i \rangle_{i_k=0} = 0$ where the angular brackets represent the average over different histories of the system (see Section 5.1) or the average over different systems, i.e. $\langle A_i \rangle = \frac{1}{M} \sum_{i=1}^M \langle A_i \rangle$. When the averaged observable does not vanish we use the difference between the observable and its average as the fundamental quantity. The index $k=0$ indicates that the average is taken in the absence of the thermometer. We denote $\langle A_i \rangle_k$ the averaged in the presence of the thermometer. Equation (14.1) can be rewritten as

$$m \ddot{x}(t) = -\frac{\partial V(x)}{\partial x(t)} + k^2 \int_0^t ds R(t;s) x(s) + \xi(t) \quad (14.2)$$

with $R(t;s)$ the linear response of the observable A to the change in energy $E_{\text{tot}} \rightarrow E_{\text{tot}} + k \sum_{i=1}^M x A_i$ performed at time s . The force $\xi(t)$ is a sum of M independent random variables and due to the central limit theorem, it becomes a Gaussian variable with vanishing average and variance

$$\langle \xi(t) \xi(s) \rangle_k = k^2 C(t;s) = k^2 \langle A_i(t) A_i(s) \rangle_{i_k=0} \quad (14.3)$$

for large M at first order in k . Thus, the evolution of the thermometer is determined by a Langevin-like equation [cfr. Eq. (4.7)] with a correlated noise $\xi(t)$ and a retarded friction generated by the coupling to the systems. For a generic system out of equilibrium there is no relation between R and C . For the problems we are interested in there is one. Next we explore the consequences of the modification of fdt for the reading of the thermometer.

If the systems are equilibrated with their environments fdt holds and it ensures that R is related to C by $R(t;s) = 1/(k_B T) @_s C(t;s)$ ($t \rightarrow s$), with T the temperature of the thermal bath. The thermometer is then coupled to an equilibrated colored bath and it will eventually reach equilibrium with it. The reading of the thermometer is defined from the value of its asymptotic internal energy and it has to be calibrated from the characteristics of the thermometer that, of course, must be known before starting the measurement. If one takes a simple harmonic oscillator as a thermometer, one proves that the internal energy approaches $k_B T$. This is the result expected from equipartition since the oscillator has only two degrees of freedom (position and momentum).

Imagine now that the systems are glassy of the type discussed in Section 12. If one studies a system with two correlation scales such that

$$R(t;s) = \begin{cases} R_{st}(t-s) & \text{if } t-s \ll \tau_s \\ \frac{1}{t} R_{ag} \frac{s}{t} & \text{if } \frac{s}{t} = O(1) \end{cases} \quad C(t;s) = \begin{cases} C_{st}(t-s) & \text{if } t-s \ll \tau_s \\ C_{ag} \frac{s}{t} & \text{if } \frac{s}{t} = O(1) \end{cases}$$

$$R_{st}(t-s) = \frac{1}{k_B T} @_s C_{st}(t-s); \quad R_{ag} \frac{s}{t} = \frac{t}{k_B T} @_s C_{ag} \frac{s}{t}$$

with T the temperature of the thermal bath and T a different value read from the modified fdt relation. The reading of the thermometer, or its asymptotic internal energy density, is found to be [12]

$$E_{\text{therm}} = \frac{!_0 \tilde{C}(!_0; t_w)}{\sim^0(!_0; t_w)} \quad (14.4)$$

where $!_0$ is the characteristic frequency of the thermometer, $\tilde{C}(!_0; t_w)$ is the Fourier transform of the correlation function with respect to the time-difference and $\sim^0(!_0; t_w)$ is the out of phase susceptibility defined in Eq. (5.8).

If the characteristic frequency $!_0$ is very high, the thermometer evaluates the evolution during the first step of the relaxation $t \rightarrow s$, one finds $E_{\text{therm}} = k_B T$ and one identifies T with the temperature of the system. Instead, if the characteristic frequency is very low, the thermometer examines the behavior of the system in the long time scales, $s/t = O(1)$ in the example, one finds $E_{\text{therm}} = k_B T$ and one identifies T as the temperature of the system.

One can easily generalize this discussion to a problem with many correlation scales, each with a different value of the effective temperature. In order to measure them it is sufficient to tune the characteristic frequency of the oscillator to the desired scale.

A concrete realization of this measurement corresponds to a generalization of the Brownian motion experience of Perrin in which one follows the evolution of a tracer immersed in the fluid. If the latter is equilibrated at temperature T , after a short equilibration period, each component of the averaged kinetic energy of the tracer approaches $k_B T/2$. Instead, if the fluid evolves out of equilibrium, one can choose the mass of the particle (that plays the role of the characteristic frequency in the previous discussion) in order to examine the rapid dynamics, or the slow dynamics. The tracer acquires an averaged kinetic energy $E_{\text{kin}} = k_B T/2$ with

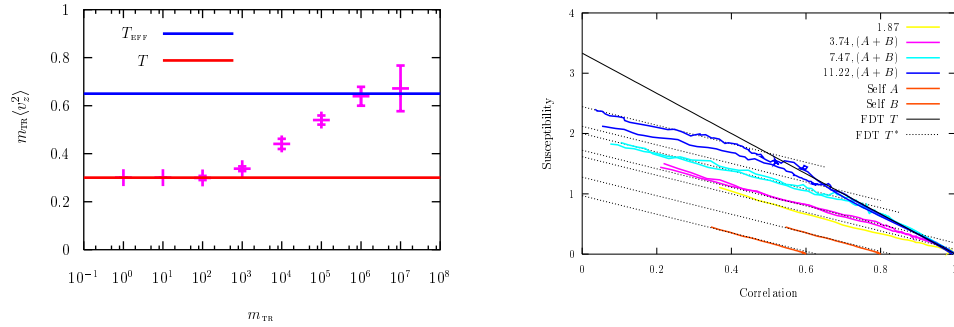


Figure 20: A Lennard-Jones liquid with two types of particles, A and B, in its liquid phase under homogeneous shear. Left: the asymptotic value of the transverse component of the averaged kinetic energy of the tracer particle normalized by k_B , $T_{\text{coeff}} = m_{\text{tr}} \langle v_z^2 \rangle / k_B$, against its mass. Right: Parametric plot between the linear response integrated over a time-interval of length t_w , $(k; t_w)$, and the incoherent scattering function $C(k; t_w)$. The four first curves correspond to $k = 1.87; 3.74; 7.47; 11.22$. The self-displacement is also shown. The equilibrium straight line of slope $1/(k_B T)$ is represented by a black line while the black dotted parallel straight lines have slopes $1/(k_B T)$. From Ref. [121].

T the value of the effective temperature in the time scale explored. Berthier and J-L Barrat [121] performed this measurement in a numerical experiment using a dense liquid modeled as in Eq. (2.4) under homogeneous shearing in contact with a thermal bath at temperature T as a fluid. They chose a Lennard-Jones particle as a tracer with mass m_{tr} . The left panel shows the asymptotic value of the transverse component of the averaged kinetic energy (transverse to the shearing rate direction) as a function of the mass of the tracer. One clearly sees how the effective temperature $T = m_{\text{tr}} \langle v_z^2 \rangle / k_B$ interpolates between the value T at small masses and the value $T > T$ for large masses. The trend can be easily understood. A very light tracer easily reacts to the quick bombardment of the particles in the fluid and it feels the temperature of the bath via the rapid scale of relaxation. A heavy tracer instead can only move via large rearrangements of the fluid and these correspond to the slow part of the relaxation. The transition between the two values is very smooth and it occurs over several orders of magnitude in the mass. The consistency of the explanation, i.e. the relation between T and the fdt relation, will become explicit in Section 14.1.2.

A complementary discussion on thermometric measurement of T_{eff} and, in particular, of the effect of not having well-separated time-scales, appeared in [41, 128].

14.1.2 Zeroth law

A temperature, even if it is defined out of equilibrium, should control the direction of heat flows and the partial equilibration between observables in interaction. (Two observables interact if and only if the crossed linear response $R_{AB}(t; t^0)$, as defined in Eq. (5.5), does not vanish.)

With a pair of observables A and B one constructs two self and two cross correlations and responses. In each correlation scale the fdt relation is modified by a constant factor with which one constructs the effective temperature. If the notion of an effective temperature is correct, two interacting observables that evolve in the same time-scale should acquire the same value of T_{eff} . The equilibration between different observables is well defined only in the limit of small heat, or energy, exchanges. This limit is achieved in a free relaxing system when the waiting time becomes very long or in a driven system rendered stationary when the non-conservative force vanishes. It is only possible for observables evolving in the same time-scale (note that even a single observable can have several values of the effective temperature when examined on different time-scales). We call partial equilibrations those arriving in the same time-scale. In contrast, if the two observables A and B do not interact they should evolve in different time-scales.

The property of partial equilibration has been proven analytically for the fully connected models solved in Section 12 [112] and, later, for all perturbative approximation of more realistic models under the assumption of there being a slow dynamics with a sharp separation of time-scales [72, 130]. It can be seen numerically as follows. Take, e.g., two spin models with different exchange strengths, J_1 and J_2 in contact with the same thermal bath at temperature T and couple them linearly with a term $\sum_{i=1}^N s_i \phi_i$ where s_i and ϕ_i are the dynamic variables of each system and ϕ is the coupling constant. (Other couplings are, of course, possible.) When $\phi = 0$ the two systems evolve independently and their T_{eff} 's in the aging scale take different values. If we now let the coupled system ($\phi > 0$) evolve it will reach an asymptotic limit (roughly when the energy of the full system decays very slowly). In this limit we trace the fdt parametric plots for the two self and cross C and R 's. We observe that if $\phi < \phi_c$ the cross responses vanish and the effective temperatures still take different values in the aging scales that are now forced to evolve with different scalings. Instead, if $\phi > \phi_c$, the cross responses do not vanish, the two systems lock and T_{eff} in the aging scale acquires the same value for both self and cross fdt relations. Note that for the manifold, all modes have the same value of the effective temperature in the same correlation scale. This is achieved internally and it means that all modes are in interaction.

Partial equilibrations have been tested numerically by Berthier and J-L Barrat [121] in the dense homogeneously sheared liquid discussed in Section 14.1.1 (partial equilibrations simply relaxation Lennard-Jones mixture were studied by Kob and J-L Barrat in [58]). The relevant correlators for this system are the wave vector dependent incoherent scattering functions and their associated responses. Berthier and Barrat measured these two-time functions for the same and different species and several values of the wave vector. Figure 20 shows the parametric fdt plots. All the curves have a broken line form with a first part with slope $-1 = (\beta_b T)$ and a second part with a common slope $-1 = (\beta_b T)$. The value T is identical to the result found monitoring the kinetic energy of the tracer (see Section 14.1.1) demonstrating that the scenario is consistent. Note that in this case we cannot tune the coupling between different wave vectors as we did when we externally coupled the two spin model. The fact that T_{eff} in the slow scale is the same for all wave

vectors studied shows that they interact. This is also seen from the fact that the cross responses do not vanish. Coupled oscillator models with parallel or sequential Monte Carlo dynamics do and do not partially equilibrate, respectively. [129]. In the latter case the thermal conductivity is very small and one is in situation in which, effectively, $\tau < \tau_c$.

Intriguingly, the fact that each time-scale has its own effective temperature has been shown to fail in two models. These are the trap model [48] and the 1d Ising chain at $T = 0$ [48, 119, 120] when special perturbations are applied. In both cases one can construct observables that evolve in the same time-scale but have different values of the effective temperatures. In the first case, the failure might be ascribed to the fact that the model does not have an equilibrium state. This is not the case in the second model though. The origin of the failure might then be related to having used special observables, see the discussion in [48]. Still another pathology was already signaled for this problem: the global correlation and response decay in a single time-scale but the asymptotic $\chi(C)$ is a curve contradicting the notion of a correlation-scale dependent effective temperature. It is quite plausible that this problem is also related to the failure of the relation between dynamics and statics discussed in Section 13.10. A good understanding of the conditions under which this property holds is still lacking. Experiments in laponite show some mismatch between the value of T_{eff} found with mechanical and electrical measurements. The reason for this is unclear [61].

One can also verify that the heat exchanges go from the higher values of T_{eff} to lower ones. However, it is still not clear why one can have a partial equilibration to a higher value of T_{eff} than those of the two independent observables, as it has been obtained analytically for some solvable fully-connected models.

14.1.3 Auxiliary thermal baths

A supplementary verification of the thermodynamic character of the effective temperature comes from the study of the action of complex thermal baths on the dynamics of simple systems, as discussed in Section 14.1.3, or glassy systems.

We found that an arbitrarily weak auxiliary bath with $\gamma(0)$ small has an important effect provided it is sufficiently slow and its temperature is within the range of values of the effective temperatures of the slow dynamics. The (slow) time dependence of all C and R 's are affected by a time rescaling $t \rightarrow K(t)$. This is such that the time-scale which has an effective temperature equal to the temperature of the auxiliary bath, say T_1 , is locked to the time-scale of the bath. In particular, if we couple an aging system with a bi-valued $T_{\text{eff}} = (T; T')$ to a composite stationary bath with two time scales, $\gamma_1 \neq 0$ and $\gamma_2 > 0$ and two temperatures T and T_2 , respectively, we find that the system becomes stationary if $T_2 > T'$, and is hardly affected if $T_2 < T'$. More generally, an aging system with multiple effective temperatures, $T_{\text{eff}}(C)$, becomes partially stationary for all the time-scales with $T_2 > T_{\text{eff}}(C)$, but still ages for time-scales with $T_2 < T_{\text{eff}}(C)$. We found this behavior in Monte Carlo simulations of the 3d Ising model [130].

14.2 Temperature fixing by susy breaking

For any model one can derive a set of integro-differential equations that couple all two-point functions. These admit a representation in terms of the super-correlator $Q(a;b)$. In the asymptotic limit in which we neglect the time-derivatives, these equations are invariant under any change of supercoordinates, a , that have unit superjacobian [162]. Fixing the time-reparametrisation (the function $h(t)$ in each correlation scale) and the value of the effective temperature corresponds to breaking this large symmetry group to a subgroup [130].

14.3 Fictive temperatures

"Fictive temperatures" are phenomenological concepts that have been used to describe experimental data [131] (see also [132]). The basic idea has been to claim that, when crossing T_g , the system remembers its equilibrium configuration before the quench and it remains effectively at a higher temperature T_f . Several refined prescriptions to extract time and preparation dependences of T_f have been proposed. The relation between T_{eff} and T_f has been discussed in [112]. Here we simply stress that even if the same basic idea can be used to interpret T_{eff} , the latter has the properties of a thermodynamic temperature while this is not obvious for T_f .

14.4 Nonequilibrium thermodynamics

Once equipped with a bona fide effective temperature the natural next step is to try to construct a thermodynamics for such systems out of equilibrium. This has been proposed by Nieuwenhuizen [133] based on two previous results: (1) similar constructions done using the fictive temperatures by Tool, Moynihan and others [131]. (2) the relation between the dynamics and the tap approach that we shall discuss in Section 15. The idea is to define generalized thermodynamic potentials in which T_{eff} intervenes as a supplementary parameter (one can also include other state variables as an effective pressure, etc.). For the fully connected models these potentials have a precise meaning based on the tap analysis (Section 15). Their validity for more realistic models is still an open problem.

14.5 Statistical mechanics

Edwards measure

In the 80s Edwards proposed that the stationary properties of dense granular matter under a weak forcing can be determined with a flat distribution of the blocked configurations, i.e. those in which no grain is able to move) at the chosen density [134]. Note that this is possible in granular matter since the external temperature is irrelevant. Following this "microcanonical" approach the logarithm of the number of blocked configurations at constant density defines an entropy from which one obtains a compactivity by simple derivation with respect to the density. Extending this prescription one can define an Edwards' temperature for

soft systems by considering blocked configurations at fixed energy and computing $1/(k_B T_{\text{edw}}) = \partial S_{\text{edw}}(E)/\partial E$.

Edwards' temperature can be calculated explicitly for the fully connected models at zero external temperature (again using techniques discussed in Section 15). Surprisingly, one finds that its actual value coincides with the value taken by T_{eff} defined from the modification of fdt in a purely dynamic calculation. This result has boosted the study of solvable models in low dimensionalities analytically and more realistic systems numerically to check if the coincidence goes beyond the fully-connected case. Until now, several models where Edwards' distribution yield very good results have been exhibited [122, 135] while some others where it fails have also been shown (e.g. the random field Ising model [122]). In the latter cases one finds a well-defined T_{eff} while Edwards' measure fails to give the correct results. The result of including additional constraints on the configurations counted have also been analysed and naturally improve the results derived from Edwards' measure. This area of research is very active and more work is necessary to determine the limits of validity of Edwards' proposal.

The definition of Edwards' measure is unambiguous since it is a zero temperature entity based on the study of minima of the potential energy. An extension to finite T necessitates the analysis of a free-energy landscape. This can be done analytically for fully-connected models as explained in Section 15. In finite d cases for which one is forced to use numerical techniques it is not, however, obvious how to define, let alone compute, the entropy $(-k_B \ln Z)$.

Inherent structures

The inherent structure approach of Stillinger and Weber [136] has been recently revisited and extended to study dynamic properties of glass formers and glasses [137]. The original approach, even if static, is close to the ideas of Edwards. At the static level it consists in dividing the partition function in inherent structures, or pockets of configurations around minima of the potential energy, and transforming the sum into sums over minima and the configurations associated to them. In order to connect with the dynamics, one computes the entropy of the inherent structures and then derives an inherent structure temperature with a similar prescription to the one of Edwards. The sampling of the inherent structures numerically is a non-trivial issue.

A critical analysis of the applicability of this approach at finite temperatures has been presented by Biroli and Monasson [142] who stressed the need of analyzing the free-energy, instead of the potential energy, at finite T . They also compared with the tap analysis discussed in Section 15. Having said this, the use of the inherent structure approach has been rather successful when confronted to T_{eff} [137].

15 Metastable states

The aim of the tap approach is to define and study a free-energy density as a function of the relevant order parameters [56]. Its stationary points are the (stable and unstable) metastable states. For a fully connected Ising magnet the tap free-

energy density simply depends on the averaged global magnetization and, below T_c , has the form drawn on the right panel of Fig. 1. The vanishing global magnetization is not a good order parameter for disordered spin systems and one is forced to introduce all local ones. The approach can be extended to describe classical and quantum systems in and out of equilibrium [143, 144]. Under different names similar approaches appear in other branches of condensed matter physics. The density functional theory of the inhomogeneous electron gas in solids or the dynamic mean-field theory of strongly correlated electrons are very similar in spirit to the tap approach [91].

The clearest way of deriving the tap free-energy density for disordered models is based on two ingredients: one identifies an adequate perturbative expansion, and one Legendre transforms the standard free-energy density with respect to a well-chosen set of parameters. When these two choices are correctly done, only a finite number of terms in the expansion do not vanish for typical configurations of disorder for infinite dimensional models. In finite d one can attempt a large d expansion [146].

For spin-glasses at low $-T$ the tap free-energy density has an infinite number of stationary points. The tap approach gives us access to the complete organization of metastable states of any type of stability (minima, saddles of all types, maxima). In particular, this has been analysed in great detail for the p spin model and the like since we expect it to mimic what occurs in real glassy systems though in an exaggerated manner.

In the following we first derive the tap free-energy density for a generic spin model with Ising or spherical variables. Next we summarize the consequences of this approach for the p spin spherical model. We also briefly explain how the number of metastable states is computed and how this depends on the parameters in the model. We explain how the approach is generalized to deal with dynamic properties. This full set of results gives us a complementary view of the non-equilibrium dynamics and serves as the basis for an image of the dynamics of finite d glassy models.

15.1 Equilibrium

Before describing the tap approach let us summarize the equilibrium behavior of the mean-field models as derived from the analysis of its disordered averaged free-energy density $[f] = [\ln Z]_T/N$ with the replica trick. Again the three classes, ferromagnetic-like ($p = 2$), glassy-like ($p > 3$) [167] and spins-glass-like (sk) [9] models have different characteristics.

For the spherical p spin model with $p > 3$ [167] the standard Parisi Ansatz [69] yields a static transition at T_s from a paramagnetic phase where a replica symmetric Ansatz solves the problem to a glassy phase where a one step replica symmetry breaking Ansatz is needed. At low T 's, the breaking point parameter, x , and the Edwards-Anderson order parameter, $q_{ea} = N^{-1} \sum_i [s_i]^2$, in the Parisi matrix are fixed by requiring that the free-energy density be a maximum. This yields a static transition temperature, T_s , given by the set of equations $T_s = y p = (2y) (1 - y)^{p-2}$ and $2 = p = 2y(1 - y + \ln y) = (1 - y^2)$. One can check that $T_s < T_d$. The static transition is discontinuous in the sense that q_{ea} jumps at T_s but it is of second

order thermodynamically since all susceptibilities are continuous across T_s . The equilibrium energy density at $T = 0$ is given by the implicit equation $2y = p = \frac{1}{q} [E(T=0) - E^2(T=0) - E_{th}^2] = (p-1)$. One checks that $E_{eq} < E_1 = E_{th}$.

A modified prescription to determine the breaking point, x , in the one step Ansatz yields different results. If instead of extremizing with respect to x one requires that the solution be marginally stable by setting the replicon eigenvalue of the matrix of quadratic fluctuations [175] to zero, leads to a different solution with a dynamical meaning. (All other eigenvalues are positive.) Namely, one finds a transition from the paramagnetic to the glassy phase at a higher temperature that coincides with the dynamical critical temperature found with a purely dynamical calculation, T_d . Moreover, q_{ea} coincides with the dynamical one and the breaking point x yields the ratio $T = T_{eff}$. Consequently, all one-time quantities as the asymptotic energy density and generalized susceptibilities coincide with the ones found dynamically (e.g. $E = E_{th}$). The fact that with the condition of marginal stability we access the region of phase space reached dynamically is due to the fact that with both we search for the path of steepest descent from the threshold level, as explained below.

When $p = 2$ instead [108], the replica solution below T_s is replica symmetric with a non-vanishing q_{ea} and marginally stable. The static transition is continuous, dynamical and static transition temperatures coincide, $T_s = T_d$, and $x = T = T_{eff} = 0$ [109]. The gap between the threshold and the equilibrium level collapses and the static energy density is the value reached dynamically, $E_{eq} = E_1$. Still the nonequilibrium dynamics does not stop in finite times with respect to N .

For $p < 2$ the equilibrium calculation needs a full replica symmetry breaking solution [9]. This can be interpreted as being equivalent to having a sequence of correlation scales in the nonequilibrium dynamics. The static transition is continuous, the static and dynamical q_{ea} are identical, the relation in (13.4) holds and all one-time quantities coincide with the equilibrium values. The static solution is also marginally stable.

From these three paragraphs one observes that the structure of the static and dynamical solution of purely potential mean-field problems is indeed very similar. One can propose a "dictionary"

rs	, 2 corr. scales, the aging one with $T_{eff} = T > 1$
1 step rsb	, 2 corr. scales, the aging one with $T_{eff} = T < +1$
full rsb	, 1 corr. scales, the aging ones with $T_{eff}(C) < +1$

while remembering that the replica solution that describes the statistical properties of the region of phase space reached dynamically has to be determined using the condition of marginal stability and not equilibrium. This connection between replicas and dynamics has been extensively exploited to use the replica trick as a substitute for dynamics. In fact, partial information about dynamics as the dynamical critical temperature, the value of T_{eff} , etc. is thus obtained. One has to keep in mind though that many aspects of the dynamics go beyond static calculations. Features like the existence of an effective temperature have been shown in models

with trivial statics [53, 54] or above the dynamic transition when non-potential or time-dependent forces are included [19, 26].

15.2 Static tap approach

In the introduction to this Section we announced that two choices facilitate the derivation of the tap free-energy density. In order to use a good perturbative expansion we weight a part of the original Hamiltonian with a parameter β . For the p spin model we simply propose

$$H(\beta; \mathbf{s}) = \sum_{i_1 < \dots < i_p} J_{i_1, \dots, i_p} s_{i_1} \dots s_{i_p} \quad (15.5)$$

In other models we weight the higher order interactions with β without modifying the quadratic terms. The idea is to expand in powers of β and set $\beta = 1$ at the end of the calculations to recover the original model [145, 146].

The second important step in the derivation is the choice of the order parameters to use in the Legendre transform of the free-energy density. For spin models these are the averaged local magnetizations m_i and a global spin constraint l . The Legendre transform reads

$$(\beta; \mathbf{m}_i; l; h_i) = \ln \text{Tr}_{\mathbf{s}_i} e^{-H(\beta; \mathbf{s}) + \sum_{i=1}^N h_i (s_i - m_i) - \frac{\beta}{2} \sum_{i=1}^N (s_i^2 - l)} \quad (15.6)$$

The trace represents a sum over all configurations of the spins, e.g. $\text{Tr}_{\mathbf{s}_i} = \prod_{i=1}^N \sum_{s_i=-1}^1$ for Ising and $\text{Tr}_{\mathbf{s}_i} = \int_{-1}^1 \prod_{i=1}^N ds_i$ for spherical variables. Requiring stationarity with respect to the Lagrange multipliers h_i and l one obtains

$$m_i = \langle s_i \rangle \text{ and } l = \frac{1}{N} \sum_{i=1}^N \langle s_i^2 \rangle \quad (15.7)$$

for all values of β . The angular brackets indicate the statistical average over the spins using the full Boltzmann weight in (15.6). Since the rhs depend on h_i and these equations can be inverted to yield $h_i(\beta; \mathbf{m}_i; l)$ and $l(\beta; \mathbf{m}_i; l)$, that one substitutes in (15.6) to write β as a function of $(\beta; \mathbf{m}_i; l)$. Henceforth we drop the parameter dependence and simply note β . The introduction of the parameter allows us to express β as a power series in β :

$$\beta = \sum_{n=0}^{\infty} \frac{\partial^n \beta(\beta; \mathbf{m}_i; l)}{\partial \beta^n} \frac{\beta^n}{n!} \quad (15.8)$$

For the p spin model and the like this is equivalent to a high T expansion. In other cases it is an expansion around an "equivalent" free theory. Interestingly enough only a finite number of terms contribute to the series for fully connected models. For finite dimensional cases a truncated series yields an approximation around mean-field.

The zero-th order term depends on the nature of the spins considered:

$$\begin{aligned} \text{ising} &= \sum_{i=1}^N \frac{1+m_i}{2} \ln \frac{1+m_i}{2} + \frac{1-m_i}{2} \ln \frac{1-m_i}{2} ; \\ \text{sph} &= \frac{N}{2} \ln 1 - \frac{1}{N} \sum_{i=1}^N m_i^2 : \end{aligned}$$

These are the entropies of N independent Ising or spherical spins constrained to have local magnetizations m_i . The first order term is proportional to

$$\begin{aligned} \frac{\partial \langle \dots \rangle}{\partial} \Big|_{=0} &= \sum_{i_1 \dots i_p} J_{i_1 \dots i_p} h_{i_1} \dots h_{i_p} \Big|_{=0} + \sum_{i=1}^N \frac{\partial h_i}{\partial} h_{i_1} \dots m_{i_1} \Big|_{=0} \\ \sum_{i=1}^N \frac{\partial}{\partial} h_{i_1}^2 \Big|_{=0} &= \sum_{i_1 \dots i_p} J_{i_1 \dots i_p} m_{i_1} \dots m_{i_p} : \end{aligned} \quad (15.9)$$

In the first equality, the last two terms on the rhs vanish due to Eqs. (15.7). The average in the first term factorizes since it has to be taken with the free-action ($\beta = 0$). The quadratic term in the expansion is proportional to

$$\frac{\partial^2 \langle \dots \rangle}{\partial^2} \Big|_{=0} = \sum_{i_1 \dots i_p} Y_{i_1 \dots i_p} \quad (15.10)$$

with $Y_{i_1 \dots i_p} = J_{i_1 \dots i_p} s_{i_1} \dots s_{i_p} (s_{i_1} - m_{i_1}) m_{i_2} \dots m_{i_p} \dots m_{i_1} \dots m_{i_{p-1}} (s_{i_p} - m_{i_p})$. This term has been computed using the following identities. First, the variation of in Eq. (15.6) with respect to m_i and 1 yields $h_i = \frac{\partial \langle \dots \rangle}{\partial m_i}$ and $\frac{\partial}{\partial} = \frac{2}{N} \frac{\partial \langle \dots \rangle}{\partial 1}$. Taking the variation with respect to and evaluating at $\beta = 0$ one has

$$\frac{\partial h_i}{\partial} \Big|_{=0} = \frac{\partial^2 \langle \dots \rangle}{\partial m_i \partial} \Big|_{=0} ; \quad \frac{\partial}{\partial} \Big|_{=0} = \frac{2}{N} \frac{\partial^2 \langle \dots \rangle}{\partial 1 \partial} \Big|_{=0} \quad (15.11)$$

Now, the contributions $O(N)$ are proportional to $J_{i_1 \dots i_p}^2$ and these can be estimated by replacing its value by $p \equiv (2N^{p-1})$ since $J_{i_1 \dots i_p} \approx p \equiv (2N^{p-1})$. As done for the first order term we factorize the thermal averages evaluated at $\beta = 0$ and

$$\frac{\partial \langle \dots \rangle_{\text{ising}}}{\partial^2} \Big|_{=0} = 2N \frac{1}{2} \mathcal{Q}_a \left(\frac{1}{2} \mathcal{Q}_a \right) \quad (15.12)$$

$$\frac{\partial \langle \dots \rangle_{\text{sph}}}{\partial^2} \Big|_{=0} = \frac{2}{2} N \mathcal{P} \left(\frac{1}{2} \mathcal{Q}_a \right) \quad (15.13)$$

where we introduced the overlap or (static) Edwards-Anderson parameter,

$$\mathcal{Q}_{\text{Ea}} = \frac{1}{N} \sum_{i=1}^N m_i^2 : \quad (15.14)$$

Higher order terms in the series expansion are sub-leading in N and do not contribute in the thermodynamic limit. Thus, for these mean-field models the tap free-energy density is made of three terms: the zero-th order has an entropic origin, the first order is the interaction term in the mean-field approximation which is exact for fully connected models, and the second order is the reaction or Onsager term.

15.3 The tap equations

The variation of the tap free-energy density, ϕ , with respect to m_i (and 1 for the spherical model) yields the tap equations. For the spherical model one finds [147]

$$\frac{m_i}{(1 - q_a)} = \frac{1}{p} \sum_{(i_2, \dots, i_p) \in i} J_{i i_2 \dots i_p} m_{i_2} \dots m_{i_p} - \frac{p(p-1)}{2} q_a^{p-2} (1 - q_a) m_i \quad (15.15)$$

$$= \frac{1}{1 - q_a} + \frac{p-2}{2} (1 - q_a)^{p-1} : \quad (15.16)$$

The study of these equations is simplified by defining the angular variables $\hat{m}_i = \frac{m_i}{\sqrt{q_a}}$ that verify the spherical constraint $\hat{m}_i^2 = 1$. Multiplying Eqs. (15.15) by \hat{m}_i and summing over i we rewrite them in terms of the zero-temperature energy density $E = \frac{1}{N} \sum_{i_1 < \dots < i_p} J_{i_1 \dots i_p} \hat{m}_{i_1} \dots \hat{m}_{i_p}$:

$$E = \sum_{i_2 < \dots < i_p} J_{i_2 \dots i_p} \hat{m}_{i_2} \dots \hat{m}_{i_p} : \quad (15.17)$$

The overlap q_{ea} is related to E by

$$pE = \frac{1}{q_a^{(p-2)/2} (1 - q_a)} \left[1 + \frac{p(p-1)}{2} (1 - q_a)^2 q_a^{p-2} \right] : \quad (15.18)$$

Equation (15.17) does not depend on T while (15.18) does. The multiplicity of solutions at a given E is entirely determined by Eq. (15.17), see Section 15.5. The existence or not of these solutions has to be tested with Eq. (15.18). The remaining Eq. (15.16) reads

Conveniently rewritten Eq. (15.18) is quadratic and yields

$$q_a^{(p-2)/2} (1 - q_a) = \frac{k_B T}{p-1} E \frac{q_a}{E^2 - E_{th}^2} \quad \text{with } E_{th} = \frac{2(p-1)}{p} : \quad (15.19)$$

This equation admits a real solution only if $E < E_{th}$, the threshold energy density at $T = 0$. The minus (plus) sign corresponds to a minimum (maximum) of the free-energy. The physical q_{ea} is then associated to the minus sign. With this choice, q_{ea} takes its maximum value on the threshold and then monotonically decreases until reaching its minimum value on the equilibrium level, $q(E_{th}) = q_a(E) = q_a(E_{eq})$.

For fixed E and T the lhs in Eq. (15.19) has a bell shape form. When $T \rightarrow 0$, $q_{ea} \rightarrow 1$ and $(1 - q_a)$ is finite. The maximum is located at $q_{ea} = (p-2)/p$ and it has a height $2/p \cdot (p-2)/p^{(p-2)/2}$. Each solution at $T = 0$ that corresponds to a given E can be followed to finite T until it disappears at $T = T(E)$ when the lhs reaches the maximum. One can check that the tap solutions do not merge nor bifurcate as a function of T . Then at any temperature T we label the tap solutions with their associated zero-temperature energy density E .

Plugging E_{th} in Eq. (15.18) we find that the overlap q_{ea} is given by the equation

$$\frac{p(p-1)}{2} q_{th}^{p-2} (1 - q_{th})^2 = (k_B T)^2 : \quad (15.20)$$

The threshold energy density E_{th} and the overlap q_{th} coincide with the asymptotic value of the dynamic energy density and the Edwards-Anderson parameter at $T = 0$, respectively. Thus, the nonequilibrium dynamics approaches asymptotically the threshold level.

15.4 Stability of, and barriers between, the tap solutions

The spectrum of the free-energy Hessian around a stationary point of the tap free-energy is a shifted semi-circle. The lowest eigenvalue λ_{min} is greater than zero for sub-threshold free-energy densities (or zero-temperature energy density). This means that for $E < E_{th}$ typical stationary states are minima. Instead, near the threshold λ_{min} drops to zero as [12]

$$\lambda_{min}(f; T) = \frac{P}{q_{th}} (f_{th} - f) \quad (15.21)$$

and the stationary states on the threshold are typically marginal in the sense that they have many flat directions.

Even if the connection between dynamics and the static tap free-energy landscape is not obvious a priori, it has been proposed and used in several works [11, 12]. The formalism in Section 15.8 and [148] settles it on a firm ground. If one imagines that the dynamics can be viewed as the displacement of a representative point in the free-energy landscape, not only the organization minima, saddles and maxima has to be known but also how do the barriers between these stationary points scale with N . Few results about barriers exist and, in short, they are the following. The barriers between threshold states vanish when $N \rightarrow 1$ [3, 149] and there is no sharp separation between them. This has been proven by analyzing the constrained complexity, related to the number of threshold states that have an overlap q with a chosen one ($\mathcal{C}(q) = N^{-1} \sum_{i=1}^N \sum_{j=1}^N \delta(q - q_{ij})$ where \sim and \sim are the two configurations). This complexity decreases with increasing values of q and it vanishes as a power law at $q = q_{th}$. This means that one can find threshold states that are as similar as required to the chosen one. The threshold level is then a series of flat connected channels. The non-equilibrium dynamics starting from random (typical) initial conditions approaches this level asymptotically and it never stops since the system drifts in a slower and slower manner as time evolves following these flat directions [12]. On the other hand, the barriers between equilibrium and metastable states have been estimated to be $O(N)$ [147, 149]. One can guess that the barriers between sub-threshold tap states also scale with N . For finite N the dynamics should penetrate below the threshold and proceed by thermal activation. An Arrhenius-like time will then be needed to descend from one level to the next. Naturally one should see another kind of separation of time-scales develop. Simulations of the p-spin model for finite N confirm the existence of metastable states below the threshold. This is most clearly seen following the evolution of the energy density of the model weakly perturbed with a non-potential force. One sees periods of trapping in which the energy-density is fixed to a given value and periods in which the system escapes the confining state and surfs above the threshold until being trapped in a new state [18, 26, 19] (see also [160] a numerical study of the finite N p-spin model).

15.5 Index dependent complexity

At low T 's the number of stationary points is exponential in N . This suggests to define the complexity $\chi_J(E)$:

$$\chi_J(E) = \lim_{N \rightarrow \infty} \frac{1}{N} \ln N_J(E); \quad (15.22)$$

where $N_J(E)$ is the number of solutions with energy density E . Actually, one can refine the study by grouping the stationary points of the tap free-energy density into classes according to the number of unstable directions. Thus, minima are saddles of index 0, saddles with a single unstable direction have index 1 and so on and so forth. The complexity of each kind of saddle is $\chi_{Jk}(E) = \lim_{N \rightarrow \infty} \frac{1}{N} \ln N_{Jk}(E)$, where k denotes the index of the considered saddles. For the spherical spin model, their average over disorder, $\bar{\chi}_k = [\chi_{Jk}]$, are ordered in such a way that [150]

$$\begin{aligned} \chi_0(E) &> \chi_1(E) > \chi_2(E) > \dots & \text{for all } E < E_{th} \\ \chi_0(E) &= \chi_1(E) = \chi_2(E) = \dots & \text{if } E = E_{th} \end{aligned}$$

Thus, when $E < E_{th}$ minima are exponentially dominant in number with respect to all other saddle points. Moreover, one proves that the complexities vanish at a k -dependent value of E . The complexity of minima is the last one to disappear at E_{eq} .

15.6 Weighted sums over tap solutions

The thermodynamics at different T is determined by the partition function, Z_J . De Dominicis and Young [151] showed that the equilibrium results obtained with the replica trick or the cavity method are recovered from the tap approach when one writes Z_J as a weighted sum over the tap stationary states.

Indeed, if one divides phase space into pockets of configurations that surround the stationary points of the tap free-energy one can carry out the statistical sum on each sector of phase space:

$$Z_J = \sum_s \exp(-H_J(s)) = \sum_s^P \exp(-H_J(s)) \quad (15.23)$$

where the index s labels the tap solutions and \sum_s^P represents a restricted sum over the configurations that belong to the pocket associated to the solution s . In order to make this separation precise one needs to assume that the barriers separating the pockets diverge in such a way to avoid ambiguities when associating a configuration to a tap solution. The restricted sum is related to the free-energy of the tap solution $\exp(-F_J(s)) = \sum_s^P \exp(-H_J(s))$ and the partition function becomes $Z_J = \sum_s^P \exp(-F_J(s))$. Thus, any statistical average can be computed using the weight $\exp(-F_J(s))/Z_J$. The sum over solutions can be replaced by an integral over free-energies if one introduces their degeneracy $N_J(\beta; f)$ and their associated complexity, $\chi_J(\beta; f) = \lim_{N \rightarrow \infty} \frac{1}{N} \ln N_J(\beta; f)$, with $f = F/N$,

$$Z_J = \int df \exp[N(\chi_J(\beta; f) - f)] : \quad (15.24)$$

The complexity is a self-averaging quantity, we then write $\chi(\beta; f) = \langle \chi(\beta; f) \rangle$. When $N \rightarrow \infty$ the integral is dominated by the solutions that minimize the generalized free-energy, $f = f(\beta; f)$. This is achieved either by $f = f_{\min}$ with $\chi(\beta; f_{\min}) = 0$ or by states that do not have the minimum free-energy if their complexity is finite, in which case [138]

$$= \frac{\partial \langle \chi(\beta; f) \rangle}{\partial f} = Z_{\chi} \exp[-N (f - \langle \chi(\beta; f) \rangle)] : \quad (15.25)$$

Minima of the generalized free-energy density with higher ($f > f_{\min}$) or lower ($f < f_{\min}$) free-energy density are metastable.

From the analysis of the partition function one distinguishes three temperature regimes [11, 138]:

$$\text{Above the dynamic transition } T > T_d = \frac{r}{2(p-1)^{1/r}} :$$

The paramagnetic or liquid solutions $m_i = 0$, dominate the partition sum, $Z \sim \exp(-N f^m)$. States with $m_i \neq 0$ exist in this range of temperatures but they do not dominate the sum.

Between the static and dynamic transitions $T_s < T < T_d$:

The paramagnetic state is fractured into an exponential in N number of non-trivial tap solutions with $m_i \neq 0$. Their free-energy density and the partition sum are given by Eq. (15.25). Each of these states has a rather high free-energy that is counterbalanced by the entropic contribution. Besides the states that dominate the partition sum, a very large number of other metastable states, with higher and lower free-energy density, also exist but are thermodynamically irrelevant. It turns out that f coincides with the extrapolation of f^m from $T > T_d$ to this temperature region even if the paramagnetic solution does not exist. Note that in this temperature regime the standard replica calculation fails since it tells us that the equilibrium state is the simple paramagnet. Remarks on this method are able to extract more precise information about the non-trivial states contributing to equilibrium [149].

Below the static transition $T < T_s$.

An infinite though not exponential in N number of states with the minimum free-energy density dominate the sum. The complexity $\chi(\beta; f)$ vanishes and this is associated to an entropy crisis. This is similar to the argument used by Kauzmann to justify the existence of a dynamic crossover at $T_g > T_s$ since, otherwise, the projection of the difference between the liquid and the crystal entropy would vanish at T_K . In this sense, this model realizes the Kauzmann paradox at T_s .

15.7 Accessing metastable states with replicas

The replica trick can be improved to access the non-trivial metastable states existent between T_s and T_d [169, 138, 139] using a "pinning-eld" or a "cloning method". Let us sketch how the latter works. Consider x copies or clones of the system's coupled

by an attractive, infinitesimal (but extensive) interaction. The free energy for the system of x clones reads:

$$f_{Jx} = \lim_{N \rightarrow \infty} \frac{1}{N} \ln Z_{Jx} = \lim_{N \rightarrow \infty} \frac{1}{N} \ln \int d\mathbf{f} \exp[-N (x f^2 - \beta \mathcal{H}(\mathbf{f}))] \quad (15.26)$$

using the formalism described in the previous Subsection. On the other hand, the free-energy density of the x clones can also be computed with the replica approach:

$$f_{Jx} = \lim_{N \rightarrow \infty} \frac{1}{N} [\ln Z_{Jx}] = \lim_{N \rightarrow \infty} \lim_{n \rightarrow 0} \frac{1}{Nn} \ln [Z_{Jx}^n] \quad (15.27)$$

where we used the fact that the free-energy density is self-averaging. Since the attractive coupling between the x clones is infinitesimal, the computation of the rhs of Eq. (15.27) reduces to the calculation of $\lim_{n \rightarrow 0} (x=n^0) \ln [Z_{Jx}^{n^0}]$, where the replica symmetry between the n groups of x -replicas ($n^0 = nx$) is explicitly broken. When the system is in the replica symmetric phase ($T_s < T$), the problem becomes one where one has to study one-step replica symmetry breaking solutions non-optimized with respect to x :

$$\lim_{N \rightarrow \infty} \frac{1}{N} \ln \int d\mathbf{f} \exp[-N (x f^2 - \beta \mathcal{H}(\mathbf{f}))] = x \text{Ext}_{q_{\text{ea}}} f_{\text{rep}}(q_{\text{ea}}; \beta; x); \quad (15.28)$$

where f_{rep} is the free-energy-density computed by using replicas, q_{ea} is the Edwards-Anderson parameter and x is the breakpoint or the size of the blocks in the replica matrix. (For simplicity we consider that the inter-state overlap q_1 equals zero [9].) Since the integral on the lhs of Eq. (15.28) is dominated by a saddle point contribution, one finds that, for a given T , fixing the value of x one selects the states with a given free-energy-density F . The relationship between f and x reads

$$x = \frac{\partial \mathcal{H}(\beta; f)}{\partial f} : \quad (15.29)$$

Note that within this framework one does not optimize with respect to x . Instead, x is a free parameter and, by changing the value of x , one selects different groups of metastable states. Inversely, choosing a value of the free-energy density one determines an "effective temperature" $T_{\text{eff}} = T/x$. This value coincides, indeed, with the dynamic result for T_{eff} in the aging scale when $f = f_{\text{th}}$. Otherwise, it gives a free-energy level dependent effective temperature. If one pursues the empirical relation between this parameter and the dynamic effective temperature this result means that when the system evolves in sufficiently long time-scales as to penetrate below the threshold it takes different values of T_{eff} depending on the deepness it reached.

Mézard and Parisi generalised this approach to search for a Kauzmann critical temperature ($T_K = T_s$) and characterise the thermodynamic properties of the glassy phase below T_s in finite interacting particle systems. The mean-field nature of the approach has been stressed by Thalmann [41] who showed that there is no lower critical dimension.

15.8 Dynamics and quantum systems

The derivation of the tap equations presented in Section 15.2 can be generalized to treat other problems as the real-time dynamics [143] of the same models or their quantum extensions [144]. Again, the procedure can be made easy if one correctly chooses the perturbative expansion and the order parameters. To study the real-time dynamics of the classical problem one is forced to Legendre transform with respect to the time-dependent local magnetization, the two-time correlation and the response [143]. The presentation is further simplified when one uses the susy notation introduced in Section 8.2 that renders the dynamic formalism very close to the static one. For quantum problems in equilibrium one uses the Matsubara representation of the partition function and then Legendre transform with respect to the imaginary-time correlation as well as the local magnetizations [144]. In order to derive tap equations for a quantum problem in real-time one should use the Schwinger-Keldysh formalism.

The derivation and study of dynamic tap equations justifies the interpretation of the asymptotic non-equilibrium dynamics in terms of the local properties of the tap free-energy density landscape. Biroli [143] showed that the dynamics in the tap free-energy landscape is in general non-Markovian due to the presence of memory terms in the dynamic tap equations. In the very long-time limit and for random initial conditions the contribution of these terms vanishes and one proves that the dynamics is a relaxation following α directions in the tap free-energy landscape (the threshold) as proposed in [12, 3].

16 Conclusions

We discussed the behaviour of a family of disordered models that yield a mean-field description of the glass transition and dynamics of super-cooled liquids and glasses. The relevance of these models to describe structural glasses was signaled and explained by Kirkpatrick, Thirumalai and Wolynes in the 80s [11]. Their nonequilibrium dynamics and hence the connection with other systems far from equilibrium started to develop more recently [12].

In short, their behaviour is the following. The dynamic transition arises when the partition function starts being dominated by an exponentially large number of metastable states yielding a finite complexity. The static transition instead is due to an entropy crisis, i.e. it occurs when the complexity vanishes and the number of states is no longer exponential in N , just as in the Adam-Gibbs-DiMarzio scenario [177]. These transitions mimic, in a mean-field way, the crossover to the glassy phase at T_g and the putative static transition at T_o (or T_K) of fragile glasses, see Fig. 2-left [11].

The equilibrium dynamics close and above T_d coincides with the one obtained with the mode-coupling approach [11]. It describes the relaxation of super-cooled liquids and it contains its most distinctive feature of having a two step decorrelation. The first step is ascribed to the motion of particles within the cages made by their neighbours while the second one is the structural relaxation related to the

destruction of the cages.

Below T_d the equilibration time diverges with the size of the system and the models do not equilibrate any longer with their environments (unless one considers times that grow with the size of the system) [12]. This is very similar to the situation encountered in real systems below T_g . The experimental time-window is restricted and one is not able to equilibrate the samples any longer below T_g . Aging effects as shown in Fig. 7 are captured. The correlations still decay to zero but they do in a waiting-time dependent manner. Their decay also occurs in two steps separated by a temperature-dependent plateau at a value related to the size of the cages. One can interpret their stiffness as increasing with the age of the system given that the beginning of the structural relaxation is delayed and slowed down for longer waiting-times.

The nonequilibrium dynamics below T_d approaches a threshold level of ϕ at directions in phase space and it never goes below this level in finite times with respect to the size of the system [12]. The aging dynamics corresponds to the slow drift of the point representing the system in the slightly tilted set of channels that form the threshold. The motion that is transverse to the channels is related to thermal fluctuations and the first stationary step of the relaxation towards q_{ea} , that characterises then the transverse "size" of the channel. The longitudinal motion along the channels is related to the structural relaxation. The tilt is proportional to the magnitude of the time-derivatives and these become less and less important as time passes. In more generality one interprets the long but finite time nonequilibrium dynamics following saddles that are the borders between basins of attraction of more stable states in phase space [3].

For times that scale with the size of the system, N , the sharp dynamic transition is avoided, the system penetrates below the threshold via activation and it approaches equilibrium in much longer time-scales. Metastable states below the threshold are typically minima [147, 150] (the fact that they are local minima can be checked studying the dynamics with initial conditions set to be in one of them [157, 139, 18]). This structure allows one to describe the cooling rate effects described in Fig. 2-right. For large but finite N and sufficiently slow cooling rate, the system penetrates below the threshold via activation when this is facilitated by T , i.e. when passing near T_d . To which level it manages to arrive (roughly speaking to which of the curves in the figure) depends on how long it stays close to T_d . The slower the cooling rate the lower level the system reaches with the ideal "equilibrium" glass corresponding to an infinitely slow cooling [158].

The region of phase space reached asymptotically in the thermodynamic limit is the threshold of ϕ at directions. The replica analysis of the partition function gives an alternative way of determining its statistical properties. Indeed, by evaluating the partition function on a marginally stable saddle-point in replica space one selects the threshold "states". Dynamic information such as the value of q_{ea} is thus obtained with a pseudo-static calculation. Other facts as, for instance, the scaling of the correlation are not accessible in this way.

One of the hallmarks of the glassy nonequilibrium dynamics is the modification of the relation between correlations and responses, namely, the fluctuation-dissipation

theorem. In mean-field models for structural glasses one finds that the integrated linear response is in linear relation with the associated correlation with a proportionality constant that takes the equilibrium value $1/(k_B T)$ when the correlation is above the plateau and it takes a different value $1/(k_B T')$ when it goes below the plateau [12]. This behaviour has been found in a number of finite dimensional glassy models numerically [58, 53, 54, 55].

The behavior just described corresponds to a family of mean-field disordered models to which the p spin models with $p \geq 3$ and the Potts glass belong. Other two families exist and they are related to ferromagnetic domain growth and spin-glasses. Two representative models are the spherical p spin model with $p = 2$ and the SK model, respectively. They are characterised by different scalings of the correlations in the aging regime and by different forms of the modification of fdt. The classification in families according to the nonequilibrium behaviour has a static counterpart given by the structure of replica symmetry breaking in the low-T phase, see Section 15.1.

The modification of fdt allows one to define an observable and correlation-scale dependent effective temperature [112]. Fast observables like the kinetic energy are equilibrated with the environment and the effective temperature equals the thermal bath temperature for them. Other observables though show different values of the effective temperature depending on the time-scales on which one investigates them. The effective temperature has a thermodynamical meaning even if defined out of equilibrium. In particular, it can be directly read with a thermometer coupled to the desired observable and a zero-th law holds for interacting observables that evolve in the same time-scale. As one should have expected the effective temperature shares some of the qualitative features of the phenomenological effective temperatures [131]. For instance, a system that is quenched from high temperatures has effective temperatures that take higher values than the temperature of the bath, etc. At the mean-field level, when $N \rightarrow 1$, it is history independent but one expects it to depend on the preparation of the sample for finite size and finite dimensional systems. (This is in close relation to the discussion above on cooling rate effects.) There is still no precise determination of which are the necessary conditions a nonequilibrium system has to fulfil to ensure the existence of well-behaved effective temperatures. A clear condition are the need to reach a dynamic regime in which the dynamics is slow and heat exchanges are weak.

Once the effective temperature has been identified one interprets the behaviour in the low T phase as follows: the system adjusts to a situation in which each observable sees two baths, one is the white external one and the one characterising the fast motion of the particles, the other is coloured and at a different temperature T' . The latter is generated by the interactions. In more complex systems { as mean-field spin-glasses } the asymptotic regime might be multithermalised with several time-scales each with its own value of the effective temperature. These results, first derived explicitly for p spin fully-connected models [112] actually hold for any resummation of the perturbative approach that keeps an infinite subset of diagrams (the mca being one such example). The structure of time-scales and values of the effective temperature is related to the breaking of supersymmetry down to a residual

group [130].

The structure of the free-energy landscape can be computed exactly for mean-field models in general, and for the spherical spin model in particular [147, 12, 150, 149, 171]. We expect its main features to be reproduced (at least in a smooth way) in real glassy systems. The free-energy landscape at fixed and low T has a structure as the one roughly sketched in Fig. 21. A pictorial image of the aging process can be quite helpful to understand it. Imagine that one fills phase space with water whose level reaches a free-energy density value, say, f . At high levels of the water, i.e. for high free-energy densities, the landscape has only some few isolated stationary states. Looking at the landscape from above one only sees some maxima that are represented as islands in the second panel in the figure. Lowering the water level the islands grow in size and some of them merge: land bridges develop. Lowering still the water level, it eventually reaches a threshold, that corresponds to $f = f_{th}$, where land percolates. One is left with a labyrinthic path of water as drawn schematically in the third panel that represents a top view of the landscape. This level is "marginal" since the bottom of the water channels is almost completely flat. Draining water from the system the "connectivity" of paths is reduced until the water level goes below the threshold, $f < f_{th}$, where minima dominate. In the fourth panel we represent them as lakes immersed in land. Lowering the water level one sees the sizes of the lakes diminish and some of them dry. These minima exist until the lowest level, $f = f_{eq}$. A "gap" in free-energy density separates the threshold and the equilibrium levels.

This picture allows us to give a natural interpretation of the nonequilibrium dynamics following a quench. Initially, the system is in a conformation typical of high- T , thus, its initial "free-energy density" is very high. This corresponds to a high level of water that fills the landscape. As time passes, water abandons the landscape in such a way that the quantity of water progressively diminishes lowering its level. The system's conformation can be associated to a ship and its evolution to the displacements of the ship sailing on the water. Initially, the water level is very high and the ship can move very rapidly far away from its initial position. It only sees some very few isolated islands that it simply avoids along its motion and the dynamics is very fast. As time passes the water level goes down. Roughly speaking we can associate the speed of drainage with the magnitude of the rate of change of the energy-density. When it approaches the threshold the available path becomes a series of rivers forming a very intricate network. The ship can still follow this network without remaining trapped in any conning region. Its motion, however, gets slower and slower. In finite times with respect to N the water level does not go below the threshold. But for longer times that scale with N it does. When such long times are attained the ship remains trapped in lakes. For still longer times the higher lakes dry and, if the ship got trapped in one of them it must be transported through the land to reach other lakes at lower levels. This action represents an activated process. Part of this image was introduced by Sibani and Hömann phenomenologically [152]. The spin models and the like realise it explicitly. All quantitative features of the landscape here described with words have been, or in principle can be, calculated analytically. The use of this image has been

ultimately justified by the dynamic tap approach of Biroli [143].

The value taken by the effective temperature is in direct relationship with the structure of the free-energy landscape. Indeed, again for p-spin model and the like, it has been shown analytically that the asymptotic value T reached for long but finite times with respect to N is given by $T = \partial \phi(\beta; f) / \partial \beta j_{f_{th}}$, with the complexity [138]. For even longer times such that the system penetrates below the threshold one expects the effective temperature to take different values related to the complexity at lower free-energy density levels. The Edwards-Anderson parameter, q_{ea} , also changes since $q_{ea}(f)$. In the longest time-scale such that equilibrium is reached and q_{ea} equals the equilibrium value also obtained with a replica calculation using the standard maximization prescription to determine the breaking point parameter x . This result is intimately related to Edwards' estimate for granular matter [34, 33] and also to the more recent use of a estimate over inherent structures [136] to describe the nonequilibrium dynamics of glasses [137, 160, 161]. Note that these, being defined using the potential energy-density landscape, are valid only at zero temperature (see, e.g. [142]). However, extensive numerical checks recently performed suggest that the approach, even if not obviously correct at finite T , yields a very good approximation [137].

Within this picture two distinct regimes would appear in the low- T isothermal dynamics of real systems: a mean-field-like one when the system approaches a pseudo-threshold of stable directions in phase space and a slower activated regime in which the system jumps over barriers to relax its excess energy density and very slowly progress towards equilibrium. How and if the aging properties in the first and second regime resemble is a very interesting open problem.

The existence of a threshold plays a fundamental role in explaining several features of many experimental observations in such diverse systems as driven granular matter, the rheological properties of complex liquids and glasses, etc. Just to cite two examples, trapping and Reynolds dilatancy effects in granular matter [33, 26] as well as the existence of a static yield stress and thixotropic behaviour in some rheological experiments [19] can be interpreted in terms of threshold and subthreshold states. These features support the claim that this free-energy structure exists in real physical systems. Moreover, maybe not surprisingly, this structure also appears in optimisation problems such as xor-sat and k-sat that can be mapped to dilute p-spin models at zero temperature. In this context the control parameter is the number of requirements over the number variables, α , and the static transition, α_s , is related to the sat-unsat transition while the dynamic transition, $\alpha_d < \alpha_s$ corresponds to the value where greedy algorithms fail to find the existing solutions [153].

All these arguments can be adapted to include quantum fluctuations. The statics is studied with the Matsubara replicated partition function [174], metastability with an extension of the tap approach [144] and the real-time dynamics with the Schwinger-Keldysh formalism [85, 106]. The picture that arises is very similar to the one above with some intriguing new ingredients as the emergence of truly first order transitions close to the quantum critical point [176, 174], highly non-trivial effects due to the quantum environments [144], a waiting-time dependent quantum -

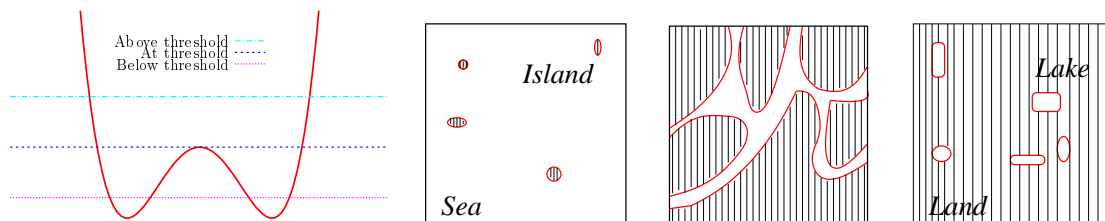


Figure 21: Left: a 1d simplified sketch of the free-energy density. Three top views of the free-energy landscape: above, at and below the threshold.

to-classical crossover in the dynamic scaling, etc.

The models we studied in these notes have quenched random interactions. Real glassy systems of the structural type do not. One may wonder if this is an important deficiency of the approach or if similar results can be obtained for models with no disorder. A large variety of models of mean-field type, or defined on large d spaces, with no explicit quenched disorder and having the same phenomenology have been introduced in recent years [166, 140]. Finite d models with similar, eventually interrupted, dynamic behaviour have also been exhibited [55, ?, 53, 54]. Their existence supports the belief that the scenario here summarized goes beyond simple modelling. Indeed, it is at the basis of several conjectures for the behaviour of other nonequilibrium systems with slow dynamics that have been later checked numerically. It has also motivated several experimental investigations in a variety of systems.

17 Perspectives

We would like to end these notes by mentioning some of the directions for future development in this area. Within the "mean-field" approach there remain at least two important open technical problems to complete their analytic solution:

Matching. Having approximated the dynamic equations as explained in the text we are not able to determine the complete scaling form of correlations and responses. In models like the p -spin spherical we cannot fix the scaling function $h(t)$. Going beyond the asymptotic solution requires to solve the matching of the solution at short time-differences with the one at long time-differences. This is a very tough mathematical problem.

Dynamics at finite time-scales. In order to penetrate below the threshold in p -spin spherical models and approach equilibrium one has to consider times that grow with N and include instanton solutions to describe the activated dynamics below T_d . This will smoothen the dynamic transition and convert it into a crossover. It will also possibly allow the mode-coupling and similar approaches to yield more accurate quantitative predictions.

Even though the models we discussed are mean-field we believe that the general picture developed holds beyond this limit. Some numerical and experimental tests

support this belief. Still, one would like to justify this claim theoretically. Some of the lines of research that are now being followed with this aim are:

Dynamics of dilute disordered models. These are disordered spin models on random graphs. Even if still mean-field they include some spatial fluctuations that one can study numerically and analytically [88, 154]. Moreover, their relation to optimisation problems make them interesting per se.

Dynamic heterogeneities. Supposedly these are nanoscale regions in supercooled liquids and glasses that are very important in determining the glass transition and the dynamics. They have been studied numerically and experimentally so far and one would like to have a theoretical model including and describing them. A step in this direction was followed in [84] where a sigma-model-like description for the spin-glass problem was introduced. This led to proposing that the distribution of the coarse-grained local correlations and responses should be constrained to follow the global relation $\langle C \rangle$; this proposal was checked numerically in [117] for the 3d Ising and studies on other disordered models are underway. The study of these distributions in real glasses as well as the development of a complete analytical description are problems that deserve further study.

Dynamic functional renormalisation group (frg). It would be very interesting to extend the frg to attack nonequilibrium situations with aging dynamics.

Field relations for finite d systems. Many questions about the form of the relations between global responses and correlations in real systems can be raised. Do all systems undergoing domain growth in $d > 1$ have two time scales with the slower one characterised by $T \rightarrow \infty$? Can a situation as the one found for the SK model be realised, i.e. does any real system have an effective temperature with more than two values (T and T^*)?

Relations between statics and dynamics. A link between the nonequilibrium field relations and Parisi's $P(q)$ was found in some mean-field models (note that it does not hold for models with a threshold as the p-spin). It was then argued that it should hold in finite d systems under certain assumptions [155]. The long-lasting debate about the nature of the spin-glass phase has now been rephrased in nonequilibrium terms, the question now being what is the form of the asymptotic $\langle C \rangle$ plot. Recent experiments address this problem [32]. Analytical results for finite d models are yet not available.

Thermodynamics and statistical mechanics out of equilibrium. From a more generic viewpoint, the development of a thermodynamics and statistical mechanics for models that evolve slowly out of equilibrium is a very important issue. Some progress in both directions has been made recently. One should try to establish these proposals in a less phenomenological way.

All these problems are challenging and very interesting. Many more could be added to this short list. We can expect to see progress in this very active area of research in the near future.

A Generalized Langevin equations

In this Appendix we derive a generalized Langevin equation starting from time-reversal microscopic equations for the motion of the system and the constituents of the bath. We use the simplest image of a thermal bath that is given by an ensemble of harmonic oscillators with masses m and frequencies ω , $\omega = 1, \dots, N$ and, for simplicity, we consider a system made of a single particle with mass M . We consider the one-dimensional case to simplify the notation. The generalization to more complex systems and/or to more complicated baths and higher dimensions is straightforward [156]. We call $q; p$ and $x; p$, $\omega = 1, \dots, N$ the positions and momenta of the particle and oscillators, respectively. The Hamiltonian of the total system is of the form (4.1),

$$H = \frac{p^2}{2M} + V(q) + \frac{1}{2} \sum_{\omega=1}^N \frac{c^2}{m \omega^2} q^2 + \sum_{\omega=1}^N \frac{p^2}{2m} + \frac{1}{2} \sum_{\omega=1}^N m \omega^2 x^2 - \sum_{\omega=1}^N c q x ;$$

All these terms have been discussed in Section 4.1.1. Hamilton's equations for the particle are

$$\dot{q}(t) = \frac{p(t)}{M} ; \quad \dot{p}(t) = -\frac{\partial V(q)}{\partial q(t)} - \sum_{\omega=1}^N \frac{c^2}{m \omega^2} q(t) + \sum_{\omega=1}^N c x_{\omega}(t) ; \quad (A.1)$$

while the dynamic equations for each member of the environment read

$$\dot{x}_{\omega}(t) = \frac{p_{\omega}(t)}{m} ; \quad \dot{p}_{\omega}(t) = -m \omega^2 x_{\omega}(t) + c q(t) ; \quad (A.2)$$

showing that they are all forced massive harmonic oscillators. These equations are readily solved yielding

$$x_{\omega}(t) = x_{\omega}(0) \cos(\omega t) + \frac{p_{\omega}(0)}{m \omega} \sin(\omega t) + \frac{c}{m \omega} \int_0^t dt' \sin(\omega(t-t')) q(t') \quad (A.3)$$

with $x_{\omega}(0)$ and $p_{\omega}(0)$ the initial coordinate and position at time $t = 0$ when the particle has been set in contact with the bath. The replacement of this expression in the last term on the rhs of Eq. (A.1), implies

$$\dot{p}(t) = -\frac{\partial V(q)}{\partial q(t)} - \sum_{\omega=1}^N \frac{c^2}{m \omega^2} q(t) + \sum_{\omega=1}^N \frac{c}{m \omega} \int_0^t dt' \sin(\omega(t-t')) q(t') \quad (A.4)$$

with the kernel given by

$$K(t-t') = \sum_{\omega=1}^N \frac{c^2}{m \omega^2} \cos(\omega(t-t')) ; \quad (A.5)$$

and the time-dependent force given by

$$F(t) = \sum_{\omega=1}^N \frac{c}{m \omega} p_{\omega}(0) \sin(\omega t) + \sum_{\omega=1}^N c x_{\omega}(0) \cos(\omega t) ; \quad (A.6)$$

Usually, the environments are made of ensembles of equilibrated entities at a chosen temperature T . Then, $f_p(0); x(0)g$ are initially distributed according to

$$P(f_p(0); x(0)g) = \frac{\exp(-H_{\text{env}}[f_p(0); x(0)g])}{\int \exp(-H_{\text{env}}[f_p(0); x(0)g])} : \quad (\text{A } .7)$$

It is convenient to assume that equilibrium distribution is shifted with respect to the coupling to the particle at the initial time; this allows one to eliminate the last term in Eq. (A .4). As when including the counter-term, we choose

$$H_{\text{env}} = \sum_{\alpha=1}^N \left[\frac{m \omega_{\alpha}^2}{2} x_{\alpha}^2 + \frac{c}{m \omega_{\alpha}} q(0) \cos(\omega_{\alpha} t) x_{\alpha} \right] : \quad (\text{A } .8)$$

Defining a new noise $\xi(t) = \sum_{\alpha=1}^N \frac{c}{m \omega_{\alpha}} \cos(\omega_{\alpha} t) q(0)$, it is a Gaussian random variable with

$$\langle \xi(t) \rangle = 0 \quad \text{for all times}; \quad (\text{A } .9)$$

$$\langle \xi(t) \xi(t') \rangle = k_B T \delta(t - t') \quad (\text{A } .10)$$

and the Langevin equation simplifies to

$$\dot{p}(t) = -\frac{\partial V(q)}{\partial q(t)} + \xi(t) + \sum_{\alpha=1}^N \int_0^t dt' \gamma_{\alpha}(t-t') q(t') : \quad (\text{A } .11)$$

A random force with non-vanishing correlations on a finite support is usually called a colored noise.

Interestingly enough, $\langle \xi(t) \xi(t') \rangle$ and the noise-noise correlation are proportional, with a constant of proportionality of value $k_B T$. This is a generalized form of the fluctuation-dissipation relation, and it applies to the environment. In this derivation it is clear that it is a consequence of having assumed the equilibration of the bath.

The third term on the rhs of Eq. (A .11) represents a rather complicated friction force. Its value at time t depends explicitly on the history of the particle at times $0 \leq t' \leq t$. The memory kernel $\gamma(t-t')$ plays the rôle of a retarded friction function. This term makes Eq. (A .11) non-Markovian.

Different choices of the environment are possible by selecting different ensembles of harmonic oscillators. The simplest choice, that leads to an approximate Markovian equation, is to consider identical oscillators coupled to the particle via the coupling constants $c = N$ but having a non-trivial distribution of frequencies, that in the limit $N \rightarrow \infty$, can be treated as continuous. This allows one to introduce the spectral density $I(\omega)$ and rewrite the kernel as

$$\gamma(t-t') = \frac{c^2}{m} \int_0^{\infty} d\omega I(\omega) \frac{\cos(\omega(t-t'))}{\omega} : \quad (\text{A } .12)$$

For a Debye distribution of frequencies

$$I(\omega) = \frac{3\omega^2}{\omega_D^3} \quad (\omega_D \text{ is } \omega_D) \quad \text{one has} \quad \gamma(t-t') = \frac{3c^2}{m \omega_D^2} \frac{\sin(\omega_D(t-t'))}{\omega_D(t-t')} : \quad (\text{A } .13)$$

If β_D is sufficiently large, $\delta(t - t^0)$ can be approximated by a delta function, $\delta(t - t^0) = 2\delta(t - t^0)$ with $\beta_D = 3c^2 = (2m\beta_D^2)$, and Eq. (A.4) becomes Markovian.

Different environments are characterized by different choices of the spectral density $I(\omega)$ at small ω . For example, one has an Ohmic ($s = 1$), sub-Ohmic ($s < 1$) or super-Ohmic ($s > 1$) bath if $I(\omega) \propto \omega^s$ for $\omega \rightarrow 0$.

B The Kubo formula

The Kubo formula relates the linear response to the asymmetric correlation of a quantum process. It holds at the level of the linear response even if the system is out of equilibrium. The linear response reads

$$\begin{aligned} R_{AB}(t; t^0) &= \frac{1}{\hbar} \frac{1}{Z(\hbar_B)} \text{Tr} \left[\hat{U}_t(\hbar_B) \hat{A}(0) \hat{U}_t^{-1}(\hbar_B) \hat{B}(0) \right]_{\hbar_B=0} \\ &= \frac{1}{Z^2(\hbar_B)} \frac{1}{\hbar} \frac{1}{Z(\hbar_B)} \text{Tr} \left[\hat{U}_t(\hbar_B) \hat{A}(0) \hat{U}_t^{-1}(\hbar_B) \hat{B}(0) \right]_{\hbar_B=0} \\ &\quad + \frac{1}{Z(0)} \text{Tr} \left[\frac{\hat{U}_t(\hbar_B)}{\hbar} \hat{A}(0) \hat{U}_t^{-1}(\hbar_B) + \hat{U}_t(\hbar_B) \hat{A}(0) \frac{\hat{U}_t^{-1}(\hbar_B)}{\hbar} \right]_{\hbar_B=0} \end{aligned}$$

where $U_t(\hbar_B)$ is the evolution operator, $U_t(\hbar_B) = \exp[-i\hbar\hat{H}]$ for all infinitesimal time intervals except from the one going from $t^0 = 2$ to $t^0 + \epsilon = 2$ where it takes the form $U_t(\hbar_B) = \exp[-i\hbar(\hat{H} - \hbar_B \hat{B})]$. See the left-panel in Fig. 8 for a graphical representation of a kick-like perturbation. Calculating the variations explicitly, and using $\hat{H}\hat{A}(t) = 0$ or $\hat{H}\hat{A}(t) = i$, we have

$$\begin{aligned} R_{AB}(t; t^0) &= \frac{1}{Z(0)} \text{Tr} \left[\frac{i}{\hbar} \left(\hat{B}(t^0) U_t(0) \hat{A}(0) U_t^{-1}(0) + U_t(0) \hat{A}(0) \hat{B}(t^0) U_t^{-1}(0) \right) \right]_{\hbar_B=0} \\ &= \frac{i}{\hbar} \langle \hat{A}(t); \hat{B}(t^0) \rangle_i : \end{aligned} \quad (\text{B.1})$$

C The response in a Langevin process

By the definition the linear response is given by

$$\frac{\langle \hat{q}(t) \rangle_i}{\hbar(t^0)} = \frac{1}{\hbar(t^0)} \int_0^t dt \langle \hat{q}(t) \hat{q}(t^0) \rangle_i = \int_0^t dt \langle \hat{q}(t) \hat{q}(t^0) \rangle_i \hbar(t^0)$$

with S_{eff} defined in Eq. (8.6) and evaluated at vanishing sources. The rhs immediately leads to $R(t; t^0) = \langle \hat{q}(t) \hat{q}(t^0) \rangle_i$, i.e. Eq. (8.7).

The proof of the relation (8.8) is slightly more involved. The correlation between coordinate and noise can be obtained from the variation with respect to $\hat{q}(t; t^0)$ of the generating functional (8.3) once the identities (8.4) and (8.5) have been used and the source

$$\int_0^t dt^{\text{eff}} \hat{q}(t^{\text{eff}}; t^{\text{eff}}) \hat{q}(t^{\text{eff}}) \quad (\text{C.1})$$

has been added. Integrating over the noise and keeping only the linear terms in the effective action since all others will vanish when setting $\bar{\eta} = 0$

$$\text{Linear terms} = \frac{k_B T}{2} \int dt_1 dt_2 dt_3 dt_4 [(t_1; t_2) q(t_1) (t_2; t_3) i\dot{q}(t_4) (t_4 - t_3) + i\dot{q}(t_1) (t_1 - t_2) (t_2; t_3) (t_4; t_3) q(t_4)] : \quad (\text{C } 2)$$

The variation with respect to $(t; t^0)$ yields $(k_B T) = 2 \int dt^0 [(t^0; t^0) + (t^0; t^0)] hq(t) i\dot{q}(t^0) i = hq(t) (t^0) i$.

D Grassmann variables and supersymmetry

Grassmann variables anticommute $\theta^2 = -\theta^2 = [;] = 0$. The integration rules are $\int d\theta = \int d\bar{\theta} = 0$ and $\int d\theta d\bar{\theta} = \int d\bar{\theta} d\theta = 1$ while the derivation is such that $\partial = \frac{\partial}{\partial \theta}$ and $\partial\bar{\theta} = \frac{\partial}{\partial \bar{\theta}}$.

In the supersymmetric formalism used in Section 8 one enlarges the usual "bosonic" space to include two conjugate Grassmann variables θ and $\bar{\theta}$: $\theta = (t; \bar{\theta})$. A "superfield" and its "supercorrelator" are then defined as

$$(a) \quad q(t) + \theta(t) \bar{\theta} + \bar{\theta}(t) \theta + i\dot{q}(t) \bar{\theta} ; \quad Q(a; b) = h(a) (b) i ; \quad (\text{D } 1)$$

$b = (t^0; \bar{\theta})$. The latter encodes the usual correlations $hq(t)q(t^0) i$, $hq(t)i\dot{q}(t^0) i$, $hi\dot{q}(t)q(t^0) i$, $hi\dot{q}(t)i\dot{q}(t^0) i$, as well as "fermionic" correlators $hq(t) (t^0) i$, $h\bar{\theta}(t)i\dot{q}(t^0) i$, $h\bar{\theta}(t) (t^0) i$, etc. The solutions we construct and study are such that all correlators that involve only one fermionic variable θ and $\bar{\theta}$ vanish. We are then left with the usual four correlators purely bosonic correlators and the fermion bilinears. One proves that the latter equal the linear response. If, moreover, we only consider causal solutions, $\hat{Q}(t; t^0) = hi\dot{q}(t)i\dot{q}(t^0) i = 0$ and

$$Q(a; b) = C(t; t^0) (\bar{\theta}^0 - \bar{\theta}) (R(t; t^0) - R(t^0; t)) ; \quad (\text{D } 2)$$

Convolutions, or operational products, and Hadamard, or simple products, are defined as

$$\begin{aligned} Q_1(a; b) \otimes Q_2(b; c) &= \int db Q_1(a; b) Q_2(b; c) ; \\ Q_1(a; b) \otimes Q(a; b) &= Q_1(a; b) Q_2(a; b) ; \end{aligned} \quad (\text{D } 3)$$

respectively, with $db = dt d\bar{\theta} d\theta$.

For correlators of the causal form (D 2), the convolution and the Hadamard product respect the structure of the correlator. Indeed, the result of the convolution is again of the form (D 2) with

$$\begin{aligned} C_{\text{conv}}(t; t^0) &= \int dt^0 [C_1(t; t^0) R_2(t^0; t^0) + R_1(t; t^0) C_2(t^0; t^0)] ; \\ R_{\text{conv}}(t; t^0) &= \int dt^0 R_1(t; t^0) R_2(t^0; t^0) ; \end{aligned} \quad (\text{D } 4)$$

and the result of the Hadamard product is also of the form (D.2) with

$$\begin{aligned} C_{\text{had}}(t; t^0) &= C_1(t; t^0)C_2(t; t^0); \\ R_{\text{had}}(t; t^0) &= C_1(t; t^0)R_2(t; t^0) + C_2(t; t^0)R_1(t; t^0); \end{aligned} \quad (\text{D.5})$$

The Dirac delta function is defined as $\delta(t - t^0) = \delta(t - t^0) \delta(t - t^0)$.

E Integrals in the aging regime

Integrals of the form

$$I_1(t) = \int_0^t dt^0 A(t; t^0) B(t; t^0) \quad (\text{E.1})$$

appear, for example, in the equation for $\chi(t)$. We separate the integration time interval as in Eq. (12.8). If t is chosen to be a finite time, $A(t; t^0)$ and $B(t; t^0)$ in the first interval can be approximated by $A(t; 0)$ that vanishes when $t \rightarrow 1$. Since the integration interval is finite, this term can be neglected. In the second interval the functions vary in the aging regime and in the third interval they vary in the stationary regime. Thus

$$\begin{aligned} I_1(t) &= \int_0^t dt^0 A_{\text{ag}}(t; t^0) B_{\text{ag}}(t; t^0) + \int_t^{t^0} dt^0 A_{\text{st}}(t; t^0) + \lim_{t \rightarrow 1} \lim_{t^0 \rightarrow 1} A(t; t^0) \\ &\quad B_{\text{st}}(t; t^0) + \lim_{t \rightarrow 1} \lim_{t^0 \rightarrow 1} B(t; t^0) : \end{aligned}$$

We assume that this separation is sharp and that we can neglect the corrections associated to mixing of the three regimes. In the third term we replaced A and B in terms of $A_{\text{st}}, B_{\text{st}}$. We can now replace the lower limit of the first integral by 0 and its upper limit by t . In addition, assuming that B is proportional to the response,

$$\lim_{t \rightarrow 1} \lim_{t^0 \rightarrow 1} B(t; t^0) = 0; \quad (\text{E.2})$$

and that A is a function of the correlation such that

$$\lim_{t \rightarrow 1} \lim_{t^0 \rightarrow 1} A(t; t^0) = A_{\text{qea}} \quad (\text{E.3})$$

we have

$$I_1(t) = \int_0^t dt^0 A_{\text{ag}}(t; t^0) B_{\text{ag}}(t; t^0) + A_{\text{qea}} \int_0^1 dt^0 B_{\text{st}}(t^0) + \int_0^1 dt^0 A_{\text{st}}(t^0) B_{\text{st}}(t^0)$$

where the upper limit tending to infinity is $t \rightarrow 1$.

Another type of integrals is: $I_2(t; t^0) = \int_{t^0}^t dt^0 A(t; t^0) B(t^0; t^0)$. In particular, if $B = 1$, $A(t; t^0) = R(t; t^0)$, $t^0 = 0$ and $t \rightarrow 1$, this integrals yields the static susceptibility. If instead, t^0 is long and t too we have the type of integral appearing in the equation for the response. Let us assume that t and t^0 are far apart; we start by dividing the time interval in three subintervals

$$\int_{t^0}^t = \int_{t^0}^{t^0} + \int_{t^0}^t + \int_t^t \quad (\text{E.4})$$

and by approximating the functions A and B assuming that they have a two-step decay as the one in Sections 11.1 and 11.2:

$$I_2(t; t^0) = \int_{t^0}^t dt^0 A_{ag}(t; t^0) B(t^0 - t^0) + \int_{t^0}^t dt^0 A_{ag}(t; t^0) B_{ag}(t^0; t^0) + \int_{t^0}^t dt^0 A(t - t^0) B_{ag}(t^0; t^0) : \quad (E.5)$$

In the first term $B(t - t^0)$ can be replaced by $B(t - t^0) = \lim_{t \rightarrow \infty} \lim_{t^0 \rightarrow 1} B(t; t^0) + B_{st}(t - t^0)$. The same applies to A in the last term. All functions vary fast in the stationary regime but very slowly in the aging regime. The next assumption is that functions in the aging regime that are convoluted with functions in the stationary regime, can be considered to be constant and taken out of the integrals. That is to say

$$I_2(t; t^0) = A_{ag}(t; t^0) \int_{t^0}^t dt^0 B(t^0 - t^0) + \int_{t^0}^t dt^0 A_{ag}(t; t^0) B_{ag}(t^0; t^0) + B_{ag}(t; t^0) \int_{t^0}^t dt^0 A(t - t^0) + A_{ag}(t; t^0) \int_{t^0}^t dt^0 B(t^0 - t^0) + \int_{t^0}^t dt^0 A_{ag}(t; t^0) B_{ag}(t^0; t^0) + B_{ag}(t; t^0) \int_{t^0}^t dt^0 A(t - t^0) ; \quad (E.6)$$

where we used $t \rightarrow \infty$ and $t^0 \rightarrow 1$. When this integral appears in the equation for the response, $A(t^0)$ and $B(t^0)$ are proportional to the response function since one is the response itself and the other is the self-energy. Using $\int dt$ the integrals in the first and third term can be computed in the classical limit or they can be expressed as functions of the correlation in the quantum case. The second term instead depends exclusively on the aging dynamic sector.

All other integrals can be evaluated, in the large-time limit, in a similar way.

Acknowledgements The author specially thanks J. Kurchan for his collaboration on this and other subjects, and G. Semerjian for very useful discussions and the careful correction of the manuscript. LFC is ICTP research scientist, acknowledges financial support from the Guggenheim Foundation and the ACI "Algoritmos d'optimisation et systemes desordones quantiques" and thanks the Universities of Buenos Aires and La Plata (Argentina) and Harvard University for hospitality during the preparation of these notes.

References

- [1] A. J. Bray, Adv. in Phys. 43 (1994) 357.
- [2] See, e.g. D. S. Fisher, Physica A 263, 222 (1999).

- [3] J.Kurchan and L.Laboux, J.Phys.A 29, 1929 (1996).
- [4] Many review articles describe the phenomenology of super-cooled liquids and glasses. See, e.g. M.D.Ediger, C.A.Angell and S.R.Nagel, J.Phys.Chem. 100,13200 (1996), P.G.Debenedetti and F.R.Stillinger, Nature 410, 259 (2001).W.Kob in this volume.
- [5] One can think as the super-cooled liquid as a metastable state in the usual sense: its properties can be computed using a restricted partition function and, in particular, the dynamics is stationary and satisfies fdt even if the system is not equilibrated in its true most favorable state { the crystal. The glass, instead, is also metastable but of a different kind: one cannot describe all its properties with a stationary probability distribution.
- [6] E. Weeks and D. Weitz, Phys. Rev. Lett. 89, 095704 (2002).
<http://www.physics.emory.edu/faculty/weeks/>
- [7] K.Binder and A.P.Young, Rev.Mod.Phys. 58, 801 (1986).K.Fischer and J.Hertz, Spin-glasses, (Cambridge Univ.Press., Cambridge, 1991).
- [8] V.Dotsenko, M.Feigel'man and L.B.Ioffe, Spin-glasses and related problems, Soviet Scientific Review, 15, Harwood, 1990.S.L.Ginzburg, Sov.Phys.JETP 63, 439 (1986).
- [9] M.Mezard, G.Parisi and M.A.Virasoro, Spin-glasses and beyond (World Scientific, Singapore, 1987).
- [10] H.Kawamura and M.S.Li, Phys.Rev.Lett.87, 187204 (2001).H.Kawamura, cond-mat/0210012 and refs. therein.
- [11] T.R.Kirkpatrick and D.Thirumalai, Phys.Rev.Lett. 58, 2091 (1987); Phys. Rev.B 36, 5388 (1987).T.R.Kirkpatrick and P.Wolynes, Phys. Rev.B 36, 8552 (1987).
- [12] L.F.Cugliandolo and J.Kurchan, Phys.Rev.Lett. 71 173 (1993).
- [13] For a review see J-P Bouchaud, L.F.Cugliandolo, J.Kurchan and M.Mezard, in Spin glasses and random fields, A.P.Young ed. (World Scientific, 1998).
- [14] W.Wu et al, Phys. Rev. Lett. 67, 2076 (1991).W.Wu et al, Phys. Rev. Lett. 71, 1919 (1993).T.F.Rosenbaum, J.Phys.C 8, 9759 (1996).E.Courtens, J. Phys.Lett. (Paris) 43, L199 (1982); Phys. Rev. Lett. 52, 69 (1984).E.Matsushita and T.Matsubara, Prog.Theor.Phys. 71, 235 (1984).R.Pirc, B.Tadic and R.Blinic, Z.Phys.B 61, 69 (1985); Phys. Rev.B 36, 8607 (1987).
- [15] S.Rogge, D.Natelson and D.D.Oshero, Phys. Rev. Lett. 76, 3136 (1996).S.Rogge, D.Natelson, B.Tigner and D.D.Oshero, Phys. Rev.B 55, 11256 (1997).D.Natelson, D.Rosenberg and D.D.Oshero, Phys. Rev. Lett. 80, 4689 (1998).

- [16] A. Vaknin, Z. Ovadyahu, M. Pollak, Phys. Rev. Lett. 84, 3402 (2000). Z. Ovadyahu, in this volume.
- [17] M. Cates, in this volume. A. Adjari, in this volume.
- [18] L. F. Cugliandolo, J. Kurchan, P. Le Doussal and L. Peliti, Phys. Rev. Lett. 78, 350 (1997).
- [19] L. Berthier, PhD Thesis, ENS-Lyon, France, 2001 and cond-mat/0209394.
- [20] R. Graham, Springer Tracts in Modern Physics 66 (Springer, Berlin, 1973).
- [21] J. D. Ferry, Viscoelastic properties of polymers (Wiley, New York, 1980). R. G. Larson, The structure of rheology of complex fluids (Oxford Univ. Press, Oxford, 1990).
- [22] H-M Jaeger, S.R. Nagel and R.P. Behringer, Rev. Mod. Phys. 68, 1259 (1996). J-P Bouchaud, in this volume.
- [23] C. Josserand, A. Tkachenki, D. M. Mueth and H. M. Jaeger, Phys. Rev. Lett. 85, 3632 (2000). J. Torok, S. Krishnamurthy, J. Kertesz and S. Roux, cond-mat/0003070. F. Restagno, C. Ursini, H. Gayvallet, E. Charlaix, cond-mat/0209210.
- [24] M. Sellitto, Europ. J. Phys. B 4, 135 (1998). M. Nicodem i, Phys. Rev. Lett. 82, 3734 (1999). M. Nicodem i and A. Coniglio, Phys. Rev. Lett. 82, 916 (1999). A. Barrat and V. Loreto, J. Phys. A 33, 4401 (2000). M. Sellitto and J. J. Arenzon, Phys. Rev. E 62, 7793 (2000). J. Talbot, G. Tarjus and P. Viot, Europ. J. E 5, 495 (2001). M. Sellitto, Phys. Rev. E 060301R (2001). J. Berg and A. Mehta, Advances in Complex Systems 4, 309 (2001).
- [25] A. Barrat, V. Colizza and V. Loreto, cond-mat/0205285.
- [26] L. Berthier, L. F. Cugliandolo and J. L. Iguain, Phys. Rev. 63, 051302 (2001).
- [27] G. Blatter et al, Rev. Mod. Phys. 66, 1125 (1994). T. Giamarchi and P. Le Doussal, Statics and dynamics of disordered elastic systems in 'Spin-glasses and random fields', A. P. Young ed. (World Scientific, Singapore, 1998). T. Nattermann and S. Scheidl, Adv. Phys. 49, 607 (2000).
- [28] T. Giamarchi, cond-mat/0205099.
- [29] L. C. E. Struick, Physical aging in amorphous polymers and other materials (Elsevier, Houston, 1976).
- [30] The geometrical properties of low-energy excitations in spin-glasses are the subject of present debate. See, e.g. J. Houdayer, F. Krzakala, and O. C. Martin, Eur. J. Phys. B 18, 467 (2000). F. Krzakala, PhD Thesis Univ. Paris Sud, France, 2002. M. Palassini and A. P. Young, Phys. Rev. Lett. 85, 3017

(2000). J. Lamarcq et al *Europhys. Lett.* 58, 321 (2002). The geometrical properties of growing objects has been discussed in H. Yoshino, K. Hukushima and H. Takayama, cond-mat/0202110 and cond-mat/0203267. H. Castillo et al (in preparation).

- [31] The aging properties in spin-glasses are reviewed in E. Vincent et al *Slow dynamics and aging in glassy systems*, in Sitges 1996, ed. M. Rub (Springer-Verlag, Berlin, 1997). P. Nordblad and P. Svendlidh, *Experiments on spin-glasses in Spin-glasses and random fields*, A. P. Young ed. (World Scientific, Singapore, 1998).
- [32] D. Herisson and M. Ocio, *Phys. Rev. Lett.* 88, 257202 (2002). D. Herisson, PhD Thesis, Univ. Paris Sud, France, 2002. M. Ocio in this volume.
- [33] J. Kurchan, *Rheology and how to stop aging*, in "Jamming and rheology: constrained dynamics in microscopic and macroscopic scales", ITP, Santa Barbara, 1997, ed. S. F. Edwards et al.
- [34] L. Berthier, J-L Barrat and J. Kurchan, *Phys. Rev. E* 61, 5464 (2000).
- [35] L. Bellon, S. Ciliberto and C. Laroche, *Europhys. Lett.* 51, 551 (2000). A. Knaebel, M. Bellour, J-P Munch, V. Viasno, F. Lequeux and J. L. Harden, *Europhys. Lett.* 52, 73 (2000). M. Clabre, R. Borrega and L. Leibler, *Phys. Rev. Lett.* 85, 4819 (2000). L. Cipelletti, S. Manley, R. C. Ball and D. A. Weitz, *Phys. Rev. Lett.* 84, 2275 (2000). C. Derac, A. Ajdari, G. Ducouret, F. Lequeux, *C. R. Acad. Sci. (Paris) IV-PHYS* 1, 1115 (2000). C. Derac, A. Ajdari, F. Lequeux, *Eur. Phys. J E* 4, 355 (2001).
- [36] L. F. Cugliandolo, J. Kurchan and P. Le Doussal, *Phys. Rev. Lett.* 76, 2390 (1996).
- [37] A. Barrat, *Phys. Rev. E* 57, 3629 (1998). H. Yoshino, *Phys. Rev. Lett.* 81, 1493 (1998).
- [38] F. Portier et al cond-mat/01. F. Portier, PhD Thesis, Univ. Paris-Sud, France, 2002.
- [39] See also the measurements in S. O. Valenzuela and V. Bekeris, *Phys. Rev. Lett.* 84, 4200 (2000), *ibid* 86, 504 (2001).
- [40] R. Exartier and L. F. Cugliandolo, *Phys. Rev. B* 66, 012517 (2002).
- [41] R. Exartier, PhD thesis, Paris VI, France, 2001.
- [42] C. Simon, private communication.
- [43] A. Kolton, R. Exartier, L. F. Cugliandolo, D. Domínguez and N. Gronbech-Jensen, cond-mat/0206042.

- [44] D. Bonn, S. Tanase, B. Abou, H. Tanaka and J. Meunier, Phys. Rev. Lett. 89, 015701 (2002).
- [45] J-P Bouchaud, J. Phys. I (France) 2 (1992) 1705. J. P. Bouchaud and D. S. Dean; J. Phys. I (France) 5 (1995) 265. C. Monthus and J-P Bouchaud, J. Phys. A 29, 3847 (1996). B. Rinn, P. Maas and J-P Bouchaud, Phys. Rev. Lett. 84, 5403 (2000).
- [46] E. Bertin and J-P Bouchaud, J. Phys. A 35, 3039 (2002).
- [47] M. Sasaki and K. Nemoto, J. Phys. Soc. Jpn. 68, 1148 (1999).
- [48] S. Fielding and P. Sollich, cond-mat/0107627, cond-mat/0209645. S. Fielding, P. Sollich and P. Mayer, cond-mat/0111241, J. Phys. C. S. Fielding, PhD Thesis Univ. Edinburgh UK 2000.
- [49] M. V. Feigel'man and V. M. Vinokur, J. Phys. (France), 49, 1731 (1988). J. Dyre, Phys. Rev. Lett. 58, 792 (1987); Phys. Rev. B 51, 12276 (1995).
- [50] W. L. McMillan, J. Phys. C 17, 3179 (1984) Phys. Rev. B 31, 340 (1985). A. J. Bray and M. A. Moore, J. Phys. C 17, L463 (1984) and in Heidelberg Colloquium in Glassy Dynamics, Lecture Notes in Physics 275, ed. J. L. van Hemmen and I. Morgenstern (Springer, Berlin, 1988). G. Koper and H. J. Hilhorst, J. Phys. (France) 49, 429 (1988). D. S. Fisher and D. Huse, Phys. Rev. B 38, 373 (1988).
- [51] See the articles in Glassy behaviour in kinetically constrained models, F. Ritort and P. Sollich eds., Barcelona 2002, J. Phys. C 14, 1381 (2002) and references therein.
- [52] J. D. Shore, M. Holtzer and J. P. Sethna, Phys. Rev. B 46, 11376 (1992).
- [53] J. Kurchan, L. Peliti and M. Sellitto, Europhys. Lett. 39, 365 (1997).
- [54] J-P Garrahan and M. E. J. Newman, Phys. Rev. E 62, 7670 (2000). D. S. Sherrington, L. Davison, A. Buhot and J. P. Garrahan, J. Phys. C 14, 1673 (2002). A. Buhot and J. P. Garrahan, Phys. Rev. E 64, 021505 (2002), J. Phys. C 14, 1499 (2002), Phys. Rev. Lett. 88, 225702 (2002).
- [55] G. Biroli and M. Mezard, Phys. Rev. Lett. 88, 225702 (2002). A. Lipowski, J. Phys. A 30, 7365 (1997). A. Lipowski and D. A. Johnston, Phys. Rev. E 61, 6375 (2000). M. Weigt and A. K. Hartmann, cond-mat/0210054.
- [56] D. J. Thouless, P. W. Anderson and R. G. Palmer, Phil. Mag. 35, 593 (1977).
- [57] J-O Andersson, J. Mattson and P. Svedlindh, Phys. Rev. B 46, 8297 (1992).
- [58] An incomplete list of references where the nonequilibrium evolution of different glassy systems has been studied numerically is the following. Spin models: H. Rieger, Annual reviews of computational physics II, 295 (World Scientific,

Singapore, 1995). Spin-glasses: S. Franz and H. Rieger, *J. Stat. Phys.* 79, 749 (1995). E. Marinari et al *J. Phys. A* 31, 2611 (1998). J. Kisker, L. Santen, M. Schreckenberg and H. Rieger, *Phys. Rev. B* 53, 6418 (1996). H. Rieger, *Physica A* 224, 267 (1996). Particle models with Lennard-Jones interactions: G. Parisi, *Phys. Rev. Lett.* 79, 3660 (1997). W. Kob and J-L Barrat, *Phys. Rev. Lett.* 78, 4581 (1997); *Eur. Phys. J B* 13, 319 (2000). J-L Barrat and W. Kob, *Europhys. Lett.* 46, 637 (1999). R. di Leonardo et al, *Phys. Rev. Lett.* 84, 6054 (2000). Models for silica glasses: H. Wahlen and H. Rieger, *J. Phys. Soc. Jpn* 69 Suppl. A 242 (2000). Frustrated lattice gases: A. Fierro, A. de Candia and A. Coniglio, *Phys. Rev. E* 62, 7715 (2002). M. Sellitto, *Eur. J. B* 4, 135 (1998). J. J. Arenzon, F. Ricci-Tersenghi and D. A. Starob, *Phys. Rev. E* 62, 5978 (2000). F. Ricci-Tersenghi, D. A. Starob, J. J. Arenzon, *Phys. Rev. Lett* 84 4473 (2000). Oscillator models: L. L. Bonilla, F. G. Padilla and F. Ritort, *Physica A* 25, 315 (1998). Spin models with dipolar interactions: J. Tolza, F. Tamarit and S. A. Cannas, *Phys. Rev. B* 48, R8885 (1998).

- [59] M. Picco, F. Ricci-Tersenghi and F. Ritort, *Eur. Phys. J B* 21, 211 (2001).
- [60] T. Grigera and N. Israeloff, *Phys. Rev. Lett.* 83, 5083 (2000).
- [61] L. Bellon, S. Ciliberto and C. Laroche, *Europhys. Lett.* 53, 5038 (1999). S. Ciliberto in this volume.
- [62] L. F. Cugliandolo, D. R. Gempel, J. Kurchan and E. Vincent, *Europhys. Lett.* 48, 699 (1999).
- [63] U. Weiss, *Quantum dissipative systems*, Series in modern condensed matter physics 10 (World Scientific, Singapore, 1999).
- [64] Note that the sign of the mass term generated by the coupling to the environment is negative. If strong enough, it may render unstable an initially stable potential well. One way to avoid this problem is to introduce the counterterm. One could also think that the coupling to the bath must be very weak and that the last term must vanish by itself (say, $\text{all } c_a \rightarrow 0$). However, this might be problematic when dealing with the stochastic dynamics since a very weak coupling to the bath implies also a very slow relaxation. It is then conventional to include the counterterm to cancel the mass renormalization.
- [65] J. Zinn-Justin; "Quantum Field Theory and Critical Phenomena" (Clarendon Press, Oxford, 1989).
- [66] R. Zwanzig, *J. Stat. Phys.* 9, 215 (1973).
- [67] J-P Hansen and A. MacDonald, *Theory of simple liquids*, (Academic Press, New York, 1976).
- [68] G. Parisi, *Statistical Field Theory*, Frontiers in Physics, Lecture Notes Series (Addison-Wesley, 1988).

- [69] G. Parisi, in this volume.
- [70] R. Kubo, M. Toda and N. Hashitume, *Statistical Physics II: Non-equilibrium Statistical Mechanics* (Springer Verlag, Berlin, 1992).
- [71] N. Pottier and A. Mauger, *Physica A* 282, 77 (2000), *ibid* 291, 327 (2001). N. Pottier, cond-mat/0205307.
- [72] L. F. Cugliandolo and J. Kurchan, cond-mat/9911086, *Frontiers in magnetism*, J. Phys. Soc. Japan, *Physica A* 263, 242 (1999).
- [73] C. P. Martin, E. Siggia and H. A. Rose, *Phys. Rev. A* 8, 423 (1973), H. K. Janssen, *Z. Phys. B* 23, 377 (1976) and *Dynamics of critical phenomena and related topics*, *Lecture notes in physics* 104, C. P. Enz ed. (Springer Verlag, Berlin, 1979).
- [74] J. Schwinger, *J. Math. Phys.* 2, 407 (1961). L. V. Keldysh, *Zh. Eksp. Teor. Fiz.* 47, 1515 (1964), *Sov. Phys JETP* 20, 235 (1965). P. Danielewicz, *Ann. Phys.* 152, 239 (1984).
- [75] C. de Dominicis, *Phys. Rev. B* 18, 4913 (1978).
- [76] E. Gozzi, *Phys. Rev. D* 30 (1984) 1218.
- [77] J. Kurchan, *J. Phys. I (France)* 1, 1333 (1992).
- [78] L. F. Cugliandolo and J. Kurchan, *Phil. Mag. B* 71, 50 (1995).
- [79] Note that the nonequilibrium correlation and response functions are self-averaging.
- [80] A. Houghton, S. Jain and A. P. Young, *Phys. Rev. B* 28, 2630 (1983).
- [81] L. F. Cugliandolo, D. R. Grompel and C. A. da Silva Santos, unpublished.
- [82] H. Sompolinsky and A. Zippelius, *Phys. Rev. Lett.* 45, 359 (1981), *Phys. Rev. B* 25, 274 (1982).
- [83] H. Sompolinsky and A. Zippelius, *Phys. Rev. Lett.* 50, 1297 (1983).
- [84] C. Chamon, M. P. Kennett, H. Castillo and L. F. Cugliandolo, cond-mat/0109150, *Phys. Rev. Lett.* (to appear).
- [85] L. F. Cugliandolo and G. Lozano, *Phys. Rev. Lett.* 80, 4979 (1998); *Phys. Rev. B* 59, 915 (1999).
- [86] R. Monasson, *J. Phys. A* 31, 513 (1998).
- [87] C. de Dominicis and P. Mottingham, *J. Phys. A* 20, L1267 (1987), *ibid* L365.
- [88] G. Semerjian and L. F. Cugliandolo, cond-mat/0204613.

- [89] L.F. Cugliandolo and P. Le Doussal, Phys. Rev. E 53, 152 (1996).
- [90] H. Sompolinsky, Phys. Rev. Lett. 47, 935 (1981).
- [91] A. Georges, Exact functionals, effective actions and (dynamical) mean-field theories: some remarks in Windsor 2001. A. Georges, G. Kotliar, W. Krauth and M. J. Rozenberg, Rev. Mod. Phys. 68, 13 (1996).
- [92] J-P Bouchaud, L.F. Cugliandolo, J. Kurchan and M. Mezard, Physica A 226, 243 (1996).
- [93] K. Kawasaki, Recent Res. Devel. Stat. Phys. 1, 41 (2001). K. Kawasaki and B-S Kim, cond-mat/0110536. E. Zaccarelli et al, Europhys. Lett. 55 157 (2001). E. Zaccarelli, PhD Thesis, Dublin 2000. J-L Barrat, Mode coupling theories, in Cargèse Summer School Glass physics, 1999.
- [94] R. Kraichnan; J. Fluid. Mech. 7, 124 (1961).
- [95] S. Franz and J. Hertz; Phys. Rev. Lett. 74 (1995) 2114.
- [96] S. Franz and M. Mezard; Europhys. Lett. 26, 209 (1994); Physica A 209, 48 (1994).
- [97] T. Halpin-Healey and Y.C. Zhang, Phys. Rep. 254 (1995) 217.
- [98] For reviews, see W. Gotze, in Liquids, freezing and glass transition, Les Houches 1989, JP Hansen, D. Levesque, J. Zinn-Justin Eds, North Holland. W. Gotze, L. Sjogren, Rep. Prog. Phys. 55 (1992) 241. W. Gotze, J. Phys. C 11 A 1 (1999).
- [99] E. Leutheusser, Phys. Rev. A 29, 2765 (1984).
- [100] U. Bengtzelius, W. Gotze and A. Sjolander, J. Phys. C 17, 5915 (1984).
- [101] W. Gotze and T. Voigtman, cond-mat/0001188.
- [102] A. Latz, J. Phys. C 12, 6353 (2000). cond-mat/9911025, cond-mat/0106068
- [103] K. Kawasaki and B-S Kim, Phys. Rev. Lett. 86, 3582 (2001).
- [104] L.F. Cugliandolo and J. Kurchan, J. Phys. A 27, 5749 (1994).
- [105] L.F. Cugliandolo, D.S. Dean and J. Kurchan, Phys. Rev. Lett. 79, 2168 (1997).
- [106] M.P. Kennett and C. Cham on, Phys. Rev. Lett. 86, 1622 (2001). M.P. Kennett, C. Cham on and Y. Ye, Phys. Rev. B 64, 224408 (2001). M.P. Kennett, PhD Thesis Princeton Univ. 2002. G. Biroli and O. Parcollet, Phys. Rev. B 65, 094414 (2002). H. Westfahl Jr., J. Schmalian and P.G. Wolynes, cond-mat/0202099.

- [107] M . Hazewinkel, Formal groups and applications Academic Press, New York, 1978.
- [108] J.M .Kosterlitz, D .J.Thouless and R .C . Jones, Phys. Rev. Lett. 36, 1217 (1976).
- [109] P . Shukla and S. Singh, J. Phys. C 14, L81 (1981). S. Ciuchi and F. de Pasquale, Nucl. Phys. B 300 [FS22], 31 (1988). L. F. Cugliandolo and D . S. Dean, J. Phys. A 28, 4213 (1995); *ibid* L453 (1995).
- [110] B. Kim and A .Latz, Europhys. Lett. 53, 660 (2001). H .Homer, unpublished.
- [111] S. Franz and F. Ricci-Tersenghi, Phys. Rev. E 61, 1121 (2000). L. Berthier, J-L Barrat and J. Kurchan, Phys. Rev. E 63, 016105 (2001). D . A . Stariob, Europhys. Lett. 55, 726 (2001).
- [112] L. F. Cugliandolo, J. Kurchan and L. Peliti, Phys. Rev. E 55, 3898 (1997).
- [113] A . Barrat and L. Berthier, Phys. Rev. Lett. 87, 087204 (2001).
- [114] H .Eissfeller and M . Opper, Phys. Rev. Lett. 68, 2094 (1992).
- [115] W . Kob, in this volume.
- [116] J. Kurchan, Phys. Rev. E 66, 017101 (2002).
- [117] H . Castillo, C . Cham on, L. F. Cugliandolo and M . P. Kennett, cond-mat/0112272, Phys. Rev. Lett. 88, 237201 (2002).
- [118] L. F. Cugliandolo, D . R. Grempe, G . Lozano, H . Lozza and C . A . da Silva Santos, Phys. Rev. B 66, 014444 (2002).
- [119] F. Corberi, E. Lippiello and M . Zannetti, Phys. Rev. E 63, 061506 (2001), Eur. Phys. J B 24, 359 (2000).
- [120] C. Godreche and J-M Luck J. Phys. A 33, 1151 (2000). E. Lippiello and M . Zannetti, Phys. Rev. E 61, 3369 (2000). F. Corberi, C . Castellano, E . Lippiello and M . Zannetti, Phys. Rev. E . (to appear).
- [121] L. Berthier and J-L Barrat, Phys. Rev. Lett. 89, 095702 (2002), J. Chem . Phys. 116, 6228 (2002).
- [122] A . Barrat, J. Kurchan, V . Loreto and M . Sellitto, Phys. Rev. Lett. 85, 5034 (2000).
- [123] H . Maske and J. Kurchan, Nature 415, 614 (2002).
- [124] L. Berthier, P. Holdsworth, M . Sellitto, J. Phys. A 34, 1805 (2001).
- [125] E. Marinari, G . Parisi, F. Ricci-Tersenghi and J. J. Ruiz-Lorenzo, J. Phys. A 31, 2611 (1998).

- [126] P. Hohenberg and B. Shraiman, *Physica D* 37, 109 (1989).
- [127] J-L Barrat, private communication.
- [128] R. Exartier and L. Peliti, *Eur. Phys. J. B* 16, 119 (2000).
- [129] A. Garriga and F. Ritort, *Eur. Phys. J. B* 20, 105 (2000), *ibid* 21, 115 (2001).
- [130] L. F. Cugliandolo and J. Kurchan, *Physica A* 263 242 (1999).
- [131] A. Q. Tool, *J. Am. Ceram. Soc.* 29, 240 (1946). R. Gardon and O. S. Narayanaswamy, *J. Am. Ceram. Soc.* 53, 380 (1970). O. S. Narayanaswamy, *J. Am. Ceram. Soc.* 54, 491 (1971). C. T. Moynihan et al *J. Am. Ceram. Soc.* 59, 12 (1976). G. W. Scherer, *J. Am. Ceram. Soc.* 67, 504 (1984). J. Jackle, *Rep. Prog. Phys.* 49, 171 (1986). G. W. Scherer, *J. Non-Cryst. Solids* 123, 75 (1990).
- [132] S. F. Edwards, in *Disorder in condensed matter physics* (Oxford Science Pub., 1991).
- [133] T. M. Nieuwenhuizen, *Phys. Rev. Lett.* 80, 5580 (1998). *Phys. Rev. E* 61, 267 (2000).
- [134] S. F. Edwards in *Disorder in condensed matter physics* Oxford Science Publications, 1991 and in *Granular matter: an interdisciplinary approach*, A. M ehta ed. (Springer-Verlag, New York, 1994).
- [135] J. J. Brey, A. P rados and B. Sanchez-Rey, *Phys. Rev. E* 60, 5685. A. Fierro, M. Nicodemi and A. Coniglio, cond-mat/01-7134. J. Berg and A. M ehta, cond-mat/0108225. A. Lefevre and D. S. Dean, *Phys. Rev. Lett.* 86, 5631 (2001), *J. Phys. A* 34, L213 (2001), cond-mat/0111331. J. Berg, S. Franz, M. Sellitto, *Eur. Phys. J. B* 26, 349 (2002).
- [136] F. H. Stillinger and T. A. Weber, *Phys. Rev. A* 25, 978 (1982); *Science* 225, 983 (1984). S. Sastry, P. G. Debenedetti and F. H. Stillinger, *Nature* 393, 554 (1998). S. Sastry, *Nature*, 409, 164 (2001).
- [137] W. Kob, J-L Barrat, F. Sciortino and P. Tartaglia, cond-mat/9910476. W. Kob, F. Sciortino and P. Tartaglia, *Phys. Rev. Lett.* 83, 3214 (1999). P. de Gregorio et al cond-mat/0111018. C. Donati, F. Sciortino and P. Tartaglia, *Phys. Rev. Lett.* 85, 1464 (2000). F. Sciortino and P. Tartaglia, *Phys. Rev. Lett.* 86, 107 (2001). R. Di Leonardo, L. Angelani, G. Parisi, G. Ruocco, A. Scala and F. Sciortino, cond-mat/0106214. S. Mossa, E. La Nave, P. Tartaglia and F. Sciortino, cond-mat/0209181
- [138] R. Monasson, *Phys. Rev. Lett.* 75, 2847 (1995).
- [139] S. Franz and G. Parisi, *J. Physique I* 5, 1401 (1995).

- [140] M .M ezard and G .Parisi, Phys.Rev.Lett.82, 747 (1998).J.Phys.C 11 A 157 (1999).
- [141] F .Thalman, J.Chem .Phys.116, 3378 (2002).
- [142] G .B ioli and R .M onasson, Europhys. Lett. 50, 155 (2000).
- [143] G .B ioli, J.Phys. A 32, 8365 (1999).
- [144] G .B ioli and L .F .Cugliandolo, Phys.Rev.B 64, 014206 (2001).
- [145] T .P lefka, J.Phys. A 15, 1971 (1982).
- [146] A .G eorges and J .S .Yedidia, J.Phys. A 24, 2173 (1991).
- [147] J .K urchan, G .Parisi and M .A .V irasoro, J.Physique I 3, 1819 (1993).
- [148] G .B ioli, J.Phys. A 32, 8365 (1999).
- [149] A .C avagna, I .G iardina and G .Parisi, J.Phys. A 30, 7021 (1997).
- [150] A .C avagna, I .G iardina and G .Parisi, Phys.Rev.B 57 11251 (1998).
- [151] C .de D om inicis and A .P .Young, J.Phys. A 16 2063 (1983).
- [152] P .S ibani, Phys. Rev. B 35, 8572 (1987) K .H .H o mann and P .S ibani, Z .Phys. B 80, 429 (1990)
- [153] O .C .M artin, R .M onasson and R .Zecchina, Theor. Comp .Sc.265, 3 (2001).
F .R icci-Tersenghi, M .W eight and R .Zecchina, Phys.Rev E 63, 026702 (2001).
S .Franz, M .Leone, F .R icci-Tersenghi and R .Zecchina, Phys. Rev. Lett. 87, 127209 (2001).
- [154] A .B arrat and R .Zecchina, Phys.Rev.E 59, R1299 (1999).A .M ontanari and F .R icci-Tersenghi, cond-m at/0207416.
- [155] S .Franz, M .M ezard, G .Parisi and L .P eliti, Phys.Rev.Lett.81, 1758 (1998);
J.Stat.Phys. 97, 459 (1999).
- [156] R .P .Feynman and F .L .Vernon, Jr, Ann.Phys.24, 114 (1963).
- [157] D .Thirumalai and T .R .K irkpatrick, Phys.Rev.B 38, 4881 (1988).A .B arrat, R .Burioni and M .M ezard, J.Phys A 29, L81 (1996).
- [158] Note that many glass formers have a crystalline structure that corresponds to most convenient equilibrium con guration.How much does the crystalline uence the behaviour or the glass is an interesting still unanswered question, see the discussion in [159]
- [159] T .S .G rigera and N .E .Israelo , Phil.M ag.B 82, 313 (2002).A .C avagna, I .G iardina and T .S .G rigera, cond-m at/0207165.

- [160] A .C risanti and F .R itort, Europhys.Lett. 52, 640 (2000), Physica A 280, 155 (2000).
- [161] A .C avagna, Europhys.Lett. 53, 490 (2001). K .B roderix, K .K .B hattacharya, A .C avagna, A .Z ippelius and I. G iardina, AIP Conference Proceedings, 553, 23 (2001).
- [162] S.Franz and J.Kurchan, Europhys.Lett. 20, 197 (1992).
- [163] D .S .F isher, P .L e D oussal, C .M onthus, Phys. Rev. Lett. 80 3539 (1998), Phys. Rev. E 64, 066107 (2001).
- [164] L .L aboux and P .L e D oussal, Phys. Rev. E . 57 6296 (1998).
- [165] A .V .L opatin and L .B .I o e, Phys. Rev. B 60, 6412 (1999), Phys. Rev. Lett. 84, 4208 (2002).
- [166] J.P .B ouchaud and M .M ezard; J.Phys. I (France) 4 (1994) 1109. E .M arinari, G .P arisi and F .R itort; J.Phys. A 27 (1994) 7615; J.Phys. A 27 (1994) 7647. L .F .C ugliandolo, J. Kurchan, G .P arisi and F .R itort, Phys. Rev. Lett. 74, 1012 (1995). P .C handra, L .B .I o e and D .S herington, Phys. Rev. Lett. 75, 713 (1996). P .C handra, M .V .F eigel'm an, L .B .I o e and D .M .K agan, Phys. Rev. B 56, 11553 (1997). G .F ranzese and A .C oniglio, Phys. Rev. E 58, 2753 (1998); Phys. Rev. E 59, 6409 (1999), Phil.M ag. B 79, 1807 (1999). A .F ierro, G .F ranzese, A .de C andia, A .C oniglio, Phys. Rev. E 59, 60 (1999).
- [167] A .C risanti and H -J Som m ers, Z .Phys. B 87, 341 (1992).
- [168] A .J .L eggett, S .C hakravarty, A .T .D orsey, M .P .A .F isher, A .G arg, W .Z werner, Rev. M od. Phys. 59, 1 (1987).
- [169] T .R .K irkpatrik and D .T hirumalai, Phys. Rev. B 36, 5388 (1987).
- [170] C .G odreche and J-M Luck, J.Phys. A 33, 9141 (2000). M .H enkel, M .P iem -ling, C .G odreche and J-M Luck, Phys. Rev. Lett. 87, 265701 (2001). A .P icone and M .H enkel, J.Phys. A 35, 5572 (2002). M .H enkel, hep-th/0205256. P .C alabrese and A .G ambassi, Phys. Rev. E 65, 066120 (2002), cond-m at/0207452, cond-m at/0207487,
- [171] A .C avagna, I. G iardina and G .P arisi, cond-m at/9702069.
- [172] I.K .O no, C .S .O 'H em, D .J .D urian, S .A .L anger, A .J .L iu and S .R .N agel, Phys. Rev. Lett. 89, 095703 (2002). L .A ngelani, G .R uocco, F .S ciortino, P .T artaglia and F .Z amponi, cond-m at/0205182 and F .Z amponi, tesi di Laurea, Univ. di Roma I, 2001.
- [173] A .E .K oshelev and V .M .V inokur, Phys. Rev. Lett. 73, 3580 (1994). I .A ranson, A .E .K oshelev and V .M .V inokur, Phys. Rev. B 56, 5136 (1997).

- [174] L.F.Cugliandolo, D.R.G ren peland C.A.da Silva Santos, Phys.Rev.Lett. 85, 2589, (2000), Phys.Rev.B 64, 014402 (2001).
- [175] A.J.B ray and M.A.M oore, J.Phys.C 12, L441 (1979).
- [176] T.M.N iuwenhuizen and F.R itort, Physica A 250, 89 (1996).
- [177] J.H.G ibbs and E.A.diM arzio, J.Chem.Phys. 28, 373 (1958). G.A dam s and J.H.G ibbs, J.Chem.Phys. 43, 139 (1965).